Transition Metal-Catalyzed Transformations of *N*-Arylindazolones to Fused-Diazaheterocycles *via* C-C/C-N Bond Formations

THESIS

Submitted in partial fulfillment

of the requirements for the degree of

DOCTOR OF PHILOSOPHY

by

MAHESHA C. K.

ID. NO. 2018PHXF0009P

Under the supervision of

Dr. RAJEEV SAKHUJA

BITS Pilani

Pilani | Dubai | Goa | Hyderabad

DEPARTMENT OF CHEMISTRY
BIRLA INSTITUTE OF TECHNOLOGY AND SCIENCE
PILANI (RAJASTHAN) INDIA
2023

BIRLA INSTITUTE OF TECHNOLOGY AND SCIENCE
PILANI (RAJASTHAN)

CERTIFICATE

This is to certify that the thesis entitled "**Transition Metal-Catalyzed Transformations of *N*-Arylindazolones to Fused-Diazahetrocycles *via* C-C/C-N Bond Formations**" submitted by **Mr. MAHESHA C. K.**, ID No. **2018PHXF0009P** for the award of Ph.D. Degree of the Institute embodies the original work done by him under my supervision.

Signature in full of the Supervisor

Name in capital block letters: **Dr. RAJEEV SAKHUJA**
Designation: Professor, Birla Institute of Technology and Science Pilani, Pilani Campus, Rajasthan India.

Date:

Dedicated
to My
Parents

ACKNOWLEDGEMENTS

First and foremost, I would like to express my deep sense of gratitude to my Ph.D. supervisor Dr. Rajeev Sakhuja providing me his continuous support, supervision and encouragement throughout my doctoral research. His dynamic personality and motivational talk has always boosted me to do hard work in my challenging days.

I am very grateful to DST-SERB for providing initial three years financial support through a DST-funded research proposal. I would also take this opportunity to express my whole-hearted gratitude to Prof. Souvik Bhattacharyya (Vice-Chancellor, BITS Pilani), Prof. Sudhirkumar Barai (Director, BITS Pilani, Pilani Campus), Prof. S. K. Verma (Dean, Administration) and Prof. Shamik Chakraborty (Associate Dean, AGSRD) for providing necessary facilities throughout my research work, and financial support in the last two years.

I am very much thankful to our collaborator Prof. Sanjay K. Mandal, IISER Mohali, for his timely help in providing X-ray crystal structures of the synthesized compounds.

I am very much grateful to my Doctoral Advisory Committee members, Prof. Anil Kumar and Prof. Indresh Kumar. Their insightful suggestions and comments have broadened the perspectives related to research.

I want to extend my sincere thanks to Prof. Bharti Khungar (Convener, Departmental Research Committee, Department of Chemistry, BITS Pilani, Pilani Campus) and Prof. Indresh Kumar (Head, Department of Chemistry, BITS Pilani, Pilani Campus) for their kind support.

I am very much obliged to Prof. S. C. Sivasubramanian, Prof. Dalip Kumar, Prof. Paritosh Shukla, Prof. Shamik Chakraborty and Prof. Madhushree Sarkar for their valuable teaching in the course work carried by me, which has helped me to gain deep knowledge of chemistry.

I am highly thankful to Dr. Kiran Bajaj for her valuable discussions and timely suggestions that helped me to solve many critical problems in my research.

I am immensely thankful for the cooperation and affection received from all the faculty members of the Department of Chemistry, BITS Pilani, which has made me to stay confident in the campus.

As an organic chemist, it is hard to think without NMR and HRMS facility. Therefore, I am very much grateful to the BITS Pilani and DST-FIST for providing financial support for the necessary instrumentation facilities at BITS Pilani, Pilani Campus. During my stay at Pilani Campus, I got an opportunity to work on the NMR instrument for four years; for this I am deeply acknowledging the immense support and friendly behavior of Dr. Vikki Narayan Shinde, Mr. Prakash Taur, Mr. Ram, Mr. Atul, Mr. Prakash N Swami, Ms. Jyoti Yadav, and lab technician, Mr. Abhishek that helped towards the smooth running of the NMR machine. Also, I would like to acknowledge the HRMS team for providing the results on time.

I would like to acknowledge my seniors, Dr. Abdul Shakoor, Dr. Santosh Kumari, Dr. Devesh S Agarwal, and fellow labmates, Dr. Karishma, Ms. Sushma, Mr. Narendra, Mr. Somnath, Ms. Disha and Ms. Nisha Gangwar who have always helped me in need.

I am extremely thankful to office staff and lab. staff (Department of Chemistry), especially Ms. Pushpa, Mr. Suresh and Mr. Nandalal for allowing me to access the general lab. equipments.

"*The world is a better place when you have found the people who make up your friendship circle*"
I realized the beauty of this sentence when I got my dearest friends, Mr. Mallikarjuna D, Dr. Amol P. Pawar, Ms. Neha, Mr. Sumit K. Agarwal, Ms. Gurpreet, Mr. Praksh P. Taur, Dr. Vikki N. Shinde, Mr. Pramod Raichure, Ms. Soumana Joarder, Mr. Dhritabrata Pal, Ms. Divya Rathod, Ms. Pragya, Mr. Bharath Kaushik and Mr. Atul Dolas, who accepted all good and bad things very patiently and always supported me in every situation.
My special thanks to 3110 lab fellows Dr. P.O.V. Reddy, Dr. Santhosh Khandagale, Dr. M. Vimal, Dr. Manish K. Mehra, Mr. Bintu Kumar, Ms. Monika Malik, Mr. Narasimha Verma, Ms. Prakriti Sarf, Ms. Nandini Roy for their immense support without any boundaries.
Earnest thanks to Dr. Moyna Das, Dr. Shiv Dhiman, Dr. Mamtha Devi Sharma, Mr. Dhananjay S Nipte, Mr. Yadaw Nagre and Ms. Shivani for their moral support and timely help.
Especially in this case I cannot forget the help received from my CSIR-NIIST-Trivandrum friends. I must say my research life started there in NIIST. Dr. Jamsheena Vellekkatt, Dr. Challa Chandra Sekhar, Dr. Veena K. S, Dr. Arun K. Tangarasu, Mr. Sadasivarao Ginjupalli supported enormously in my two years of NIIST journey.
My extensive wholehearted acknowledgements to my primary and high school teachers who taught me to become a gentle man in this society especially, Ms. Renuka, Ms. Shammem Unnisa, Ms. Anuradha, Ms. Vanaja, Ms. Usha, Ms. Sibul, Ms. Bharathi, Ms. Suvarana Kumari, Mr. Mohana Kalluraya, Mr. Sham Sundar Bhat are the main reason why I have reached this level.
I extend my profound thanks to my college lecturers, Mr. Nagaraj and Mr. Shet Prakash M. who really develop my curiosity towards Organic Chemistry.
I am truly blessed with the love of my relatives and the support I have received from my family that cannot be overstated. Mr. Krishnappa C. N (my father), Ms. Ratnamma (my mother), Mr. Tejaswi C.K (my brother), and Ms. Kavya R (my wife) supported me in all my best and worst conditions. They are the real backbone to my strength, and I am using this platform to acknowledge them.

Date: **Mahesha C. K.**

ABSTRACT

The construction of carbon–carbon (C–C) bonds are of perennial interest to organic and medicinal chemists, extending carbon frameworks for preparing pharmacological active molecular architectures, agrochemicals and natural products. In this concern, transition metal-catalyzed directing group-assisted cross-dehydrogenative coupling has emerged as a powerful tool to construct C-C/C-hetero bonds. Strikingly, indazol-3-one nucleus has been recognized as a privileged scaffold that constitute an integral part of functionalized and indazolo-fused heterocycles with interesting biological activities. Particularly, the functionalization of *N*-aryl-1,2-dihydro-3*H*-indazol-3-ones was explored only to a limited extent at the time of commencement of this work. The current thesis entitled "**Transition Metal-Catalyzed Transformations of *N*-Arylindazolones to Fused-Diazaheterocycles *via* C-C/C-N Bond Formations**" has been successfully executed in due diligence of sustainable chemistry, and the thesis has been divided into four chapters.

The first chapter of the thesis is divided in two sub-parts (**Chapter 1A** and **Chapter 1B**). **Chapter 1A** summarizes an overview on transition metal-catalyzed cross-dehydrogenative coupling (CDC) strategies proceeded *via* C-H activation/functionalization approach, and general mechanistic pathways involved in such protocols. Further, the chapter briefly describes the importance of indazol-3-one scaffold, and the rationale for pursuing this research work by exploring the directing group ability of inbuilt cyclic amide group in *N*-aryl-1,2-dihydro-3*H*-indazol-3-ones and aiming to functionalize it with varied coupling partners primarily *via* chelation-assisted transition metal-catalyzed C-H activation notion. **Chapter 1B** presents an efficient synthesis of diversely substituted indazolo[1,2-*a*]indazolylidenes obtained by the [4+1] annulation of *N*-aryl-1,2-dihydro-3*H*-indazol-3-ones and acrylates *via* Ru^{II}-catalyzed cross-dehydrogenative coupling strategy using KPF_6 as an additive and CsOAc as a base in toluene.

The second chapter of the thesis aims at synthesizing three series of functionalized indazolo[1,2-*a*]cinnolines *via* directing group-assisted transition metal-catalyzed C-H activation approach. **The second chapter** of the thesis is divided in three sub-parts (**Chapter 2A**, **Chapter 2B** and **Chapter 2C**). **Chapter 2A** describes an external reducing agent-free strategy for the [4+2] annulation of *N*-aryl-1,2-dihydro-3H-indazol-3-ones with easily accessible nitroolefins to afford hydroxyimino-decorated indazolo[1,2-*a*]cinnolines under Rh^{III}-catalyzed conditions using NaOAc as an additive in ethanol. **Chapter 2B** discloses an efficient Ir^{I}-catalyzed methodology to access indazolo[1,2-a]cinnoline carboxylates by the annulation of *N*-aryl-1,2-dihydro-3*H*-indazol-3-ones with *α*-diazo carbonyl compounds using $AgSbF_6$ as an additive in DCE. **Chapter 2C** discloses solvent/additive-controlled strategies for the synthesis of two regioisomeric forms of indazolo[1,2-*a*]cinnolines possessing internal and exocyclic double bonds through Pd^{II}-catalyzed oxidative annulation of *N*-aryl-1,2-dihydro-3*H*-indazol-3-ones with allenoates.

The third chapter (**Chapter 3**) of the thesis describes a one-pot Pd^{II}-catalyzed protocol for the unprecedented transformations of 1-aryl- and 2-arylindazolones to 1,2-(hetero)aryl and 2,3-(hetero)aryl 2,3-dihydroquinazolin-4(1H)-ones respectively, by reacting them with *N*-tosylhydrazones through carbene insertion into N-N Bond.

Finally, in **the fourth chapter** (**Chapter 4**) of the thesis, brief conclusions of each chapter are presented along with the future scope of the research work.

LIST OF TABLES

LIST OF FIGURES

LIST OF ABBREVATIONS/SYMBOLS

Abbreviation/Symbol	Description
α	Alpha
β	Beta
δ	Chemical shift in parts per million
°C	Degree centigrade
σ	Sigma
π	Pi
Å	Angstrom
%	Percentage
ACN	Acetonitrile
Ar	Aryl
Aq	Aqueous
AgOAc	Silver acetate
AdCOOH	1-Adamantane carboxylic acid
ADA	Adenosine deaminase
atm	Atmosphere
Bn	Benzyl
t-BuOH	*tert*-Butyl alcohol
^{13}C	Carbon-13
$CDCl_3$	Deuterated Chloroform
$Cu(OAc)_2$	Copper acetate
Calc.	Calculated
COD	Cyclooctadiene
CCDC	Cambridge Crystallographic Data Center
m-CPBA	*meta*-Chloroperoxybenzoic acid
d	Doublet
dd	Doublet of doublet
DG	Directing Group
DCE	1,2-Dichloroethane
DEAD	Diethyl azodicarboxylate
DCM	Dichloromethane

DMF	*N*,*N*-Dimethylformamide
DMSO-d_6	Deuterated dimethylsulfoxide
DMA	Dimethylacetamide
DMSO	Dimethylsulfoxide
ESI-MS	Electron Spray Ionization-Mass Spectrometry
Et_2O	Diethyl ether
EtOAc	Ethyl acetate
EtOH	Ethanol
EWG	Electron Withdrawing Group
EDG	Electron Donating Group
equiv.	Equivalent
g	Gram
h	Hours
HFIP	Hexafluoroisopropanol
HRMS	High Resolution Mass Spectrometry
Hz	Hertz
^{i}Pr	Isopropyl
J	Coupling constant
KOAc	Potassium acetate
KIE	Kinetic Isotopic Effect
k_H	Protonated rate constant
k_D	Deuterated rate constant
P_H	Protonated product constant
P_D	Deuterated product constant
LiO^{t}Bu	Lithium tertiary butoxide
LiOAc	Lithium acetate
LAH	Lithium Aluminium Hydride
LC/MS	Liquid Chromatography/Mass Spectrometry
mp	Melting point
m	Meta
m	Multiplet
mL	Millilitre

mg	Milligram
MHz	Megahertz
min	Minutes
mmol	Millimole
mol %	Mole percent
MeOH	Methanol
MeOD	Deuterated Methanol
NaOAc	Sodium acetate
NEt_3	Triethyl amine
NMR	Nuclear Magnetic Resonance
Nu	Nucleophile
o	Ortho
OTf	Triflouromethanesulfonate
ORTEP	Oak Ridge Thermal Ellipsoid Plot
p	Para
Py	Pyridine
PhMe	Toluene
PhCl	Chlorobenzene
PIDA	Phenyl iodonium diacetate
PivOH	Pivalic acid
$PhCO_2H$	Benzoic acid
ppm	Parts per million
rt	Room temperature
s	Singlet
SET	Single Electron Transfer
S_EAr	Electrophilic Aromatic Substitution
t	Triplet
t-AmOH	*tert*-Amyl alcohol
td	Triplet of doublets
TFA	Trifluoroacetic acid
TEMPO	(2,2,6,6-Tetramethylpiperidin-1-yl)oxyl
TFE	Trifluoroethanol

THF	Tetrahydrofuran
TLC	Thin layer chromatography
XRD	X-Ray diffraction
$Zn(OAc)_2$	Zinc acetate

TABLE OF CONTENTS

Chapter 2B. Iridium-Catalyzed [4+2] Annulation of *N*-Arylindazolones with *α*-Diazo Carbonyl Compounds to access Indazolo[1,2-*a*]cinnoline Carboxylates

Chapter 2C. Palladium-Catalyzed [4+2] Annulation of *N*-Arylindazolones with Allenoates to access Indazolo[1,2-*a*]cinnoline Carboxylates

Chapter 3. Palladium-Catalyzed Tandem Transformation of *N*-Arylindazolones to Disubstituted Quinazolinones through Carbene Insertion into N-N Bond

Chapter 4. Conclusions of the Thesis

Appendices

Chapter 1A

Background of the Research Work

1A.1 Transition Metal-Catalyzed C-H Bond Functionalization

Ever since the dawn of organic chemistry, the construction of carbon–carbon (C–C) bonds are of perennial interest to organic and medicinal chemists, connecting carbon frameworks that are of paramount importance for preparing pharmacological active molecular architectures, agrochemicals and natural products.[1-3] Among the plethora of methods developed, nucleophilic & electrophilic additions and substitutions, pericyclic and radical chain reactions, Cope and acid/base-mediated rearrangements have been predominantly employed to construct C-C bonds in a conventional fashion for decades.[4-5] However, a sudden hike in C-C bond forming strategies was observed with the advent of cross-coupling reactions, involving metal-catalyzed coupling of activated and less-activated electrophiles (aryl/vinyl/benzyl/allyl/alkyl halides/tosylates, amides, esters *etc.*) with an organometallic nucleophile.[6-11] Though, the need for additional steps for pre-functionalization of starting materials and the production of substantial by-products embarks the overall cross-coupling reactions as cumbersome processes, yet their illustrious applications towards fostering industrially valuable molecules in high yields have successively outshined these protocols for more than a decade. Such extensive work on transition metal-catalyzed electroneutral cross-coupling reactions was recognized in the form of Nobel Prize in Chemistry-2010 for Pd-catalyzed cross-couplings in organic synthesis.[12] Interestingly, with the maturity of the chemistry of cross-coupling reactions, transition metal-catalyzed Csp^2-H, Csp-H and Csp^3-H bond activation reactions *via* cross-dehydrogenative coupling (CDC) have added new dimensions to the flourishing modern synthetic organic chemistry, whereby unprecedented reaction mechanisms have been observed by the eye-catching roles played by Co, Cu, Pd, Ru, Rh and Ir catalysts, resulting in the assembling of complex heterocyclic frameworks with ease.[13-16]

In fact, Glaser report on Cu-mediated homo-oxidative dimerization of terminal alkynic C–H bonds to a conjugated diyne in 1869 has been considered as the first report on the direct generation of C–C bonds *via* CDC strategy.[17-18] Following this, Iataaki, Tanaka, and Yamaguchi's groups independently disclosed benzene dimerization to afford biphenyl under Pd-catalyzed, Rh/photocatalytic and thermal conditions, respectively.[19-21] However, the work in the area of CDC remains explored only to a limited extent for several decades. This may be attributed to the electronic mismatch between the coupling of two negatively charged carbon atoms of two isolated C-H bonds, and the thermodynamically unfavorable release of molecular hydrogen as a by-product in a typical CDC reaction. However, the usage of appropriate sacrificial oxidant can help in

formation of possible intermediates, such as carbocation/radical during the oxidative H-removal of C-H bond. This oxidative coupling can categorized into reactions with internal oxidants and external oxidants, respectively. Alternatively, the use of appropriate metal ion can facilitate the formation of a transition-metal complex by the activation of C-H bond, which upon subsequent reaction with C-H bond of another molecule results in the formation of C-C bond[22] (Figure 1A.1.1).

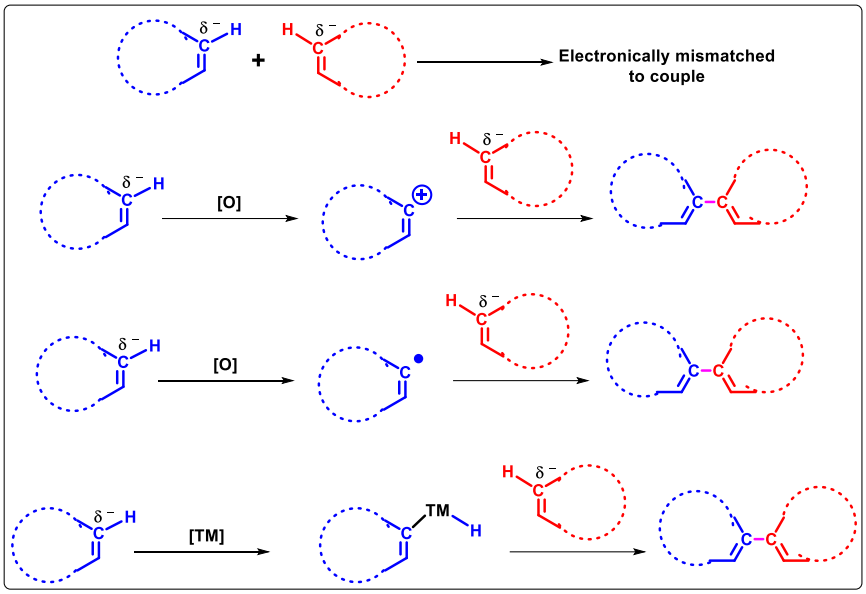

Figure 1A.1.1 General scheme for requirement of CDC reactions

Over the decades, a gradual increase in the development of CDC strategies by modulating the oxidant nature have been monitored, whereby the lesser reactive non-acidic Csp^2-H bonds in a variety of aromatic/heteroaromatic substrates have been triggered by coordination to a transition metal center to form an organometallic complex *via* C-H bond cleavage through a strategy termed as "C-H activation".[23-26] Broadly, C-H activation has been classified under two classes: (i) outer-sphere mechanism involving the interaction of an active ligand coordinated to the metal-center with the C-H bond, and (ii) inner-sphere mechanism favoring a direct involvement of C-H bond with transition metal to form a metal-alkyl or metal-aryl organometallic complex, which is usually followed by its reaction with either a ligand bound to the metal center or with an external reagent. Certainly, in the inner sphere mechanism, C-H bond interacts with transition metal through a charge transfer either from metal based filled dπ orbital to σ* orbital of the coordinated C-H bond, or from the filled σ(C-H) bond to an empty metal dσ orbital. The propensity of a metal center towards particular C-H bond governs the selectivity of inner-sphere C-H bond functionalization process, and is less dependent on C-H bond strength that prevents over-oxidation. Furthermore,

inner-sphere pathways are primarily favored by diamagnetic complexes that perform two-electron chemistry and avoids radical pathways. In contrast, the selectivity in outer-sphere C-H bond activation process favors the reaction of weaker C-H bonds (tertiary, benzylic, allylic, or alpha to heteroatoms), and activation occurs for metals in high oxidation states with reactive imido, oxo or carbene ligands attached to it. Either of these phenomena can lead to weakening and eventual breaking of C-H bond. The type of mechanism is completely dependent on nature and oxidation state of the metal. Notably, since electron-deficient high-valent late transition metals (*e.g.* Pd^{II}, Ru^{II}, Ir^{III} and Rh^{III}) possess low energy dπ and dσ electrons, hence charge transfer will occur from C-H orbitals to empty metal-based orbitals through a process called "electrophilic C-H activation", such as concerted metalation-deprotonation (CMD).[27-28] In striking contrast, the "nucleophilic C-H activation" involving the role of low-valent electron-rich metals (*e.g.* Rh^{I} and Ir^{I}), often undergoes oxidative addition into C–H bonds that gets benefited by the addition of external strongly binding ligands, such as phosphines, *N*-heterocyclic carbenes or bidentate nitrogen-containing molecules for further tuning the reactivity of the reaction.[27] It is noteworthy that mechanistic pathways followed by different organic substrates often remains debatable unless supported by computational studies.

In the domain of modern flourishing organic synthesis, the overall process involving transformation of C-H bonds into C-C and C-Het bonds (Het = N, O or X) in hetero(arenes) under metal-free or metal-catalyzed conditions, has been broadly popularized as C-H functionalization. With regard to the above described C-H activation notion, astonishing C-H functionalization strategies with varied coupling partners have been disclosed in the past decade using Pd,[29] Rh,[30] Ir,[31] Ru,[32] Cu,[33] Co,[34] Mn[35] and Re[36] catalytic systems, allowing unlimited access to libraries of functionalized (hetero)arenes in fewer steps, and generating lesser by-products (Figure 1A.1.2).

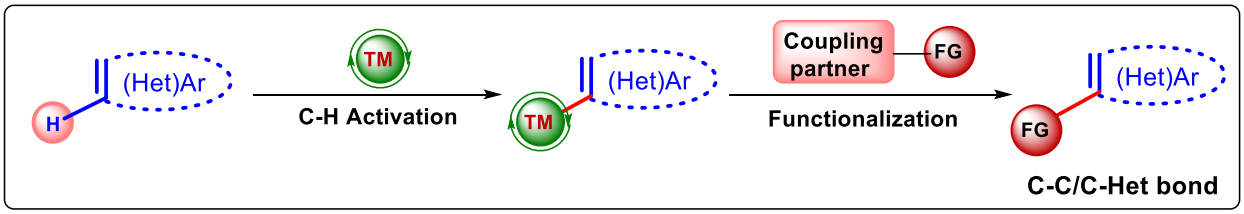

Figure 1A.1.2. General representation of C-H bond activation and functionalization

A few selective examples on transition metal-catalyzed (Pd, Rh, Ru, Ir)[28,37-38] C-H functionalization/annulation strategies with functional group inducing reagents or coupling

partners, employing a variety of ligands, oxidants, bases and/or additives are shown in Figure 1A.1.3.

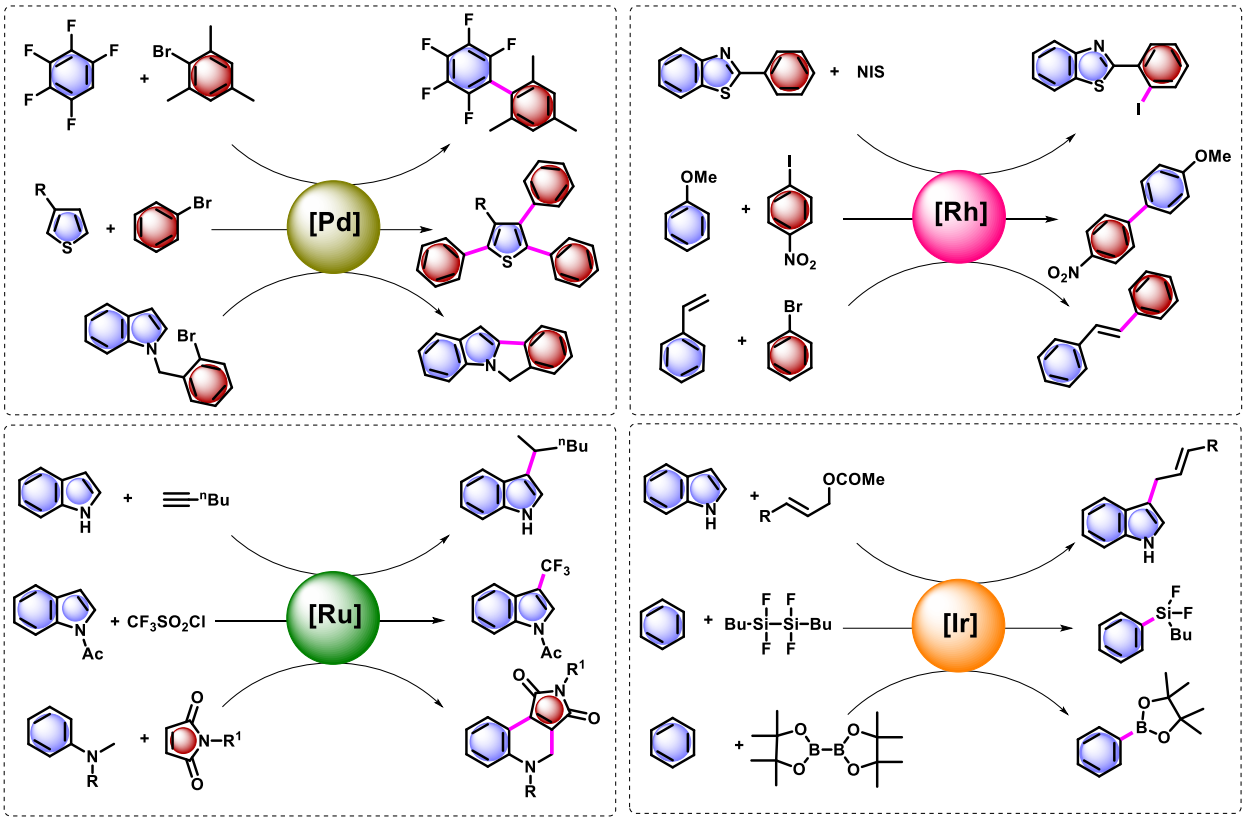

Figure 1A.1.3. Selective examples of C-H bond functionalization/annulation *via* Pd, Rh, Ru and Ir-catalysis

In spite of great success on the above described undirected C-H activation processes, the fundamental issues on regioselective functionalization, and the reactivity of inert C-H bonds are not completely addressed. In recent years, these issues have been resolved to a large extent by the employability of a directing group (DG) in close proximity to inert C-H bonds to be functionalized, applying C-H bond activation chemistry.

1A.2 Directing Group (DG)-Mediated Chelation-Assisted C-H Bond Functionalization

The reactivity and the regioselective functionalization of the C-H bonds in heterocyclic compounds is mainly controlled by the electronic effects of heteroatoms, however, the selective functionalization of inert and non-biased Csp^2-H or Csp^3-H bonds in aromatic or aliphatic compounds are particularly challenging because of absence for a metal-coordinating site at the substrate in close proximity to such bonds. To overcome this, installation of a proximal directing

group (DG)/ (hetero atom-bearing DG) possessing a pair of electrons facilitate the possibility of high site-selective C-H activation by coordinating reversibly to a transition metal, forming a chelated-metallocyclic intermediate, thereby bringing it into close proximity to the C–H bond to be functionalized. Thus, proximal directing groups not only induces the site-selectivity, but also leads to higher reactivity by enhancing the effective concentration of the metal catalyst[39-40] (Figure 1A.2.1).

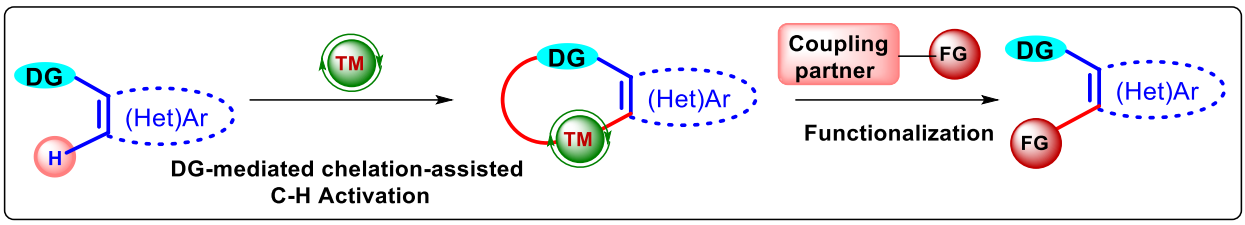

Figure 1A.2.1 General representation of directing group (DG)-mediated chelation-assisted C-H bond functionalization

In this domain, the first report by Murai's group in 1993 achieved the Ru^{II}-catalyzed carbonyl group-assisted regioselective *ortho*-C-H hydroarylation of arenes with alkenes.[41] Following this interesting outcome, the chelation-assisted C-H bond activation strategy has been immensely employed towards the rapid synthesis of complex molecules by directly coupling electron-rich/deficient (hetero)arenes with varied functional group-inducting reagents or coupling partners to succeed either C-H functionalization and/or subsequent cyclization in a convenient manner.[42]

Broadly two types of DG-assisted C-H functionalization strategies have been applied: (i) in-built DG-assisted C-H activation, in which coordinating functional group (DG) is a part of (hetero)arene system, and (ii) temporary or removable DG-assisted C-H activation, in which there is a stepwise installation and removable of a traceless directing group (TDG) for aiding functionalization. Alternatively, a one-step process involving *in-situ* installation of a transient directing group, subsequent functionalization, followed by dissociation of DG can be adopted (Figure 1A.2.2). In these strategies, the in-built DGs or externally installed DGs should be stable and does not interfere in the reaction. However, it is quite likely that the certain modifiable directing groups (MDGs) undergoes extra functionalization/cyclization step after the targeted C-H functionalization, leading to the formation of unprecedented annulated products through a series of cascade sub-steps. In the above processes, removable directing groups (RDGs) are usually removed from the target compound during a final synthetic step, while non-removable directing groups (NRDGs) are maintained in the final compound, thus restricting their versatility.

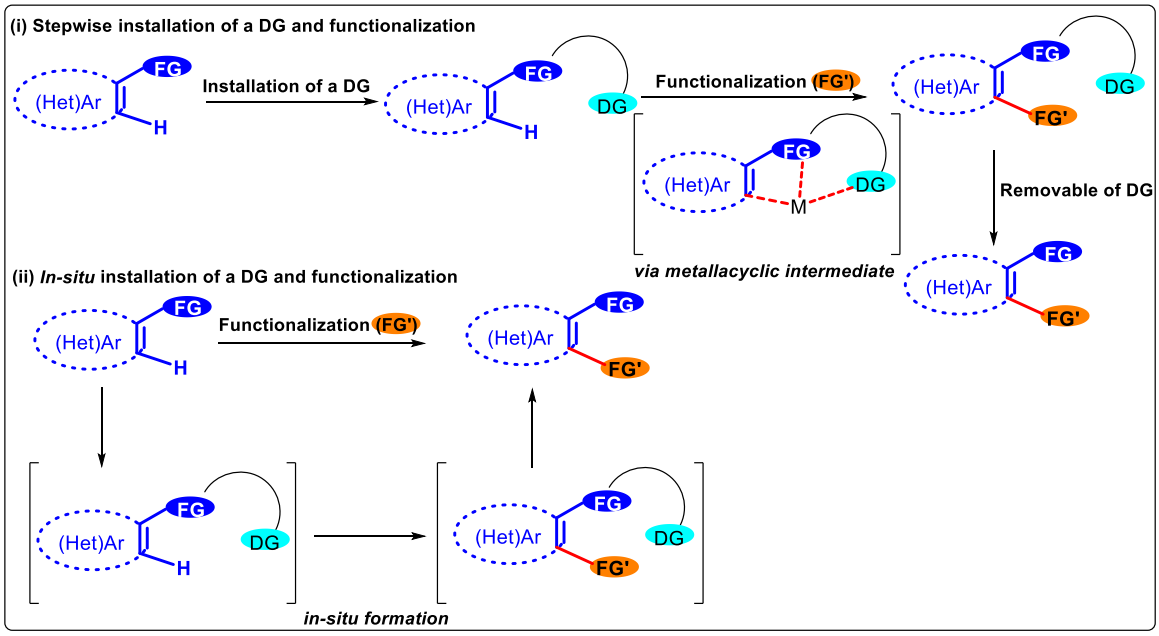

Figure 1A.2.2 Classes of DG-mediated chelation-assisted C-H functionalization

In this realm, a variety of strong and weak directing groups have been identified based on their structure (*e.g.* denticity, coordinating atoms and moieties) to achieve site-selective C-H functionalization in varying yields at an inert neighboring C-H bond site *via* chelation-assisted C-H bond activation strategy under transition-metal catalysis.[43] A few examples include, functionalities, such as amine, amide, imine, carboxylic acid, ester, ketone, nitrile, oxime, hydrazine, urea, carbamate, sulfoximine, phosphine oxide, cyanide *etc.*, and *N*-heterocycles, such as pyridine, pyrimidine, triazole, pyrazole, oxadiazole, benzothiazole, 8-aminoquinoline, picolinamide *etc.* (Figure 1A.2.3). Thermodynamically favored five- and six-membered metallocyclic intermediates with these directing groups, along with the kinetic lability of 3dn metal ions provides energetically advantageous reaction pathways. However, the thermodynamic stability of the isolable metallacyclic complexes formed with strongly coordinating directing groups refrains the C-H functionalization step due to lack of reactivity. In sharp contrast, a number of ligands have been discovered that primarily drives the C-H activation step to match the weakly coordinating directing groups. A few selective examples on varied directing group-mediated transition metal-catalyzed (Pd, Rh, Ru, Ir)[44-48] C-H functionalization strategies are shown in Figure 1A.2.4.

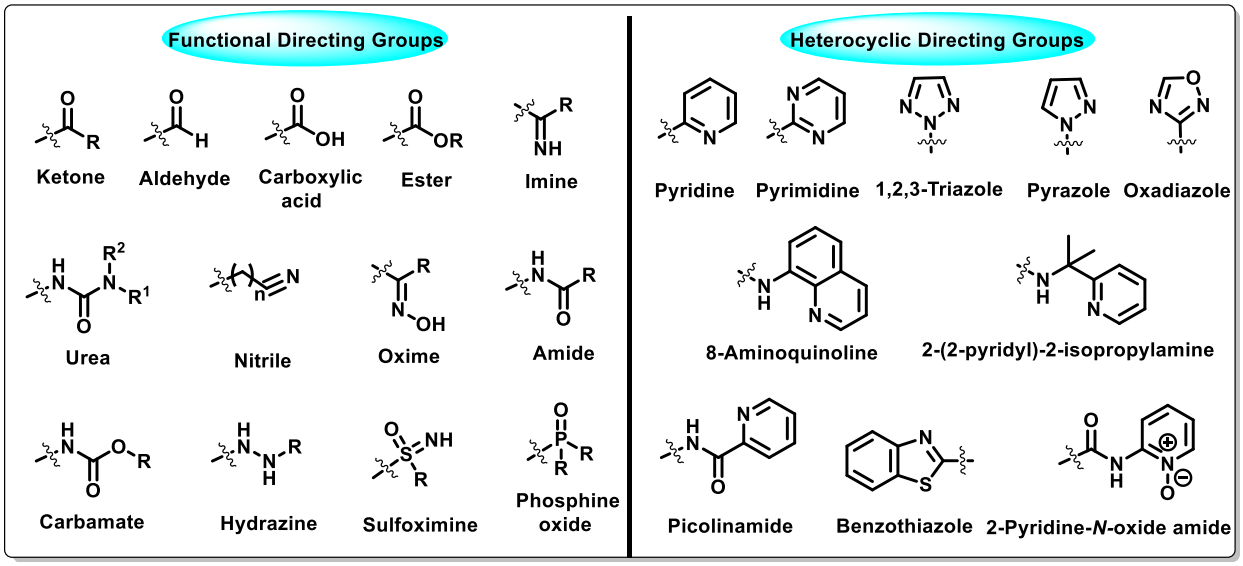

Figure 1A.2.3 Representative examples of directing groups explored in C-H activation strategy

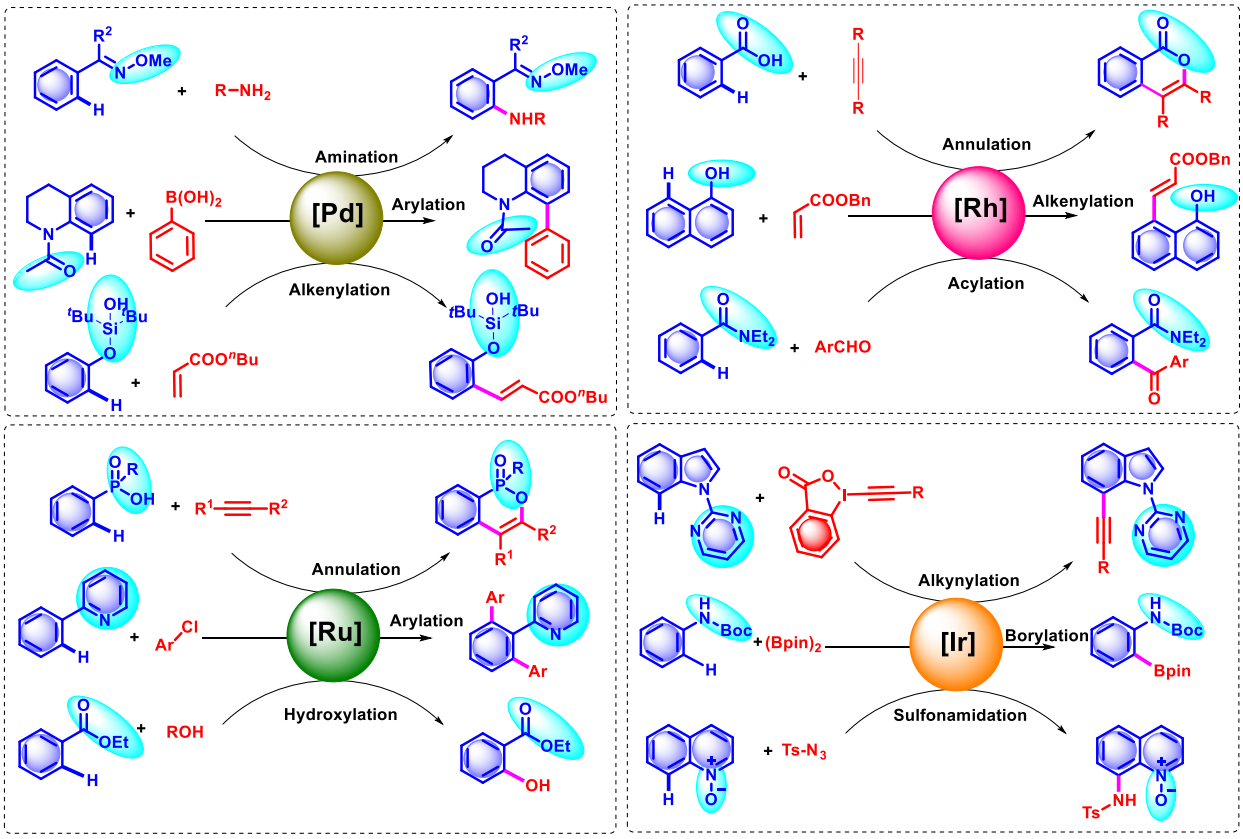

Figure 1A.2.4. Selective examples of directing group-mediated C-H bond functionalization *via* Pd, Rh, Ru and Ir-catalysis

1A.3 Amide Functionality as a Directing Group

Amide group is a ubiquitous functionality found in several natural products, drug candidates, agrochemicals, polymers, dyes and synthetic intermediates.[49-52] The planarity of amide bond and high degree of nitrogen lone pair delocalization render it stability and inertness.[43] In addition, the presence of nitrogen and oxygen atoms imparts it ligand ability to coordinate with the transition metals for generating thermodynamically stable cyclometallated intermediates. In particular, *N*-substituted secondary and tertiary amides (CONH-alkyl/aryl, CONH-alkoxyl) have been extensively employed as the strong directing groups for site-selective functionalization of the (hetero)arenes *via* proximal C-H bond activation in a regio- and chemoselective manner. Furthermore, due to ability of the amidic N-H bond to be entangled in C-N bond formation with appropriate electrophilic coupling partners, subsequent coupling of amidic directing group with the newly generated functional groups have been documented under metal-catalyzed conditions, generating annulated azaheterocycles in an atom-economical fashion. A few functionalized or annulated products prepared by the established methodologies, including alkylation, arylation, alkenylation, alkynylation, allylation, intramolecular cyclization *via* amide-directed chelation-assisted C-H activation approach under Rh, Ru, Ir, Pd, Co, Mn catalysis[53-56] are given in Figure 1A.3.1.

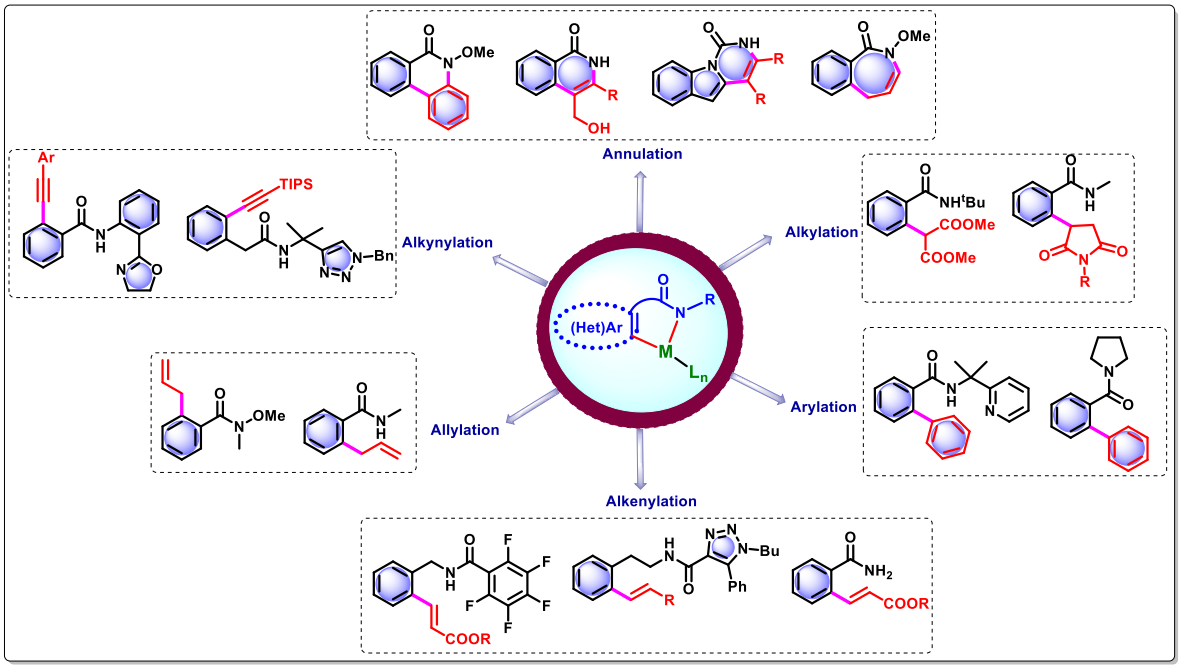

Figure 1A.3.1 Selective examples of functionalized or annulated products prepared by amide-directed C-H activation approach

Most importantly, the contributions by transition metals, such as Rh, Ru, Ir, Pd in the area of DG-assisted C-H activation approaches are gigantic and worth discussing.

1A.4 Palladium Catalysis

Palladium, discovered by William Hyde Wollaston in 1803, is one of the late-transition metal having atomic number 46 and electronic configuration [Kr] $4d^{10}$. Among the myriad of important transition metal-catalyzed synthetic organic transformations, palladium-catalyzed Heck coupling, and other cross-coupling reactions, such as Kumada, Stille, Negishi, Suzuki–Miyaura, Hiyama, Tsuji–Trost allylation, and Buchwald–Hartwig amination using organohalides and other surrogates are particularly valuable tools in synthetic organic chemistry, resulting in the construction of C-C, C-N and C-O bonds.[57-58] Organic Chemists have extensively tuned the reactivity of different palladium catalysts by varying the ligand, base, solvent, temperature and additives to achieve unprecedented targeted molecules with the generation of minimum waste by-products, hence palladium-catalyzed reactions are generally considered as eco-friendly chemical processes, exhibiting high functional group tolerance and excellent stereo- and regioselectivity[59-60] (Figure 1A.4.1).

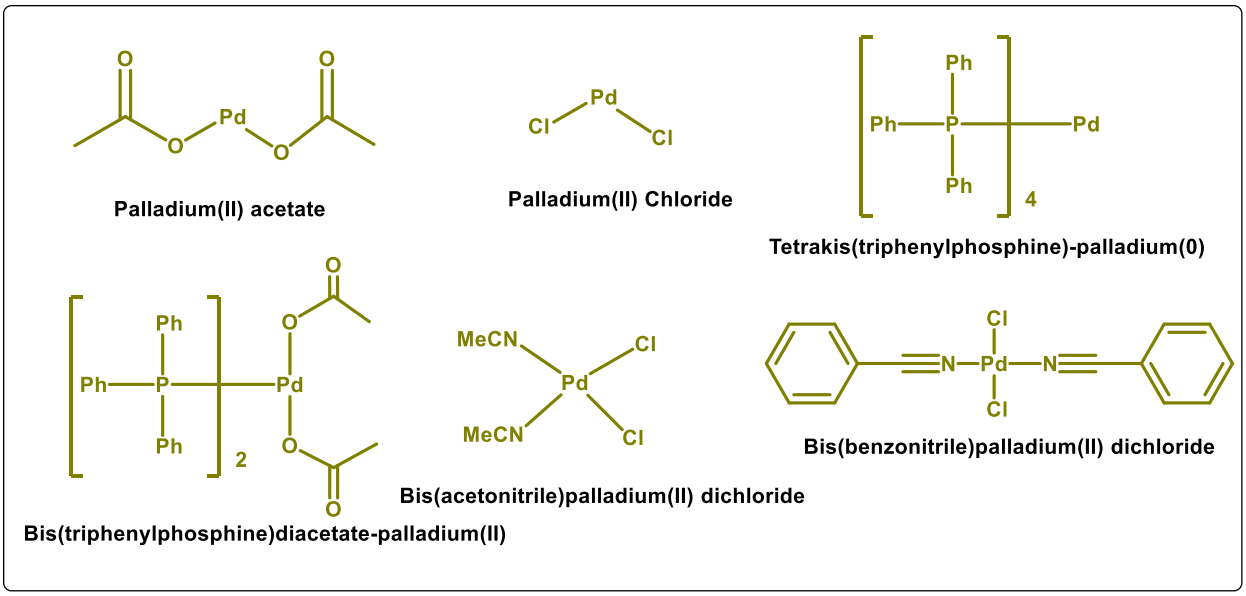

Figure 1A.4.1 Selective examples of palladium complexes used in organic synthesis

1A.5 Ruthenium Catalysis

A rare transition metal ruthenium (Ru) was first discovered and isolated by Karl Earns in 1844 from the residue of a sample of platinum ore obtained from the Ural mountains. Ruthenium metal is the 74th most abundant metal on the earth with an atomic number 44, and its electronic

configuration is [Kr]$4d^7 5s^1$. Ruthenium complexes have been employed as outstanding and attractive catalysts due to their high reactivity under mild conditions, good selectivity, ease of conversion within variable oxidation states (Ru^0/Ru^{II}, Ru^{II}/Ru^{IV}, and $Ru^{II}/^0$) in catalytic cycles, compatibility with varied oxidants, stability under air or moisture and economically profitable in comparison to Pd, Pt, Ir and Rh catalysts. As a result, a variety of ruthenium complexes have been extensively used in several directing group-mediated functionalization methodologies, such as olefination,[61] annulation,[62] oxygenation,[63] nitrogenation,[63] halogenation,[64] amidation,[65] arylation,[66] carboxylation,[67] silylation[68] and sulfonation[69] *etc.*, in recent years (Figure 1A.5.1).

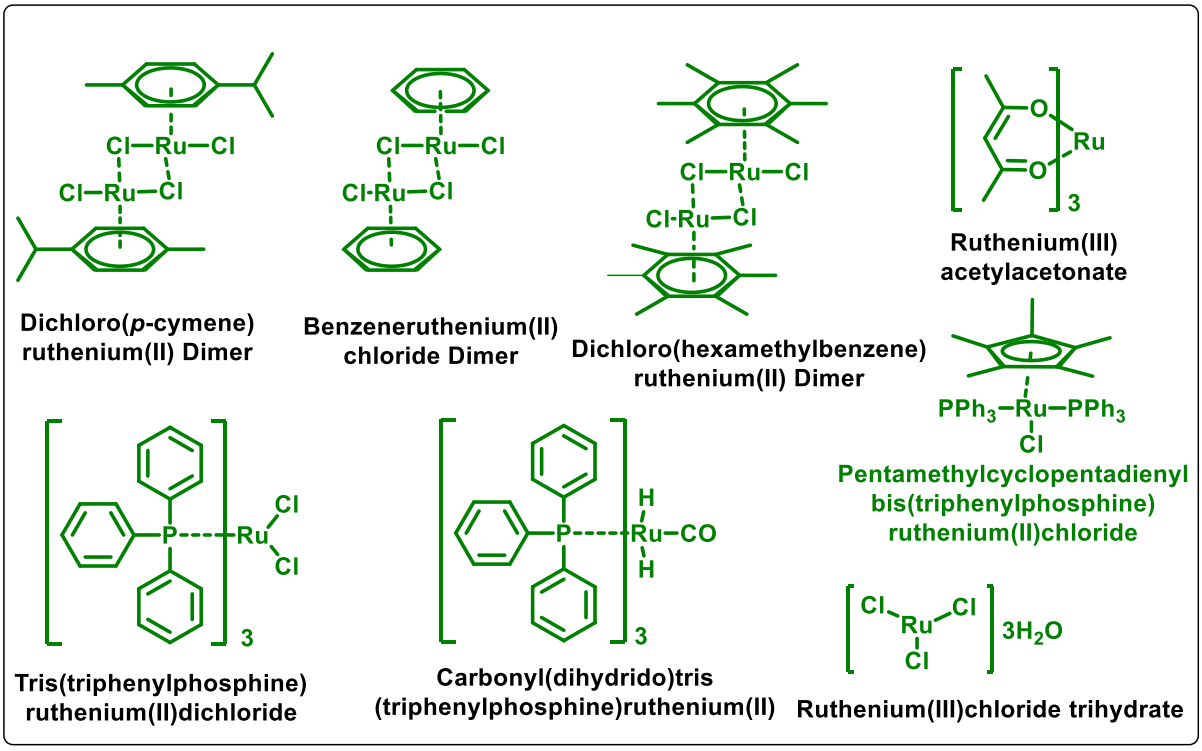

Figure 1A.5.1 Selective examples of ruthenium complexes used in C-H activation approaches

1A.6 Rhodium Catalysis

Rhodium was discovered by William Wollaston in 1803from the platinum or nickel ores, having atomic number 45 and electronic configuration [Kr]$4d^8 5s^1$. In recent years, considerable advancements in rhodium-catalyzed C-H functionalization has been attempted to access C-C, C-N, C-O and C-X bond formations in a convenient manner.[70-71] In most of the coupling reactions, rhodium-catalysis shows good site selectivity and reactivity to activate the inert C-H bonds to generate reactive organometallic intermediates. Rh^{III}/Rh^{I} oxidation state change has been prominently monitored in catalytic cycles in most C-H activation methodologies, including

Monsanto acetic acid process.[72] Wilkinson's catalyst is one of the well-known rhodium containing catalyst used for hydrogenation of alkenes. Despite the generally high coast of rhodium complexes, these are highly desirable in C-H functionalization transformations due to ecofriendly nature, easy to handle as it is much stable under air or moisture, good functional group tolerance and high efficiency even with very low catalyst loading. Hence, several Rh-catalyzed directing group-mediated C-H functionalization reactions, such as allylation,[73] alkylation,[74] arylation,[75] halogenation,[76] hydroarylation,[77] alkenylation,[78] amidation,[79] annulation[80] *etc.* have been documented in high yields by using a variety of rhodium catalysts (Figure 1A.6.1).

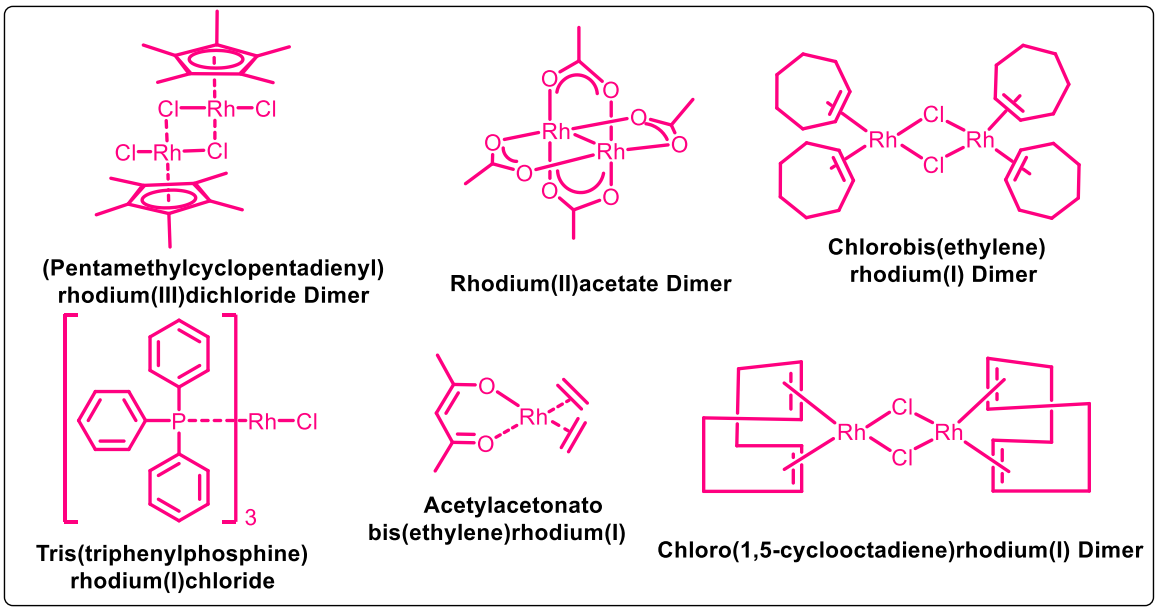

Figure 1A.6.1 Selective examples of rhodium complexes used in C-H activation approaches

1A.7 Iridium Catalysis

Iridium is a second-densest naturally-occurring metal, and most corrosion resistant even at very high temperatures. It was discovered in 1803 by Smithson Tennant from insoluble impurities in natural platinum. Iridium is having an atomic number 77 and electronic configuration $[Xe]4f^{14}5d^{7}6s^{2}$. Though, iridium complexes are found to be effective for the explored methodologies under mild reaction conditions, however, comparatively lesser research has been documented by using iridium complexes employing C-H activation notion. Some of the iridium complexes used in alkylation,[81] alkenylation,[82] borylation,[83] alkane metathesis,[84] hydroarylation[85] methodologies are listed below (Figure 1A.7.1).

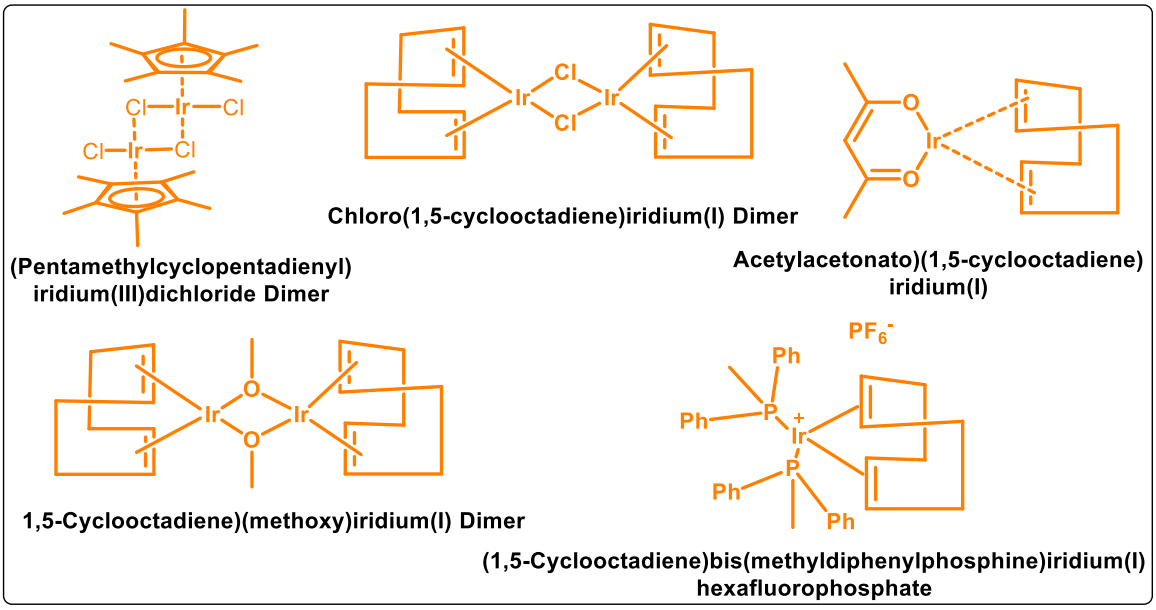

Figure 1A.7.1 Selective examples of iridium complexes used in C-H activation approaches

1A.8 Importance of Indazole

Benzodiazines, such as indazole (**I**), phthalazine (**II**) and cinnoline (**III**) derivatives are well reported to possess versatile pharmacological profiles, including anticonvulsant, antitumor, antihypertensive, antidiabetic, anti-inflammatory, anticancer behavior[86-89] (Figure 1A.8.1).

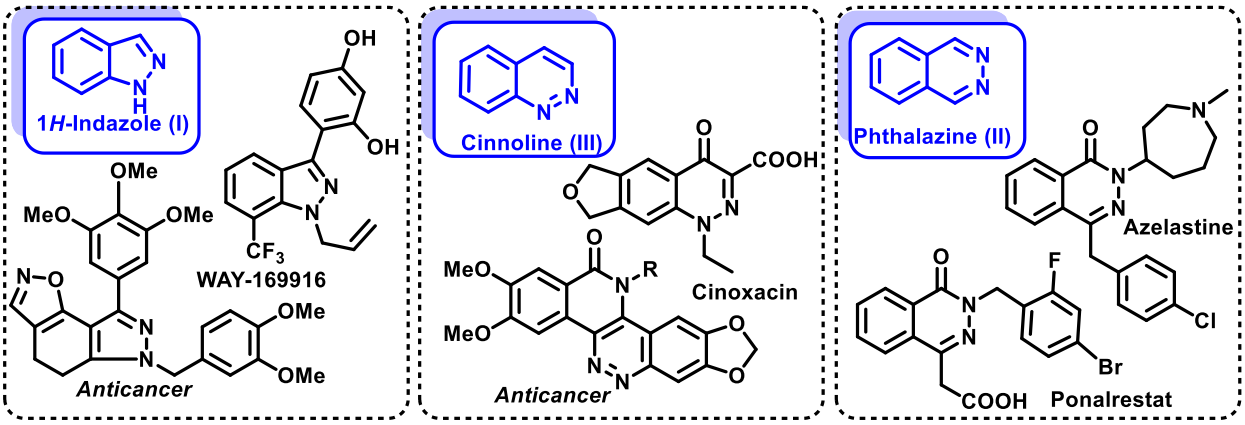

Figure 1A.8.1 Selective examples of indazole (**I**), phthalazine (**II**), and cinnoline (**III**) based biologically active molecules

Accordingly, functionalized and fused-indazoles have been perceived as emerging and interesting targets because of their varied medicinal and material chemistry related applications.[87-90] In particular, indazolone moiety constitute an integral part of several fused and functionalized derivatives with interesting biological activities, such as antibacterial,[91] anti-inflammatory,

antitumor,[92] antiasthmatic,[93] antihyperlipidemic,[94] antidiabetic,[95] antipsychotic,[96] antichagasic[97] *etc* (Figure 1A.8.2).

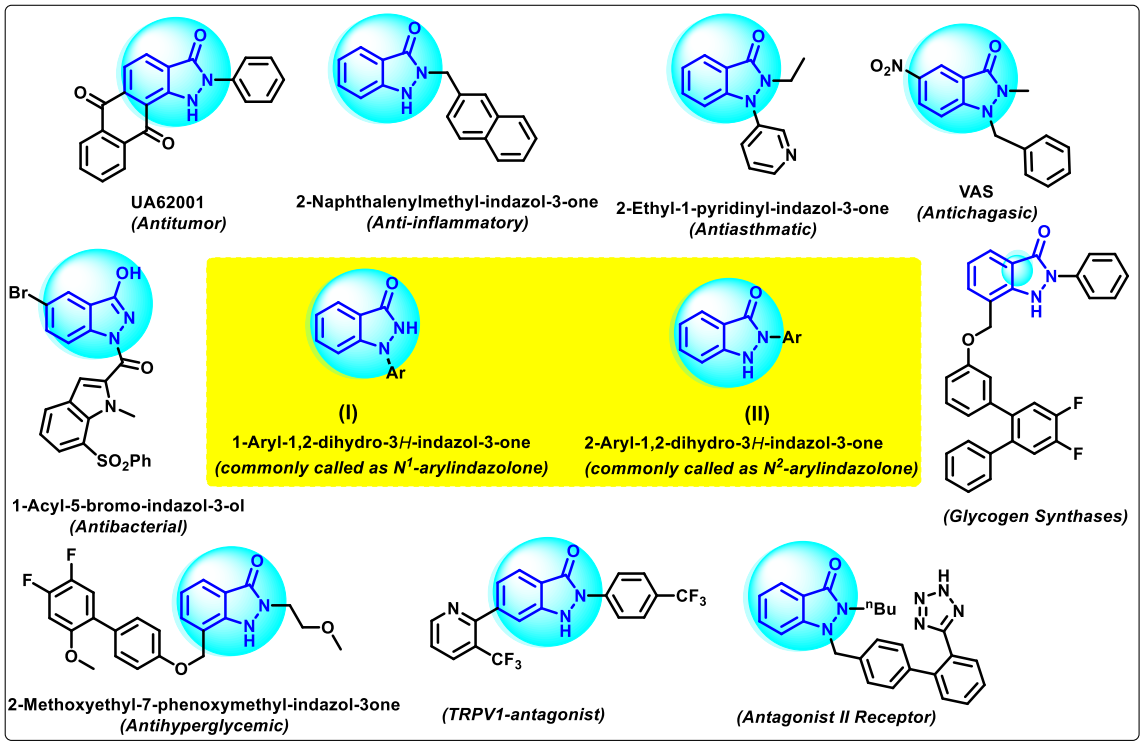

Figure 1A.8.2 Selective examples of biologically relevant indazolones

Despite these promising applications, it has been observed that previous synthetic wisdom on functionalized and fused-indazolones unanimously focused on application of conventional acid/base mediated strategies or multi-component reactions. During the initiation of our research work on indazolones derivatives, the functionalization of 1-aryl or 2-aryl-1,2-dihydro-3*H*-indazol-3-ones (**I**, and **II**) was only explored to a limited extent. Anticipating the inbuilt cyclic amide/amine-directing group capability of 1-aryl or 2-aryl-1,2-dihydro-3*H*-indazol-3-ones, we undertook the task of performing chelation-assisted transition metal-catalyzed transformation of these *N*-arylindazolones to different fused-diazaheterocycles by C-C and C-N bond formations using a variety of coupling partners at the expense of previously described C-H activation notion.

1A.9 References

1. Heravi, M. M.; Zadsirjan, V.; Saedi, P.; Momeni, T. *RSC Advances* **2018**, *8*, 40061-40163.
2. Marco, A. B. F.; Luiz, C. D.; Ives, A. L.; Ellen, C. P.; Emilio, C. L. *Current Organic Synthesis* **2015**, *12*, 547-564.
3. Knölker, H.-J.; Reddy, K. R. *Chemical Reviews* **2002**, *102*, 4303-4428.

4. Isobe, H.; Yamanaka, S.; Yamaguchi, K.; *International Journal of Quantum Chemistry* **2003**, *95*, 532-545.
5. Fleming, I. *Pericyclic reactions*. Oxford University Press, USA: **2015**.
6. Yu, D.-G.; Li, B.-J.; Shi, Z.-J. *Accounts of Chemical Research* **2010**, *43*, 1486-1495.
7. Corbet, J.-P.; Mignani, G. *Chemical Reviews* **2006**, *106*, 2651-2710.
8. Suzuki, A. *Journal of Organometallic Chemistry* **1999**, *576*, 147-168.
9. Stanforth, S. P. *Tetrahedron* **1998**, *54*, 263-303.
10. Cardenas, D. J. *Angewandte Chemie International Edition* **2003**, *42*, 384-387.
11. Kambe, N.; Iwasaki, T.; Terao, J. *Chemical Society Reviews* **2011**, *40*, 4937-4947.
12. Johansson Seechurn, C. C.; Kitching, M. O.; Colacot, T. J.; Snieckus, V. *Angewandte Chemie International Edition* **2012**, *51*, 5062-5085.
13. Huang, C.-Y.; Kang, H.; Li, J.; Li, C.-J. *The Journal of Organic Chemistry* **2019**, *84*, 12705-12721.
14. Miura, M.; Nomura, M. *Cross-coupling Reactions* **2002**, 211-241.
15. Daugulis, O.; Do, H.-Q.; Shabashov, D. *Accounts of Chemical Research* **2009**, *42*, 1074-1086.
16. Bellina, F.; Rossi, R. *Chemical Reviews* **2010**, *110*, 1082-1146.
17. Glaser, C. *Berichte der Deutschen Chemischen Gesellschaft* **1869**, *2*, 422-424.
18. Glaser, C.; *Justus Liebigs Annalen der Chemie* **1870**, *154*, 137-171.
19. Iataaki, H.; Yoshimoto, H. *The Journal of Organic Chemistry* **1973**, *38*, 76-79.
20. Sakakura, T.; Sodeyama, T.; Tokunaga, Y.; Tanaka, M. *Chemistry Letters* **1987**, *16*, 2211-2214.
21. Nakada, M.; Aimin, Y.; Kawakami, S.; Iwaki, S.; Yamaguchi, T. *Bulletin of the Chemical Society of Japan* **1989**, *62*, 3392-3393.
22. Tian, T.; Li, Z.; Li, C.-J. *Green Chemistry* **2021**, *23*, 6789-6862.
23. Das, R.; Kumar, G. S.; Kapur, M. *European Journal of Organic Chemistry* **2017**, *2017*, 5439-5459.
24. Carvalho, R. L.; Dias, G. G.; Pereira, C. L.; Ghosh, P.; Maiti, D.; Silva Júnior, E. N. d. *Journal of the Brazilian Chemical Society* **2021**, *32*, 917-952.
25. Gallego, D.; Baquero, E. A. *Open Chemistry* **2018**, *16*, 1001-1058.
26. Inoue, M.; Tsurugi, H.; Mashima, K. *Coordination Chemistry Reviews* **2022**, *473*, 214810.
27. Hashiguchi, B. G.; Bischof, S. M.; Konnick, M. M.; Periana, R. A. *Accounts of Chemical Research* **2012**, *45*, 885-898.

28. Kuhl, N.; Hopkinson, M. N.; Wencel-Delord, J.; Glorius, F. *Angewandte Chemie International Edition* **2012**, *51*, 10236-10254.

29. Giri, R.; Thapa, S.; Kafle, A. *Advanced Synthesis & Catalysis* **2014**, *356*, 1395-1411.

30. Song, G.; Li, X. *Accounts of Chemical Research* **2015**, *48*, 1007-1020.

31. Liu, B.; Yang, L.; Li, P.; Wang, F.; Li, X. *Organic Chemistry Frontiers* **2021**, *8*, 1085-1101.

32. Gramage-Doria, R.; Bruneau, C. *Coordination Chemistry Reviews* **2021**, *428*, 213602.

33. Jadhav, A. P.; Ray, D.; Rao, V. B.; Singh, R. P. *European Journal of Organic Chemistry* **2016**, *2016*, 2369-2382.

34. Pototschnig, G.; Maulide, N.; Schnürch, M. *Chemistry–A European Journal* **2017**, *23*, 9206-9232.

35. Cano, R.; Mackey, K.; McGlacken, G. P. *Catalysis Science & Technology* **2018**, *8*, 1251-1266.

36. Urbina, K.; Tresp, D.; Sipps, K.; Szostak, M. *Advanced Synthesis & Catalysis* **2021**, *363*, 2723-2739.

37. Naveen, T. *Tetrahedron* **2021**, *84*, 132025.

38. Sandtorv, A. H. *Advanced Synthesis & Catalysis* **2015**, *357*, 2403-2435.

39. Rani, G.; Luxami, V.; Paul, K. *Chemical Communications* **2020**, *56*, 12479-12521.

40. Wang, K.; Hu, F.; Zhang, Y.; Wang, J. *Science China Chemistry* **2015**, *58*, 1252-1265.

41. Rej, S.; Ano, Y.; Chatani, N. *Chemical Reviews* **2020**, *120*, 1788-1887.

42. Ackermann, L.; Vicente, R.; Kapdi, A. R. *Angewandte Chemie International Edition* **2009**, *48*, 9792-9826.

43. Chen, Z.; Wang, B.; Zhang, J.; Yu, W.; Liu, Z.; Zhang, Y. *Organic Chemistry Frontiers* **2015**, *2*, 1107-1295.

44. Yu, D.-G.; Li, B.-J.; Shi, Z.-J. *Tetrahedron* **2012**, *68*, 5130-5136.

45. Arockiam, P. B.; Bruneau, C.; Dixneuf, P. H. *Chemical Reviews* **2012**, *112*, 5879-5918.

46. Tsang, Y. L.; Choy, P. Y.; Leung, M. P.; He, X.; Kwong, F. Y. *Organic Chemistry Frontiers* **2022**.

47. Liao, Y.; Liu, F.; Shi, Z.-j. *Chemical Communications* **2021**, *57*, 8059-8062.

48. Yoshino, T.; Satake, S.; Matsunaga, S. *Chemistry–A European Journal* **2020**, *26*, 7346-7357.

49. Kumari, S.; Carmona, A. V.; Tiwari, A. K.; Trippier, P. C. *Journal of Medicinal Chemistry* **2020**, *63*, 12290-12358.

50. Yan, K.; Wang, J.; Wang, Z.; Yuan, L.; *Chemical Communications* **2023,** *advance article*.

51. Guo, X.; Facchetti, A.; Marks, T. J. *Chemical Reviews* **2014**, *114*, 8943-9021.

52. Ishi-i, T.; Shinkai, S. *Supermolecular Dye Chemistry* **2005**, 119-160.

53. Park, J.; Son, J. *European Journal of Organic Chemistry* **2022**, *2022*, e202200465.

54. Zhu, C.; Wang, R.; Falck, J. R. *Chemistry–An Asian Journal* **2012**, *7*, 1502-1514.

55. Wang, C.; Chen, F.; Qian, P.; Cheng, J. *Organic & Biomolecular Chemistry* **2021**, *19*, 1705-1721.

56. Yuan, Y.-C.; Goujon, M.; Bruneau, C.; Roisnel, T.; Gramage-Doria, R. *The Journal of Organic Chemistry* **2019**, *84*, 16183-16191.

57. Wu, X. F.; Anbarasan, P.; Neumann, H.; Beller, M. *Angewandte Chemie International Edition* **2010**, *49*, 9047-9050.

58. Sain, S.; Jain, S.; Srivastava, M.; Vishwakarma, R.; Dwivedi, J. *Current Organic Synthesis* **2019**, *16*, 1105-1142.

59. Girard, S. A.; Knauber, T.; Li, C. J. *Angewandte Chemie International Edition* **2014**, *53*, 74-100.

60. Wu, Y.; Wang, J.; Mao, F.; Kwong, F. Y. *Chemistry–An Asian Journal* **2014**, *9*, 26-47.

61. Li, B.; Ma, J.; Wang, N.; Feng, H.; Xu, S.; Wang, B. *Organic Letters* **2012**, *14*, 736-739.

62. Song, L.; Zhang, X.; Tang, X.; Van Meervelt, L.; Van der Eycken, J.; Harvey, J. N.; Van der Eycken, E. V. *Chemical Science* **2020**, *11*, 11562-11569.

63. Thirunavukkarasu, V. S.; Kozhushkov, S. I.; Ackermann, L. *Chemical Communications* **2014**, *50*, 29-39.

64. Wang, L.; Ackermann, L. *Chemical Communications* **2014**, *50*, 1083-1085.

65. Pan, C.; Abdukader, A.; Han, J.; Cheng, Y.; Zhu, C. *Chemistry–A European Journal* **2014**, *20*, 3606-3609.

66. Ackermann, L.; Vicente, R. *CH Activation* **2009**, 211-229.

67. Barlow, H. L.; Teskey, C. J.; Greaney, M. F. *Organic Letters* **2017**, *19*, 6662-6665.

68. Kakiuchi, F.; Matsumoto, M.; Tsuchiya, K.; Igi, K.; Hayamizu, T.; Chatani, N.; Murai, S. *Journal of Organometallic Chemistry* **2003**, *686*, 134-144.

69. Saidi, O.; Marafie, J.; Ledger, A. E.; Liu, P. M.; Mahon, M. F.; Kociok-Köhn, G.; Whittlesey, M. K.; Frost, C. G. *Journal of the American Chemical Society* **2011**, *133*, 19298-19301.

70. Sasmal, S.; Prakash, G.; Dutta, U.; Laskar, R.; Lahiri, G. K.; Maiti, D. *Chemical Science* **2022**, *13*, 5616-5621.

71. Li, C.; Huang, H.; Xiao, F.; Zhao, B.; Deng, G.-J. *Organic Chemistry Frontiers* **2022**, *9*, 822-830.

72. Ji, W.; Zhang, S.; Dong, F.; Feng, N.; Lan, L.; Li, Y.; Ma, Y.; Sun, Y. *Arabian Journal for Science and Engineering* **2022**, 1-10.

73. Ma, C.; Li, C.; Bai, J.; Xiao, J.; Zhai, Y.; Guo, Y.; Ma, S. *ACS Catalysis* **2022**, *12*, 10141-10146.

74. Ramachandran, K.; Anbarasan, P. *Organic Letters* **2022**, *24*, 6745-6749.

75. Wang, D.; Li, M.; Shuang, C.; Liang, Y.; Zhao, Y.; Wang, M.; Shi, Z. *Nature Communications* **2022**, *13*, 1-10.

76. Dhiman, A. K.; Sharma, U. *Handbook of CH-Functionalization* **2022**, 1-25.

77. Pagès, L.; Abed Ali Abdine, R.; Monnier, F.; Taillefer, M. *European Journal of Organic Chemistry* **2022**, *2022*, e202200724.

78. Alisha, M.; Philip, R. M.; Anilkumar, G. *Journal of Organometallic Chemistry* **2022**, *959*, 122207.

79. Ban, T.; Vu, H.-M.; Zhang, J.; Yong, J.-Y.; Liu, Q.; Li, X.-Q. *The Journal of Organic Chemistry* **2022**, *87*, 5543-5555.

80. Meng, H.; Xu, H.; Zhou, Z.; Tang, Z.; Li, Y.; Zhou, Y.; Yi, W.; Wu, X. *Green Chemistry* **2022**, *24*, 7012-7021.

81. Yamauchi, D.; Yamakawa, K.; Nishimura, T. *Organic Letters* **2022**, *24*, 6828-6833.

82. Zhou, B.; Deng, S.; Xu, Y.; Qi, X.; Dong, G. *Journal of the American Chemical Society* **2022**, *144*, 23230-23238.

83. Gillaizeau, I.; Dondasse, I.; Nicolas, C.; Mimoun, L.; Sukach, V.; Meudal, H. *European Journal of Organic Chemistry* **2022**, *2022*, e202101302.

84. de Souza, W. C.; Correia, J. T. M.; Matos, P. M.; Kisukuri, C. M.; Carneiro, P. S.; Paixão, M. W. *European Journal of Organic Chemistry* **2022**, *2022*, e202101376.

85. Cooper, P.; Dalling, A. G.; Farrar, E. H.; Aldhous, T. P.; Grélaud, S.; Lester, E.; Feron, L. J.; Kemmitt, P. D.; Grayson, M. N.; Bower, J. F. *Chemical Science* **2022**, *13*, 11183-11189.

86. Desai, N.; Jadeja, D.; Mehta, H.; Khasiya, A.; Shah, K.; Pandit, U. *Springer* **2022**, *2022*, 143-189.

87. Nie, S. M.; Zhang, X.; Wang, Z. X.; Su, G. F.; Pan, C. X.; Mo, D. L. *Advanced Synthesis & Catalysis* **2022**.

88. Mahmoud, E. M.; Shongwe, M.; Moghadam, E. S.; Moghimi-Rad, P.; Stoll, R.; Abdel-Jalil, R. *Journal of Biosciences C* **2022**.

89. Türkeş, C.; Arslan, M.; Demir, Y.; Çoçaj, L.; Nixha, A. R.; Beydemir, Ş. *Journal of Molecular Recognition* **2022**, *35*, e2991.

90. Uppulapu, S. K.; Alam, M.; Kumar, S.; Banerjee, S. K. *Current Topics in Medicinal Chemistry* **2022**.

91. Dawood, N. H.; Ali, N. H. *Journal of Pharmaceutical Negative Results* **2022**, 3178-3190.

92. Bedi, P.; Alanazi, A. K.; Bose, R.; Pramanik, T. Biointerface Research in Applied Chemistry **2022**, *13*, 2023.

93. Zheng, Y.-C.; Shu, B.; Zeng, Y.-F.; Chen, S.-Y.; Song, J.-L.; Liu, Y.-Z.; Xiao, L.; Liu, X.-G.; Zhang, X.; Zhang, S.-S. *Organic Chemistry Frontiers* **2022**, *9*, 5185-5190.

94. Chen, S. Y.; Zheng, Y. C.; Liu, X. G.; Song, J. L.; Shu, B.; Zheng, T.; Xiao, L.; Zhang, S. S.; Cao, H. *Advanced Synthesis & Catalysis* **2022**, *364*, 3302-3309.

95. Xie, G.; Vlocskó, R. B.; Török, B. *Elsevier* **2022,** 201-279.

96. Kang, J. Y.; Kim, S.; Moon, J.; Chung, E.; Kim, J.; Kyung, S. Y.; Kim, H. S.; Mishra, N. K.; Kim, I. S. *ACS Omega* **2022**, *7*, 14712-14722.

97. Bhattacharjee, S.; Laru, S.; Hajra, A. *Organic & Biomolecular Chemistry* **2022**, *20*, 8893-8897.

Chapter 1B

Ruthenium-Catalyzed [4+1] Annulation of *N*-Arylindazolones with Acrylates to access Indazolo[1,2-*a*]indazolylidenes

1B.1 Introduction

As discussed in the background section that indazole is ubiquitous in nature,[1-3] and it constitutes an integral part of several natural-occurring and synthetic indazolo-fused derivatives. Nigellicine obtained from *N*. sativa (an annual flowering plant) is a naturally-occurring alkaloid that contains indazole nucleus.[4] In Southwest Asia, the seeds of *N*. sativa plant have been used for thousands of years as a spice, and for the treatment of several diseases.[5] Nigeglanine and Nigellidine are also naturally-occurring alkaloids that contains indazole nucleus (Figure 1B.1.1). In addition, some of the indazole derivatives have exhibited promising activity to cure Alzhemer's disease, Schizophrenia, auto imune & degenerative and cancer cell proliferative disorders.[6-17]

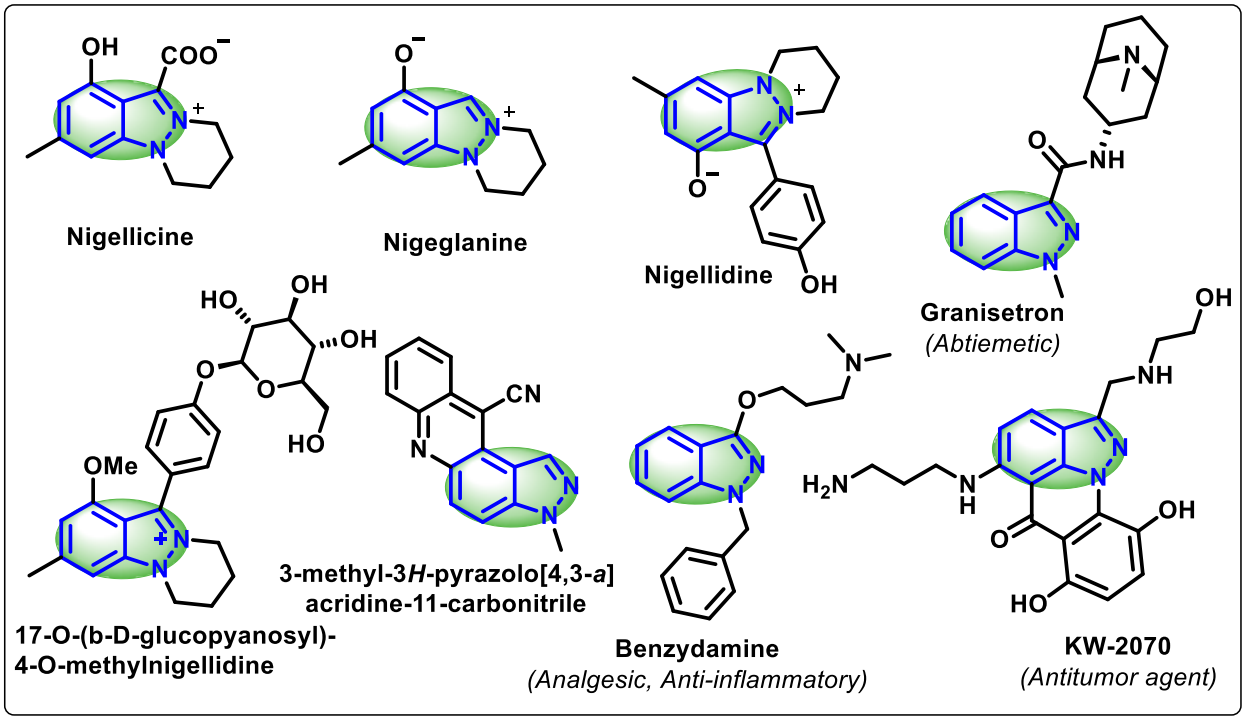

Figure 1B.1.1 Selective examples of naturally-occurring and synthetic fused-indazoles with diverse applications

Starting from different heterocyclic scaffolds, various transition metal-catalyzed strategies have been established for the construction of indazole nucleus over them in recent years. For example, *N*-aryl-2,3-dihydopthalazine-1,4-diones (**1**) are one of the reactive diazaheterocyclic motifs possessing cyclic amide directing group that have been reasonably explored for preparing numerous series of functionalized indazolo-fused phthalazine-diones using varied coupling partners. For example, in the year 2018, Ji's group disclosed a [4+1] oxidant-free annulation strategy for the coupling between *N*-aryl-2,3-dihydopthalazine-1,4-diones (**1**) and propargyl

alcohols (**2**) under Rh^{III}-catalysis, yielding functionalized indazolo-fused phthalazine-diones (**3**) in good yields (Scheme 1B.1.1a).[18] Yu and coworkers stabilized two independent strategies to achieve penta- and tetracyclic indazolo-fused phthalazine-diones (**5** & **7**) by using substituted cyclic diazo naphthalenones (**4**) and benzylic allenes (**6**) as coupling partners under Rh^{III}-catalyzed conditions in acetonitrile (Scheme 1B.1.1b-c).[19-20] The former strategy resulted a series of spirocyclic indazolo-fused phthalazine-diones with a quaternary carbon center.

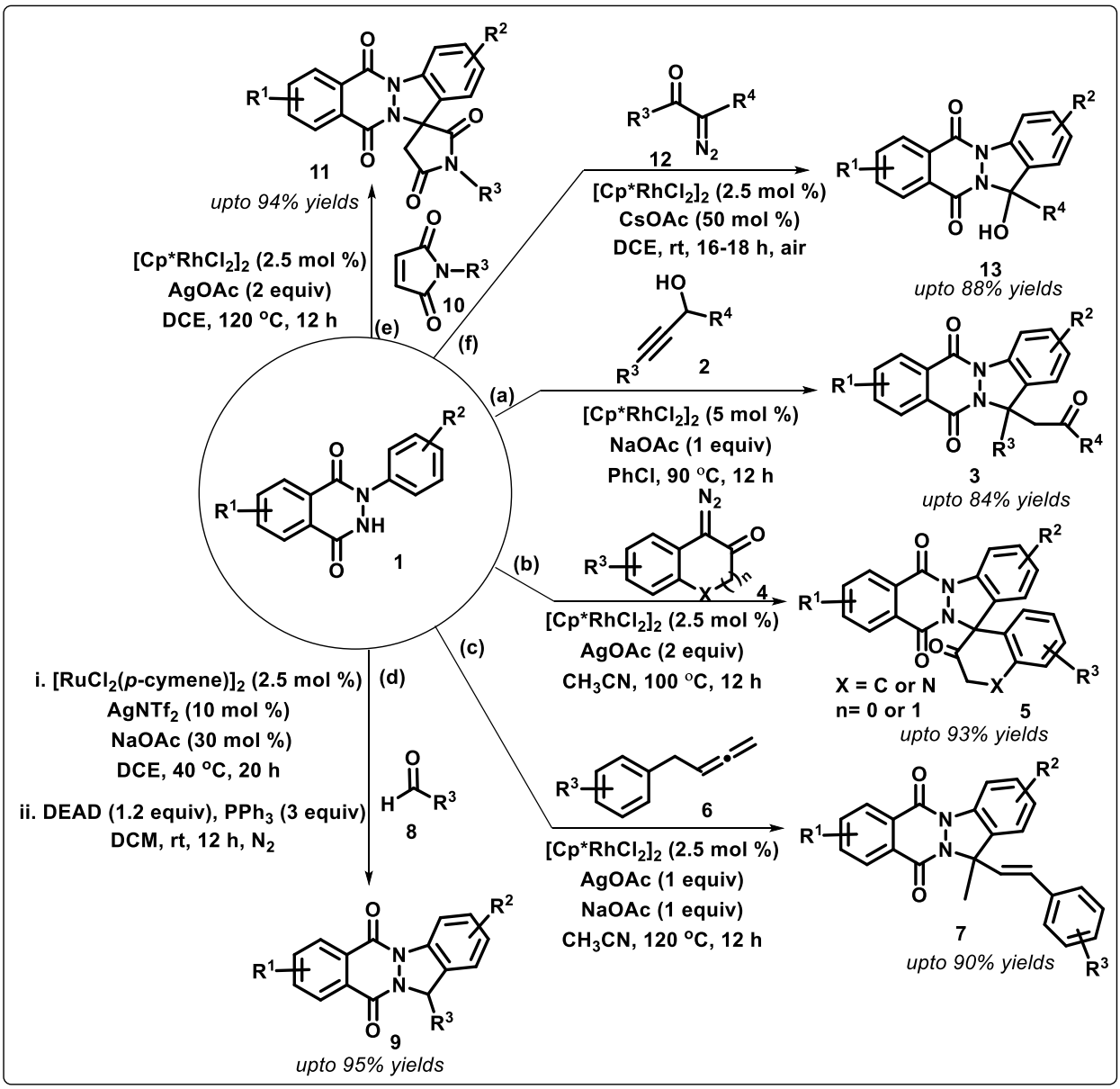

Scheme 1B.1.1 Rh/Ru-catalyzed strategies to access indazolo-fused phthalazinone-diones

In 2021, Kim *et al.* developed a two-step strategy to build an array of tetracyclic indazolo-fused phthalazine-diones (**9**) by coupling *N*-aryl-2,3-dihydopthalazine-1,4-diones (**1**) with aldehydes (**8**). In this pathway, *N*-aryl-2,3-dihydopthalazine-1,4-diones (**1**) underwent Csp^2-H activation with the aid of Ru^{II}-catalyst to furnish *o*-functionalized hydroxyalkylated phthalazine-diones, which further underwent intramolecular Mitsunobu cyclization to produce the target products (**9**) in good-to-excellent yields (Scheme 1B.1.1d).[21] Another interesting Rh^{III}-catalyzed protocol for preparing a series of indazolo-fused phthalazine-diones spirocyclized with pyrrolidine scaffold (**11**) was reported by our group by annulating *N*-aryl-2,3-dihydrophthalazine-1,4-diones (**1**) with maleimides (**10**) in dichloroethane (Scheme 1B.1.1e).[22] In another one-step approach by our group, a series of unprecedented hydroxy-dihydroindazolo-fused phthalazine-diones (**13**) were prepared by [4+1] annulation of *N*-aryl-2,3-dihydrophthalazine-1,4-diones (**1**) with *α*-diazo carbonyl compounds (**12**) in presence of CsOAc under Rh^{III}-catalysis (Scheme 1B.1.1f).[23]

In contrast, a few more indazolo-fused heterocycles have also been prepared by constructing other heterocyclic moieties on indazole derivatives *via* transition metal-catalyzed C-H activation notion. For example, pentacyclic fused- and spirocyclic indazoles (**15** & **16**) were prepared by Zhang and Fan, starting from 2-arylindazoles (**14**) and *N*-substituted maleimdies (**10**) under Rh^{III}-catalysis with the aid of different additives, such as ADA and DIPEA (Scheme 1B.1.2).[24]

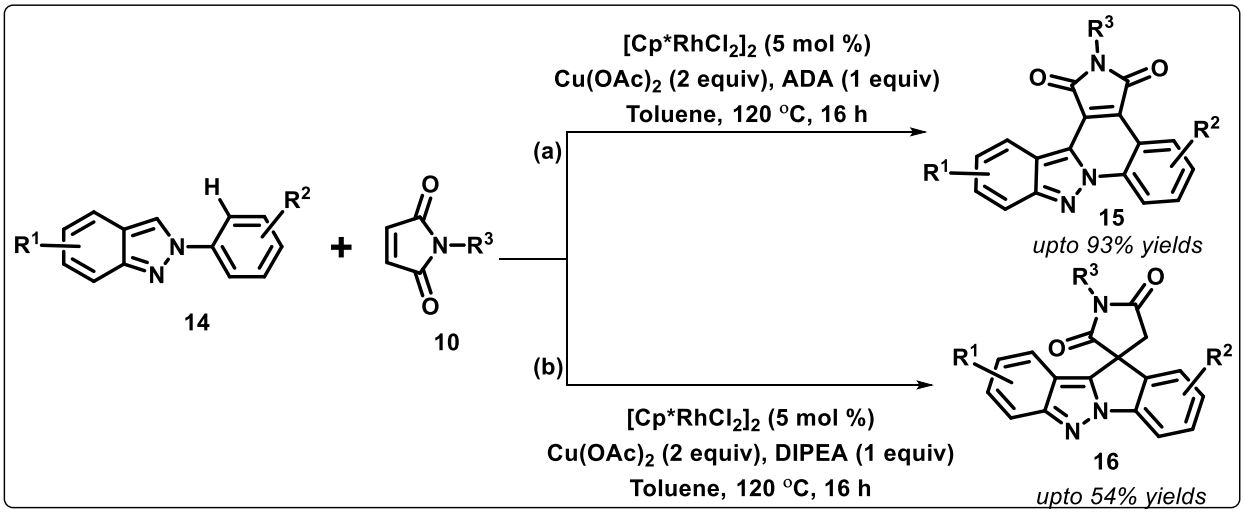

Scheme 1B.1.2 Rh-catalyzed additive-driven strategies to access fused- and spirocyclized indazoles

Recently, Kim *et al.* systematically investigated the coupling between *N*-aryl-2,3-dihydroindazol-3-ols (**17**) and maleimides (**10**) under Rh^{III}-catalyzed conditions and obtained

spirosuccinimide bearing *N*-arylindazolones (**18**) in major amounts, in addition to the isolation of *ortho*-succinimido *N*-arylindazolones (**19**) in minor amounts (Scheme 1B.1.3).[25]

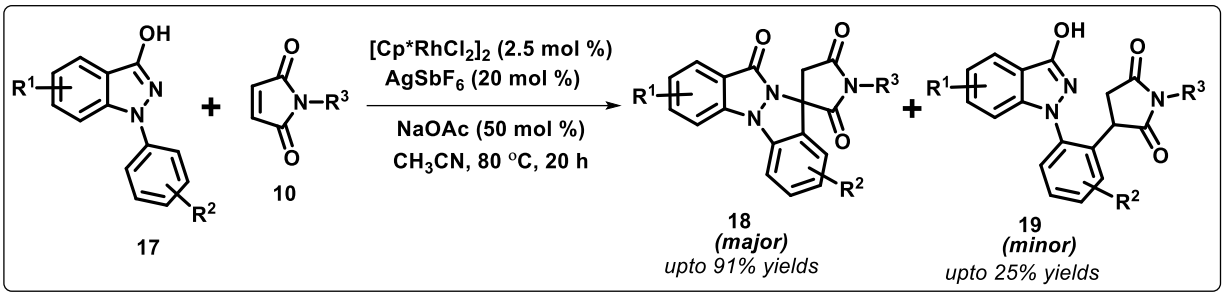

Scheme 1B.1.3 Rh-catalyzed synthesis of spirosuccinimides and *ortho*-succinimido *N*-arylindazolones

A part from the above explored coupling partners, *α, β*-unsaturated carbonyl compounds, such as acrylates (**20**) have also been explored as activated olefins in various catalytic, tandem or sequential cross-dehydrogenative couplings (CDC) to access functionalized/fused (hetero)arenes.[26-29] The insertion of acrylates into (hetero)aryl C-H bonds have primarily resulted in alkylation (hydroarylation) products,[30-32] however in a few cases, the alkenylated products have been found to be obtained by the oxidation of hydroarylated products in presence of an oxidant.[33-35] In this context, remarkable practical progress has been monitored to achieve C*sp*^{2}-H alkenylation on numerous (hetero)arenes, employing varied directing groups by using $Ru^{II}/AgSbF_6$ catalytic system. For example, o*rtho*-alkenylation of aryl esters[36] (**21**) and aryl carbamates[37] (**23**) were achieved efficiently under the Ru^{II}-catalysis by their cross-dehydrogenative couplings with acrylates (**20**) with the assistance of weekly-directing groups, esters and carbamates, respectively (Scheme 1B.1.4a-b). Similarly, Ru^{II}-catalyst allowed the cross-dehydrogenative alkenylation of *N*-aryl-1,2,3-triazoles (**25**) with acrylates (**20**) with the aid of strong directing triazole group[38] (Scheme 1B.1.4c). Jeganmohan's group disclosed Ru^{II}-catalyzed chelation-assisted C*sp*^{2}–H alkenylation of aromatic ketones[39] (**27**), aromatic amides, aromatic ketoximes, and anilides[40] (**29**) with olefins, including acrylates (**20**) to provide Heck-type products (**30**) in a high regio- and stereoselective manner (Scheme 1B.1.4d-e). Zhao and coworkers separately achieved *ortho*-alkenylation of *N*-alkylanilines[41] (**31**) and C-4 alkenylation of 3-acetylcoumarins[42] (**33**) with various acrylates (**20**), using pivaloyl and modifiable ketone directing groups, respectively (Scheme 1B.1.4f-g). Very recently, Kumar *et al*. disclosed a controlled strategy for *ortho*-alkenylation of electron-deficient benzamides (**35**) with activated

olefins (**20**) using a weakly coordinating primary amide group under Ru^{II}-catalysis, producing *ortho*-alkenylated benzamide derivatives (**36**) with high mono- and diastereoselectivity (Scheme 1B.1.4h).[43]

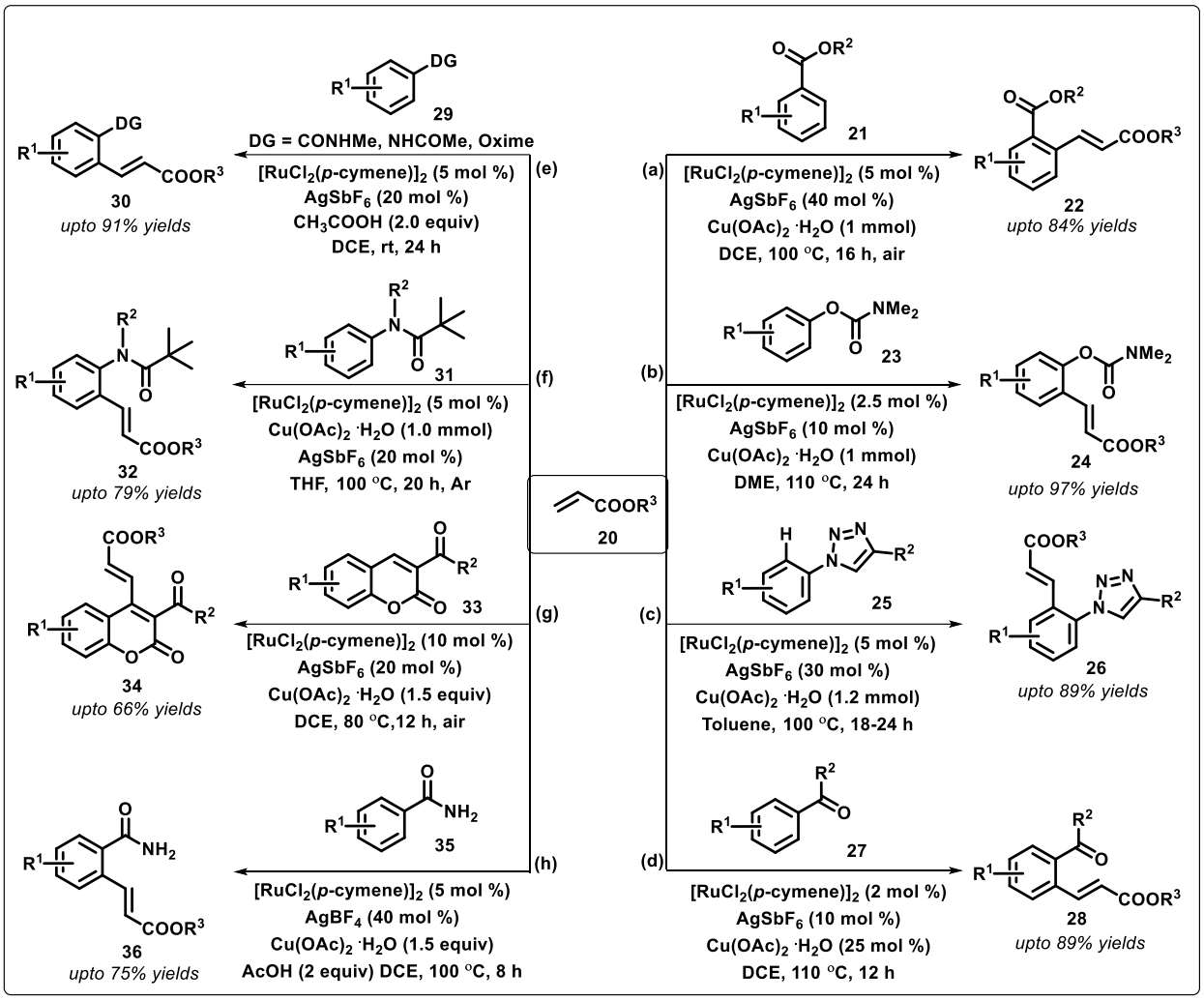

Scheme 1B.1.4 Ru-catalyzed strategies for Csp^2-H alkenylation of (hetero)arenes using acrylates

Furthermore, highly regioselective alkenylations at C-2 and C-4 positions in indoles (**37** & **39**) with acrylates (**20**) have been accomplished by Prabhu *et al*., employing carbonyl-directing groups at *N*-1 and *C*-3 positions, respectively under Ru^{II}-catalysis (Scheme 1B.1.5a-b).[44-45] Furthermore, Zhao and coworkers established a Ru^{II}-catalyzed strategy for selective C-7 alkenylation in indolines (**41**) with acrylates (**20**) by using simple pivaloyl as a directing group[41] (Scheme 1B.1.5c).

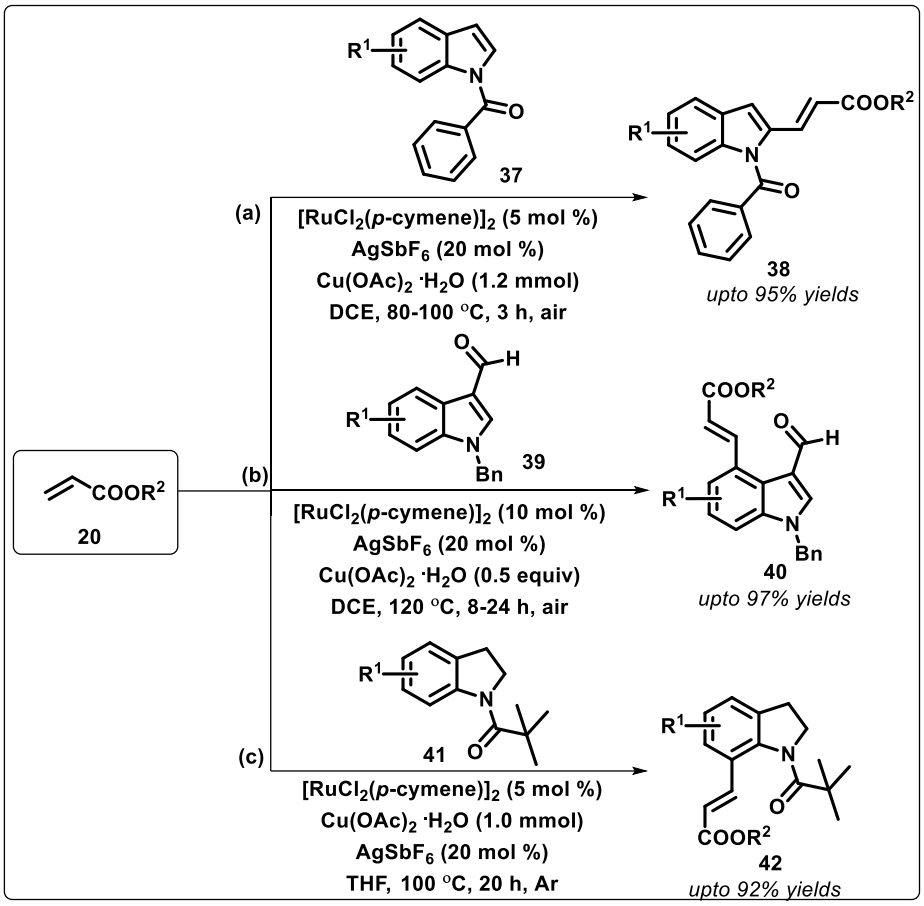

Scheme 1B.1.5 Ru-catalyzed regioselective alkenylation of indoles/indolines using acrylates

Interestingly, cross-dehydrogenative *ortho*-alkenylation followed by Michael addition has also been recorded in several cases, producing fused-heterocycles in appreciable yields. For example, Ackermann's group prepared lactones (**44**) by the annulation of benzoic acid derivatives (**43**) and acrylates (**20**) under the shadow of Ru^{II}-catalysis using $Cu(OAc)_2$ as an oxidant in water as a green solvent (Scheme 1B.1.6a).[46] Similarly, the same group also reported the synthesis of cyclic benzamides (**46**) by the alkenylation followed by cyclization of acrylates (**20**) to *N*-tosylbenzamides (**45**) under Ru^{II}-catalysis (Scheme 1B.1.6b).[47] Huang and coworkers established a catalyst-controlled two-step protocol for the synthesis of 6-alkylidene-6*H*-isoindo[2,1-*a*]indoles (**48**) by Rh and Pd–catalyzed couplings between 2-arylindoles (**47**) and acrylates (**20**) (Scheme 1B.1.6c).[48] Furthermore, in the domain of transition-metal catalyzed C-H functionalization on benzodiazines, Kianmehr *et al.* established a Ru^{II}-catalyzed strategy for [4+1] cycloaddition between *N*-arylpyridazine-diones/*N*-arylphthalazine-diones (**49**) and acrylates (**20**) to furnish pyridazino[1,2- *a*]indazoles/indazolo[1,2-*b*]phthalazines (**50**) in water as

green solvent (Scheme 1B.1.6d).[49] Similarly, Peng, Yu and their coworkers reported a Rh^{III}-catalyzed [4+1] strategy for the synthesis of pyrrolo[2,1-*b*]quinazolin-9(1*H*)-one (**52**) from 2-arylquinazolin-4-ones (**51**) and acrylates (**20**) (Scheme 1B.1.6e).[50]

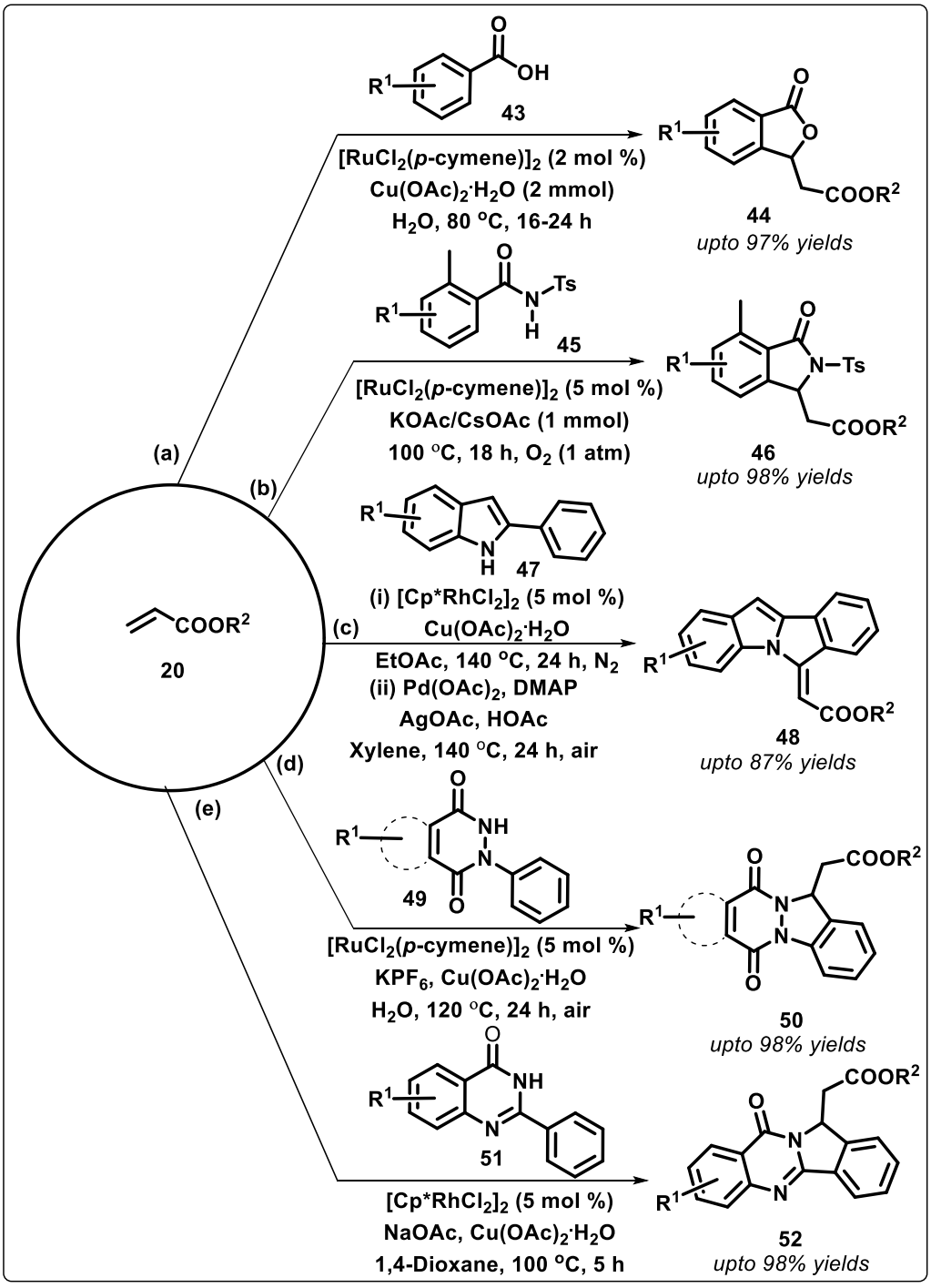

Scheme 1B.1.6 Ru/Rh-catalyzed annulation strategies to access fused-heterocycles using acrylates

Interestingly, the functionalization of *N*-arylindazolones remains unexplored with acrylates. In the backdrop of the above discussion, and anticipating the potential directing group ability of indazolone moiety, we envisioned that *N*-arylindazolones could be selectively functionalized using acrylates under metal-catalyzed conditions in a one-pot manner.

In this chapter, we present our systematic results on the accomplished Ru-catalyzed [4+1] annulation between *N*-aryl-1,2-dihydro-3*H*-indazol-3-ones (**53**) and acrylates (**20**) *via* sequential *ortho*-alkenylation-oxidative aza-Michael addition to afford indazolo[1,2-*a*]indazolylidenes (**54**) in high yields (Scheme 1B.1.7).

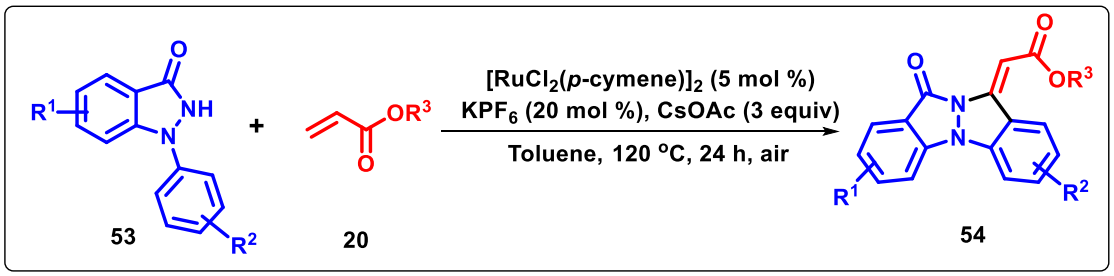

Scheme 1B.1.7 Ru-catalyzed [4+1] annulation strategy for the synthesis of indazolo[1,2-*a*]indazolylidenes using acrylates

1B.2 Results and Discussion

We commenced our investigations by optimizing the reaction conditions for the coupling of 1-phenyl-1*H*-indazol-3(2*H*)-one (**53a**) and ethyl acrylate (**20a**) as model substrates to afford an anticipated fused annulated product under Ru-catalyzed conditions. The reaction between **53a** (1 equiv) and **20a** (3 equiv) did not initiate in absence or presence of only base or additive using $[RuCl_2(p\text{-cymene})]_2$ as catalyst in DCE at 100 °C up to 24 h (Table 1B.2.1, entries 1–3). Pleasantly, the coupling proceeded in presence of CsOAc (1 equiv) and $AgSbF_6$ (20 mol %) under Ru-catalyzed condition to give ethyl (*E*)-2-(12-oxo-10*H*,12*H*-indazolo[1,2-*a*]indazol-10-ylidene)acetate (**54aa**) in 30% yield (Table 1B.2.1, entry 4). The structure of **54aa** was unambiguously confirmed by detailed ^1H NMR, ^{13}C NMR, COSY, HSQC and HRMS analysis. The use of alternate bases, such as NaOAc, KOAc provided no product at all, while detrimental yield (16%) of **54aa** was obtained by using AgOAc under similar experimental conditions (Table 1B.2.1, entries 5–7). Alternatively, the replacement of $AgSbF_6$ with KPF_6 furnished 56% of **54aa** (Table 1B.2.1, entry 8). Solvent screening studies indicated THF, MeOH and CH_3CN to be completely ineffective in producing **54aa** at all (Table 1B.2.1, entry 9), while the use of toluene was found to be most beneficial, affording **54aa** in 65% yield (Table 1B.2.1, entry 10).

Table 1B.2.1 Selective optimization[a] studies for the synthesis of **54aa**

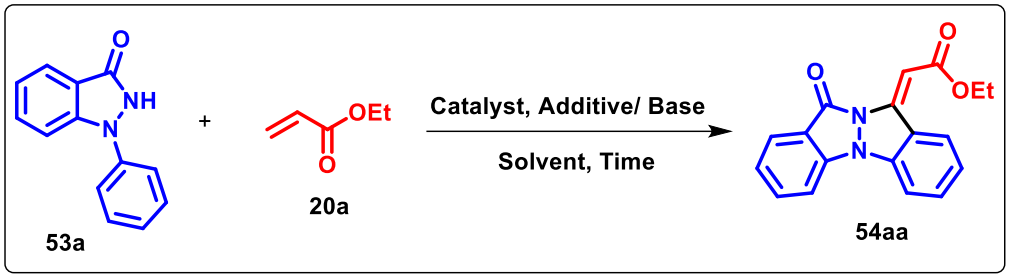

S. No.	Catalyst (5 mol %)	Additive (20 mol %)	Base (equiv)	Solvent	Yield[b] of 54aa (%)
1.	$[RuCl_2(p\text{-cymene})]_2$	-	-	DCE	NR
2.	$[RuCl_2(p\text{-cymene})]_2$	-	CsOAc (1)	DCE	-
3.	$[RuCl_2(p\text{-cymene})]_2$	$AgSbF_6$	-	DCE	-
4.	$[RuCl_2(p\text{-cymene})]_2$	$AgSbF_6$	CsOAc (1)	DCE	30
5.	$[RuCl_2(p\text{-cymene})]_2$	$AgSbF_6$	NaOAc (1)	DCE	-
6.	$[RuCl_2(p\text{-cymene})]_2$	$AgSbF_6$	KOAc (1)	DCE	-
7.	$[RuCl_2(p\text{-cymene})]_2$	$AgSbF_6$	AgOAc (1)	DCE	16
8.	$[RuCl_2(p\text{-cymene})]_2$	KPF_6	CsOAc (1)	DCE	56
9.	$[RuCl_2(p\text{-cymene})]_2$	KPF_6	CsOAc (1)	THF/MeOH/CH_3CN	NR
10.	$[RuCl_2(p\text{-cymene})]_2$	KPF_6	CsOAc (1)	Toluene	65
11.	$[RuCl_2(p\text{-cymene})]_2$	KPF_6	CsOAc (2)	Toluene	69
12.	$[RuCl_2(p\text{-cymene})]_2$	KPF_6	CsOAc (2.5)	Toluene	70
13.	$[RuCl_2(p\text{-cymene})]_2$	KPF_6	CsOAc (3)	Toluene	72
14.	$[RuCl_2(p\text{-cymene})]_2$	KPF_6	CsOAc (4)	Toluene	73
15[c].	$[RuCl_2(p\text{-cymene})]_2$	KPF_6	CsOAc (3)	Toluene	73
16[d].	$[RuCl_2(p\text{-cymene})]_2$	KPF_6	CsOAc (3)	Toluene	75
17.	$RuCl_2(PPh_3)_3$	KPF_6	CsOAc (3)	Toluene	28
18.	$RuCl_3.\chi H_2O$	KPF_6	CsOAc (3)	Toluene	20
19.	$[Cp^*RhCl_2]_2$	KPF_6	CsOAc (3)	Toluene	48
20.	$[Cp^*IrCl_2]_2$	KPF_6	CsOAc (3)	Toluene	32
21.	$Pd(OAc)_2$	KPF_6	CsOAc (3)	Toluene	NR
22[e].	$[RuCl_2(p\text{-cymene})]_2$	KPF_6	CsOAc (3)	Toluene	48

[a]Reaction conditions: The reactions were carried out with **53a** (0.23 mmol) and **20a** (0.69 mmol) in presence of a catalyst/additive (as indicated) in 4 mL of solvent at 100 °C for 24 h in a sealed tube. [b]Isolated yields after column chromatography. [c]Reaction temperature = 110 °C for 24 h. [d]Reaction temperature = 120 °C for 24 h. [e]Reaction under nitrogen atmosphere; NR = No Reaction; "–" few faintly visible spots on TLC.

Gratifyingly, the incremental use of base from 1 to 3 equivalents produced **54aa** in 72% yield, which further got elevated to 75% by performing the same reaction at 120 °C for 24 h (Table 1B.2.1, entries 11–16). Finally, to examine the efficiency of the proposed strategy with other

catalysts, independent reactions were performed using $RuCl_2(PPh_3)_3$, $RuCl_3 \cdot \chi H_2O$, $[Cp^*RhCl_2]_2$ and $[Cp^*IrCl_2]_2$ as catalysts; all of these were found be less effective, yielding **54aa** in comparatively lower yields (Table 1B.2.1, entries 17–20). While catalytic amount of $Pd(OAc)_2$ did not trigger any reaction between the model substrates (Table 1B.2.1, entry 21). Notably, the yield of **54aa** drastically decreased by performing Ru-catalyzed reaction under nitrogen atmosphere (Table 1B.2.1, entry 22). The representative ^1H and ^{13}C NMR spectra of **54aa** are shown in Figure 1B.2.1 and Figure 1B.2.2, respectively.

Having optimized conditions in hand, we next explored the scope and limitation of this Ru-catalyzed *ortho*-functionalization/cyclization protocol. Initially, the reactivity of various 1-aryl-1,2-dihydro-3*H*-indazol-3-ones (**53**) were examined with ethyl acrylate (**20a**) under the optimized conditions (Scheme 1B.2.1). A variety of 1-aryl-1,2-dihydro-3*H*-indazol-3-one possessing electron-donating (substrates **53b**: R^2 = 4-Me, **53c**: R^2 = 4-OMe) and electron-withdrawing substituents (substrates **53d**: R^2 = 4-F, **53e**: R^2 = 4-Cl, **53f**: R^2 = 4-Br, **53g**: R^2 = 3-Cl, **53h**: R^2 = 3-NO_2) at different positions on aryl group, were well tolerated for the coupling with **20a** to deliver their corresponding indazolo-fused indazolylidenes (**54ba**–**54ha**) in 55–89% yields (Scheme 1B.2.1). Further, disubstituted 1-aryl-1,2-dihydro-3*H*-indazol-3-one possessing electron-donating/withdrawing groups (substrates **53i**: R^2 = 2,4-di-Cl, **53j**: R^2 = 3-Cl-4-Me) produces desirable products (**54ia**–**54ja**) in 75–83% yields. In general, electron-withdrawing substitutions at *m*-position of aryl group were more favorable as compared to electron-donation groups at *o*-/*p*-positions in furnishing their respective products in comparatively higher yields. Similarly, 1-aryl-1,2-dihydro-3*H*-indazol-3-one substituted with a weakly electron-withdrawing group (substrate **53k**: R^1=5-Br) on the indazolone scaffold was observed to be good in the formation of expected annulation product (**54ka**). After extensive screening of the N-arylindazolones substrates, we next move to test the potential of various acrylates (**20b**–**h**) with 1-aryl-1,2-dihydro-3*H*-indazol-3-ones (**53**) (Scheme 1B.2.1). The coupling of methyl acrylate (**20b**) with 1-aryl-1,2-dihydro-3*H*-indazol-3-ones (substrates **53a**: R^2 = H, **53g**: R^2 = 3-Cl, **53h:** R^2 = 3-NO_2) produces the corresponding products (**54ab**, **54gb**–**54hb**) in 68–78% yields, which was slightly lower than what was obtained with ethyl acrylate. While, for (tetrahydrofuran-2-yl)methyl acrylate (**20c**), the attempted 1-aryl-1,2-dihydro-3*H*-indazol-3-one (substrates **53a**: R^2 = H, **53g**: R^2 = 3-Cl, **53h**: R^2 = 3-NO_2, **53i**: R^2 = 2,4-di-Cl; & **53k**: R^1 = 5-Br) comfortably furnishes respective indazolo-fused indazolylidenes (**54ac**, **54gc**–**54ic**, **54kc**) in 80–85% yields.

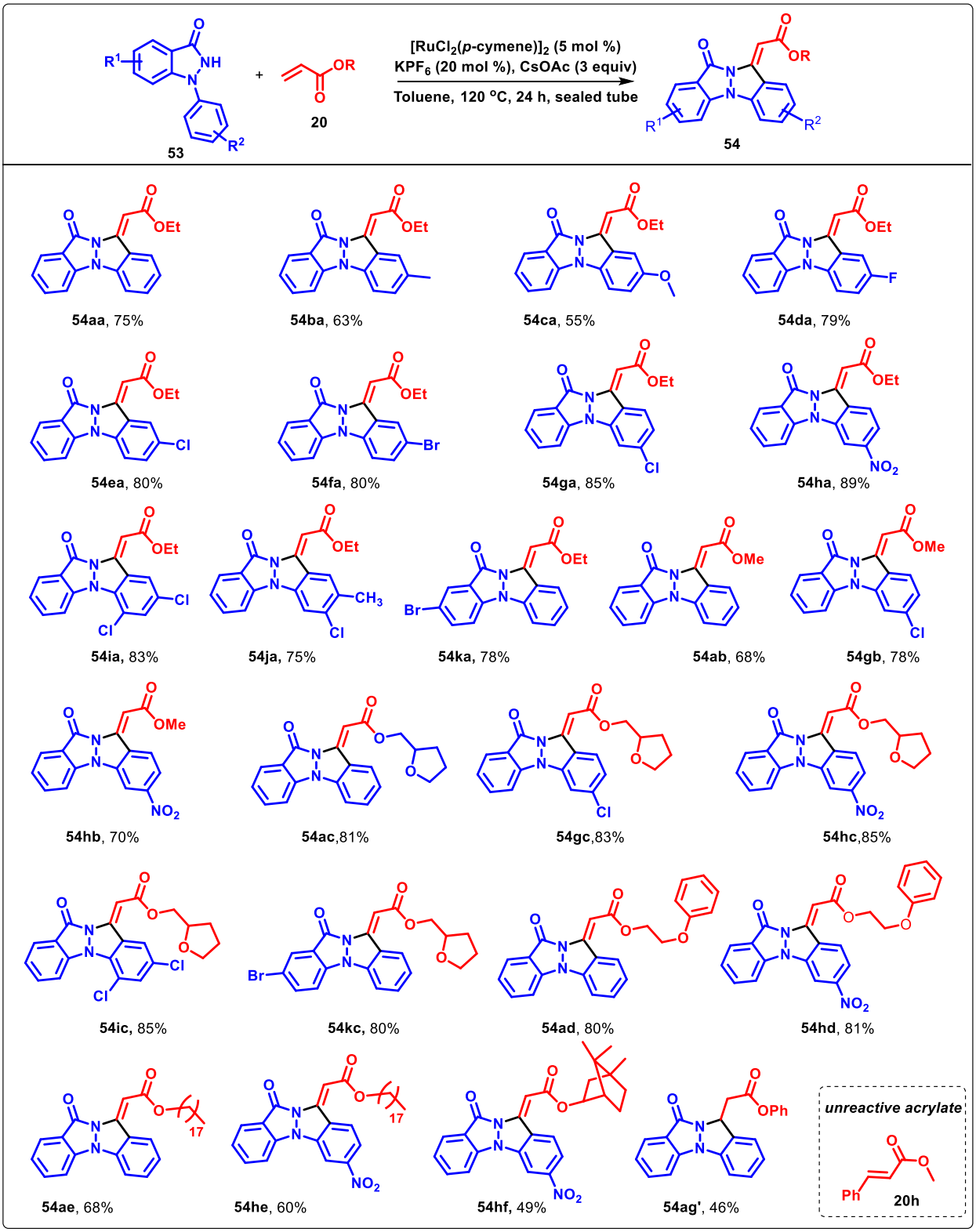

Scheme 1B.2.1 Substrate scope of 1-aryl-1,2-dihydro-3*H*-indazol-3-ones and acrylates

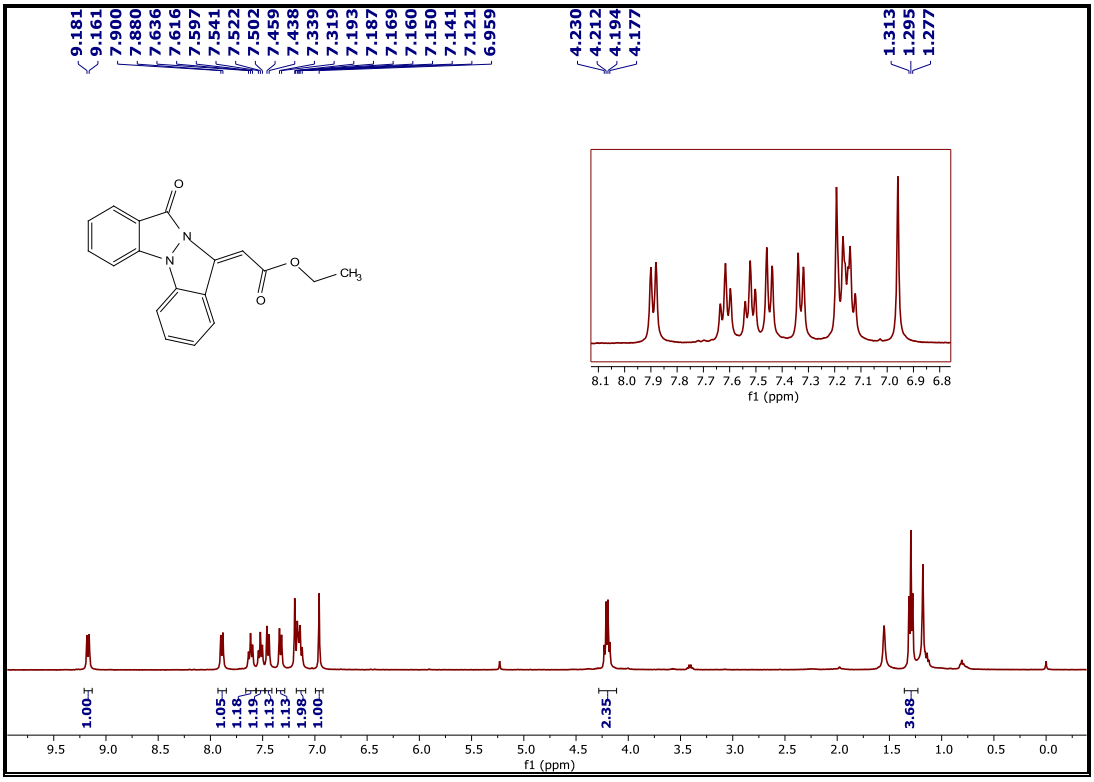

Figure 1B.2.1 ^{1}H NMR Spectrum of **54aa**

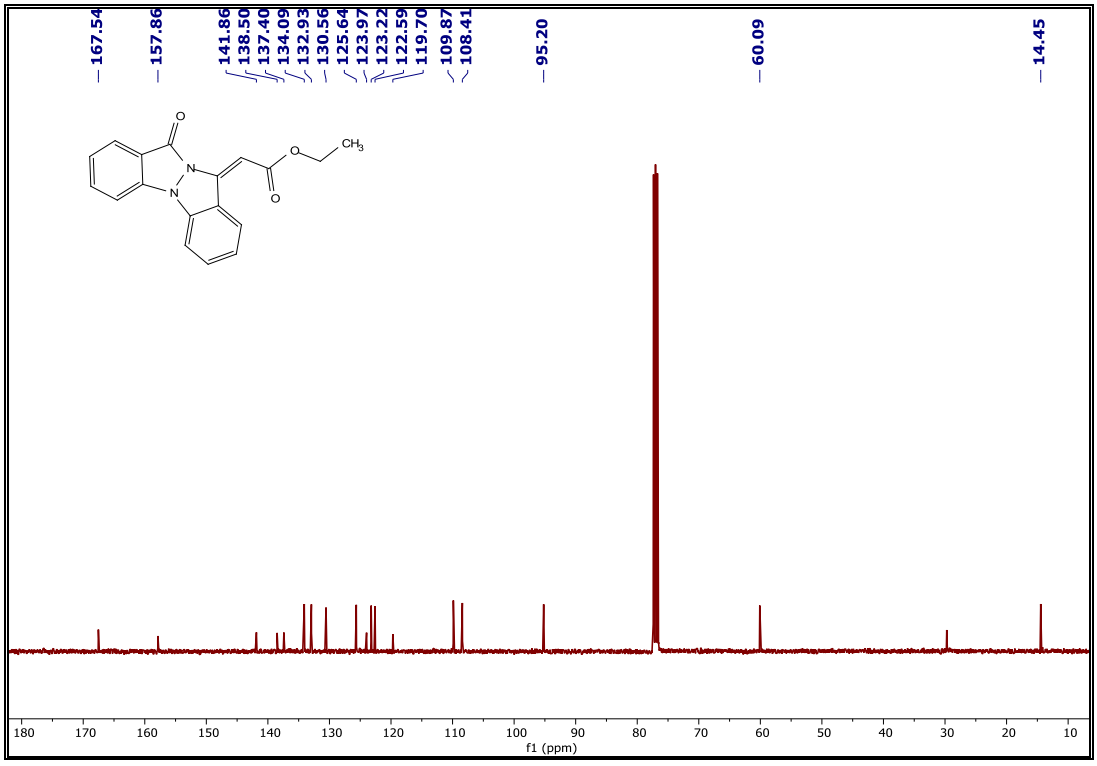

Figure 1B.2.2 ^{13}C NMR Spectrum of **54aa**

Similarly, coupling of 2-phenoxyethyl acrylate (**20d**) with **53a** & **53h** (R^2 = H & 3-NO_2) afforded **54ad** and **54hd**, respectively in high yields under optimized conditions. Further, the reaction of **53a** & **53h** with stearyl acrylate (**20e**) yielded **54ae** and **54he** in 68% and 60% respectively. Interestingly, isobornyl acrylate (**20f**) was not found to be an effective coupling partner for the desired transformation with **53a**, yielding traces of product; however, with nitro-substituted 1-phenyl-1,2-dihydro-3*H*-indazol-3-one (**53h**), **54hf** was isolated in 49% yield. To our surprise, phenyl acrylate (**20g**) on coupling with **53a** afforded un-oxidized annulated product (**54ag'**) in 46% yield, while methyl cinnamate (**20h**) failed to react at all under standard conditions.

As a representative example, single crystals of **54ad** were grown in DCM, the structure of **54ad** was unambiguously confirmed by single crystal X-ray analysis. An ORTEP diagram (CCDC no. 1985703) of **54ad** is shown in figure 1B.2.3.

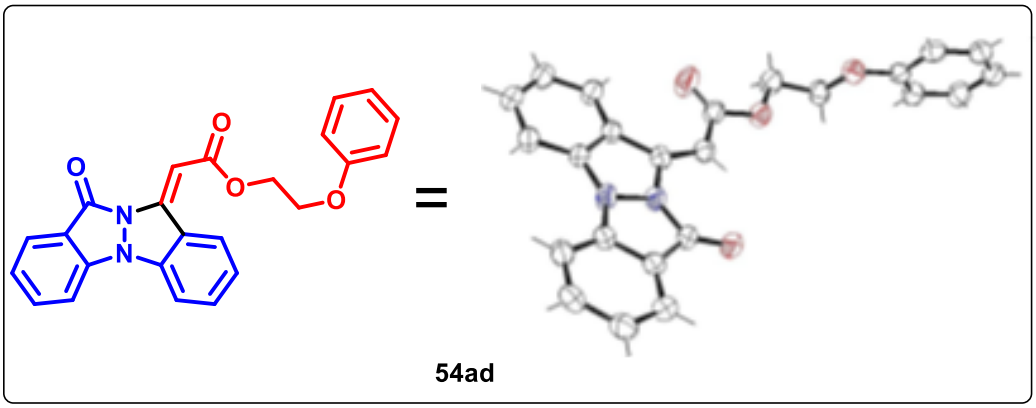

Figure 1B.2.3 ORTEP Diagram of **54ad**

To confirm the mechanistic pathway of the established protocol, a few preliminary studies were carried. Firstly, the reaction between **53a** and **20a** did not furnish **54aa** in absence of [$RuCl_2$(*p*-cymene)]$_2$ using CsOAc as a base and KPF_6 as an additive in toluene at 120 °C (Scheme 1B.2.2i). Also since the combination of CsOAc and KPF_6 drastically improved the reactivity between the two coupling partners during optimization studies; the formation of active complex, [Ru^{II}OAc(*p*-cymene)]$^+$[PF_6]$^-$, in concordance with the earlier reports, could be affirmed. No considerable declination in the yield of **54aa** was observed by carrying the reaction between **53a** and **20a** in presence of TEMPO (3 equiv) as a radical quencher, thereby eliminating the possibility of radical mechanism for the established protocol (Scheme 1B.2.2ii). An attempt to isolate any of the possible intermediate was made. Fascinatingly, the reaction of **53i** and **20a** under Ru-catalyzed optimized conditions afforded **54ia**′ after 10 h at 100 °C in toluene, which

was isolated in 60% yield along with the isolation of 19% of **54ia**. This clearly indicated slow, albeit simultaneous oxidation of **54ia'** to **54ia** as the reaction proceeds. **54ia'** on reaction with CsOAc at 120 °C furnished 88% of **54ia** in 10 h (Scheme 1B.2.2iii). This affirmed **54ia'** to be an active intermediate in this protocol. A deuterium labelling experiment when performed by reacting **53a** under Ru-catalyzed optimized conditions using D_2O, produced 66% of a mixture of bis(*ortho*-deuterated)1-phenyl-1*H*-indazol-3(2*H*)-one (**53a**–***d*₂**) and **53a** (87: 13), after 15 h of heating in toluene at 120 °C (Scheme 1B.2.2iv). This remarkable incorporation of deuterium atoms (~87%) at both the *ortho*-C-H bonds under Ru^{II} catalysis indicated the possibility of reversible nature of C-H bond dissociation step. The intermolecular competition experiment when performed with a mixture of **53a** and **53a**–***d*₂** under standard conditions gave a kinetic isotopic effect (KIE) of P_H/P_D = 3.1, while a k_H/k_D value of 2.9 was obtained by performing two parallel reactions of substrates **53a** and **53a**–***d*₂**, indicating C-H bond cleavage probably occurred in the rate-determining step (Scheme 1B.2.2v).

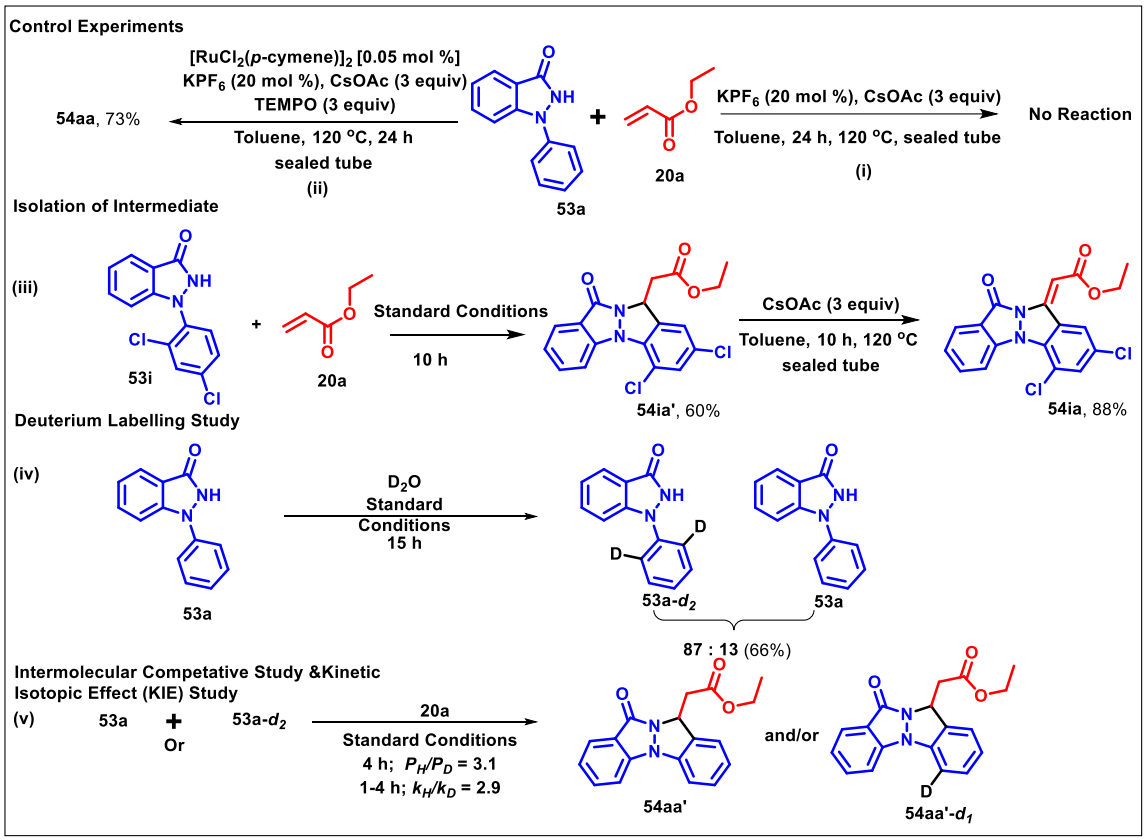

Scheme 1B.2.2 Mechanistic investigations

On the basis of our preliminary mechanistic results and literature precedents,[51-54] a plausible mechanism is proposed (Scheme 1B.2.3). The reaction is believed to be initiated by the

activation of dimeric $[RuCl_2(p\text{-cymene})]_2$ by KPF_6 to generate monomeric Ru^{II} active species, $[RuOAc(p\text{-cymene})]^+[PF_6]^-$; which furnishes the ruthenacyclic intermediate **A** upon cyclometalation *via* N-H assisted C-H activation. Thereafter, vinylic coordination and subsequent C-C insertion affords species **C** *via* **B**. Later, **C** on *β*-hydride-elimination forms **D**, which reductively eliminates the *o*-alkenylated product **E** along with the regeneration of Ru^{II} catalyst for the next catalytic cycle. Finally, intramolecular aza-Michael addition in **E** gives **54aa'**, which on dehydrogenation in aerial oxygen produces the desired product **54**.

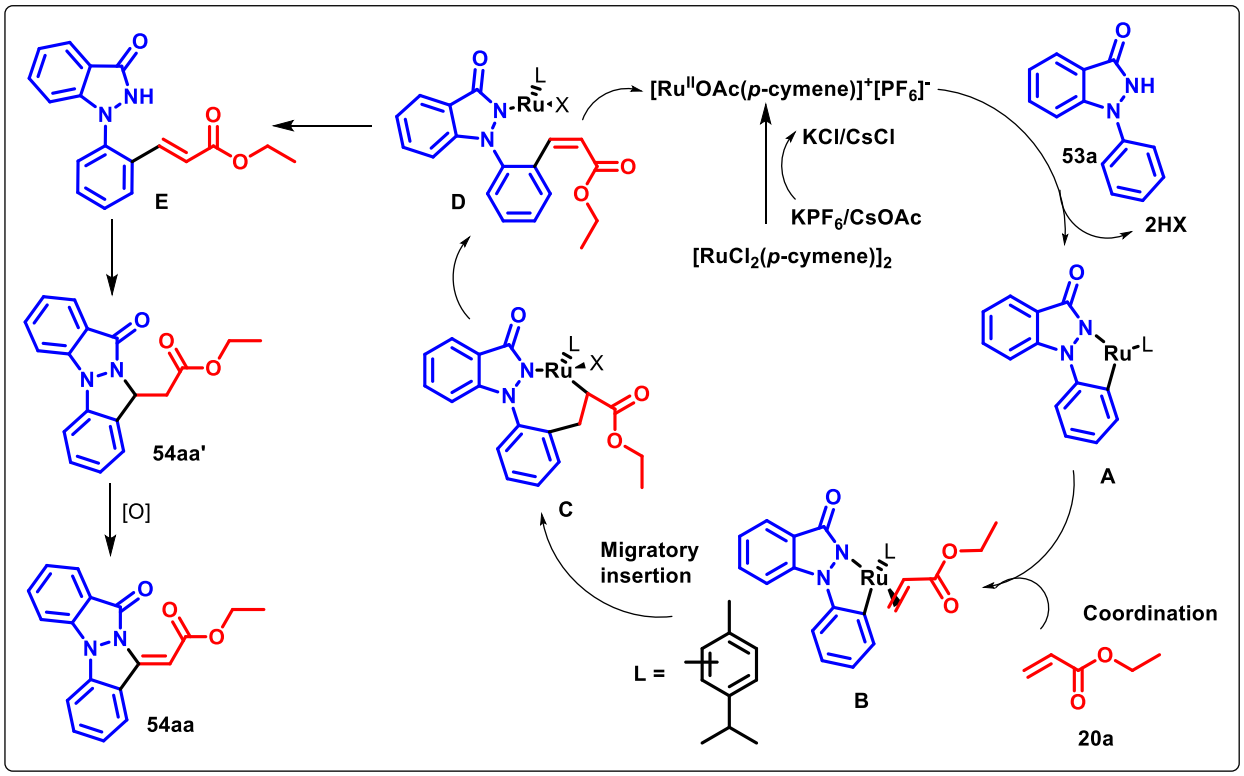

Scheme 1B.2.3 Plausible mechanistic pathway

In summary, we have disclosed a facile annulation strategy for the synthesis of diversely substituted indazolo[1,2-*a*]indazolylidenes through a one-pot coupling between 1-aryl-1,2-dihydro-3*H*-indazol-3-one and acrylates under Ru-catalyzed conditions. The reaction proceeded through the *ortho*-alkenylation on 1-aryl-1,2-dihydro-3*H*-indazol-3-one *via* directing group influence of cyclic amide group, followed by oxidative intramolecular aza-Michael addition. Good functional group tolerance and synthesis modularity highlighted the broad utility of the described synthetic methodology in organic synthesis.

1B.3 Experimental Section

General Considerations

Commercially available reagents were used without purification. Commercially available solvents were dried by standard procedures prior to use. Nuclear magnetic resonance spectra were recorded on a 400 MHz spectrometer, and the chemical shifts are reported in δ units, parts per million (ppm), relative to residual chloroform (7.26 ppm) in the deuterated solvent. The following abbreviations were used to describe peak splitting patterns when appropriate: s = singlet, d = doublet, t = triplet, dd = doublet of doublets, and m = multiplet. Coupling constants, *J*, are reported in hertz (Hz). The ^{13}C NMR spectra are reported in ppm relative to $CDCl_3$ (77.0 ppm). Melting points were determined on a capillary point apparatus equipped with a digital thermometer and are uncorrected. High resolution mass spectra were recorded on an Agilent Technologies 6545 Q-TOF LC/MS by using electrospray mode. Column chromatography was performed on silica gel (100-200) mesh using a varying ratio of ethyl acetate/hexanes as an eluent.

General procedure for the synthesis of 1-aryl-1,2-dihydro-3*H*-indazol-3-ones (53)

Step 1: To a stirred solution of aryl hydrazine hydrochloride (**56**) (4.0 mmol, 1.0 equiv) and 2-halobenzoic acid (**55**) (4.0 mmol, 1.0 equiv) in dry DMF (10 mL) were added triethyl amine (8 mmol, 2 equiv), EDC·HCl (4.4 mmol, 1.1 equiv), HOBt (4.4 mmol, 1.1 equiv), and DMAP (0.2 mmol, 5.0 mol %), and the mixture was stirred for 24 h at room temperature. The reaction was quenched with water, and the mixture was extracted with EtOAc (50 mL×2). The organic layers were washed with water and dried over Na_2SO_4, and the solvent was evaporated in *vacuo*. The residue was purified by recrystallization with EtOAc to afford 2-halobenzohydrazides (**57**) used for the next step.

Step 2: A mixture of 2-halobenzohydrazide (0.5 mmol), L-proline (0.2 mmol, 40 mol %), and *t*-BuOK (1.0 mmol, 2.0 equiv) in dry DMSO (1.5 mL) was stirred at 100 °C for 24 h. The reaction was quenched with a saturated $NaHCO_3$ solution, and the mixture was extracted with EtOAc (40 mL×2). The organic layers were dried over Na_2SO_4, and the solvent was evaporated in *vacuo*. The residue was purified by recrystallization with EtOAc to afford 1-aryl-1,2-dihydro-3*H*-indazol-3-one (**53**).

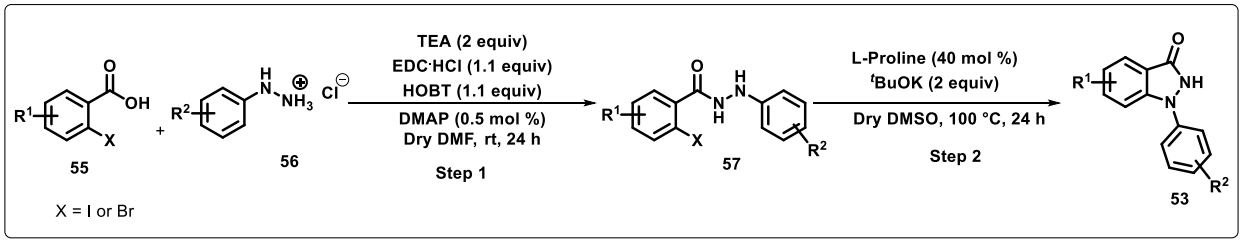

Scheme 1B.3.1 Synthesis of 1-aryl-1,2-dihydro-3*H*-indazol-3-ones

General procedure for the synthesis of indazolo[1,2-*a*]indazolylidenes (54)

To a stirred solution of 1-aryl-1*H*-indazol-3(2*H*)-one (**53**) (50 mg, 1 equiv) and acrylate (**20**) (3 equiv) in toluene (4 mL) in a sealed tube, $[RuCl_2(p\text{-cymene})]_2$ (0.05 equiv), KPF_6 (0.2 equiv) and CsOAc (3 equiv) were added at room temperature. The reaction was stirred and heated at 120 °C for 24 h, and the progress of the reaction was monitored by TLC. After the completion of the reaction, the reaction mixture was extracted in EtOAc (15 mL×2), and the combined organic extracts were dried over anhydrous sodium sulfate and concentrated under vacuum to yield a crude mixture. The crude mixture was purified by column chromatography using ethyl acetate/hexanes (2:8) as an eluent system to furnish the desired product (**54**).

Ethyl (*E*)-2-(12-oxo-10*H*,12*H*-indazolo[1,2-*a*]indazol-10-ylidene)acetate (54aa). Yellow

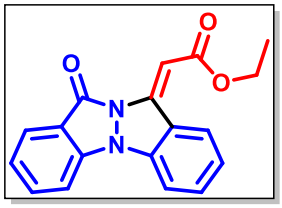

solid, 55 mg (75%); mp: 155-156 °C; ^{1}H NMR (400 MHz, $CDCl_3$) δ 9.17 (d, J = 8.2 Hz, 1H), 7.89 (d, J = 7.9 Hz, 1H), 7.61 (t, J = 7.8 Hz, 1H), 7.52 (t, J = 7.7 Hz, 1H), 7.44 (d, J = 8.3 Hz, 1H), 7.32 (d, J = 8.1 Hz, 1H), 7.17 – 7.12 (m, 2H), 6.95 (s, 1H), 4.20 (q, J = 7.1 Hz, 2H), 1.29 (t, J = 7.1 Hz, 3H); ^{13}C NMR (100 MHz, $CDCl_3$) δ 167.5, 157.9, 141.9, 138.5, 137.4, 134.1, 132.9, 130.6, 125.6, 124.0, 123.2, 122.6, 119.7, 109.9, 108.4, 95.2, 60.1, 14.4; HRMS (ESI-TOF) (*m/z*) calculated $C_{18}H_{15}N_2O_3^+$: 307.1082, found 307.1108 $[M + H]^+$.

(*E*)-Ethyl 2-(8-methyl-12-oxoindazolo[1,2-*a*]indazol-10(12*H*)-ylidene)acetate (54ba). Yellow

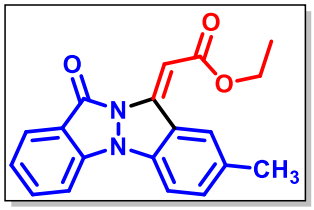

solid, 45 mg (63%); mp: 151-152 °C; ^{1}H NMR (400 MHz, $CDCl_3$) δ 9.08 (s, 1H), 8.00 (dd, J = 8.8, 1.2 Hz, 1H), 7.72 – 7.68 (m, 1H), 7.52 (d, J = 8.3 Hz, 1H), 7.44 (dd, J = 8.1, 1.6 Hz, 1H), 7.33 (d, J = 8.3 Hz, 1H), 7.25 (t, J = 7.6 Hz, 1H), 7.05 (s, 1H), 4.30 (q, J = 7.1 Hz, 3H), 2.48 (s, 3H), 1.39 (t, J = 7.1 Hz, 3H); ^{13}C NMR (100 MHz, $CDCl_3$) δ 167.6, 158.0, 142.0, 138.7, 135.7, 134.0, 133.9, 133.1, 130.4, 129.8, 125.6, 122.3, 119.6, 109.8, 108.2, 95.0, 60.0, 21.4, 14.5; HRMS (ESI-TOF) (*m/z*) calculated $C_{19}H_{17}N_2O_3^+$: 321.1234, found 321.1222 $[M + H]^+$.

(*E*)-Ethyl 2-(8-methoxy-12-oxoindazolo[1,2-*a*]indazol-10(12*H*)-ylidene)acetate (54ca).

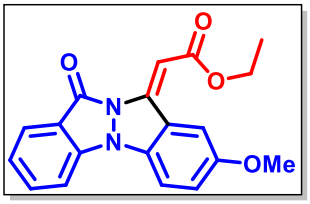

Yellow solid, 38 mg (55%); mp: 134-135 °C; ^{1}H NMR (400 MHz, $CDCl_3$) δ 8.95 (d, J = 2.6 Hz, 1H), 7.98 (d, J = 7.9 Hz, 1H), 7.71 – 7.67 (m, 1H), 7.50 (d, J = 8.3 Hz, 1H), 7.35 (d, J = 8.8 Hz, 1H), 7.25 – 7.21 (m, 2H), 7.03 (s, 1H), 4.29 (q, J = 7.1 Hz, 2H), 3.94 (s, 3H), 1.38 (t, J = 7.1 Hz, 3H); ^{13}C NMR (100 MHz, $CDCl_3$) δ 167.6, 158.3, 155.9, 142.2, 139.2, 134.1, 132.4, 125.7, 124.9, 122.2, 121.8, 119.4, 112.9, 109.6, 109.3, 95.2, 60.1, 56.0, 14.4; HRMS (ESI-TOF) (*m/z*) calculated $C_{19}H_{17}N_2O_4^+$: 337.1183, found 337.1194 $[M + H]^+$.

(*E*)-Ethyl 2-(8-fluoro-12-oxoindazolo[1,2-*a*]indazol-10(12*H*)-ylidene)acetate (54da). Yellow

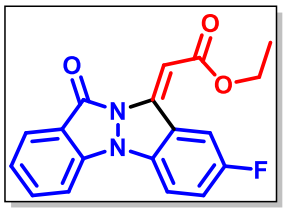

solid, 56 mg (79%); mp: 189-190 °C; ^{1}H NMR (400 MHz, $CDCl_3$) δ 9.10 – 9.07 (m, 1H), 7.99 (dt, J = 7.8, 1.0 Hz, 1H), 7.74 –7.69 (m, 1H), 7.51 (dt, J = 8.3, 0.8 Hz, 1H), 7.40 – 7.35 (m, 2H), 7.29 – 7.35 (m, 1H), 7.04 (s, 1H), 4.29 (q, J = 7.1 Hz, 2H), 1.39 (t, J = 7.1 Hz, 3H); ^{13}C NMR (100 MHz, $CDCl_3$) δ 167.3, 159.7, 157.7 ($^{1}J_{C–F}$ = 87.5 Hz), 141.4, 139.0, 134.3, 125.8, 125.2 ($^{3}J_{C–F}$ = 10.6 Hz), 122.8, 120.6 ($^{2}J_{C–F}$ = 25.4 Hz), 119.6, 117.2 ($^{2}J_{C–F}$ = 27.8 Hz), 109.7, 109.1 ($^{3}J_{C–F}$ = 8.5 Hz), 96.0, 60.3, 14.4; ^{19}F NMR (100 MHz, $CDCl_3$) δ −117.66 to −117.72 (m, 1F); HRMS (ESI-TOF) (*m/z*) calculated $C_{18}H_{14}FN_2O_3^+$: 325.0983, found 325.0970 $[M + H]^+$.

(*E*)-Ethyl 2-(8-chloro-12-oxoindazolo[1,2-*a*]indazol-10(12*H*)-ylidene)acetate (54ea). Yellow

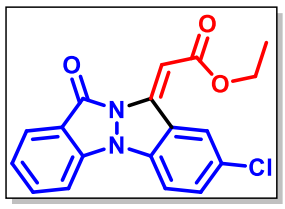

solid, 55 mg (80%); mp: 199-200 °C; ^{1}H NMR (400 MHz, $CDCl_3$) δ 9.34 (d, J = 2.1 Hz, 1H), 8.00 (d, J = 7.9 Hz, 1H), 7.72 (t, J = 7.9 Hz, 1H), 7.59 (dd, J = 8.6, 2.1 Hz, 1H), 7.51 (d, J = 8.3 Hz, 1H), 7.37 – 7.28 (m, 2H), 7.05 (s, 1H), 4.30 (q, J = 7.1 Hz, 2H), 1.39 (t, J = 7.1 Hz, 3H); ^{13}C NMR (100 MHz, $CDCl_3$) δ 167.3, 157.8, 140.8, 138.5, 136.0, 134.3, 133.1, 130.3, 128.6, 125.8, 125.3, 123.0, 119.7, 109.8, 109.2, 96.0, 60.3, 14.4; HRMS (ESI-TOF) (*m/z*) calculated $C_{18}H_{14}ClN_2O_3^+$: 341.0687, found 341.0677 $[M + H]^+$.

(*E*)-Ethyl 2-(8-bromo-12-oxoindazolo[1,2-*a*]indazol-10(12*H*)-ylidene)acetate (54fa). Yellow

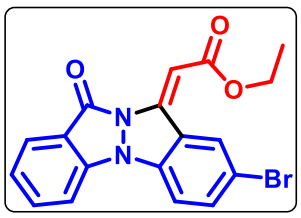

solid, 53 mg (80%); mp: 201-202 °C; ^{1}H NMR (400 MHz, $CDCl_3$) δ 9.49 (d, J = 1.9 Hz, 1H), 8.01 (d, J = 7.9 Hz, 1H), 7.75 – 7.71 (m, 2H), 7.52 (d, J = 8.3 Hz, 1H), 7.33 – 7.30 (m, 2H), 7.06 (s, 1H), 4.31 (q, J = 7.1 Hz, 2H), 1.39 (t, J = 7.1 Hz, 3H); ^{13}C NMR (100 MHz, CDCl3) δ 167.3, 157.8, 140.6, 138.4, 136.3, 135.8, 134.3, 133.2, 125.8, 125.6, 123.0, 119.8, 115.8, 109.9,

109.6, 96.1, 60.3, 14.4; HRMS (ESI-TOF) (m/z) calculated $C_{18}H_{14}BrN_2O_3^+$: 385.0182, found 385.0159 $[M + H]^+$.

(*E*)-Ethyl 2-(7-chloro-12-oxoindazolo[1,2-*a*]indazol-10(12*H*)-ylidene)acetate (54ga). Yellow solid, 59 mg (85%); mp: 180-181 °C; ^{1}H NMR (400 MHz, $CDCl_3$) δ 9.24 (d, J = 8.7 Hz, 1H), 8.00 (d, J = 7.9 Hz, 1H), 7.74 (t, J = 7.8 Hz, 1H), 7.54 (d, J = 8.3 Hz, 1H), 7.41 (d, J = 1.9 Hz, 1H), 7.33 – 7.29 (m, 1H), 7.20 (dd, J = 8.7, 1.9 Hz, 1H), 7.03 (s, 1H), 4.29 (q, J = 7.1 Hz, 2H), 1.38 (t, J = 7.1 Hz, 3H); ^{13}C NMR (100 MHz, $CDCl_3$) δ 167.5, 157.8, 141.1, 139.1, 138.4, 138.1, 134.3, 131.6, 125.8, 123.5, 123.2, 122.6, 119.9, 110.0, 108.7, 95.4, 60.2, 14.4; HRMS (ESI-TOF) (*m/z*) calculated $C_{18}H_{14}ClN_2O_3^+$: 341.0687, found 341.0674 $[M + H]^+$.

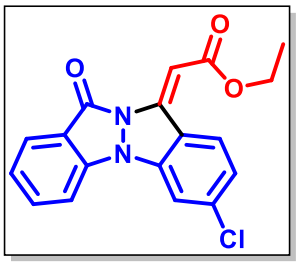

(*E*)-Ethyl 2-(7-nitro-12-oxoindazolo[1,2-*a*]indazol-10(12*H*)-ylidene)acetate (54ha). Red solid, 61 mg (89%); mp: 220-221 °C; ^{1}H NMR (400 MHz, $CDCl_3$) δ 9.51 (d, J = 8.9 Hz, 1H), 8.21 (s, 1H), 8.05 (t, J = 9.9 Hz, 2H), 7.82 (t, J = 7.9 Hz, 1H), 7.67 (d, J = 8.3 Hz, 1H), 7.37 (t, J = 7.6 Hz, 1H), 7.15 (s, 1H), 4.31 (q, J = 7.1 Hz, 2H), 1.40 (t, J = 7.1 Hz, 3H); ^{13}C NMR (100 MHz, $CDCl_3$) δ 167.0, 157.7, 150.4, 140.0, 138.4, 137.5, 134.7, 131.7, 129.1, 125.9, 123.8, 120.0, 117.9, 110.2, 103.4, 98.1, 60.6, 14.4; HRMS (ESI-TOF) (*m/z*) calculated $C_{18}H_{14}N_3O_5^+$: 352.0928, found 352.0917 $[M + H]^+$.

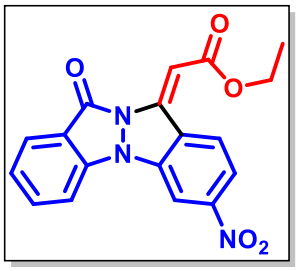

(*E*)-Ethyl 2-(6,8-dichloro-12-oxoindazolo[1,2-*a*]indazol-10(12*H*)-ylidene)acetate (54ia). Yellow solid, 56 mg (83%); mp: 230-231 °C; ^{1}H NMR (400 MHz, $CDCl_3$) δ 9.43 (d, J = 2.0 Hz, 1H), 8.42 – 8.40 (m, 1H), 7.99 (dt, J = 7.5, 1.1 Hz, 1H), 7.70 – 7.67 (m, 1H), 7.60 (d, J = 2.1 Hz, 1H), 7.33 – 7.29 (m, 1H), 7.18 (s, 1H), 4.30 (q, J = 7.1 Hz, 2H), 1.38 (t, J = 7.1 Hz, 3H); ^{13}C NMR (100 MHz, $CDCl_3$) δ 167.2, 157.9, 139.7, 139.6, 134.8, 134.2, 134.0, 129.3, 128.6, 128.0, 125.2, 123.5, 120.2, 114.7, 114.4, 95.8, 60.4, 14.4; HRMS (ESI-TOF) (*m/z*) calculated $C_{18}H_{13}Cl_2N_2O_3^+$: 375.0298, found 375.0297 $[M + H]^+$.

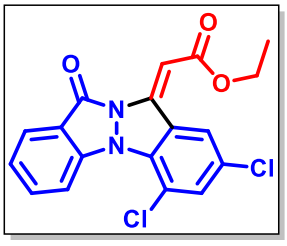

(*E*)-Ethyl 2-(7-chloro-8-methyl-12-oxoindazolo[1,2-*a*]indazol-10(12*H*)-ylidene)acetate

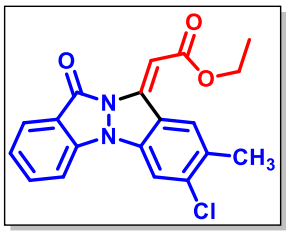

(54ja). Yellow solid, 52 mg (75%); mp: 234-235 °C; ^{1}H NMR (400 MHz, $CDCl_3$) δ 9.14 (s, 1H), 7.97 (d, J = 7.9 Hz, 1H), 7.73 – 7.69 (m, 1H), 7.49 (d, J = 8.3 Hz, 1H), 7.40 (s, 1H), 7.31 – 7.25 (m, 1H), 6.99 (s, 1H), 4.28 (q, J = 7.1 Hz, 2H), 2.46 (s, 3H), 1.38 (t, J = 7.1 Hz, 3H).; ^{13}C NMR (100 MHz, $CDCl_3$) δ 167.6, 157.9, 141.3, 139.3, 138.6, 136.4, 134.2, 131.9, 131.2, 125.7, 122.9, 122.7, 119.8, 109.9, 108.9, 95.3, 60.2, 20.2, 14.4; HRMS (ESI-TOF) (*m/z*) calculated $C_{19}H_{16}ClN_2O_3^+$: 355.0844, found 355.0842 $[M + H]^+$.

(*E*)-Ethyl 2-(2-bromo-12-oxoindazolo[1,2-*a*]indazol-10(12*H*)-ylidene)acetate (54ka). Yellow

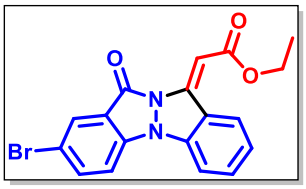

solid, 52 mg (78%); mp: 141-142 °C; ^{1}H NMR (400 MHz, $CDCl_3$) δ 9.26 (d, J = 8.2 Hz, 1H), 8.12 (d, J = 1.9 Hz, 1H), 7.80 (dd, J = 8.7, 2.0 Hz, 1H), 7.63 (t, J = 7.8 Hz, 1H), 7.44 (d, J = 8.7 Hz, 1H), 7.39 (d, J = 8.1 Hz, 1H), 7.28 – 7.25 (m, 1H), 7.06 (s, 1H), 4.30 (q, J = 7.2 Hz, 2H), 1.38 (t, J = 7.1 Hz, 3H); ^{13}C NMR (100 MHz, $CDCl_3$) δ 167.3, 156.4, 141.5, 137.0, 136.9, 136.9, 133.0, 130.7, 128.3, 124.0, 123.6, 121.2, 115.2, 111.3, 108.4, 96.2, 60.2, 14.4; HRMS (ESI-TOF) (*m/z*) calculated $C_{18}H_{14}BrN_2O_3^+$: 385.0182, found 385.0155 $[M + H]^+$.

(*E*)-Methyl 2-(12-oxoindazolo[1,2-*a*]indazol-10(12*H*)-ylidene)acetate (54ab). Yellow solid,

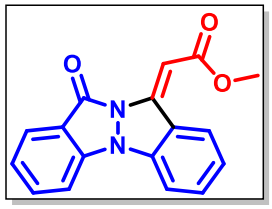

47 mg (68%); mp: 161-162 °C; ^{1}H NMR (400 MHz, $CDCl_3$) δ 9.29 (d, J = 8.2 Hz, 1H), 8.00 (dt, J = 8.0, 1.2 Hz, 1H), 7.74 – 7.70 (m, 1H), 7.63 (td, J = 8.2, 1.2 Hz, 1H), 7.56 (d, J = 8.3 Hz, 1H), 7.44 (d, J = 8.2 Hz, 1H), 7.29 – 7.24 (m, 2H), 7.08 (s, 1H), 3.84 (s, 3H).); ^{13}C NMR (100 MHz, $CDCl_3$) δ 167.9, 157.7, 142.1, 138.7, 137.5, 134.1, 133.0, 130.6, 125.7, 124.0, 123.3, 122.7, 119.8, 109.9, 108.4, 94.6, 51.3; HRMS (ESI-TOF) (*m/z*) calculated $C_{17}H_{13}N_2O_3^+$: 293.0921, found 23.0923 $[M + H]^+$.

(*E*)-Methyl 2-(7-chloro-12-oxoindazolo[1,2-*a*]indazol-10(12*H*)-ylidene)acetate (54gb).

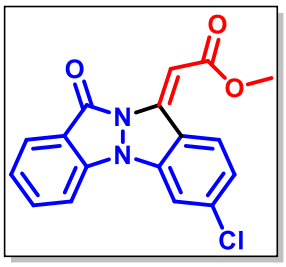

Yellow solid, 52 mg (78%); mp: 170-172 °C; ^{1}H NMR (400 MHz, $CDCl_3$) δ 9.25 (d, J = 8.7 Hz, 1H), 8.01 (d, J = 7.9 Hz, 1H), 7.77 – 7.73 (m, 1H), 7.55 (d, J = 8.3 Hz, 1H), 7.42 (d, J = 1.8 Hz, 1H), 7.32 (t, J = 7.6 Hz, 1H), 7.21 (dd, J = 8.7, 1.9 Hz, 1H), 7.04 (s, 1H), 3.84 (s, 3H); ^{13}C NMR (100 MHz, $CDCl_3$) δ 167.9, 157.8, 141.3, 139.2, 138.4, 138.1,

134.3, 131.6, 125.8, 123.6, 123.2, 122.6, 110.0, 108.7, 94.8, 51.4; HRMS (ESI-TOF) (*m/z*) calculated $C_{17}H_{12}ClN_2O_3^+$: 327.0531, found 327.0547 $[M + H]^+$.

(*E*)-Methyl 2-(7-nitro-12-oxoindazolo[1,2-*a*]indazol-10(12*H*)-ylidene)acetate (54hb). Red

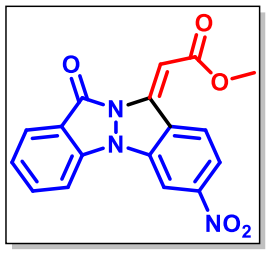

solid, 46 mg (70%); mp: 200-201 °C; ^{1}H NMR (400 MHz, $CDCl_3$) δ 9.52 (d, *J* = 8.9 Hz, 1H), 8.23 (d, *J* = 2.1 Hz, 1H), 8.09 (dd, *J* = 8.9, 2.1 Hz, 1H), 8.06 (d, *J* = 7.9 Hz, 1H), 7.84 7.80 (m, 1H), 7.68 (d, *J* = 8.3 Hz, 1H), 7.39 (t, *J* = 7.5 Hz, 1H), 3.87 (s, 3H); ^{13}C NMR (100 MHz, $CDCl_3$) δ 167.5, 157.8, 140.2, 138.4, 134.8, 131.7, 129.0, 126.0, 123.9, 120.0, 117.9, 110.3, 103.5, 97.5, 51.7; HRMS (ESI-TOF) (*m/z*) calculated $C_{17}H_{12}N_3O_5^+$: 338.0776, found 338.0756 $[M + H]^+$.

(*E*)-(Tetrahydrofuran-2-yl)methyl 2-(12-oxoindazolo[1,2-*a*]indazol-10(12*H*)-ylidene)acetate

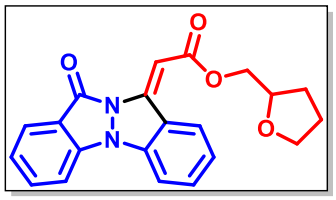

(54ac). Yellow solid, 69 mg (81%); mp: 191-192 °C; ^{1}H NMR (400 MHz, $CDCl_3$) δ 9.27 (d, *J* = 8.2 Hz, 1H), 8.00 (d, *J* = 7.9 Hz, 1H), 7.72 (t, *J* = 7.9 Hz, 1H), 7.63 (t, *J* = 7.7 Hz, 1H), 7.55 (d, *J* = 8.3 Hz, 1H), 7.43 (d, *J* = 8.2 Hz, 1H), 7.27 – 7.22 (m, 2H), 7.11 (s, 1H), 4.32 – 4.19 (m, 3H), 4.00 – 3.82 (m, 2H), 2.10 – 1.94 (m, 3H), 1.77 – 1.73 (m, 1H); ^{13}C NMR (100 MHz, $CDCl_3$) δ 167.4, 157.8, 142.2, 138.5, 137.4, 134.2, 133.0, 130.6, 125.7, 123.9, 123.2, 122.6, 119.7, 109.9, 108.4, 94.7, 68.5, 66.1, 28.2, 25.8; HRMS (ESI-TOF) (*m/z*) calculated $C_{21}H_{19}N_2O_4^+$: 363.1366, found 363.1339 $[M + H]^+$.

(*E*)-(Tetrahydrofuran-2-yl)methyl 2-(7-chloro-12-oxoindazolo[1,2-*a*]indazol-10(12*H*)-

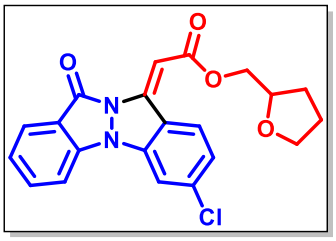

ylidene)acetate (54gc). Yellow solid, 67 mg (83%); mp: 210-211 °C; ^{1}H NMR (400 MHz, $CDCl_3$) δ 9.23 (d, *J* = 8.7 Hz, 1H), 8.00 (d, *J* = 7.8 Hz, 1H), 7.76 – 7.72 (m, 1H), 7.54 (d, *J* = 8.2 Hz, 1H), 7.41 (d, *J* = 1.9 Hz, 1H), 7.33 – 7.28 (m, 1H), 7.20 (dd, *J* = 8.8, 1.9 Hz, 1H), 7.07 (s, 1H), 4.32 – 4.18 (m, 3H), 3.99 – 3.82 (m, 2H), 2.10 – 1.92 (m, 3H), 1.78 – 1.72 (m, 1H); ^{13}C NMR (100 MHz, $CDCl_3$) δ 167.3, 157.7, 141.4, 139.2, 138.3, 138.1, 134.3, 131.7, 125.8, 123.5, 123.2, 122.5, 119.9, 110.0, 108.7, 94.8, 68.5, 66.2, 28.2, 25.7; HRMS (ESI-TOF) (*m/z*) calculated $C_{23}H_{18}ClN_2O_4^+$: 397.095, found 397.0978 $[M + H]^+$.

(*E*)-(Tetrahydrofuran-2-yl)methyl 2-(7-nitro-12-oxoindazolo[1,2-*a*]indazol-10(12*H*)-ylidene)acetate (54hc). 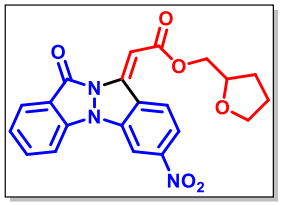

Red solid, 68 mg (85%); mp: 184-185 °C; ^{1}H NMR (400 MHz, $CDCl_3$) δ 9.49 (d, J = 8.9 Hz, 1H), 8.21 (s, 1H), 8.05 (t, J = 9.9 Hz, 2H), 7.82 (t, J = 7.7 Hz, 1H), 7.68 (d, J = 8.4 Hz, 1H), 7.38 (t, J = 7.7 Hz, 1H), 7.20 (s, 1H), 4.34 – 4.20 (m, 3H), 3.98 – 3.85 (m, 2H), 2.08 – 1.95 (m, 3H), 1.80 – 1.69 (m, 1H); ^{13}C NMR (100 MHz, $CDCl_3$) δ 166.9, 157.7, 150.4, 140.2, 138.3, 137.5, 134.8, 131.7, 129.0, 126.0, 123.9, 120.0, 117.8, 110.2, 103.5, 97.5, 68.6, 66.5, 28.1, 25.7; HRMS (ESI-TOF) (*m/z*) calculated $C_{21}H_{18}N_3O_6^+$: 408.1190, found 408.1191 $[M + H]^+$.

(*E*)-(Tetrahydrofuran-2-yl)methyl 2-(6,8-dichloro-12-oxoindazolo[1,2-*a*]indazol-10(12*H*)-ylidene)acetate (54ic). 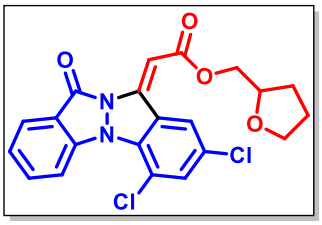

Yellow solid, 65 mg (85%); mp: 189-190 °C; ^{1}H NMR (400 MHz, $CDCl_3$) δ 9.42 (d, J = 2.1 Hz, 1H), 8.41 (d, J = 8.7 Hz, 1H), 7.98 (d, J = 7.8 Hz, 1H), 7.70 – 7.66 (m, 1H), 7.60 (d, J = 2.0 Hz, 1H), 7.32 – 7.28 (m, 1H), 7.23 (s, 1H), 4.33 – 4.18 (m, 3H), 3.99 – 3.82 (m, 2H), 2.09 – 1.94 (m, 3H), 1.76 – 1.71 (m, 1H); ^{13}C NMR (100 MHz, $CDCl_3$) δ 167.1, 157.8, 140.0, 139.6, 134.8, 134.2, 134.0, 129.3, 128.6, 127.9, 125.2, 123.5, 120.2, 114.7, 114.4, 95.2, 68.5, 66.4, 28.2, 25.7; HRMS (ESI-TOF) (*m/z*) calculated $C_{21}H_{17}Cl_2N_2O_4^+$: 431.056, found 431.0558 $[M + H]^+$.

(*E*)-(Tetrahydrofuran-2-yl)methyl 2-(2-bromo-12-oxoindazolo[1,2-*a*]indazol-10(12*H*)-ylidene)acetate (54kc). 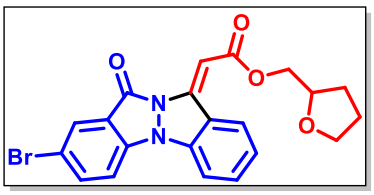

Yellow solid, 61 mg (80%); mp: 187-188 °C; ^{1}H NMR (400 MHz, $CDCl_3$) δ 9.26 (d, J = 8.1 Hz, 1H), 8.12 (d, J = 2.0 Hz, 1H), 7.80 (dd, J = 8.7, 2.0 Hz, 1H), 7.65 – 7.61 (m, 1H), 7.45 (d, J = 8.7 Hz, 1H), 7.40 (d, J = 8.1 Hz, 1H), 7.27 (m, 1H), 7.11 (s, 1H), 4.26 – 4.21 (m, 3H), 4.00 – 3.82 (m, 2H), 2.04 – 1.93 (m, 2H), 1.75 – 1.72 (m, 2H); ^{13}C NMR (100 MHz, $CDCl_3$) δ 167.2, 156.4, 141.8, 137.0, 137.0, 133.1, 132.5, 130.7, 128.3, 124.4, 123.6, 122.5, 115.2, 113.2, 111.3, 95.6, 68.5, 66.2, 28.2, 25.7; HRMS (ESI-TOF) (*m/z*) calculated $C_{21}H_{18}BrN_2O_4^+$: 441.0444, found 441.0414 $[M + H]^+$.

(*E*)-2-Phenoxyethyl 2-(12-oxoindazolo[1,2-*a*]indazol-10(12*H*)-ylidene)acetate (54ad). 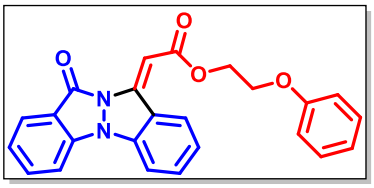

Yellow solid, 75 mg (80%); mp: 156-157 °C; ^{1}H NMR (400 MHz, $CDCl_3$) δ 9.26 (d, J = 8.2 Hz, 1H), 7.98 (d, J = 7.9 Hz, 1H), 7.71 (t, J = 7.8 Hz, 1H), 7.63 (t, J = 7.8 Hz, 1H), 7.54 (d, J = 8.3 Hz,

1H), 7.43 (d, *J* = 8.1 Hz, 1H), 7.33 (t, *J* = 7.9 Hz, 2H), 7.26 – 7.22 (m, 2H), 7.10 (s, 1H), 7.01 – 6.98 (m, 3H), 4.61 (t, *J* = 4.9 Hz, 2H), 4.31 (t, *J* = 5.0 Hz, 2H); ^{13}C NMR (100 MHz, $CDCl_3$) *δ* 167.3, 158.6, 157.9, 142.3, 138.6, 137.4, 134.2, 133.1, 130.6, 129.5, 125.7, 123.9, 123.3, 122.7, 121.1, 119.7, 114.7, 109.9, 108.5, 94.3, 66.0, 62.5; HRMS (ESI-TOF) (*m/z*) calculated $C_{24}H_{19}N_2O_4^+$: 399.1339, found 399.1337 $[M + H]^+$.

(*E*)-2-Phenoxyethyl 2-(7-nitro-12-oxoindazolo[1,2-*a*]indazol-10(12*H*)-ylidene)acetate (54hd). Red solid, 70 mg (81%); mp: 150-151 °C; ^{1}H NMR (400 MHz, $CDCl_3$) *δ* 9.50 (d, *J* = 8.9

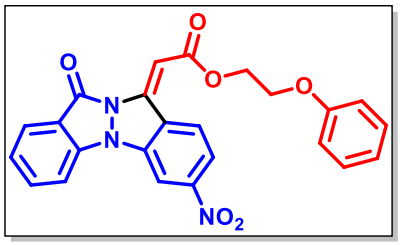

Hz, 1H), 8.22 (d, *J* = 2.1 Hz, 1H), 8.08 – 8.03 (m, 2H), 7.82 (t, *J* = 7.8 Hz, 1H), 7.68 (d, *J* = 8.3 Hz, 1H), 7.40 – 7.31 (m, 3H), 7.20 (s, 1H), 7.02 – 6.97 (m, 3H), 4.62 (t, *J* = 4.8 Hz, 2H), 4.31 (t, *J* = 4.9 Hz, 2H); ^{13}C NMR (100 MHz, $CDCl_3$) *δ* 166.9, 158.5, 157.7, 150.5, 140.4, 138.4, 137.5, 134.8, 131.7, 129.6, 128.9, 126.0, 123.9, 121.2, 120.0, 117.9, 114.7, 110.3, 103.5, 97.2, 65.9, 62.9; HRMS (ESI-TOF) (*m/z*) calculated $C_{24}H_{18}N_3O_6^+$: 444.119, found 444.1099 $[M + H]^+$.

(*E*)-Octadecyl 2-(12-oxoindazolo[1,2-*a*]indazol-10(12*H*)-ylidene)acetate (54ae). Yellow solid,

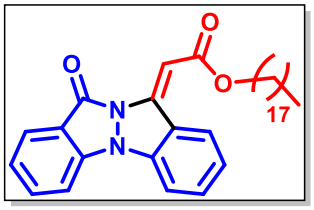

86 mg (68%); mp: 99-100 °C; ^{1}H NMR (400 MHz, $CDCl_3$) *δ* 9.28 (d, *J* = 8.1 Hz, 1H), 7.99 (d, *J* = 7.8 Hz, 1H), 7.73 – 7.69 (m, 1H), 7.63 – 7.59 (m, 1H), 7.55 (d, *J* = 8.3 Hz, 1H), 7.43 (d, *J* = 8.1 Hz, 1H), 7.25 – 7.22 (m, 2H), 7.06 (s, 1H), 4.23 (t, *J* = 6.7 Hz, 2H), 1.78 – 1.69 (m, 2H), 1.29 – 1.27 (s, 30H), 0.90 (t, *J* = 6.3 Hz, 3H); ^{13}C NMR (100 MHz, $CDCl_3$) *δ* 167.7, 157.9, 141.8, 138.5, 137.4, 134.1, 132.9, 130.6, 125.6, 124.0, 123.2, 122.6, 119.7, 109.9, 108.4, 95.3, 64.4, 31.9, 29.7, 29.6, 29.5, 29.4, 29.3, 28.9, 26.1, 22.7, 14.1; HRMS (ESI-TOF) (*m/z*) calculated $C_{34}H_{47}N_2O_3^+$: 531.3581, found 531.3557 $[M + H]^+$.

(*E*)-Octadecyl 2-(7-nitro-12-oxoindazolo[1,2-*a*]indazol-10(12*H*)-ylidene)acetate (54he). Red

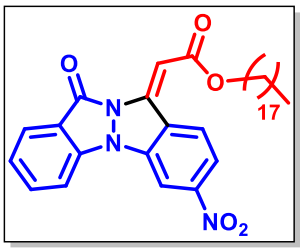

solid, 68 mg (60%); mp:110-111 °C; ^{1}H NMR (400 MHz, $CDCl_3$) *δ* 9.53 (d, *J* = 9.0 Hz, 1H), 8.22 (d, *J* = 2.1 Hz, 1H), 8.08 8.04 (m, 2H), 7.82 (t, *J* = 7.7 Hz, 1H), 7.69 (d, *J* = 8.3 Hz, 1H), 7.39 (t, *J* = 7.6 Hz, 1H), 7.17 (s, 1H), 4.24 (t, *J* = 6.7 Hz, 2H), 1.79 – 1.73 (m, 2H), 1.31 – 1.24 (s, 30H), 0.90 (t, J = 6.7 Hz, 3H); ^{13}C NMR (100 MHz, $CDCl_3$) *δ*

167.2, 157.8, 139.9, 138.4, 137.5, 134.7, 131.7, 125.9, 123.8, 120.0, 117.9, 110.3, 103.4, 100.0, 98.2, 64.8, 31.9, 29.7, 29.7, 29.6, 29.5, 29.4, 29.3, 28.8, 26.0, 22.7, 14.1; HRMS (ESI-TOF) (*m/z*) calculated $C_{34}H_{46}N_3O_5^+$: 576.3432, found 576.3431 $[M + H]^+$.

(*E*)-(1*R*,2*R*,4*R*)-1,7,7-Trimethylbicyclo[2.2.1]heptan-2-yl 2-(7-nitro-12-oxoindazolo[1,2-*a*]indazol-10(12*H*)-ylidene)acetate (54hf). Red solid, 44 mg (49%); mp: 210-211 °C; ^{1}H NMR

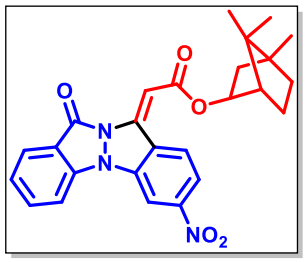

(400 MHz, $CDCl_3$) δ 9.53 (d, *J* = 8.8 Hz, 1H), 8.22 (d, *J* = 2.1 Hz, 1H), 8.08 – 8.03 (m, 2H), 7.83 (t, *J* = 7.7 Hz, 1H), 7.69 (d, *J* = 8.3 Hz, 1H), 7.39 (t, *J* = 7.6 Hz, 1H), 7.13 (s, 1H), 4.84 (t, *J* = 5.9 Hz, 1H), 1.92 (d, *J* = 5.9 Hz, 2H), 1.81 (s, 2H), 1.28 – 1.12 (m, 3H), 1.09 (s, 3H), 0.95 (s, 3H), 0.90 (s, 3H); ^{13}C NMR (100 MHz, $CDCl_3$) δ 166.8, 157.8, 139.9, 138.3, 137.5, 134.7, 131.8, 125.8, 123.8, 120.0, 117.9, 110.3, 103.4, 100.0, 98.8, 81.5, 49.0, 47.1, 45.1, 39.0, 33.9, 27.2, 20.2, 20.1, 11.6; HRMS (ESI-TOF) (*m/z*) calculated $C_{26}H_{23}N_3O_4Na^+$: 464.1586 , found 464.1660 $[M + Na - H_2O]^+$.

Ethyl 2-(6,8-dichloro-12-oxo-10,12-dihydroindazolo[1,2-*a*]indazol-10-yl)acetate (54ia').

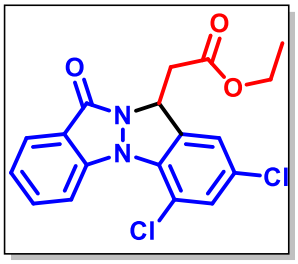

Green solid, 40 mg (60%); ^{1}H NMR (400 MHz, $CDCl_3$) δ 8.37 (d, *J* = 8.6 Hz, 1H), 7.91 (d, *J* = 7.8 Hz, 1H), 7.63 – 7.59 (m, 1H), 7.40 (d, *J* =1.9 Hz, 1H),7.34 – 7.33 (m, 1H), 7.28 (s, 1H), 5.89 (dd, *J* = 7.8, 4.0 Hz, 1H), 4.19 (q, *J* = 7.1 Hz, 2H), 3.34 (dd, *J* = 16.6, 4.1 Hz, 1H), 3.09 (dd, *J* = 16.6, 7.9 Hz, 1H), 1.24 (t, *J* = 7.1 Hz, 3H); ^{13}C NMR (100 MHz, $CDCl_3$) δ 169.4, 161.7, 143.0, 136.1, 135.4, 132.6, 131.0, 129.3, 124.2, 123.3, 123.0, 120.5, 115.7, 115.4, 61.2, 54.5, 39.0, 14.1; HRMS (ESI-TOF) (*m/z*) calculated $C_{18}H_{15}Cl_2N_2O_3^+$: 377.0459, found 377.0442 $[M + H]^+$.

Ethyl 2-(12-oxo-10,12-dihydroindazolo[1,2-*a*]indazol-10-yl)acetate (54aa'). Green solid; 54

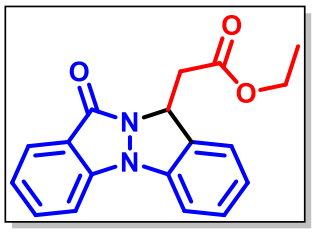

mg (74%); ^{1}H NMR (400 MHz, $CDCl_3$) δ 7.93 (d, *J* = 7.9 Hz, 1H), 7.65 (t, *J* = 7.7 Hz, 1H), 7.55 (d, *J* = 8.3 Hz, 1H), 7.42 (t, *J* = 8.0 Hz, 2H), 7.34 (d, *J* = 7.9 Hz, 1H), 7.28 – 7.24 (m, 1H), 7.11 (t, *J* = 7.5 Hz, 1H), 5.97 (dd, *J* = 7.8, 4.7 Hz, 1H), 4.20 (q, *J* = 7.1 Hz, 2H), 3.38 (dd, *J* = 16.2, 4.7 Hz, 1H), 3.09 (dd, *J* = 16.2, 7.8 Hz, 1H), 1.24 (t, *J* = 7.1 Hz, 3H).

Phenyl 2-(12-oxo-10,12-dihydroindazolo[1,2-*a*]indazol-10-yl)acetate (54ag'). Green solid, 39 mg (46%); ^{1}H NMR (400 MHz, $CDCl_3$) δ 7.94 (dt, J = 7.9, 1.0 Hz, 1H), 7.66 – 7.62 (m, 1H), 7.54 (d, J = 8.3 Hz, 1H), 7.48 (d, J = 7.5 Hz, 1H), 7.43 – 7.34 (m, 4H), 7.28 – 7.22 (m, 2H), 7.15 – 7.08 (m, 3H), 6.05 (dd, J = 7.2, 5.1 Hz, 1H), 3.58 (dd, J = 16.3, 5.1 Hz, 1H), 3.35 (dd, J = 16.3, 7.2 Hz, 1H).

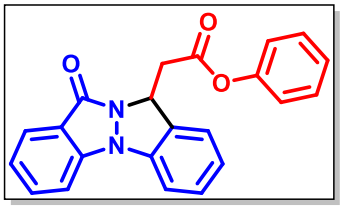

1B.4 Single Crystal X-Ray Diffraction Studies

Based on the screening the crystals of **54ad** under a microscope, one suitable crystal was mounted in a nylon loop attached to a goniometer head. Initial crystal evaluation and data collection were performed on a Kappa APEX 20 diffractometer equipped with a CCD detector (with the crystal-to-detector distance fixed at 60 mm) and sealed-tube monochromated MoKα radiation using the program APEX2.[55] Data were integrated, reflections were fitted and values of F^2 and $\sigma(F^2)$ for each reflection were obtained by using the program SAINT.[55] Data were also corrected for Lorentz and polarization effects. The subroutine XPREP[55] was used for the processing of data that included determination of space group, application of an absorption correction (SADABS),[55] merging of data, and generation of files necessary for solution and refinement. The crystal structure was solved and refined using SHELX 97.[56] The chosen space group was confirmed by the successful refinement of the structure. Positions of most of the non-hydrogen atoms were obtained from a direct methods solution. Several full-matrix least-squares/difference Fourier cycles were performed, locating the remainder of the non-hydrogen atoms. All non-hydrogen atoms were refined with anisotropic displacement parameters. All hydrogen atoms were placed in ideal positions and refined as riding atoms with individual isotropic displacement parameters. There were four independent molecules in the asymmetric unit. All figures were drawn using MERCURY V 3.0[57] and Platon.[58]

1B.4.1. Crystal data for 54ad (CCDC No. 1985703). $C_{24}H_{18}N_2O_4$, Mr = 398.40 g/mol, triclinic, space group P-1, a = 15.406(5) Å, b = 16.870(5) Å, c = 17.640(6) Å, α = 76.819(5)°, β = 70.237(5)°, γ = 62.874(4)°, V = 3825.(2) Å^3, Z = 8, T = 296(2) K, D_{calcd} = 1.384 g/cm^3; Full matrix least-square on F^2; R_1 = 0.0823, wR_2 = 0.2526 for 6092 observed reflections [I > 2σ(I)] and R_1 = 0.1694, wR_2 = 0.3042 for all 13548 reflections; GOF = 1.037.

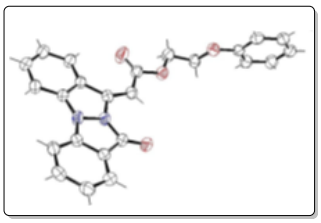

1B.5 References

1. Yuan, T.; Nahar, P.; Sharma, M.; Liu, K.; Slitt, A.; Aisa, H.; Seeram, N. P. *Journal of Natural Products* **2014**, *77*, 2316-2320.
2. Selwood, D. L.; Brummell, D. G.; Budworth, J.; Burtin, G. E.; Campbell, R. O.; Chana, S. S.; Charles, I. G.; Fernandez, P. A.; Glen, R. C.; Goggin, M. C. *Journal of Medicinal Chemistry* **2001**, *44*, 78-93.
3. Bräse, S.; Gil, C.; Knepper, K. *Bioorganic & Medicinal Chemistry* **2002**, *10*, 2415-2437.
4. Sutrisna, E.; Azizah, T.; Wahyuni, S. *Research Journal of Pharmacy and Technology* **2022**, *15*, 381-384.
5. Singh, Y.; Saxena, B. *Understanding Covid-19* **2022**, 103.
6. Frejat, F. O. A.; Zhai, H.; Cao, Y.; Wang, L.; Mostafa, Y. A.; Gomaa, H. A.; Youssif, B. G.; Wu, C. *Bioorganic Chemistry* **2022**, 105922.
7. Hamdoon, A. M.; Saleh, M. Y.; Saied, S. M. *Egyptian Journal of Chemistry* **2022**, *65*, 305-312.
8. Desai, N.; Jadeja, D.; Mehta, H.; Khasiya, A.; Shah, K.; Pandit, U. *Springer* **2022**, 143-189.
9. Kesavan, M. P.; Ravi, L.; Balachandran, C.; Thangadurai, T. D.; Aoki, S.; Webster, T. J.; Rajesh, J. *Journal of Molecular Structure* **2023**, *1274*, 134423.
10. Fonseca-Berzal, C.; Ibáñez-Escribano, A.; de Castro, S.; Escario, J. A.; Gómez-Barrio, A.; Arán, V. J. *Acta Tropica* **2022**, *234*, 106607.
11. González-Naranjo, P.; Pérez, C.; González-Sánchez, M.; Gironda-Martínez, A.; Ulzurrun, E.; Bartolomé, F.; Rubio-Fernández, M.; Martin-Requero, A.; Campillo, N. E.; Páez, J. A. *Journal of Enzyme Inhibition and Medicinal Chemistry* **2022**, *37*, 2348-2356.
12. Zhang, Y.; Zhang, J.; Wang, J.; Chen, H.; Ouyang, L.; Wang, Y. *European Journal of Medicinal Chemistry* **2022**, 114668.
13. Sangepu, V. R.; Sharma, D.; Venkateshwarlu, R.; Bhoomireddy, R. D.; Jain, K. K.; Kapavarapu, R.; Dandela, R.; Pal, M. *Journal of Molecular Structure* **2023**, *1273*, 134273.
14. Qin, J.; Cheng, W.; Duan, Y.-T.; Yang, H.; Yao, Y. *Anti-Cancer Agents in Medicinal Chemistry* **2021**, *21*, 839-860.
15. Tan, C.; Yang, S.-J.; Zhao, D.-H.; Li, J.; Yin, L.-Q. *Arabian Journal of Chemistry* **2022**, *15* 103756.
16. Cerecetto, H.; Gerpe, A.; Gonzalez, M.; Aran, V. J.; de Ocariz, C. O. *Mini Reviews in Medicinal Chemistry* **2005**, *5*, 869-878.

17. Boddapati, S. M.; Mutchu, B. R.; Saketi, J. M. R.; Gokada, M. R.; Patchipala, S. B.; Bollikolla, H. B. *Caribbean Journal of Sciences and Technology* **2021**, *9*, 20-34.

18. Wu, X.; Ji, H. *The Journal of Organic Chemistry* **2018**, *83*, 4650-4656.

19. Zhou, J.; Yin, C.; Zhong, T.; Zheng, X.; Yi, X.; Chen, J.; Yu, C. *Organic Chemistry Frontiers* **2021**, *8*, 5024-5031.

20. Yin, C.; Zhong, T.; Zheng, X.; Li, L.; Zhou, J.; Yu, C. *Organic & Biomolecular Chemistry* **2021**, *19*, 7701-7705.

21. Kim, K.; Han, S. H.; Jeoung, D.; Ghosh, P.; Kim, S.; Kim, S. J.; Ku, J.-M.; Mishra, N. K.; Kim, I. S. *The Journal of Organic Chemistry* **2020**, *85*, 2520-2531.

22. Karishma, P.; Mandal, S. K.; Sakhuja, R. *Asian Journal of Organic Chemistry* **2021**, *10*, 2580-2590.

23. Karishma, P.; Mahesha, C. K.; Agarwal, D. S.; Mandal, S. K.; Sakhuja, R. *The Journal of Organic Chemistry* **2018**, *83*, 11661-11673.

24. Guo, C.; Li, B.; Liu, H.; Zhang, X.; Zhang, X.; Fan, X. *Organic Letters* **2019**, *21*, 7189-7193.

25. Kang, J. Y.; An, W.; Kim, S.; Kwon, N. Y.; Jeong, T.; Ghosh, P.; Kim, H. S.; Mishra, N. K.; Kim, I. S. *Chemical Communications* **2021**, *57*, 10947-10950.

26. Wu, Y.; Wang, J.; Mao, F.; Kwong, F. Y. *Chemistry–An Asian Journal* **2014**, *9*, 26-47.

27. Tsang, Y. L.; Choy, P. Y.; Leung, M. P.; He, X.; Kwong, F. Y. *Organic Chemistry Frontiers* **2022**, *9*, 1992-2012.

28. Yang, L.; Huang, H. *Catalysis Science & Technology* **2012**, *2*, 1099-1112.

29. Wang, J.; Su, P.; Abdolmohammadi, S.; Vessally, E. *RSC Advances* **2019**, *9*, 41684-41702.

30. Ma, W.; Gandeepan, P.; Li, J.; Ackermann, L. *Organic Chemistry Frontiers* **2017**, *4*, 1435-1467.

31. Carral-Menoyo, A.; Sotomayor, N.; Lete, E. *ACS omega* **2020**, *5*, 24974-24993.

32. Li, B.; Dixneuf, P. H. *Ruthenium in Catalysis* **2014**, 119-193.

33. Bruneau, C.; Dixneuf, P. H. *C-H Bond Activation and Catalytic Functionalization I* **2015**, 137-188.

34. Manikandan, R.; Jeganmohan, M. *Chemical Communications* **2017**, *53*, 8931-8947.

35. Chatani, N. *Bulletin of the Chemical Society of Japan* **2018**, *91*, 211-222.

36. Graczyk, K.; Ma, W.; Ackermann, L. *Organic Letters* **2012**, *14*, 4110-4113.

37. Li, J.; Kornhaaß, C.; Ackermann, L. *Chemical Communications* **2012**, *48*, 11343-11345.

38. Tirler, C.; Ackermann, L. *Tetrahedron* **2015**, *71*, 4543-4551.

39. Padala, K.; Jeganmohan, M. *Organic Letters* **2011**, *13*, 6144-6147.

40. Manikandan, R.; Madasamy, P.; Jeganmohan, M. *ACS Catalysis* **2016**, *6*, 230-234.

41. Zhang, L.; Chen, C.; Han, J.; Huang, Z.-B.; Zhao, Y. *Organic Chemistry Frontiers* **2016**, *3*, 1271-1275.

42. Wang, Y.-J.; Wang, T.-T.; Yao, L.; Wang, Q.-L.; Zhao, L.-M. *The Journal of Organic Chemistry* **2020**, *85*, 9514-9524.

43. Baghel, A. S.; Aghi, A.; Kumar, A. *The Journal of Organic Chemistry* **2021**, *86*, 9744-9754.

44. Lanke, V.; Prabhu, K. R. *Organic Letters* **2013**, *15*, 2818-2821.

45. Lanke, V.; Ramaiah Prabhu, K. *Organic Letters* **2013**, *15*, 6262-6265.

46. Ackermann, L.; Pospech, J. *Organic Letters* **2011**, *13*, 4153-4155.

47. Bechtoldt, A.; Tirler, C.; Raghuvanshi, K.; Warratz, S.; Kornhaaß, C.; Ackermann, L. *Angewandte Chemie International Edition* **2016**, *55*, 264-267.

48. Liu, A.; Han, Q.; Zhang, X.; Li, B.; Huang, Q. *Organic Letters* **2019**, *21*, 6839-6843.

49. Gholamhosseyni, M.; Kianmehr, E. *Organic & Biomolecular chemistry* **2018**, *16*, 5973-5978.

50. Jiang, X.; Yang, Q.; Yuan, J.; Deng, Z.; Mao, X.; Peng, Y.; Yu, C. *Tetrahedron* **2016**, *72*, 1238-1243.

51. Su, L.; Yu, Z.; Ren, P.; Luo, Z.; Hou, W.; Xu, H. *Organic & Biomolecular Chemistry* **2018**, *16*, 7236-7244.

52. Wang, S.-M.; Li, C.; Leng, J.; Bukhari, S. N. A.; Qin, H.-L. *Organic Chemistry Frontiers* **2018**, *5*, 1411-1415.

53. Kona, C. N.; Nishii, Y.; Miura, M. *Organic Letters* **2018**, *20*, 4898-4901.

54. Ackermann, L. *Chemical Reviews* **2011**, *111*, 1315-1345.

55. *APEX2, SADABS and SAINT*; Bruker AXS inc: Madison, WI, USA, **2008**.

56. Sheldrick, G. M. *Acta Crystallographica* **2008**, *A64*, 112.

57. Macrae, C. F.; Bruno, I. J.; Chisholm, J. A.; Edginton, P. R.; McCabe, P.; Pidocck, E.; RodriguezMonge, L.; Taylor, T.; Van de Streek, J.; Wood, P. A. *Journal of Applied Crystallography* **2008**, *41*, 466.

58. Spek, A. L. PLATON, Version 1.62, University of Utrecht, **1999.**

Chapter 2A

Rhodium-Catalyzed [4+2] Annulation of *N*-Arylindazolones with Nitroolefins to access Hydroxyimino-decorated Indazolo[1,2-*a*]cinnolines

2A.1 Introduction

Cinnolines are highly valuable synthetic targets that are often found in many natural products, known to display interesting biological properties. The importance of cinnolines has been further demonstrated by their prevalence in a large number of synthetic analogues with luminescent and optical properties. The natural product, Schizocommunin,[1] and other synthetic molecules such as 4849F[2] and ARC-31[3] are representative examples of functionalized and fused-cinnolines with promising anticancer activity (Figure 2A.1.1). Furthermore, cinnoline-fused heterocycles have exemplified interesting anti-inflammatory, antimicrobial, analgesic, anticancer and anxiolytic activities due to their ability to interact with molecular receptors, such as CSF-1R, GABA A, H3R enzymes, including human neutrophil elastase, cyclooxygenase-2, phosphodiesterase, topoisomerases, Bruton's tyrosine kinase, *etc*.[4-16] Strikingly, fluorescent cinnoline-based dyes have been successfully employed for their cellular-based imaging applications (Figure 2A.1.1).[4-16]

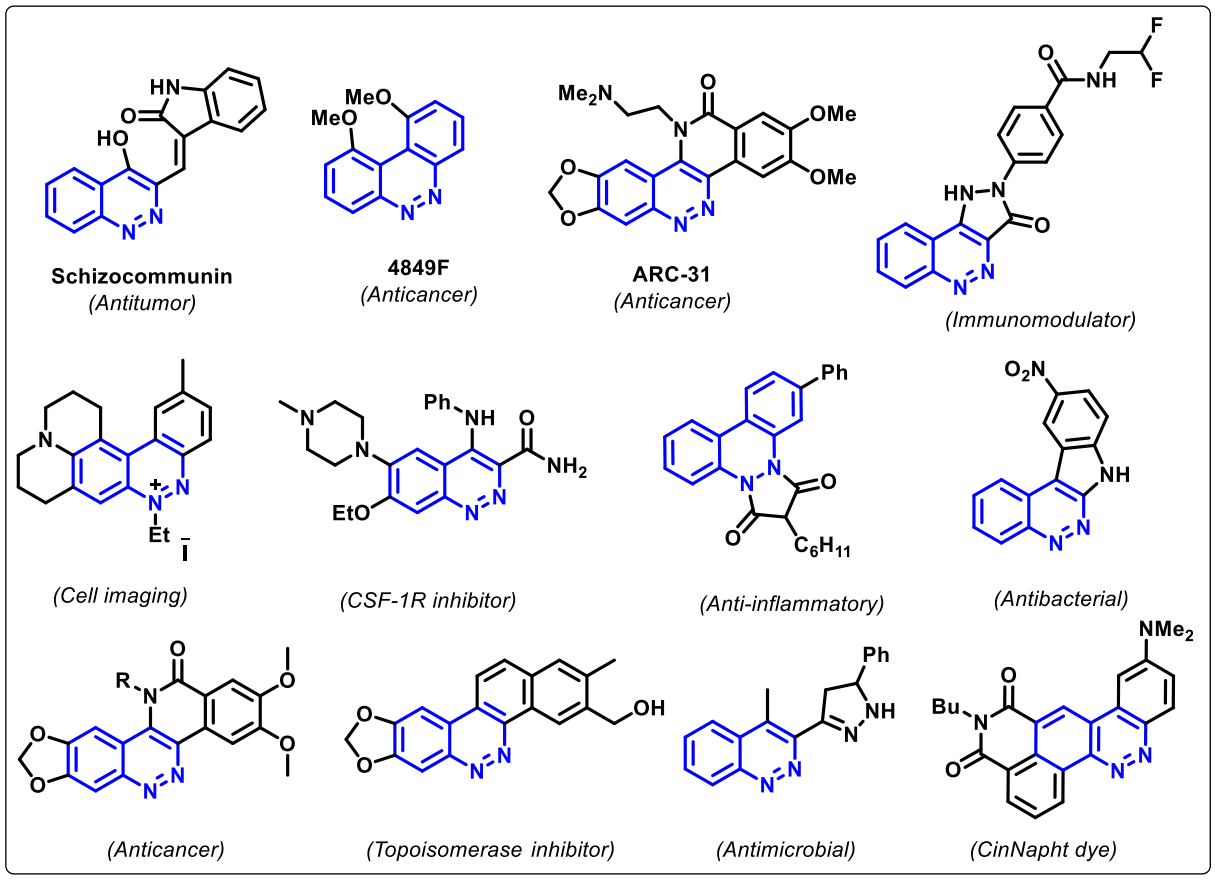

Figure 2A.1.1 Selective examples of biologically active naturally-occurring, and synthetic functionalized and fused-cinnolines

In spite of their immense synthetic, commercial, and therapeutic potential, the traditional methods for the construction of cinnoline nucleus are surprisingly limited. Thus, the strategies for the construction of cinnoline-fused heterocyclic frameworks *via* transition-metal (TM)-catalyzed oxidative annulation with varied coupling partners have received special attention in recent times. In the midst of various strategies, pyrazolo-fused cinnolines have been successfully accessed *via* transition metal-catalyzed directing group-mediated cross-dehydrogenative coupling between *N*-arylpyrazolidinones (**1**) with various coupling partners. For example, Huang and Lin groups independently reported synthesis of pyrazolo[1,2–*a*]cinnolines (**3a** and **3b**) through Rh^{III}-catalyzed [4+2] annulations of *N*-arylpyrazolidin-3-ones (**1**) with *α*-*O*-mesyl ketones (**2**) and *α*-ketodiazo compounds (**4**), respectively (Scheme 2A.1.1a-b).[17-18] In 2021, Zhao's group utilized sulfoxonium ylides (**5**) as coupling partners with to prepare 1,2-dihydro-3*H*-pyrazolo[1,2-*a*]cinnolin-3-ones (**3a**) from *N*-arylpyrazolidin-3-ones (**1**) under Ru^{II}-catalysis (Scheme 2A.1.1c).[19]

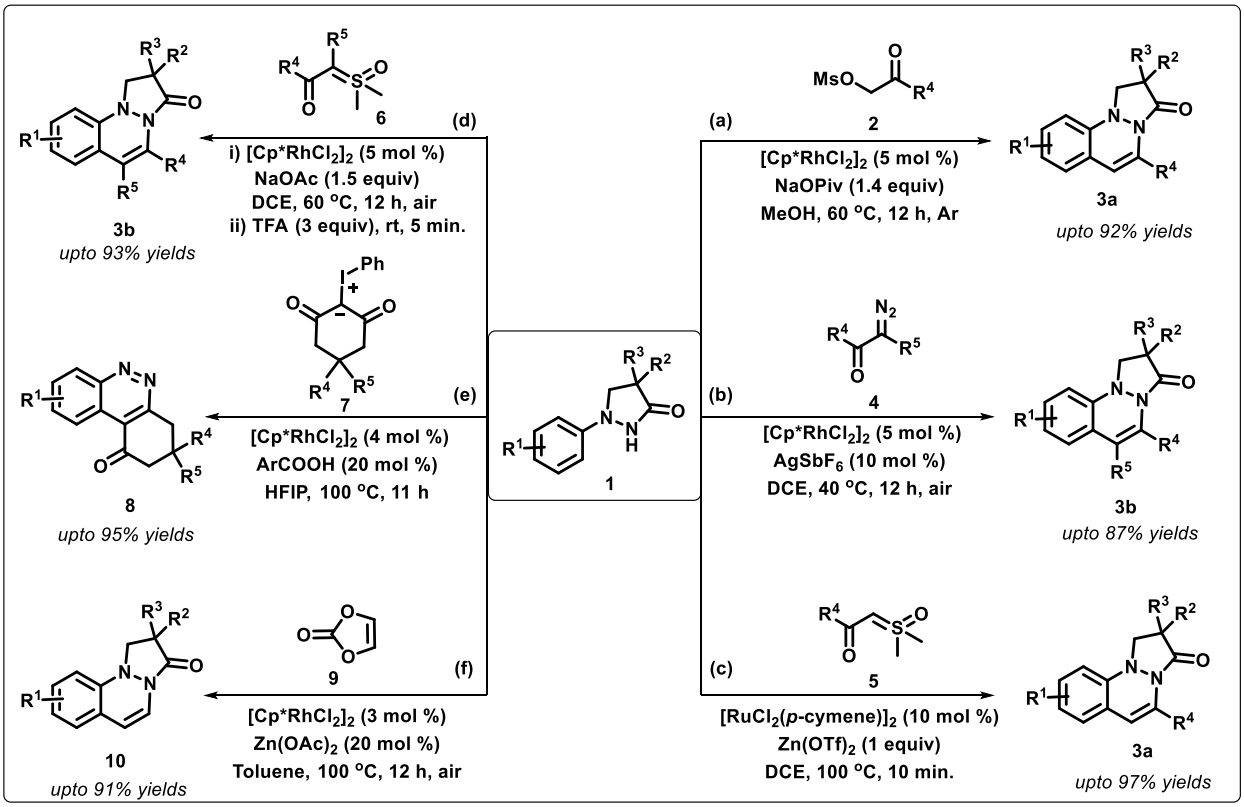

Scheme 2A.1.1 Transition metal-catalyzed synthesis of fused-cinnolines from *N*-arylpyrazolidinones

Likewise, Liu and Wang's group established another strategy to synthesize pyrazolo[1,2-*a*]cinnolines (**3b**) or their hydrogenated counterparts *via* Rh^{III}-catalyzed C−H activation of *N*-

arylpyrazolidin-3-ones (**1**), and its subsequent annulation with substituted sulfoxonium ylides (**6**) (Scheme 2A.1.1d).[20] Very recently, Li and Hu's groups established a facile route to tetrahydrobenzo[*c*]cinnolin-1(2*H*)-one (**8**) *via* annulation of *N*-arylpyrazolidin-3-ones (**1**) with iodonium ylides (**7**) under Rh^{III}-catalysis (Scheme 2A.1.1e).[21] From the inspiration of these results, Fan *et al*. developed another efficient and robust methodology to obtain 1,2-dihydro-3*H*-pyrazolo[1,2-*a*]cinnolin-3-ones (**10**) *via* Rh^{III}-catalyzed C–H functionalization and annulation of *N*-arylpyrazolidin-3-ones (**1**) with vinylene carbonate (**9**) (Scheme 2A.1.1f).[22]

Furthermore, Zhang *et al*. reported an alternative procedure to synthesis pyrazolo[1,2-*a*]cinnolines (**13**) through Rh^{III}-catalyzed oxidative coupling of *N*-aryl-1*H*-pyrazol-5(4*H*)-ones (**11**) with internal alkynes (**12**) using the assistance of amide directing group in the presence of HFIP solvent (Scheme 2A.1.2).[23]

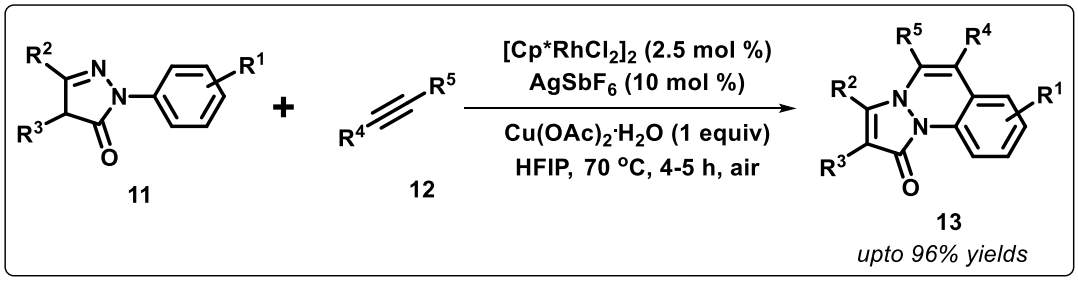

Scheme 2A.1.2 Rh^{III}-catalyzed synthesis of pyrazolo-fused cinnolines from *N*-aryl-1*H*-pyrazol-5(4*H*)-ones

In recent years, *N*-aryl-2,3-dihydrophthalazine-1,4-diones (**14**) have also been utilized as prime substrates for annulating different coupling partners to assemble phthalazino-fused cinnolines *via* C-H activation/functionalization/cyclization protocol with the assistance of Ru^{II}, Rh^{III} or Ir^{III} catalysts. For example, in the year 2015, Gandhi *et al.* established a protocol for Ru^{II}-catalyzed synthesis of phthalazino[2,3-*a*]cinnoline-8,13-dione (**16**) from *N*-aryl-2,3-dihydrophthalazine-1,4-dione (**14**) through the insertion and unusual deoxy-oxidative annulation of propargyl alcohols (**15**) (scheme 2A.1.3a).[24] Another indistinguishable method was developed by Perumal's group to construct phthalazino[2,3-*a*]cinnolines (**17**) in excellent regioselectivity by treating *N*-aryl-2,3-dihydrophthalazine-1,4-diones (**14**) with internal alkynes (**12**) under Rh^{III}-catalyzed conditions (scheme 2A.1.3b).[25] In 2018, our group, and Wang's group independently reported [4+2] annulation of *N*-aryl-2,3-dihydrophthalazine-1,4-diones (**14**) with *α*-diazo carbonyl compounds (**4** & **18**), accessing a series of phthalazino-fused cinnolines (**17** & **19**) in good-to-excellent yields under Rh^{III} and Ir^{III}-catalysis, respectively.[26-27] In both the strategies, the reaction route was

described to proceeded *via* consecutive C-H activation, carbene insertion and intermediate condensation to afford tetra- and pentacyclic fused-cinnolines (Scheme 2A.1.3c-d). Taking the advantage of vinylene carbonates (**9**) as vinyl transfer agent, Kim *et al*. achieved its [4+2] annulation with *N*-aryl-2,3-dihydrophthalazine-1,4-diones (**14**). In this process, with the usage of Rh^{III}-catalyst, the authors successfully established two different methodologies to obtain tetracyclic phthalazino-fused hydroxycinnolines[28] (**20**) and phthalazino-fused-cinnolines[29] (**21**) under mild conditions (Scheme 2A.1.3e-f).

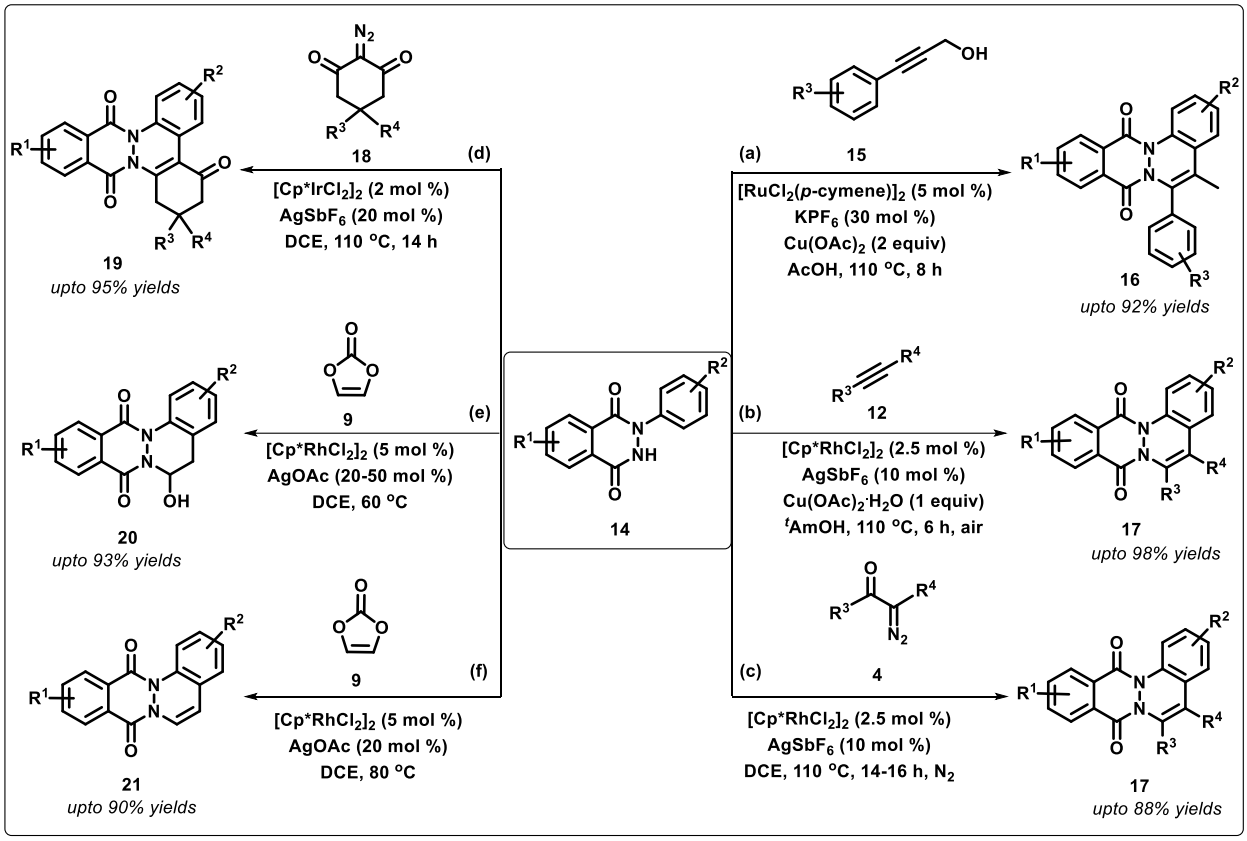

Scheme 2A.1.3 Transition metal-catalyzed synthesis of phthalazino-fused cinnolines from *N*-aryl-2,3-dihydrophthalazine-1,4-diones

In continuation, our group has also developed a two-step protocol to synthesize phthalazino-fused cinnolines (**23** & **24**) by first isolating *ortho*-acylmethylated products (**22**) *via* Ru^{II}-catalyzed *ortho*-C-H functionalization of *N*-aryl-2,3-dihydrophthalazine-1,4-diones (**14**) with *α*-carbonyl sulfoxonium ylides (**5**). These *ortho*-acylmethylated products (**22**) underwent cyclization in the presence of Lawesson's reagent or $BF_3{\cdot}Et_2O$ in DMSO to afford 6-arylphthalazino[2,3-*a*]cinnoline-8,13-diones (**23**) and 5-acyl-5,6-dihydrophthalazino[2,3-*a*]cinnoline-8,13-diones (**24**) respectively (Scheme 2A.1.4a).[30] Very similar to this work, Yu *et al.* achieved Ru^{II}-catalyzed

C−H/N−H functionalization in one-pot to access phthalazino[2,3-*a*]cinnolindiones (**24**) by the annulation of *N*-aryl-2,3-dihydrophthalazine-1,4-diones (**14**) with sulfoxonium ylides (**5**) (Scheme 2A.1.4b).[31]

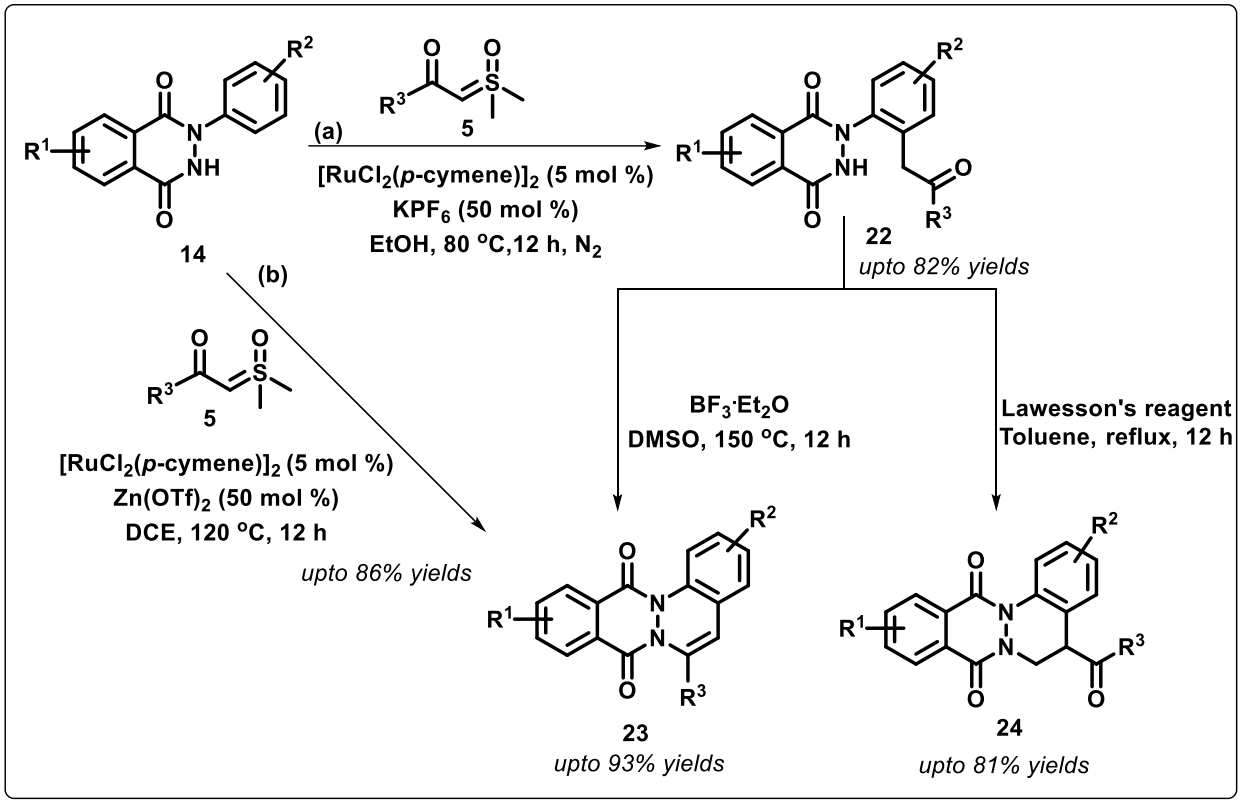

Scheme 2A.1.4 Ru-catalyzed synthesis of phthalazino-fused cinnolines from *N*-aryl-2,3-dihydrophthalazine-1,4-diones

Under the same domain, *N*-aryl-1,2-dihydro-3*H*-indazol-3-one, another pivotal heterocyclic analogue, has been explored by several eminent research groups in recent years to access indazolo-fused cinnolines *via* transition metal-catalyzed cross-dehydrogenative coupling (CDC) with different coupling partners. The first report on this system appeared in 2016 by Perumal and coworkers, in which *N*-aryl-1,2-dihydro-3*H*-indazol-3-one (**25**) and internal alkynes (**12**) were coupled to construct indazolo-fused cinnolines (**26**) *via* oxidative annulation under Rh^{III}-catalysis with the aid of $Cu(OAc)_2 \cdot H_2O$ as an oxidant (Scheme 2A.1.5a).[25] Thereafter, a few reports by other groups have been documented from the same starting material either paralleled or subsequently with the work conducted by our group (Scheme 2A.1.5).

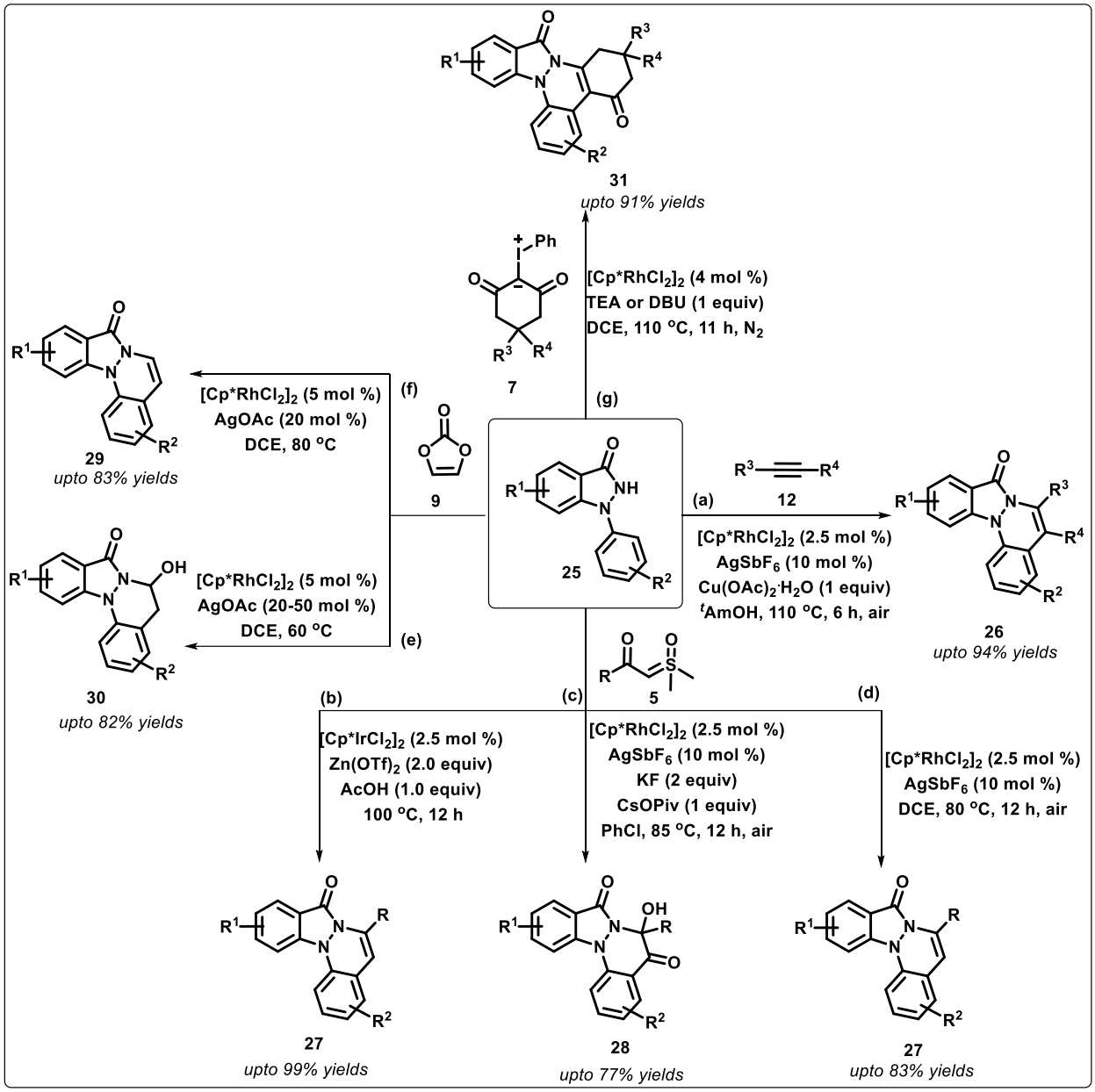

Scheme 2A.1.5 Rh/Ir-catalyzed synthesis of indazolo-fused cinnolines from *N*-aryl-1,2-dihydro-3*H*-indazol-3-ones

For example, Zhang *et al.* systematically prepared chemically divergent indazolo[1,2-*a*]cinnolines (**27** & **28**) from *N*-aryl-1,2-dihydro-3*H*-indazol-3-ones (**25**) and sulfoxonium ylides (**5**) as carbene precursors through the process of Ir^{III} and Rh^{III}-catalyzed Csp^2-H activation/oxidation/annulation cascade protocols. The showcased fused-cinnolines were found to be suitable for late-stage modification of drug molecules (Scheme 2A.1.5b-c).[32] Similar type of tetracyclic indazolo-fused cinnolines (**27**) have been synthesized by Yu's group from the same starting materials under Rh^{III}-

catalyzed conditions[21] (Scheme 2A.1.5d). Also, Kim and coworkers reported two different strategies to furnish tetracyclic indazolo[1,2-*a*]cinnolines (**29** & **30**) by using 1-aryl-1,2-dihydro-3*H*-indazol-3-ones (**25**) and vinylene carbonates (**9**) under two different Rh^{III} catalyzed conditions (Scheme 2A.1.5e-f).[29-33] Additionally, Hu's group reported only four examples of pentacyclic indazolo-fused cinnolines (**31**) from *N*-aryl-1,2-dihydro-3*H*-indazol-3-one (**25**) and easily available iodonium ylides (**7**) *via* Rh^{III}-catalyzed C-H/N-H functionalization (Scheme 2A.1.5g).[21] In addition to these reports, Hou, Xu and coworkers added another set of fruitful strategies to prepare indazolo[1,2-*a*]cinnolines (**33**) by coupling 2-aryl-1,2-dihydro-3*H*-indazol-3-one (**32**) with *α*-diazo carbonyl compound (**4**) in the presence of cationic ruthenium complex or Rh^{III}-catalysis. The reactions were believed to proceed through *ortho*-Csp^2-H activation, metal-carbene formation from diazo compounds, migratory insertion of carbine, and finally protonolysis followed by dehydration to lead to the target products (Scheme 2A.1.6a-b).[34-35]

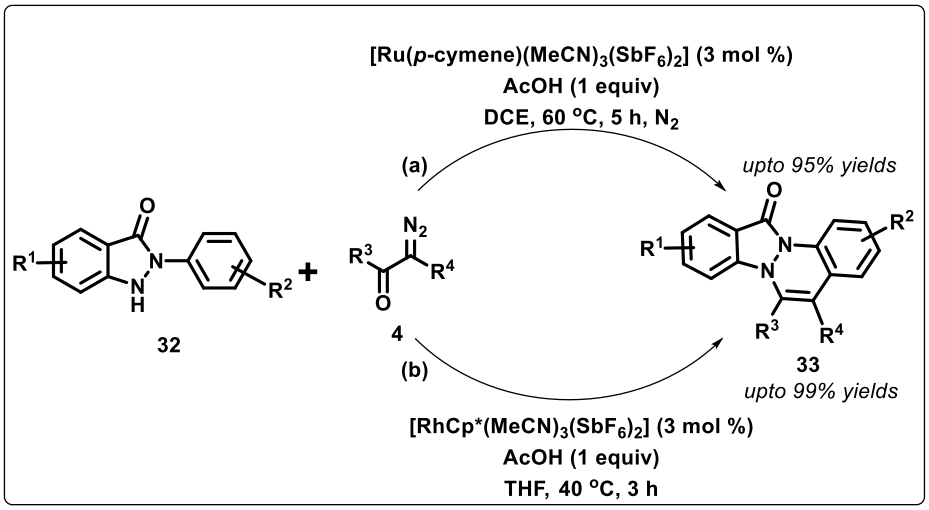

Scheme 2A.1.6 Rh/Ru-catalyzed synthesis of indazolo-fused cinnolines from 2-aryl-1,2-dihydro-3*H*-indazol-3-ones

In striking analogy to above coupling partners, nitroolefins (**34**) are intriguing electrophilic synthons that have been considerably utilized as substrates in various classical transformations, including Friedel-Crafts alkylation[36] (*e.g.* product **36**), Michael addition[37] (*e.g.* product **38**), 1,3-dipolar cycloaddition[38] (*e.g.* product **40**) and [2+2] cycloaddition reactions[39] (*e.g.* product **42**) (Scheme 2A.1.7). Moreover, they have been utilized for the synthesis of diverse chemically interesting molecules, such as oximes, hydroxylamines, nitroalkanes, aliphatic amines, and nitroso compounds. Often nitroolefins have been used as valued starting materials for constructing C-C

bonds in the total synthesis of natural products, heterocyclic compounds and asymmetric molecules.

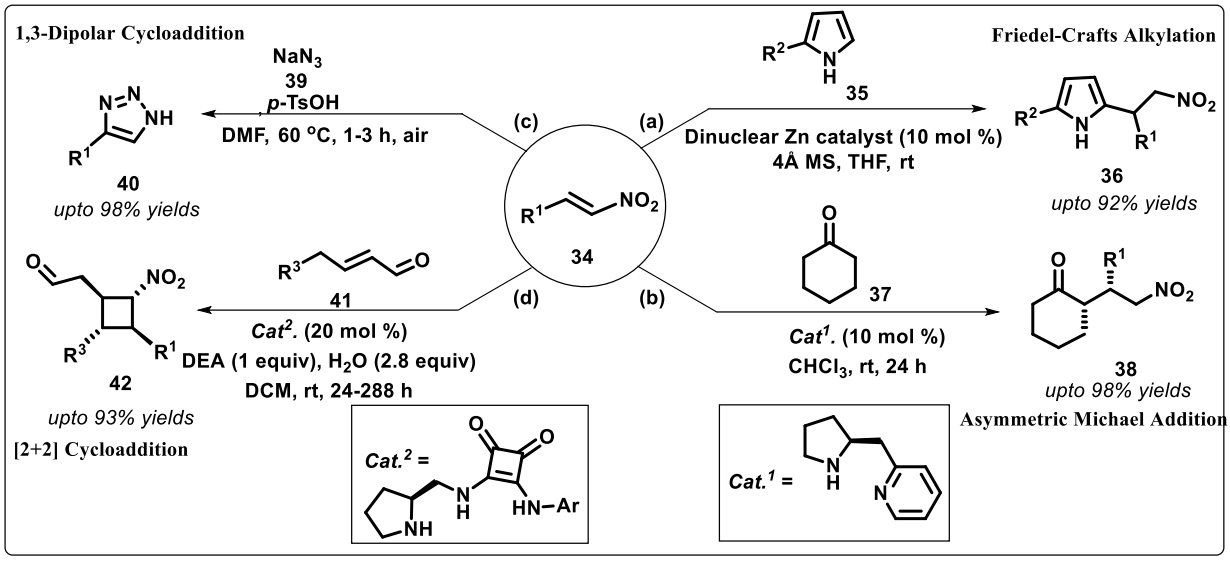

Scheme 2A.1.7 Selective exemplification of classical nitroolefin reactions

In addition, nitroolefins (**34**) have also been employed for coupling with a number of electrophiles, such as formaldehyde (**43**), acrylates (**45**), aldimines (**47**), azadicarboxylates (**49**), and ketoesters (**51**) *etc*. to prepare diversified nitro-substituted molecules (Scheme 2A.1.8).[40-44]

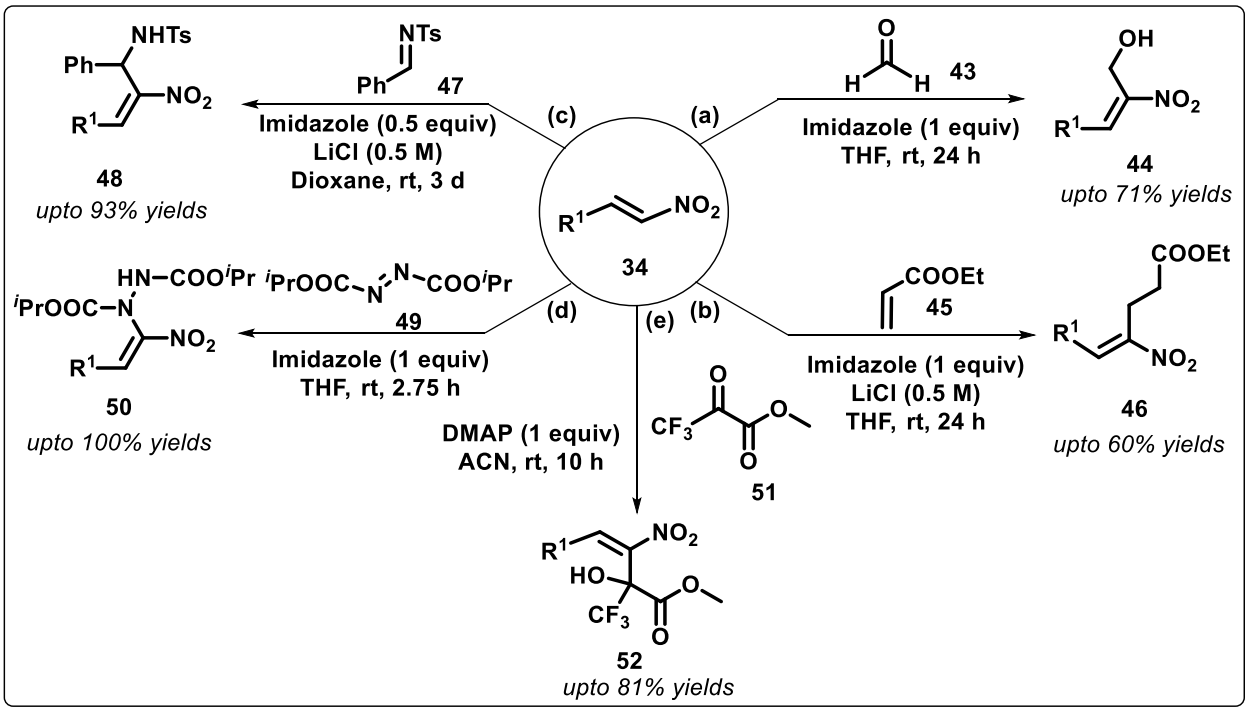

Scheme 2A.1.8 Selective exemplification of coupling of nitroolefins with various electrophiles

Recently, nitroolefins have been used for the construction of C-C bonds *via* transition metal-catalyzed organic transformations. However, the utilization of nitroolefins in the field of C-H activation/functionalization has been explored only to a limited extent. Firstly, in the year 2016, Pan's group utilized nitrostyrenes (**34**) for the C_1-benzoylation of isoquinoline *N*-oxides (**53**) *via* remote C-H activation and subsequent intramolecular oxygen atom transfer with the assistance of N-O bond as a directing group. This reaction proceeded with $Pd(OAc)_2$ as the catalyst in DMSO without employing the usage of any ligands, additives or oxidants (Scheme 2A.1.9).[45]

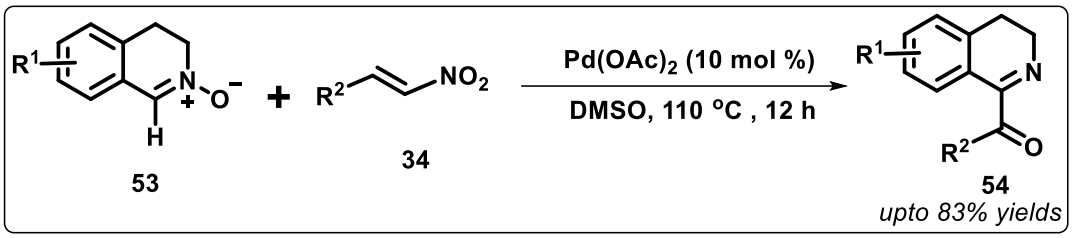

Scheme 2A.1.9 Pd-catalyzed benzoylation of isoquinoline *N*-oxides using nitroolefins

In the year 2017, Ellman *et al.* reported a strategy involving Rh^{III}-catalyzed addition of aryl and alkenyl Csp^2-H bonds to nitroolefins (**34**) to prepare nitroalkylated products (**56**) in appreciable yields. The developed strategy dictated broad range of C-H functionalization substrates (**55**) with appropriate directing groups (Scheme 2A.1.10).[46]

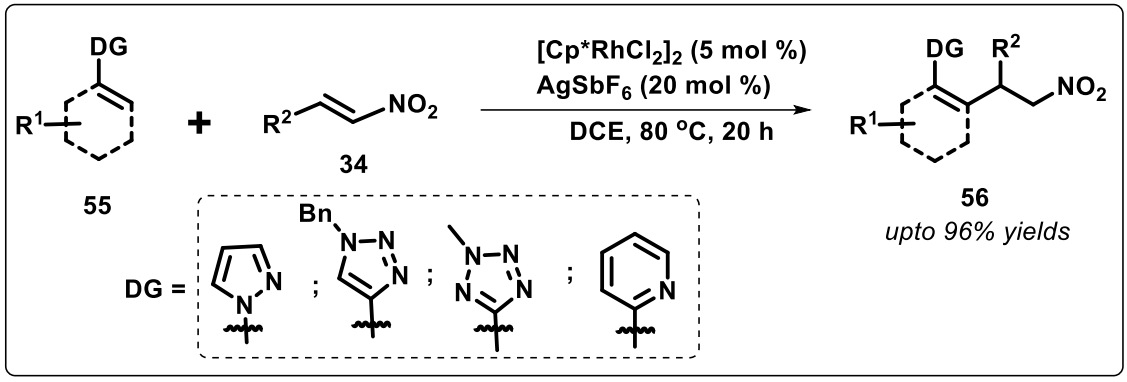

Scheme 2A.1.10 Rh-catalyzed nitroalkylation of varied substrates with nitroolefins

Chang and Li's group developed Rh^{III}-catalyzed synthesis of nitro-functionalized indenes (**58**) from arylnitrones (**57**) and nitroolefins (**34**) *via* a sequential process, involving C-H activation, migratory insertion, protonolysis and intramolecular Henry-type reaction (Scheme 2A.1.11a).[47] Similarly, Zhang *et al.* developed another facile and expeditious protocol for the synthesis of nitro and amine-functionalized indenes (**60**) from readily available starting materials, such as benzimidates (**59**) and nitroolefins (**34**) through Rh^{III}-catalyzed C-H activation and cyclization

protocol (Scheme 2A.1.11b).[48] Additionally, Kim *et al.* described Rh^{III}-catalyzed diastereoselective synthesis of nitro-functionalized 1-aminoindanes (**62**) from *N*-sulfonyl aldimines (**61**) and various activated nitroolefins (**34**) through C-H alkylation followed by intramolecular cyclization (Scheme 2A.1.11c).[49]

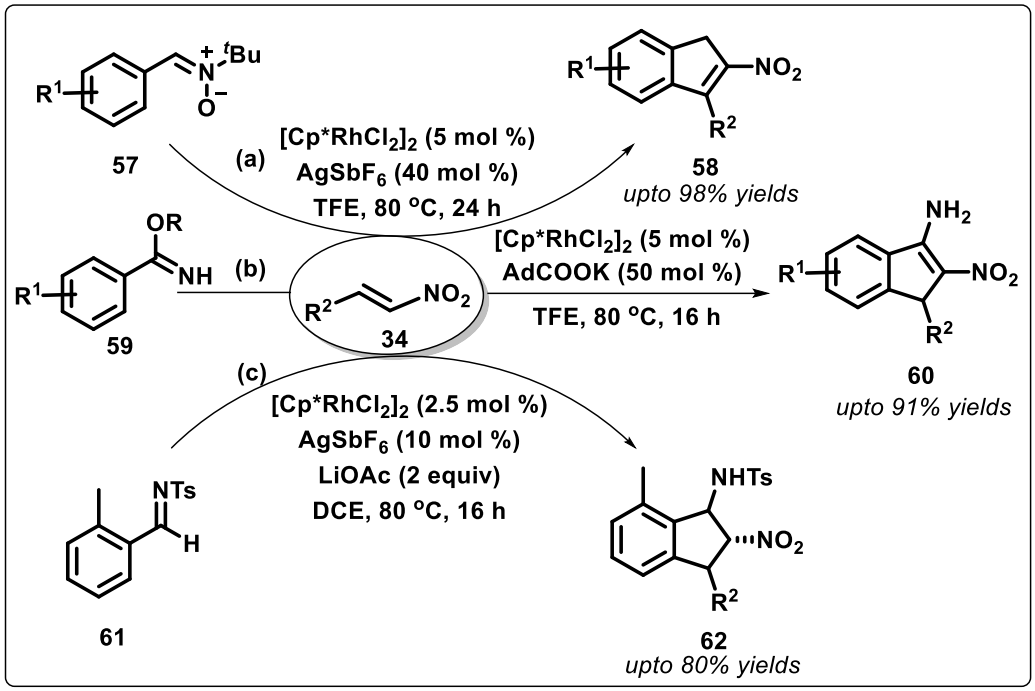

Scheme 2A.1.11 Rh-catalyzed synthesis of nitro-functionalized indenes/indanes from nitroolefins

Ellamn and Ward's group demonstrated an easy handling approach to access 4-substituted isoquinolones (**64**) by the annulation of *N*-methoxyamides (**63**) and nitroolefins (**34**) *via* amide-group directing Rh^{III}-catalyzed C-H activation, nitroalkene addition and annulation with the elimination of H_2O and nitroxyl (HNO) group (Scheme 2A.1.12).[50]

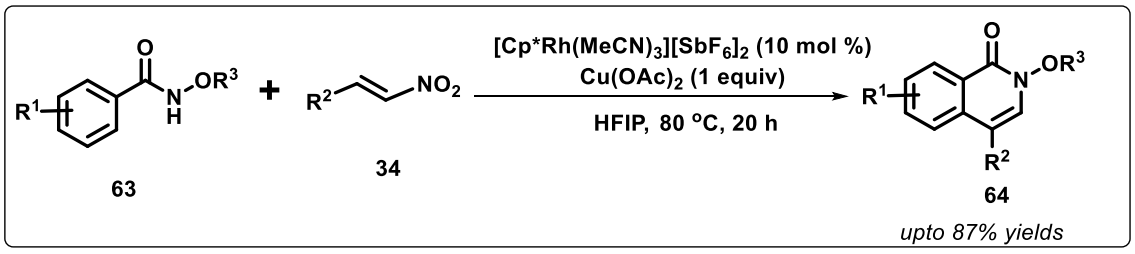

Scheme 2A.1.12 Rh-catalyzed synthesis of 4-substituted isoquinolones from nitroolefins

Deb and co-workers established an Ir^{III}-catalyzed [3+2] annulation of weakly coordinating *N*-sulfonyl ketimines (**65**) with nitroolefins (**34**) to access nitro-substituted spirocyclic benzosultams (**66**) with the generation of three consecutive stereogenic centers in a single step *via* redox-neutral

C-H functionalization (Scheme 2A.1.13a).[51] Analogously, the same group developed another [3+2] stereoselective spiroannulation of benzoxazines (**67**) with nitroolefins (**34**) to obtain nitro-substituted spirocyclic 2,3-dihydro-1,4-benzoxazine derivatives (**68**) under Rh^{III}-catalyzed conditions (Scheme 2A.1.13b).[52] Very recently in the year 2022, Xu, Li group reported a [3+2] spirocyclization protocol to construct C2-quaternary-indole-3-ones (**70**) from pseudo-indolones (**69**) and nitroolefins (**34**). In this spirocyclization process, four diasteroisomers could be selectively obtained under appropriate reaction conditions (Scheme 2A.1.13c).[53]

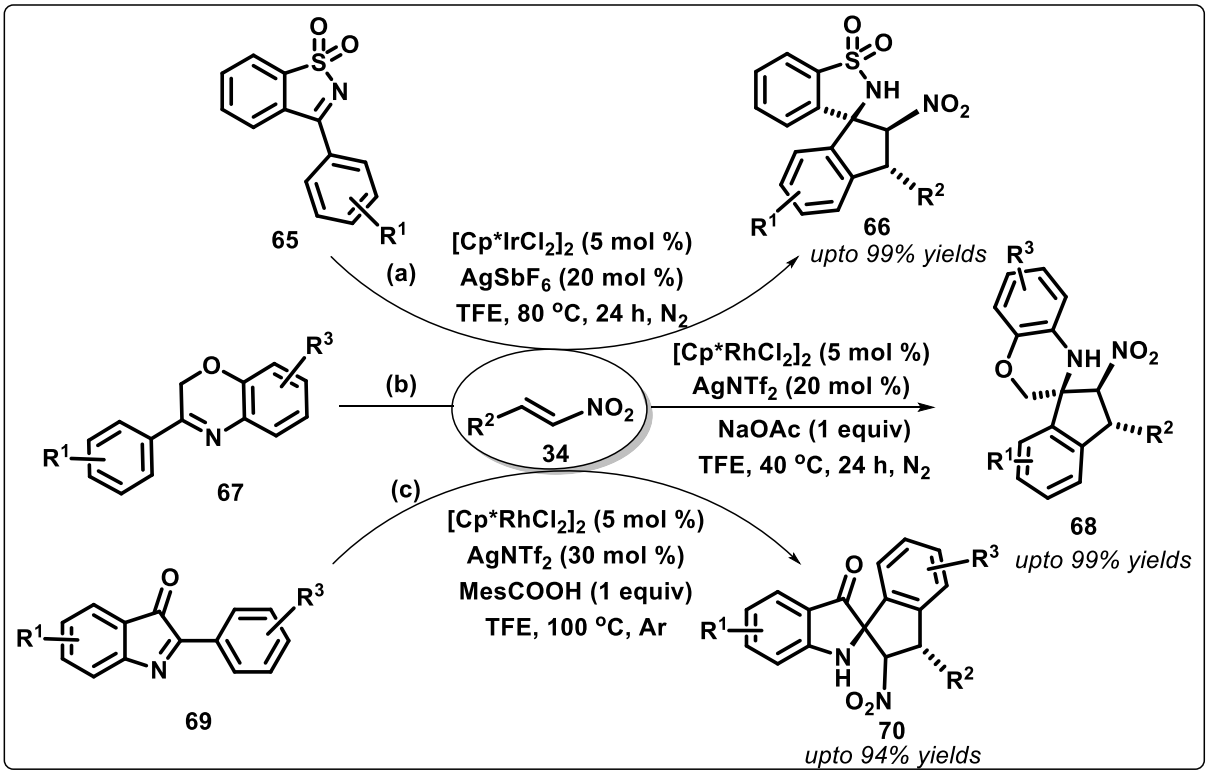

Scheme 2A.1.13 Ir- and Rh-catalyzed [3+2] spirocyclization strategies with nitroolefins

Interestingly, the functionalization of *N*-arylindazolones (**25**) remains unexplored with nitroolefins (**34**). In the backdrop of the above discussion and anticipating the potential directing group ability of indazolone moiety, we envisioned that *N*-arylindazolones could be selectively functionalized using nitroolefins under metal-catalyzed conditions. In this chapter, we present our systematic results on the accomplished Rh-catalyzed [4+2] annulation between 1-aryl-1,2-dihydro-3*H*-indazol-3-ones (**25**) and nitroolefins (**34**) *via* sequential C−H activation/olefin insertion/reduction pathway to afford hydroxyimino-decorated indazolo[1,2-*a*]cinnolines (**71**) in high yields.

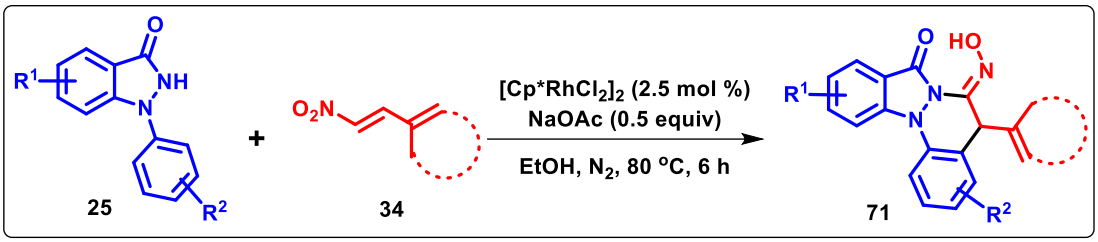

Scheme 2A.1.14 Rh-catalyzed [4+2] annulation of 1-aryl-1,2-dihydro-3*H*-indazol-3-ones with nitroolefins

2A.2 Results and Discussion

This study commenced with optimizing the reaction condition for the coupling between 1-phenyl-1,2-dihydro-3*H*-indazol-3-one (**25a**) and *β*-nitrostyrene (**34a**) as model substrates, employing rhodium catalysis (Table 2A.2.1). Unfortunately, the coupling between the model substrates did not proceed using $[Cp^*RhCl_2]_2$ as a catalyst in ethanol at varied temperature conditions (Table 2A.2.1, entry 1). The use of additives such as $Cu(OAc)_2$, Cs_2CO_3, and $AgSbF_6$ remained ineffective to initiate any reaction under Rh catalysis (Table 2A.2.1, entries 2−4). Interestingly, a combination of $[Cp^*RhCl_2]_2$ with KPF_6 or NaOAc or CsOAc promoted the coupling reaction in ethanol at 40 °C under nitrogen atmosphere to afford 6-(hydroxyimino)-5-phenyl-5,6-dihydro-8*H*-indazolo[1,2-*a*]cinnolin-8-one (**71aa**) in 32%, 45%, and 40% yields, respectively (Table 2A.2.1, entries 5−7). The structure of **71aa** was unambiguously confirmed by its detailed spectroscopic analysis, including ^1H and ^{13}C NMR, COSY, HSQC, HMBC, and HRMS. To our delight, 74% of **71aa** was obtained by carrying the coupling between **25a** and **34a** using the $[Cp^*RhCl_2]_2$/NaOAc catalytic system at 80 °C in ethanol (Table 2A.2.1, entry 8). Further optimization indicated that lowering of additive loading to 25 mol % produced a detrimental effect on the yield of **71aa**, while an increment in catalyst or additive loading did not produced any noticeable effect (Table 2A.2.1, entries 9−11). Finally, solvent screening studies suggested the sensitivity of the reaction toward the choice of solvent. The use of TFE produced comparable results, while the yield of **71aa** drastically decreased when toluene, THF, and ACN were used (Table 2A.2.1, entries 12−15). However, polar aprotic solvents such as DMF and DMSO were complete unfavorable for this transformation (Table 2A.2.1, entries 16 − 17). The coupling under an air atmosphere furnished a 48% yield of **71aa** (Table 2A.2.1, entry 18). Unfortunately, the reaction did not proceed at all using $[RuCl_2(p\text{-cymene})]_2$, $Co(OAc)_2$, and $[Ir(COD)Cl]_2$ as catalysts, under the described conditions (Table 2A.2.1, entries 19−21).

Table 2A.2.1 Selective optimization[a] studies for the synthesis of 71aa

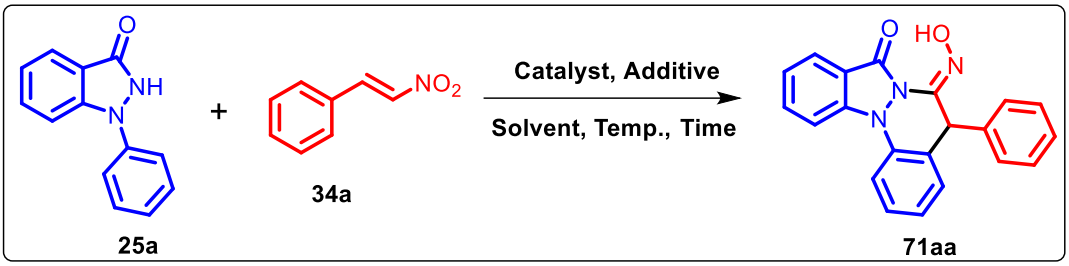

Entry	Catalyst (mol %)	Additive (mol %)	Solvent	Temp. (°C)	Yield of 71aa (%)[b]
1.	$[Cp^*RhCl_2]_2$ (2.5)	-	EtOH	25-80[c]	-
2.	$[Cp^*RhCl_2]_2$ (2.5)	$Cu(OAc)_2$ (50)	EtOH	40	-
3.	$[Cp^*RhCl_2]_2$ (2.5)	Cs_2CO_3 (50)	EtOH	40	-
4.	$[Cp^*RhCl_2]_2$ (2.5)	$AgSbF_6$ (50)	EtOH	40	-
5.	$[Cp^*RhCl_2]_2$ (2.5)	KPF_6 (50)	EtOH	40	32
6.	$[Cp^*RhCl_2]_2$ (2.5)	NaOAc (50)	EtOH	40	45
7.	$[Cp^*RhCl_2]_2$ (2.5)	CsOAc (50)	EtOH	40	40
8.	$[Cp^*RhCl_2]_2$ (2.5)	NaOAc (50)	EtOH	80	74
9.	$[Cp^*RhCl_2]_2$ (2.5)	NaOAc (25)	EtOH	80	51
10.	$[Cp^*RhCl_2]_2$ (2.5)	NaOAc (100)	EtOH	80	76
11.	$[Cp^*RhCl_2]_2$ (5)	NaOAc (50)	EtOH	80	75
12.	$[Cp^*RhCl_2]_2$ (2.5)	NaOAc (50)	TFE	80	70
13.	$[Cp^*RhCl_2]_2$ (2.5)	NaOAc (50)	Toluene	80	32
14.	$[Cp^*RhCl_2]_2$ (2.5)	NaOAc (50)	THF	80	27
15.	$[Cp^*RhCl_2]_2$ (2.5)	NaOAc (50)	ACN	80	20
16.	$[Cp^*RhCl_2]_2$ (2.5)	NaOAc (50)	DMF	80	-
17.	$[Cp^*RhCl_2]_2$ (2.5)	NaOAc (50)	DMSO	80	-
18.[d]	$[Cp^*RhCl_2]_2$ (2.5)	NaOAc (50)	EtOH	80	48[e]
19.	$[RuCl_2(p\text{-cymene})]_2$ (2.5)	NaOAc (50)	EtOH	80	
20.	$Co(OAc)_2$ (2.5)	NaOAc (50)	EtOH	80	
21.	$[Ir(COD)Cl]_2$ (2.5)	NaOAc (50)	EtOH	80	

[a]Reaction conditions: The reactions are carried out with **25a** (0.24 mmol), **34a** (0.36 mmol) in the presence of catalyst/additive (as indicated in the table) in 5 mL of solvent at specified for 6 h under nitrogen atmosphere. [b]Isolated yields after column chromatography. [c]Reaction time = 12 h. [d]Under air atmoshphere. [e]A number of minor spots appeared in addition to **71aa**.

With the optimized conditions in hand, we first examined the scope of the optimized strategy on a variety of 1-aryl-1,2-dihydro-3*H*-indazol-3-one (**25b**–**j**) using *β*-nitrostyrene (**34a**) as a coupling partner (Scheme 2A.2.1). *para*-Substituted 1-aryl-1,2-dihydro-3*H*-indazol-3-ones possessing electron-donating substituents [substrates: **25b**,**c** (R^2 = 4-CH_3 and 4-OCH_3)] reacted extremely

well with **34a** to produce the expected products, **71ba** and **71ca**, in 79 and 85% yields respectively, while *para*- or *meta*-halo-substituted 1-aryl-1,2-dihydro-3*H*-indazol-3-ones [substrates: **25d**–**g** (R^2 = 4-F, 4-Cl, 4-Br, and 3-Cl)] worked moderately well to afford their corresponding hydroxyimino-fused cinnolines (**71da**–**ga**) in 50–62% yields. Disubstituted substrates, such as 3,4-dimethyl- and 3-chloro-4- methyl-phenyl indazolone [substrates: **25h**–**i**] furnished the desired products, **71ha** and **71ia**, in 80 and 66% yields, respectively. Substitution on the indazolone moiety [substrate: **25j** (R^1 = 5-OCH_3)] undergoes smooth transformation to afford 65% of the expected product (**71ja**). Unfortunately, 1-aryl-1,2-dihydro-3*H*-indazol-3-one substrates possessing 2-Me, 2-Br and 3-NO_2, substitutions on the aryl ring remained unreactive under described conditions. The representative ^{1}H and ^{13}C NMR spectra of **71aa** are shown in Figure 2A.2.1 and Figure 2A.2.2, respectively.

We next focused our investigation on examining the use of nitroolefins for this one-pot Rh-catalyzed reductive annulation strategy (Scheme 2A.2.1). *para*-Substituted nitrostyrenes possessing electron-donating substituents [**71b**–**e** (R^3 = 4-CH_3, 4-OCH_3, 4-$N(CH_3)_2$, and 4-OH)] showcased high reactivity with 1-phenylindazolone (**25a**) to furnish the respective fused-cinnolines (**71ab**–**ae**) in 75–84% yields, while nitrostyrenes with moderately electron-withdrawing halogen substituents [**71f**–**g** (R^3 = 4-F and 4-Cl)] react with moderate reactivity with **25a** to produce the desired products (**71af**–**ah**) in 55–69% yields. The trifluoromethyl-functionalized nitrostyrene (**34i**) showed poor reactivity with **25a** to give 37% of the corresponding indazolo-fused cinnoline (**71ai**). 3,4-Dimethoxy and 3-ethoxy-4-hydroxy substituted nitrostyrenes (**34j**–**k**) offered smooth conversion to produce the corresponding products (**71aj**–**ak**) in 71–73% yields. Pleasingly, the naphthyl- and biphenyl-bearing nitroolefins (**34l**–**m**) rendered the products (**71al**–**am**) in 75–80% yield. Additionally, the reaction was well-tolerated with nitroolefins containing heterocyclic moieties such as thiophene, furan, and indole (**34o**–**q**), affording their respective annulated products (**71ao**–**aq**) in 66–72% yields. Notably, the annulation of **25a** with ((1*E*,3*E*)-4-nitrobuta-1,3-dien-1-yl)benzene (**34n**) provided only 43% yield of **71an**, while annulation of **25a** with (*E*)-1-nitrooct-1-ene (**34r**) afforded **71ar** in 48% yield. However, benzyl-substituted nitroethene, nitro- and cyano-substituted nitrostyrenes failed to produce any product under the described conditions. It is most likely that the presence of electron-withdrawing groups on the phenyl ring in nitrostyrenes decreases the nucleophilicity on C=C double bond, which further disfavors their coordination to rhodium.

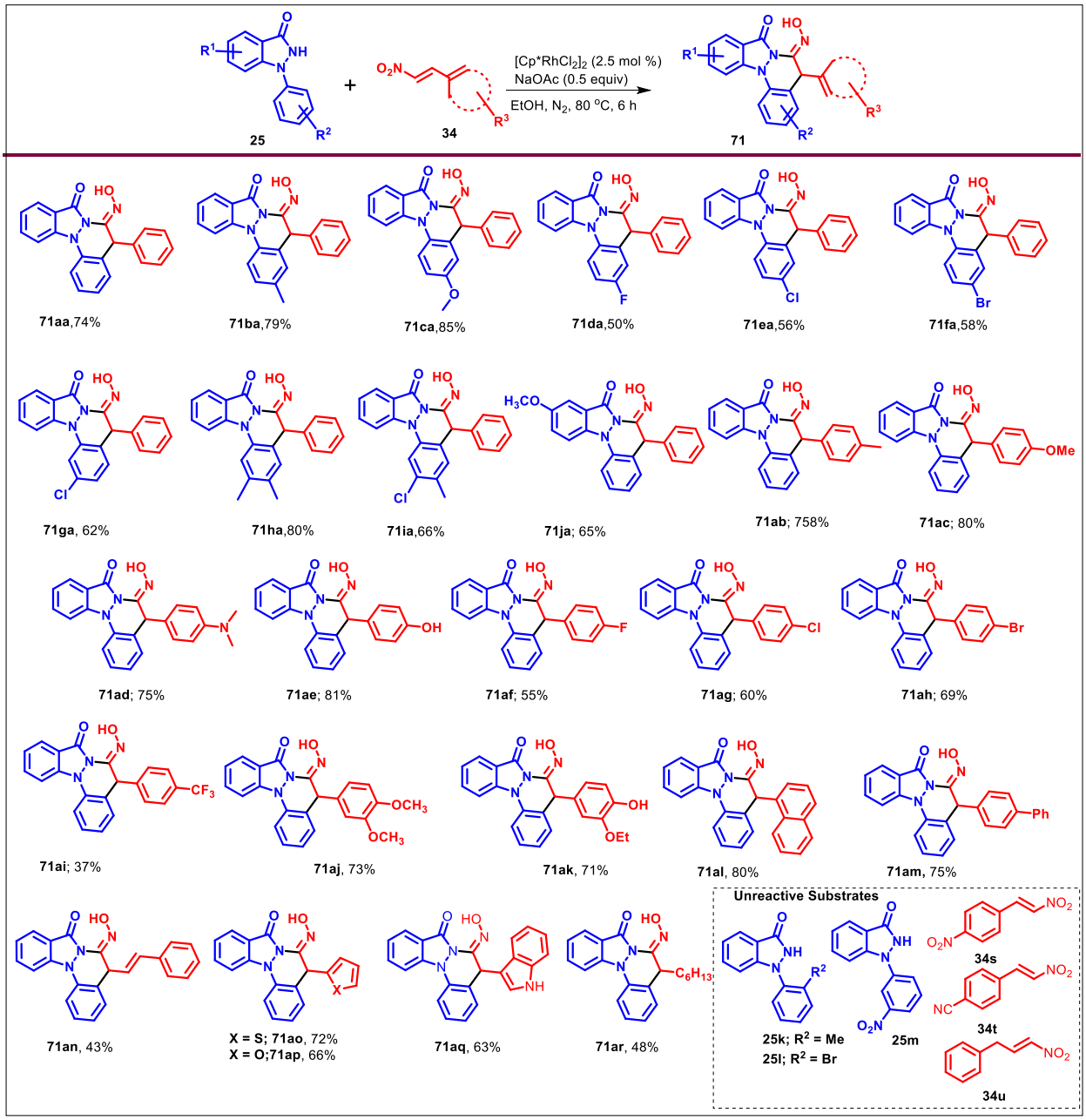

Scheme 2A.2.1 Substrate Scope for annulation of 1-aryl-1,2-dihydro-3*H*-indazol-3-ones and nitroolefins

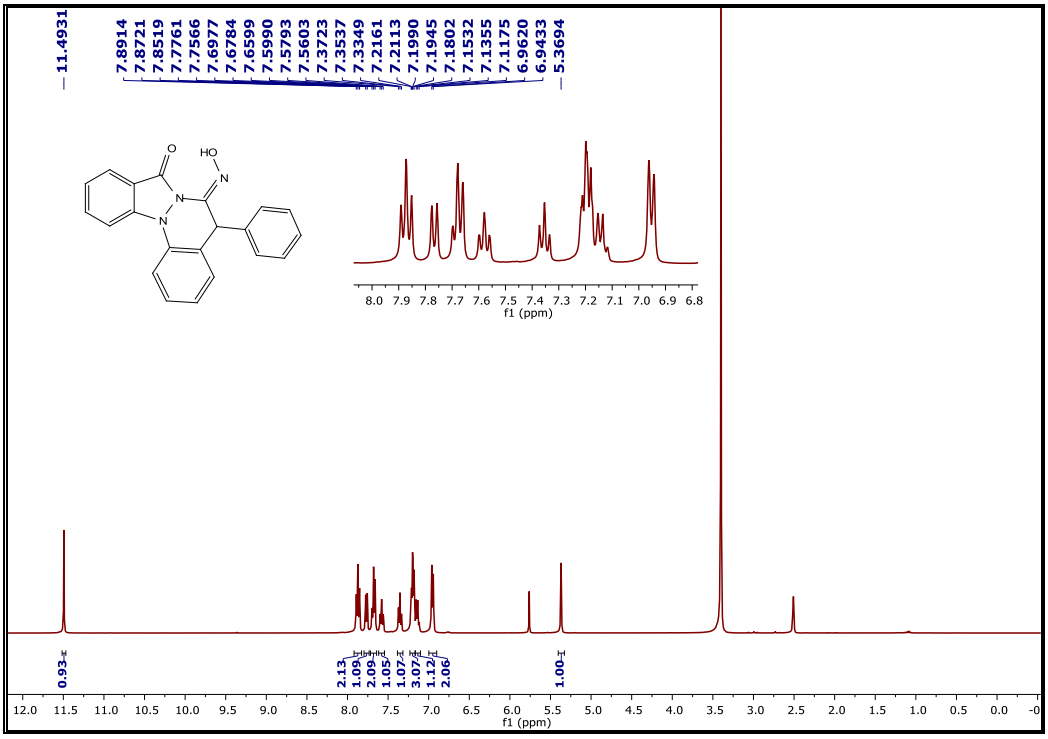

Figure 2A.2.1 ^{1}H NMR Spectrum of **71aa**

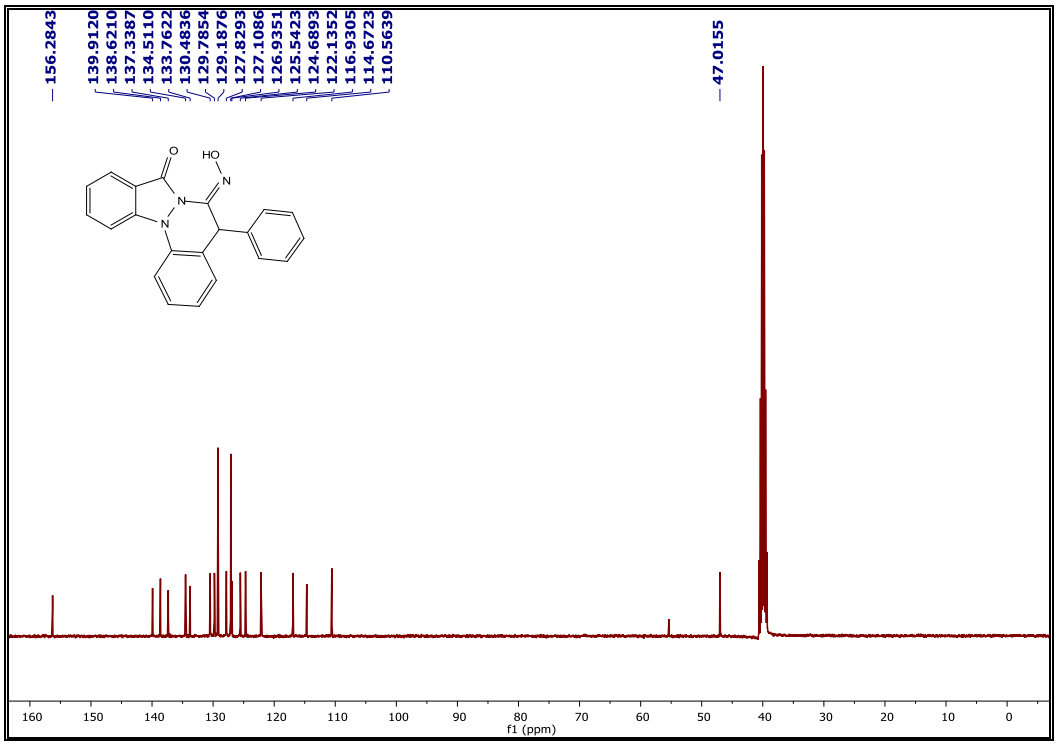

Figure 2A.2.2 ^{13}C NMR Spectrum of **71aa**

As representative examples, single crystals of **71ga** were grown in DMSO, *via* slow evaporation at room temperature. The ORTEP diagrams of **71**ga (CCDC 2040954) is shown in Figure 2A.2.3.

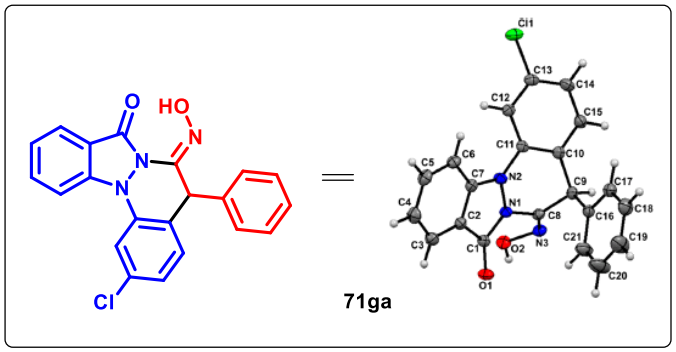

Figure 2A.2.3 ORTEP Diagram of **71ga**

Preliminary mechanistic investigations were conducted to probe the mechanism of the strategy. No considerable declination in the productivity of **71aa** was observed by carrying the reaction between **25a** and **34a** under standard conditions in the presence of TEMPO (3 equiv.) as a radical scavenger, thereby eliminating the possibility of radical mechanism for the established protocol (Scheme 2A.2.2i). Extensive incorporation (~65%) of deuterium atoms at the two *ortho*-positions was observed by carrying out the deuterium-labeling experiment on **25a** under Rh-catalyzed optimized conditions in CD_3OD, which established the reversible nature of the C−H cleavage step (Scheme 2A.2.2ii). In addition, the presence of dihydroxyamino derivative (**F**) was detected in ESI-HRMS of the crude mixture obtained by reacting **25a** with **34a** under standard conditions at 80 °C for 1.5 h (Scheme 2A.2.2iii).

On the basis of previous literature[47-48,54] and our preliminary mechanistic investigations, the reaction could be believed to be triggered by the formation of reactive $[Cp^*Rh^{III}(OAc)_2]$ species *via* acetate-ion-mediated dissociation of dimeric $[Cp^*RhCl_2]_2$ (Scheme 2A.2.3). This further activates the substrate (**25**) *via* N−H ligand exchange to produce species **A**, which subsequently furnishes a five-membered rhodacyclic intermediate (**C**) by C−H activation possibly through the SEAr mechanism *via* **B**. Next, the coordination of nitroolefine (**34**) followed by its insertion into the C_{Ar}−Rh bond generates species **E** *via* **D**. Thereafter, acetate-ion-mediated demetalation concomitant with the protonation of the two oxygen atoms of the nitro group produces **F**, along with the regeneration of active Rh^{III} species for the next catalytic cycle. Finally, dehydration in **F** leads to the oxime decorated product (**71**).

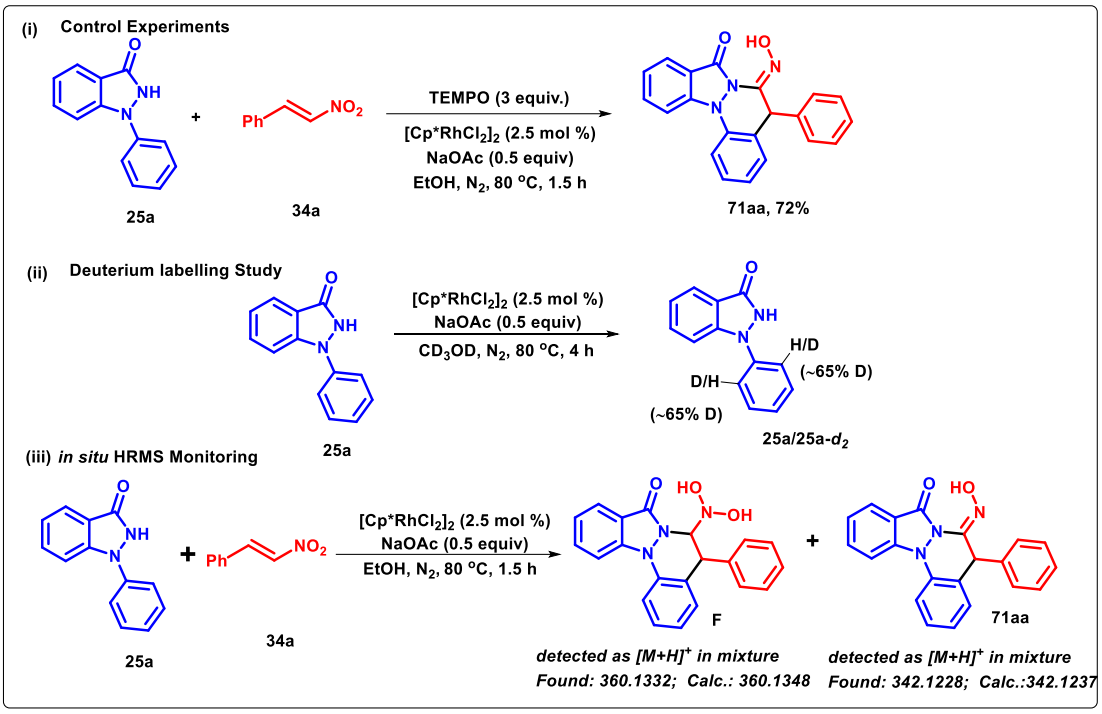

Scheme 2A.2.2 Mechanistic investigations

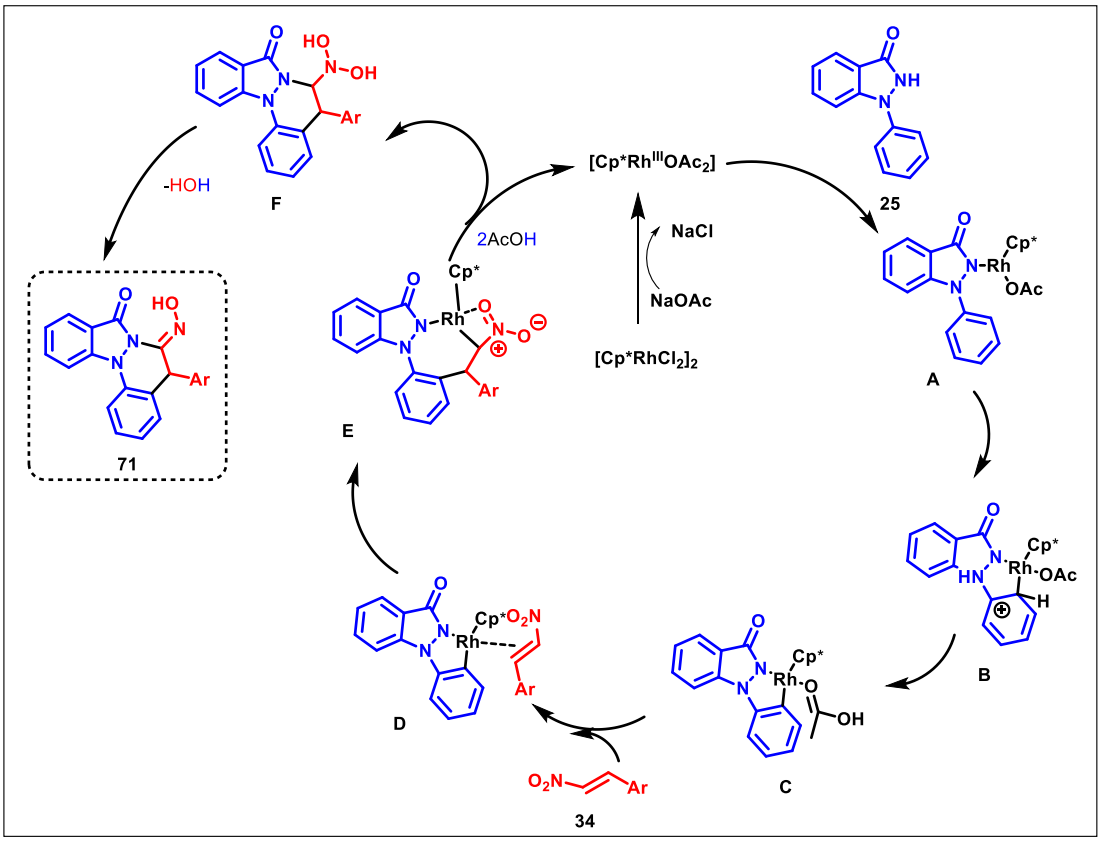

Scheme 2A.2.3 Plausible mechanistic pathway

In summary, we have disclosed a facile strategy for the reductive [4+2] annulation of 1-aryl-1,2-dihydro-3*H*-indazol-3-one with diversified nitroolefins to afford hydroxyimino-decorated indazolo[1,2-*a*]cinnolines under Rh-catalyzed conditions. The strategy provides a direct access to a variety of tetracyclic fused-cinnolines with potential applications in medicinal and material chemistry.

2A.3 Experimental Section

General considerations

Commercially available reagents were used without purification. Commercially available solvents were dried by standard procedures prior to use. Nitroolefins[55-57] were prepared according to the reported procedure. Nuclear magnetic resonance spectra were recorded on a 400 MHz spectrometer, and the chemical shifts are reported in δ units, parts per million (ppm), relative to residual chloroform (7.26 ppm) or DMSO (2.5 ppm) in the deuterated solvent. The following abbreviations were used to describe peak splitting patterns when appropriate: s = singlet, d = doublet, t = triplet, dd = doublet of doublets, and m = multiplet. Coupling constants *J* are reported in Hz. The ^{13}C NMR spectra are reported in ppm relative to deuterochloroform (77.0 ppm) or DMSO-d_6 (39.5 ppm). Melting points were determined on a capillary point apparatus equipped with a digital thermometer and are uncorrected. High-resolution mass spectra were recorded on Agilent Technologies 6545 Q-TOF LC/MS by using electrospray mode. Column chromatography was performed on silica gel (100-200) mesh using varying ratio of ethyl acetate/hexanes as eluent.

General procedure for the synthesis of hydroxyimino decorated indazolo[1,2-*a*]cinnolines (71)

To an oven-dried sealed tube with a screw cap (PTFE) containing 1-aryl-1,2-dihydro-3*H* indazol-3-one (**25**) (50 mg, 1 equiv) in EtOH (5 mL), nitroolefin (**34**) (1.5 equiv), $[Cp^*RhCl_2]_2$ (0.025 equiv), NaOAc (0.5 equiv) were added under a nitrogen atmosphere. The reaction mixture was stirred at 80 ^oC for 6 h (traced by TLC). After the completion of the reaction, the reaction mixture was cooled to room temperature, concentrated, diluted with water and extracted with EtOAc (20 mL x 2). The organic layers were combined and concentrated under *vacuo* to afford a residue, which was purified by column chromatography (SiO_2 100−200 mesh) using hexanes/EtOAc (8/2 to 7:3) as eluent systems to afford the desired product (**71**)

(*Z*)-6-(Hydroxyimino)-5-phenyl-5*H*-indazolo[1,2-*a*]cinnolin-8(6*H*)-one (71aa). White solid,

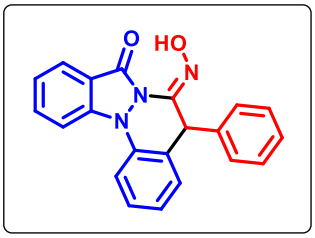

60 mg (74%); mp: 208-209 °C; ^{1}H NMR (400 MHz, DMSO-d_6) δ 11.49 (s, 1H), 7.89 (t, J = 7.6 Hz, 2H), 7.76 (d, J = 7.9 Hz, 1H), 7.70 – 7.66 (m, 2H), 7.58 (t, J = 7.8 Hz, 1H), 7.35 (t, J = 7.2 Hz, 1H), 7.22 – 7.18 (m, 3H), 7.15 – 7.11 (m, 1H), 6.95 (d, J = 7.5 Hz, 2H), 5.37 (s, 1H); ^{13}C NMR (100 MHz, DMSO-d_6) δ 156.3, 139.9, 138.6, 137.3, 134.5, 133.8, 130.5, 129.8, 129.2, 127.8, 127.1, 126.9, 125.5, 124.7, 122.1, 116.9, 114.7, 110.6, 47.0; HRMS (ESI-TOF) (*m/z*) calculated $C_{21}H_{16}N_3O_2^+$: 342.1243, found 342.1228 $[M + H]^+$.

(*Z*)-6-(Hydroxyimino)-3-methyl-5-phenyl-5*H*-indazolo[1,2-*a*]cinnolin-8(6*H*)-one (71ba).

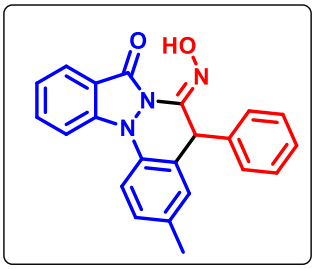

White solid, 63 mg (79%); mp: 189-190 °C; ^{1}H NMR (400 MHz, DMSO-d_6) δ 11.45 (s, 1H), 7.82 (d, J = 8.5 Hz, 1H), 7.76 (t, J = 8.6 Hz, 2H), 7.67 (td, J = 7.7, 1.3 Hz, 1H), 7.48 (d, J = 2.0 Hz, 1H), 7.39 (dd, J = 8.4, 2.0 Hz, 1H), 7.22 – 7.14 (m, 4H), 6.94 (d, J = 7.0 Hz, 2H), 5.29 (s, 1H), 2.39 (s, 3H); ^{13}C NMR (100 MHz, $CDCl_3$) δ 156.3, 140.0, 138.7, 137.5, 135.1, 134.5, 131.5, 130.7, 130.2, 129.2, 127.8, 127.1, 126.9, 124.7, 121.9, 116.8, 114.4, 110.4, 47.1, 20.9; HRMS (ESI-TOF) (*m/z*) calculated $C_{22}H_{18}N_3O_2^+$: 356.1399, found 356.1391 $[M + H]^+$.

(*Z*)-6-(Hydroxyimino)-3-methoxy-5-phenyl-5*H*-indazolo[1,2-*a*]cinnolin-8(6*H*)-one (71ca).

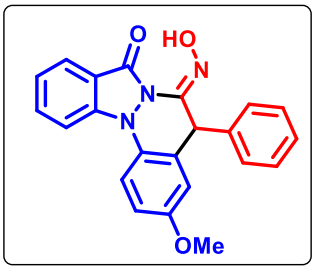

White, 68 mg (85%); mp: 190-192 °C; ^{1}H NMR (400 MHz, DMSO-d_6) δ 11.43 (s, 1H), 7.80 (d, J = 8.8 Hz, 1H), 7.74 (t, J = 8.9 Hz, 2H), 7.65 (td, J = 7.8, 1.5 Hz, 1H), 7.32 (d, J = 2.9 Hz, 1H), 7.22 – 7.12 (m, 5H), 6.96 (d, J = 7.0 Hz, 2H), 5.32 (s, 1H), 3.84 (s, 3H); ^{13}C NMR (100 MHz, $CDCl_3$) δ 157.1, 156.5, 140.0, 138.3, 137.6, 134.5, 129.2, 128.9, 127.8, 127.3, 127.1, 124.7, 121.6, 118.4, 115.4, 115.2, 114.1, 110.1, 56.1, 47.3; HRMS (ESI-TOF) (*m/z*) calculated $C_{22}H_{18}N_3O_3^+$: 372.1348, found 372.1323 $[M + H]^+$.

(*Z*)-3-Fluoro-6-(hydroxyimino)-5-phenyl-5*H*-indazolo[1,2-*a*]cinnolin-8(6*H*)-one (71da).

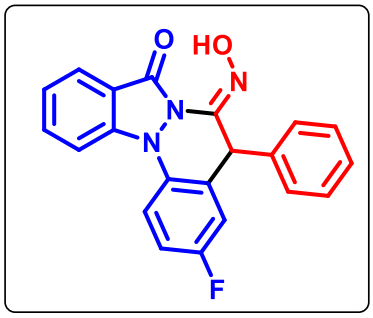

White, 40 mg (50%); mp: 160-161 °C; ^{1}H NMR (400 MHz, DMSO-d_6) δ 11.54 (s, 1H), 7.95 – 7.91 (m, 1H), 7.82 (d, J = 8.6 Hz, 1H), 7.76 (d, J = 7.8 Hz, 1H), 7.71 – 7.64 (m, 2H), 7.44 (t, J = 7.4 Hz, 1H), 7.24 – 7.16 (m, 4H), 6.95 (d, J = 7.5 Hz, 2H), 5.39 (s, 1H); ^{13}C NMR (100 MHz, DMSO-d_6) δ 159.4 ($^{1}J_{C\text{-}F}$ = 242.3 Hz), 156.4, 140.0, 138.0, 136.9, 134.6, 130.4, 129.4 ($^{3}J_{C\text{-}F}$ = 8.3 Hz), 129.3, 128.0, 127.1, 124.7, 122.2, 119.0 ($^{3}J_{C\text{-}F}$ = 8.3 Hz), 117.2 ($^{2}J_{C\text{-}F}$ = 23.7 Hz), 116.6 ($^{2}J_{C\text{-}F}$ = 22.9 Hz), 114.5, 110.3, 46.9; HRMS (ESI-TOF) (*m/z*) calculated $C_{21}H_{15}FN_3O_2^+$: 360.1148, found 360.1126 $[M + H]^+$.

(*Z*)-3-Chloro-6-(hydroxyimino)-5-phenyl-5*H*-indazolo[1,2-*a*]cinnolin-8(6*H*)-one (71ea).

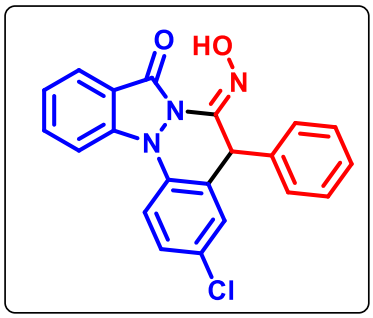

White solid, 43 mg (56%); mp: 174-175 °C; ^{1}H NMR (400 MHz, DMSO-d_6) δ 11.58 (s, 1H), 7.91 (d, J = 8.8 Hz, 1H), 7.84 (d, J = 8.6 Hz, 1H), 7.83 (d, J = 2.4 Hz, 1H), 7.77 (d, J = 7.8 Hz, 1H), 7.70 (td, J = 7.8, 1.3 Hz, 1H), 7.62 (dd, J = 8.8, 2.5 Hz, 1H), 7.24 – 7.20 (m, 3H), 7.18 – 7.16 (m, 1H), 6.95 (d, J = 8.8 Hz, 2H), 5.41 (s, 1H); ^{13}C NMR (100 MHz, DMSO-d_6) δ 156.2, 139.9, 138.1, 136.7, 134.6, 132.7, 130.0, 129.6, 129.3, 129.2, 128.9, 128.0, 127.1, 124.7, 122.5, 118.7, 114.8, 110.6, 46.6; HRMS (ESI-TOF) (*m/z*) calculated $C_{21}H_{15}ClN_3O_2^+$: 376.0852, found 376.0851 $[M + H]^+$.

(*Z*)-3-Bromo-6-(hydroxyimino)-5-phenyl-5*H*-indazolo[1,2-*a*]cinnolin-8(6*H*)-one (71fa).

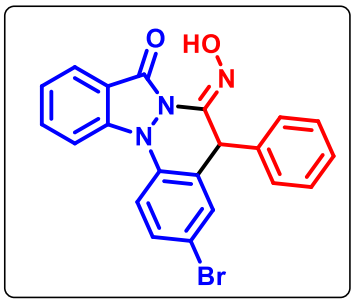

White solid, 42 mg (58%); mp: 180-181 °C; ^{1}H NMR (400 MHz, DMSO-d_6) δ 11.56 (s, 1H), 7.95 (d, J = 2.3 Hz, 1H), 7.87 (d, J = 4.8 Hz, 1H), 7.85 (d, J = 4.6 Hz, 1H), 7.77 (d, J = 7.76 Hz, 1H), 7.75 – 7.68 (m, 2H), 7.24 – 7.20 (m, 3H), 7.18 – 7.14 (m, 1H), 6.95 (d, J = 8.0 Hz, 2H), 5.42 (s, 1H); ^{13}C NMR (100 MHz, DMSO-d_6) δ 156.2, 139.8, 138.2, 136.7, 134.6, 133.1, 132.8, 132.5, 129.3, 129.2, 128.0, 127.1, 124.7, 122.5, 118.9, 117.1, 114.9, 110.7, 46.5; HRMS (ESI-TOF) (*m/z*) calculated $C_{21}H_{15}BrN_3O_2^+$: 420.0347, found 420.0358 $[M + H]^+$.

(*Z*)-2-Chloro-6-(hydroxyimino)-5-phenyl-5*H*-indazolo[1,2-*a*]cinnolin-8(6*H*)-one (71ga).

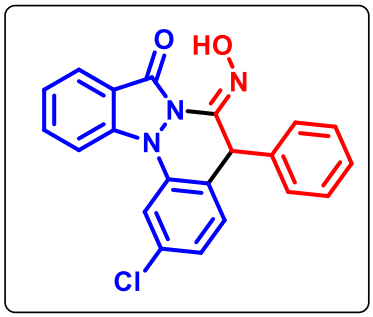

White solid, 48 mg (62%); mp: 170-171 ºC; ^{1}H NMR (400 MHz, DMSO-d_6) δ 11.52 (s, 1H), 7.92 – 7.89 (m, 2H), 7.77 (d, J = 7.7 Hz, 1H), 7.74 – 7.68 (m, 2H), 7.43 (dd, J = 8.2, 2.0 Hz, 1H), 7.26 – 7.14 (m, 4H), 6.94 (d, J = 7.9 Hz, 2H), 5.41 (s, 1H); ^{13}C NMR (100 MHz, DMSO-d_6) δ 156.2, 139.9, 138.3, 134.8, 134.7, 134.1, 132.0, 129.2, 127.9, 127.1, 125.8, 125.3, 124.7, 122.7, 116.6, 115.0, 110.9, 46.6; HRMS (ESI-TOF) (*m/z*) calculated $C_{21}H_{15}ClN_3O_2^+$: 376.0852, found 376.0851 $[M + H]^+$.

(*Z*)-6-(Hydroxyimino)-2,3-dimethyl-5-phenyl-5*H*-indazolo[1,2-*a*]cinnolin-8(6*H*)-one (71ha).

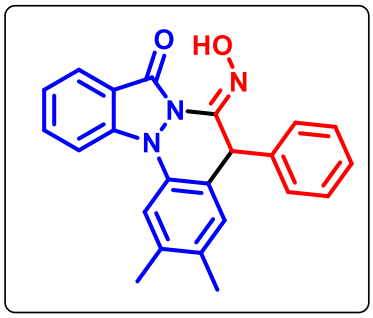

White solid, 62 mg (80%); mp: 200-201 ºC; ^{1}H NMR (400 MHz, DMSO-d_6) δ 11.41 (s, 1H), 7.90 (d, J = 8.5 Hz, 1H), 7.74 (d, J = 7.8 Hz, 1H), 7.70 7.66 (m, 2H), 7.66 (s, 1H), 7.40 (s, 1H), 7.21 – 7.13 (m, 4H), 6.94 (d, J = 7.5 Hz, 2H), 5.23 (s, 1H), 2.38 (s, 3H), 2.29 (s, 3H); ^{13}C NMR (100 MHz, DMSO-d_6) δ 156.4, 140.0, 138.9, 138.2, 137.7, 134.4, 134.0, 131.7, 131.0, 129.1, 127.8, 127.1, 124.6, 124.1, 121.8, 117.5, 114.4, 110.6, 46.7, 19.9, 19.3; HRMS (ESI-TOF) (*m/z*) calculated $C_{23}H_{20}N_3O_2^+$: 370.1555, found 370.1537 $[M + H]^+$.

(*Z*)-2-Chloro-6-(hydroxyimino)-3-methyl-5-phenyl-5*H*-indazolo[1,2-*a*]cinnolin-8(6*H*)-one

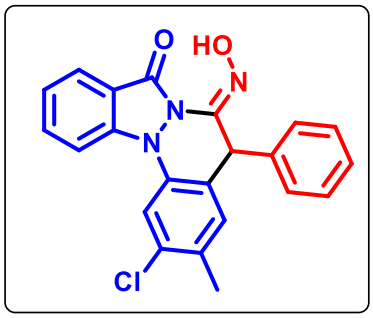

(71ia). White solid, 51 mg (66%); mp: 121-122 ºC; ^{1}H NMR (400 MHz, DMSO-d_6) δ 11.52 (s, 1H), 7.90 (s, 1H), 7.86 (d, J = 8.5 Hz, 1H), 7.76 (d, J = 7.9 Hz, 1H), 7.71 (t, J = 7.9 Hz, 1H), 7.66 (s, 1H), 7.24 – 7.15 (m, 4H), 6.95 (d, J = 7.7 Hz, 2H), 5.33 (s, 1H), 2.39 (s, 3H); ^{13}C NMR (100 MHz, DMSO-d_6) δ 156.2, 139.9, 138.3, 137.0, 134.6, 134.1, 132.7, 132.6, 132.5, 129.5, 129.2, 127.9, 127.1, 125.8, 124.6, 122.5, 117.0, 114.8, 110.7, 46.6, 19.6; HRMS (ESI-TOF) (*m/z*) calculated $C_{22}H_{17}ClN_3O_2^+$: 390.1009, found 390.1014 $[M + H]^+$.

(*Z*)-6-(Hydroxyimino)-10-methoxy-5-phenyl-5,6-dihydro-8*H*-indazolo[1,2-*a*]cinnolin-8-one

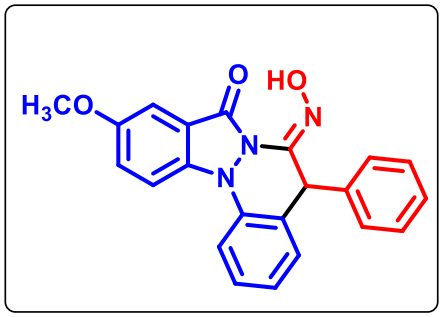

(71ja). White solid, 52 mg (65%); mp: 80-81 °C; ^{1}H NMR (400 MHz, DMSO-d_6) δ 11.45 (s, 1H), 7.84 (t, J = 8.2 Hz, 2H), 7.62 (d, J = 7.5 Hz, 1H), 7.55 (t, J = 7.7 Hz, 1H), 7.33 – 7.29 (m, 3H), 7.23 – 7.15 (m, 3H), 6.94 (d, J = 7.3 Hz, 2H), 5.34 (s, 1H), 3.80 (s, 3H); ^{13}C NMR (100 MHz, DMSO-d_6) δ 156.2, 155.2, 138.9, 137.5, 135.5, 134.2, 130.5, 129.8, 129.2, 127.8, 127.2, 126.4, 125.1, 124.4, 116.3, 115.5, 112.4, 105.2, 56.2, 47.0; HRMS (ESI-TOF) (*m/z*) calculated $C_{22}H_{18}N_3O_3^+$: 372.1348, found 372.1322 $[M + H]^+$.

(*Z*)-6-(Hydroxyimino)-5-(*p*-tolyl)-5*H*-indazolo[1,2-*a*]cinnolin-8(6*H*)-one (71ab). White solid,

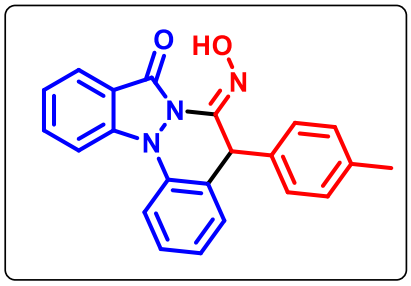

62 mg (75%); mp: 190-191 °C; ^{1}H NMR (400 MHz, DMSO-d_6) δ 11.43 (s, 1H), 7.87 (q, J = 4.2 Hz, 2H), 7.76 (d, J = 7.9 Hz, 1H), 7.71 – 7.63 (m, 2H), 7.58 (t, J = 7.8 Hz, 1H), 7.35 (t, J = 7.4 Hz, 1H), 7.20 (t, J = 7.5 Hz, 1H), 7.00 (d, J = 7.9 Hz, 2H), 6.82 (d, J = 7.8 Hz, 2H), 5.29 (s, 1H), 2.14 (s, 3H); ^{13}C NMR (100 MHz, DMSO-d_6) δ 156.3, 139.9, 137.5, 137.1, 135.5, 134.5, 133.7, 130.4, 129.7, 127.1, 127.0, 125.5, 124.7, 122.1, 116.9, 114.7, 110.6, 46.7, 20.9; HRMS (ESI-TOF) (*m/z*) calculated $C_{22}H_{18}N_3O_2^+$: 356.1399, found 356.1392 $[M + H]^+$.

(*Z*)-6-(Hydroxyimino)-5-(4-methoxyphenyl)-5*H*-indazolo[1,2-*a*]cinnolin-8(6*H*)-one (71ac).

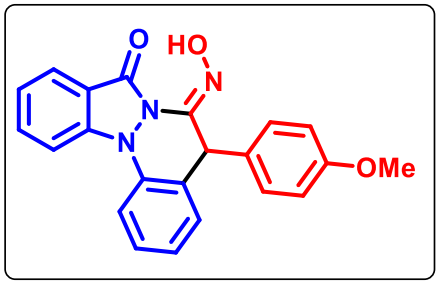

White solid, 71 mg (80%); mp: 199-200 °C; ^{1}H NMR (400 MHz, DMSO-d_6) δ 11.45 (s, 1H), 7.88 (d, J = 8.5 Hz, 2H), 7.78 – 7.56 (m, 4H), 7.35 (t, J = 7.4 Hz, 1H), 7.21 (t, J = 7.3 Hz, 1H), 6.83 (dd, J = 9.0, 8.0 Hz, 4H), 5.27 (s, 1H), 3.61 (s, 3H); ^{13}C NMR (100 MHz, DMSO-d_6) δ 158.8, 156.3, 139.9, 137.6, 134.5, 133.7, 130.4, 129.7, 128.2, 127.2, 125.5, 124.7, 122.1, 116.9, 114.7, 114.6, 110.6, 55.4, 46.3; HRMS (ESI-TOF) (*m/z*) calculated $C_{22}H_{18}N_3O_3^+$: 372.1348, found 372.1345 $[M + H]^+$.

(*Z*)-5-(4-(Dimethylamino)phenyl)-6-(hydroxyimino)-5*H*-indazolo[1,2-*a*]cinnolin-8(6*H*)-one

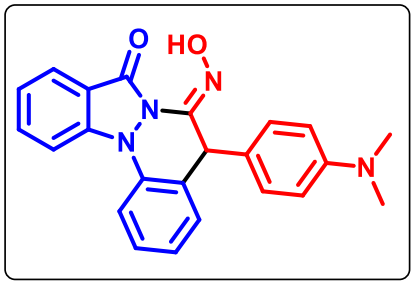

(71ad). White solid, 68 mg (75%); mp: 160-161 °C; ^{1}H NMR (400 MHz, DMSO-d_6) δ 11.37 (s, 1H), 7.89 – 7.86 (m, 2H), 7.77 (dt, J = 7.7, 1.0 Hz, 1H), 7.71 – 7.67 (m, 1H), 7.61 (dd, J = 7.6, 1.5 Hz, 1H), 7.59 – 7.54 (m, 1H), 7.34 (td, J = 7.5, 1.0 Hz, 1H), 7.20 (t, J = 7.5 Hz, 1H), 6.73 (d, J = 8.8 Hz, 2H), 6.51 (d, J = 8.9 Hz, 2H), 5.17 (s, 1H), 2.75 (s, 6H); ^{13}C NMR (100 MHz, DMSO-d_6) δ 156.3, 149.9, 139.8, 137.9, 134.5, 133.6, 130.3, 129.5, 127.7, 127.5, 125.5, 125.4, 124.7, 122.1, 116.8, 114.7, 112.7, 110.5, 46.3, 40.3; HRMS (ESI-TOF) (*m/z*) calculated $C_{23}H_{21}N_4O_2^+$: 385.1664, found 385.1661 $[M + H]^+$.

(*Z*)-6-(Hydroxyimino)-5-(4-hydroxyphenyl)-5*H*-indazolo[1,2-*a*]cinnolin-8(6*H*)-one (71ae).

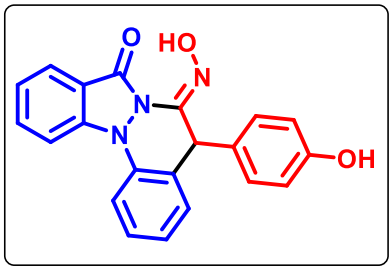

White solid, 69 mg (81%); mp: 185-186 °C; ^{1}H NMR (400 MHz, DMSO-d_6) δ 11.39 (s, 1H), 9.39 (s, 1H), 7.86 (d, J = 8.4 Hz, 2H), 7.76 (d, J = 7.8 Hz, 1H), 7.68 (t, J = 7.8 Hz, 1H), 7.61 (d, J = 7.4, 1H), 7.56 (t, J = 7.6 Hz, 1H), 7.34 (t, J = 7.5 Hz, 1H), 7.20 (t, J = 7.5 Hz, 1H), 6.73 (d, J = 8.2 Hz, 2H), 6.56 (d, J = 8.5 Hz, 2H), 5.21 (s, 1H); ^{13}C NMR (100 MHz, DMSO-d_6) δ 157.0, 156.4, 139.9, 137.8, 134.5, 133.7, 130.4, 129.6, 128.6, 128.2, 127.3, 125.5, 124.7, 122.1, 116.9, 115.9, 114.6, 110.5, 46.4; HRMS (ESI-TOF) (*m/z*) calculated $C_{21}H_{16}N_3O_3^+$: 358.1191, found 358.1167 $[M + H]^+$.

(*Z*)-5-(4-Fluorophenyl)-6-(hydroxyimino)-5*H*-indazolo[1,2-*a*]cinnolin-8(6*H*)-one (71af).

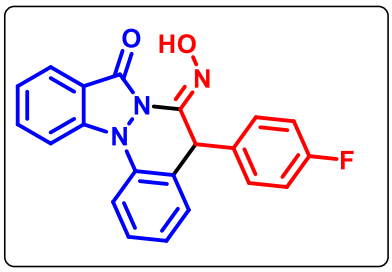

White solid, 47 mg (55%); mp: 198-199 °C; ^{1}H NMR (400 MHz, DMSO-d_6) δ 11.52 (s, 1H), 7.89 (t, J = 7.4 Hz, 2H), 7.77 (d, J = 7.8 Hz, 1H), 7.72 – 7.65 (m, 2H), 7.59 (t, J = 7.7 Hz, 1H), 7.36 (t, J = 7.5 Hz, 1H), 7.21 (t, J = 7.5 Hz, 1H), 7.06 (t, J = 8.7 Hz, 2H), 6.98 – 6.95 (m, 2H), 5.37 (s, 1H); ^{13}C NMR (100 MHz, DMSO-d_6) δ 161.7 ($^{1}J_{C\text{-}F}$ = 242.4 Hz), 156.3, 140.0, 137.2, 134.8 ($^{4}J_{C\text{-}F}$ = 2.9 Hz), 134.6, 133.8, 130.4, 129.9, 129.2 ($^{3}J_{C\text{-}F}$ = 8.3 Hz), 126.7, 125.6, 124.7, 122.2, 117.0, 116.0 ($^{2}J_{C\text{-}F}$ = 21.4 Hz), 114.7, 110.6, 46.3; HRMS (ESI-TOF) (*m/z*) calculated $C_{21}H_{15}FN_3O_2^+$: 360.1148, found 360.1124 $[M + H]^+$.

(*Z*)-5-(4-Chlorophenyl)-6-(hydroxyimino)-5*H*-indazolo[1,2-*a*]cinnolin-8(6*H*)-one (71ag).

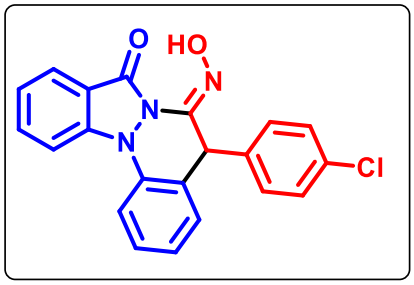

Dirty white solid, 53 mg (60%); mp: 200-201 °C; ^{1}H NMR (400 MHz, $CDCl_3$) δ 11.57 (s, 1H), 7.88 (t, J = 7.8 Hz, 2H), 7.77 (d, J = 7.8 Hz, 1H), 7.70 (t, J = 8.0 Hz, 1H), 7.65 (dd, J = 7.6, 1.5 Hz, 1H), 7.59 (td, J = 7.8, 1.5 Hz, 1H), 7.36 (t, J = 7.5 Hz, 1H), 7.28 (dd, J = 6.5, 2.1 Hz, 2H) 7.21 (t, J = 7.5 Hz, 1H), 6.94 (d, J = 8.2 Hz, 2H), 5.38 (s, 1H).; ^{13}C NMR (100 MHz, $CDCl_3$) δ 156.3 , 140.0, 137.6, 137.0, 134.6, 133.8, 132.6, 130.5, 130.0, 129.2, 129.0, 126.4, 125.7, 124.7, 122.3, 117.0, 114.6, 110.7, 46.4; HRMS (ESI-TOF) (*m/z*) calculated $C_{21}H_{14}ClN_3NaO_2^+$: 398.0672, found 398.068 $[M + Na]^+$.

(*Z*)-5-(4-Bromophenyl)-6-(hydroxyimino)-5*H*-indazolo[1,2-*a*]cinnolin-8(6*H*)-one (71ah).

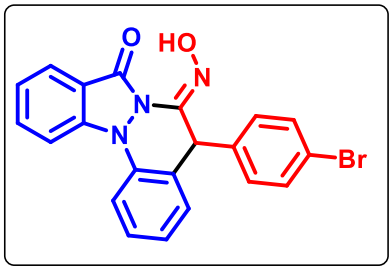

Dirty white solid, 69 mg (69%); mp: 200-201 °C; ^{1}H NMR (400 MHz, $CDCl_3$) δ 11.56 (s, 1H), 7.88 (t, J = 8.2 Hz, 2H), 7.78 – 7.57 (m, 4H), 7.42 – 7.34 (m, 3H), 7.21 (t, J = 7.6 Hz, 1H), 6.89 (d, J = 8.2 Hz, 2H), 5.36 (s, 1H); ^{13}C NMR (100 MHz, $CDCl_3$) δ 156.3, 140.0, 138.0, 136.9, 134.6, 133.8, 132.1, 130.5, 130.0, 129.4, 126.4, 125.6, 124.7, 122.3, 121.2, 117.0, 114.7, 110.7, 46.5; HRMS (ESI-TOF) (*m/z*) calculated $C_{21}H_{15}BrN_3O_2^+$: 420.0347, found 420.0328 $[M + H]^+$.

(*Z*)-6-(Hydroxyimino)-5-(4-(trifluoromethyl)phenyl)-5*H*-indazolo[1,2-*a*]cinnolin-8(6*H*)-one

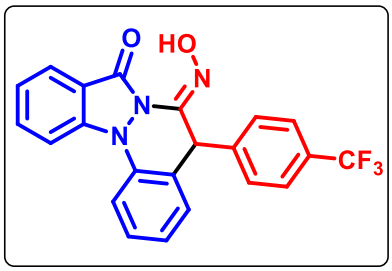

(71ai). White solid, 36 mg (37%); mp: 186-187 °C; ^{1}H NMR (400 MHz, DMSO-d_6) δ 11.61 (s, 1H), 7.90 (t, J = 8.9 Hz, 2H), 7.77 (dd, J = 8.5, 1.2 Hz, 1H), 7.72 – 7.67 (m, 2H), 7.63 – 7.58 (m, 3H), 7.37 (td, J = 7.5, 1.0 Hz, 1H), 7.23 – 7.17 (m, 3H), 5.51 (s, 1H); ^{13}C NMR (100 MHz, DMSO-d_6) δ 156.2, 143.4, 140.1, 136.7, 134.6, 133.9, 130.5, 130.1, 128.1, 126.2 (q, J_{C-F} = 3.6 Hz), 126.0, 125.8, 125.7, 124.7, 122.4, 116.9, 114.7, 110.8, 46.8; HRMS (ESI-TOF) (*m/z*) calculated $C_{22}H_{15}F_3N_3O_2^+$: 410.1116, found 410.1097 $[M + H]^+$.

(*Z*)-5-(3,4-Dimethoxyphenyl)-6-(hydroxyimino)-5*H*-indazolo[1,2-*a*]cinnolin-8(6*H*)-one

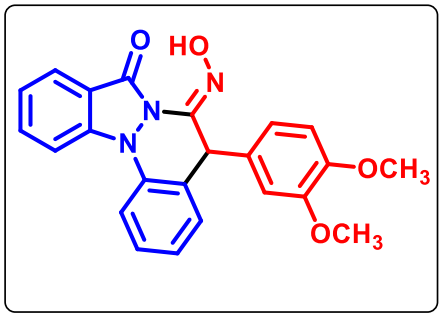

(71aj). White solid, 70 mg (73%); mp: 178-179 °C; ^{1}H NMR (400 MHz, DMSO-d_6) δ 11.46 (s, 1H), 7.88 (d, J = 8.4 Hz, 2H), 7.80 (d, J = 7.9 Hz, 1H), 7.70 (t, J = 7.9 Hz, 1H), 7.65 (d, J = 7.5 Hz, 1H), 7.58 (t, J =7.1 Hz,1H), 7.35 (t, J = 7.5 Hz, 1H), 7.21 (t, J = 7.5 Hz, 1H), 6.75 (d, J = 8.4 Hz, 1H), 6.47 (d, J = 2.2 Hz, 1H), 6.41 (dd, J = 8.3, 2.2 Hz, 1H), 5.25 (s, 1H), 3.60 (s, 6H); ^{13}C NMR (100 MHz, DMSO-d_6) δ 156.6, 149.0, 148.4, 140.1, 137.7, 134.6, 133.6, 131.0, 130.3, 129.7, 127.4, 125.6, 124.7, 122.2, 119.4, 117.3, 114.7, 112.3, 110.4, 110.3, 55.8, 55.4, 46.6; HRMS (ESI-TOF) (*m/z*) calculated $C_{23}H_{20}N_3O_4^+$: 402.1453, found 402.1440 $[M + H]^+$.

(*Z*)-5-(3-Ethoxy-4-hydroxyphenyl)-6-(hydroxyimino)-5*H*-indazolo[1,2-*a*]cinnolin-8(6*H*)-one

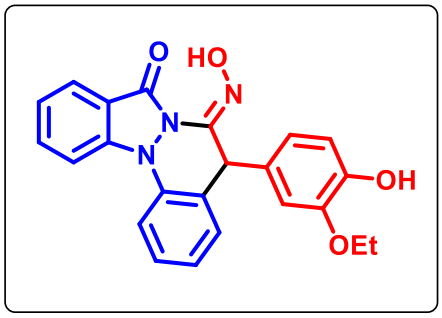

(71ak). White solid, 68 mg (71%); mp: 190-191 °C; ^{1}H NMR (400 MHz, DMSO-d_6) δ 11.40 (s, 1H), 8.90 (s, 1H), 7.87 (d, J = 8.3 Hz, 2H), 7.78 (d, J = 7.8 Hz, 1H), 7.72 – 7.67 (m, 1H), 7.63 – 7.54 (m, 2H), 7.33 (t, J = 7.5 Hz, 1H), 7.21 (t, J = 7.5 Hz, 1H), 6.57 (d, J = 8.1 Hz, 1H), 6.34 (dd, J = 8.0, 2.0 Hz, 1H), 6.30 (d, J = 2.1 Hz, 1H), 5.18 (s, 1H), 3.57 – 3.45 (m, 2H), 1.09 (t, J = 7.0 Hz, 3H); ^{13}C NMR (100 MHz, DMSO-d_6) δ 156.7, 147.0, 146.5, 140.2, 137.9, 134.5, 133.6, 130.2, 129.6, 129.4, 127.6, 125.6, 124.7, 122.1, 119.9, 117.3, 116.1, 114.7, 112.2, 110.2, 64.0, 46.6, 14.9; HRMS (ESI-TOF) (*m/z*) calculated $C_{23}H_{20}N_3O_4^+$: 402.1453, found 402.1425 $[M + H]^+$.

(*Z*)-6-(Hydroxyimino)-5-(naphthalen-1-yl)-5*H*-indazolo[1,2-*a*]cinnolin-8(6*H*)-one (71al).

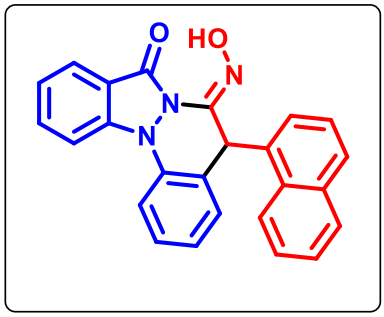

White solid, 75 mg (80%); mp: 195-196 °C; ^{1}H NMR (400 MHz, DMSO-d_6) δ 11.54 (s, 1H), 8.66 (d, J = 8.5 Hz, 1H), 8.06 (d, J = 8.6 Hz, 1H), 8.01 (d, J = 8.2 Hz, 1H), 7.94 (d, J = 8.1 Hz, 1H), 7.78 – 7.73 (m, 2H), 7.71 – 7.61 (m, 3H), 7.60 – 7.54 (m, 2H), 7.33 (t, J = 7.5 Hz, 1H), 7.21 (t, J = 7.5 Hz, 1H), 7.09 (t, J = 7.7 Hz, 1H), 6.41 (d, J = 7.1 Hz, 1H), 6.16 (s, 1H); ^{13}C NMR (100 MHz, DMSO-d_6) δ 155.9, 140.3, 137.4, 135.0, 134.5, 134.1, 133.8, 131.6, 130.4, 130.0, 129.1,

128.8, 126.9, 126.7, 126.5, 125.7, 125.6, 125.2, 124.7, 124.6, 122.2, 117.0, 114.9, 110.7, 44.5; HRMS (ESI-TOF) (*m/z*) calculated $C_{25}H_{18}N_3O_2^+$: 392.1399, found 392.1358 $[M + H]^+$.

(*Z*)-5-([1,1'-Biphenyl]-4-yl)-6-(hydroxyimino)-5*H*-indazolo[1,2-*a*]cinnolin-8(6*H*)-one

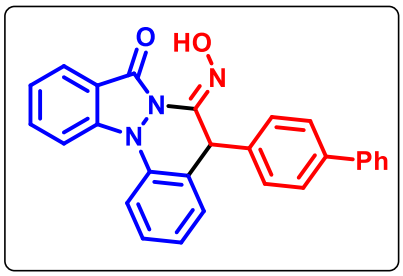

(71am). White solid, 75 mg (75%); mp: 156-157 °C; ^{1}H NMR (400 MHz, DMSO-*d*$_6$) δ 11.52 (s, 1H), 7.91 (dd, *J* = 8.5, 2.8 Hz, 2H), 7.78 (d, *J* = 7.8 Hz, 1H), 7.71 (t, *J* = 6.9 Hz, 2H), 7.60 (td, *J* = 7.9, 1.5 Hz, 1H), 7.53 (t, *J* = 8.6 Hz, 4H), 7.41 – 7.35 (m, 3H), 7.33 – 7.27 (m, 1H), 7.21 (t, *J* = 7.5 Hz, 1H), 7.04 (d, *J* = 8.1 Hz, 2H), 5.41 (s, 1H); ^{13}C NMR (100 MHz, DMSO-*d*$_6$) δ 156.3, 140.0, 139.6, 139.5, 137.8, 137.2, 134.6, 133.8, 130.5, 129.8, 129.3, 128.0, 127.7, 127.4, 127.0, 126.8, 125.6, 124.7, 122.2, 116.9, 114.8, 110.7, 46.8; HRMS (ESI-TOF) (*m/z*) calculated $C_{27}H_{20}N_3O_2^+$: 418.1555, found 418.1556 $[M + H]^+$.

(*Z*)-6-(Hydroxyimino)-5-((*E*)-styryl)-5*H*-indazolo[1,2-*a*]cinnolin-8(6*H*)-one (71an). White solid, 37 mg (43%); mp: 161-162 °C; ^{1}H NMR (400 MHz, DMSO-*d*$_6$) δ 11.51 (s, 1H), 7.91 (d, *J* = 8.5 Hz, 1H), 7.87 – 7.82 (m, 2H), 7.75 – 7.71 (m 1H), 7.57 – 7.52 (m, 2H), 7.31 (td, *J* = 7.5, 1 Hz, 1H), 7.28 – 7.14 (m, 6H), 6.36 – 6.23 (m, 2H), 4.85 (d, *J* = 5.5 Hz, 1H); ^{13}C NMR (100 MHz, DMSO-*d*$_6$) δ 156.7, 140.4, 137.1, 136.2, 134.6, 133.7, 132.3, 129.6, 129.3, 129.1, 128.4, 127.0, 126.8, 126.7, 125.7, 124.7, 122.3, 116.8, 114.9, 110.8, 45.4; HRMS (ESI-TOF) (*m/z*) calculated $C_{23}H_{18}N_3O_2^+$: 368.1399, found 368.1397 $[M + H]^+$.

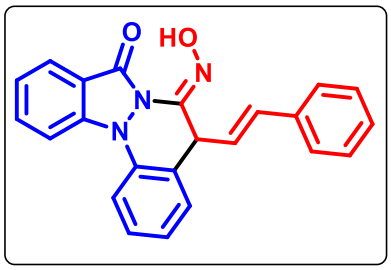

(*Z*)-6-(Hydroxyimino)-5-(thiophen-2-yl)-5*H*-indazolo[1,2-*a*]cinnolin-8(6*H*)-one (71ao). White solid, 60 mg (72%); mp: 159-160 °C; ^{1}H NMR (400 MHz, DMSO-*d*$_6$) δ 11.52 (s, 1H), 7.89 (t, *J* = 6.9 Hz, 2H), 7.81 (d, *J* = 7.8 Hz, 1H), 7.72 (t, *J* = 8.1 Hz, 1H), 7.66 (dd, *J* = 7.7, 1.5 Hz, 1H), 7.57 (t, *J* = 7.5 Hz, 1H), 7.35 – 7.29 (m, 2H), 7.23 (t, *J* = 7.5 Hz, 1H), 6.84 (t, *J* = 4.2 Hz, 1H), 6.67 (d, *J* = 3.5 Hz, 1H), 5.59 (s, 1H); ^{13}C NMR (100 MHz, DMSO-*d*$_6$) δ 156.5, 142.4, 140.1, 136.8, 134.6, 133.3, 130.1, 129.6, 127.5, 127.3, 126.5, 125.6, 125.5, 124.7, 122.2, 117.1, 114.7, 110.5, 43.1; HRMS (ESI-TOF) (*m/z*) calculated $C_{19}H_{14}N_3O_2S^+$: 348.0806, found 348.0800 $[M + H]^+$.

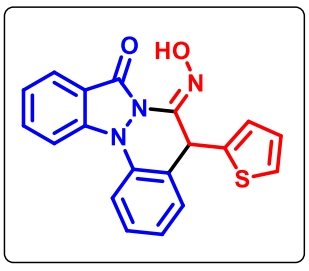

(*Z*)-5-(Furan-2-yl)-6-(hydroxyimino)-5*H*-indazolo[1,2-*a*]cinnolin-8(6*H*)-one (71ap). White

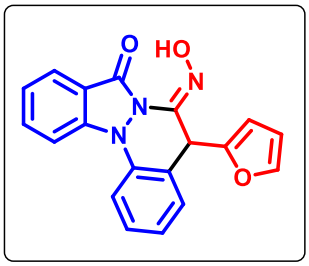

solid, 52 mg (66%); mp: 185-186 °C; ^{1}H NMR (400 MHz, DMSO-d_6) δ 11.56 (s, 1H), 7.91 – 7.86 (m, 2H), 7.82 (d, J = 7.8 Hz, 1H), 7.72 (t, J = 8.1 Hz, 1H), 7.63 (dd, J = 7.6, 1.5 Hz, 1H), 7.57 (td, J = 7.8, 1.5 Hz, 1H), 7.45 (d, J = 1.8 Hz, 1H), 7.31 (t, J = 7.5 Hz, 1H), 7.24 (t, J = 7.5 Hz, 1H), 6.23 (q, J = 1.8 Hz, 1H), 5.79 (d, J = 3.3 Hz, 1H), 5.41 (s, 1H); ^{13}C NMR (100 MHz, DMSO-d_6) δ 156.5, 151.6, 143.6, 140.4, 135.4, 134.6, 133.7, 130.0, 129.9, 125.4, 125.1, 124.7, 122.2, 117.1, 114.7, 111.1, 110.5, 107.0, 41.9; HRMS (ESI-TOF) (*m/z*) calculated $C_{19}H_{13}N_3NaO_3^+$: 354.0854, found 354.0844 $[M + Na]^+$.

(*Z*)-6-(Hydroxyimino)-5-(1*H*-indol-3-yl)-5H-indazolo[1,2-*a*]cinnolin-8(6*H*)-one (71aq).

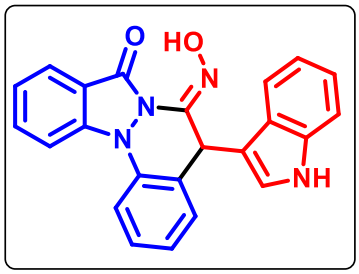

White solid, 57 mg (63%); mp: 214-215 °C; ^{1}H NMR (400 MHz, DMSO-d_6) δ 11.33 (s, 1H), 10.79 (brs, 1H), 7.91 (t, J = 7.4 Hz, 2H), 7.75 – 7.68 (m, 4H), 7.57 (t, J = 7.6 Hz, 1H), 7.33 (t, J = 7.5 Hz, 1H), 7.28 (d, J = 8.0 Hz, 1H), 7.19 (t, J = 7.5 Hz, 1H), 7.08 (t, J = 7.5 Hz, 1H), 7.01 (t, J = 7.5 Hz, 1H), 6.31 (d, J = 2.5 Hz, 1H), 5.48 (s, 1H); ^{13}C NMR (100 MHz, DMSO-d_6) δ 156.4, 140.0, 138.1, 136.7, 134.5, 133.7, 129.7, 129.4, 127.9, 126.3, 125.5, 124.7, 122.9, 122.0, 119.3, 119.2, 117.0, 114.6, 112.1, 110.5, 40.5; HRMS (ESI-TOF) (*m/z*) calculated $C_{23}H_{17}N_4O_2^+$: 381.1351, found 381.1346 $[M + H]^+$.

(*Z*)-5-Hexyl-6-(hydroxyimino)-5,6-dihydro-8*H*-indazolo[1,2-*a*]-cinnolin-8-one (71ar). White

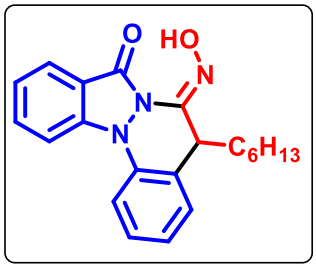

solid, 40 mg (48%); mp: 59-60 °C; ^{1}H NMR (400 MHz, DMSO-d_6) δ 11.22 (s, 1H), 7.89 (dd, J = 17.2, 8.2 Hz, 2H), 7.82 (d, J = 7.9 Hz, 1H), 7.74 (t, J = 7.6 Hz, 1H), 7.51−7.46 (m, 2H), 7.26 (t, J = 7.0 Hz, 2H), 3.89−3.84 (m, 1H), 1.40−1.15 (m, 10H), 0.79 (t, J = 6.9 Hz, 3H); ^{13}C NMR (100 MHz, DMSO-d_6) δ 156.4, 140.3, 138.1, 134.5, 133.2, 129.1, 129.0, 125.4, 124.7, 122.1, 116.9, 114.7, 110.6, 100.0, 42.8, 33.2, 31.4, 28.4, 26.9, 22.3, 14.3; HRMS (ESI-TOF) (*m/z*) calculated $C_{21}H_{24}N_3O_2^+$: 350.1868, found 350.1847 $[M + H]^+$.

2A.4. Single Crystal X-Ray Diffraction Studies

Using a suitable crystal mounted in a nylon loop that was attached to a goniometer head, initial crystal evaluation and data collection of each compound were performed on a Kappa APEX II diffractometer equipped with a CCD detector (with the crystal-to-detector distance fixed at 60 mm) and sealed-tube monochromated Mo$K\alpha$ radiation using the program APEX2.[58] Data were

integrated, reflections were fitted and values of F^2 and $\sigma(F^2)$ for each reflection were obtained by using the program SAINT.[58] Data were also corrected for Lorentz and polarization effects. The subroutine XPREP[58] was used for the processing of data that included determination of space group, application of an absorption correction (SADABS),[58] merging of data, and generation of files necessary for solution and refinement. The crystal structure was solved by direct methods using the SHELXS program of the SHELXTL package and was refined using SHELXL.[59,60] All non-hydrogen atoms were refined with anisotropic displacement parameters. All hydrogen atoms for **71ga** were located in the difference Fourier map and refined with individual isotropic displacement parameters. All hydrogen atoms for **71ga** were placed in ideal positions and refined as riding atoms with individual isotropic displacement parameters. All figures were drawn using MERCURY V 3.0.[61]

2A.4.1 Crystal data for 71ga (CCDC No. 2040954). $C_{21}H_{14}N_3O_2$, Mr = 375.80 g/mol,

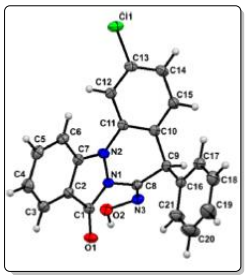

monoclinic, space group *C2/c*, a = 16.7921(6) Å, b = 14.8118(5) Å, c = 14.5882(5) Å, α = 90°, β = 104.484(1)°, γ = 90°, V = 3513.1(2) Å3 , Z = 8, T = 296(2) K, Dcalcd = 1.421 g/cm3 ; Full matrix least-square on F^2 ; R_1 = 0.0352, wR_2 = 0.1007 for 2815 observed reflections [I > 2σ(I)] and R_1 = 0.0383, wR_2 = 0.1039 for all 3110 reflections; GOF = 1.064..

2A.5 References

1. Che, T.; Chen, S.-B.; Tu, J.-L.; Wang, B.; Wang, Y.-Q.; Zhang, Y.; Wang, J.; Wang, Z.-Q.; Zhang, Z.-P.; Ou, T.-M. *Journal of Medicinal Chemistry* **2018**, *61*, 3436-3453.
2. Wang, K.; Guo, L.; Zou, Y.; Li, Y.; Wu, J. *The Journal of Antibiotics* **2007**, *60*, 325-327.
3. Satyanarayana, M.; Feng, W.; Cheng, L.; Liu, A. A.; Tsai, Y.-C.; Liu, L. F.; LaVoie, E. J. *Bioorganic & Medicinal chemistry* **2008**, *16*, 7824-7831.
4. Sony, S.; Thiruvalla, K.; George, M.; Joseph, L. *International Journal of Advance Research, Ideas and Innovations in Technology* **2018**, *4*, 1016-1021.
5. Binuja, S.; Aswathy, J. *Journal of Pharmaceutical Sciences and Research* **2019**, *11*, 2679-2683.
6. Szumilak, M.; Stanczak, A. *Molecules* **2019**, *24*, 2271.
7. Mekheimer, R. A.; Abd-Elmonem, M.; Abou Elsebaa, M.; Nazmy, M. H.; Sadek, K. U. *Physical Sciences Reviews* **2022**.
8. Ma, G.-H.; Tu, X.-J.; Ning, Y.; Jiang, B.; Tu, S.-J. *ACS Combinatorial Science* **2014**, *16*, 281-286.

9. Romeo, R.; V Giofre, S.; A Chiacchio, M. *Current Medicinal Chemistry* **2017**, *24*, 3433-3484.
10. Lewgowd, W.; Stanczak, A. *Archiv der Pharmazie: An International Journal Pharmaceutical and Medicinal Chemistry* **2007**, *340*, 65-80.
11. Giovannoni, M. P.; Schepetkin, I. A.; Crocetti, L.; Ciciani, G.; Cilibrizzi, A.; Guerrini, G.; Khlebnikov, A. I.; Quinn, M. T.; Vergelli, C. *Journal of Enzyme Inhibition and Medicinal Chemistry* **2016**, *31*, 628-639.
12. Tonk, R. K.; Bawa, S.; Chawla, G.; Deora, G. S.; Kumar, S.; Rathore, V.; Mulakayala, N.; Rajaram, A.; Kalle, A. M.; Afzal, O. *European Journal of Medicinal Chemistry* **2012**, *57*, 176-184.
13. Tian, C.; Yang, C.; Wu, T.; Lu, M.; Chen, Y.; Yang, Y.; Liu, X.; Ling, Y.; Deng, M.; Jia, Y. *Bioorganic & Medicinal Chemistry Letters* **2021**, *48*, 128271.
14. Mishra, P.; Middha, A.; Saxena, V.; Saxena, A. *Pharmaceutical and Biosciences Journal* **2016**, 74-80.
15. Keneford, J.; Lourie, E.; Morley, J.; Simpson, J.; Williamson, J.; Wright, P. *Nature* **1948**, *161*, 603-604.
16. Mahmoud, E. M.; Shongwe, M.; Moghadam, E. S.; Moghimi-Rad, P.; Stoll, R.; Abdel-Jalil, R. *Zeitschrift für Naturforschung C* **2022**.
17. Yang, C.; Song, F.; Chen, J.; Huang, Y. *Advanced Synthesis & Catalysis* **2017**, *359*, 3496-3502.
18. Li, P.; Xu, X.; Chen, J.; Yao, H.; Lin, A. *Organic Chemistry Frontiers* **2018**, *5*, 1777-1781.
19. Jin, H.-S.; Du, Y.-Z.; Zhao, Q.-Y.; Zhao, L.-M. *Organic Chemistry Frontiers* **2021**, *8*, 6350-6355.
20. Hu, S.; Han, X.; Xie, X.; Fang, F.; Wang, Y.; Saidahmatov, A.; Liu, H.; Wang, J. *Advanced Synthesis & Catalysis* **2021**, *363*, 3311-3317.
21. Li, R.; Hou, Y.-X.; Xu, J.-H.; Gao, Y.; Hu, X.-Q. *Organic Chemistry Frontiers* **2022**, *9*, 2181-2186.
22. Li, N.; Zhang, X.; Fan, X. *Tetrahedron Letters* **2022**, *103*, 153984.
23. Xing, L.; Fan, Z.; Hou, C.; Yong, G.; Zhang, A. *Advanced Synthesis & Catalysis* **2014**, *356*, 972-976.
24. Rajkumar, S.; Savarimuthu, S. A.; Kumaran, R. S.; Nagaraja, C.; Gandhi, T. *Chemical Communications* **2016**, *52*, 2509-2512.
25. Mayakrishnan, S.; Arun, Y.; Balachandran, C.; Emi, N.; Muralidharan, D.; Perumal, P. T. *Organic & Biomolecular Chemistry* **2016**, *14*, 1958-1968.

26. Karishma, P.; Mahesha, C. K.; Agarwal, D. S.; Mandal, S. K.; Sakhuja, R. *The Journal of Organic Chemistry* **2018**, *83*, 11661-11673.

27. Cai, P.; Zhang, E.; Wu, Y.; Fang, T.; Li, Q.; Yang, C.; Wang, J.; Shang, Y. *ACS Omega* **2018**, *3*, 14575-14584.

28. Lautens, M.; Marchese, A. D. *Synfacts* **2022**, *18*, 1315.

29. Kim, S.; Choi, S. B.; Kang, J. Y.; An, W.; Lee, S. H.; Oh, H.; Ghosh, P.; Mishra, N. K.; Kim, I. S. *Asian Journal of Organic Chemistry* **2021**, *10*, 3005-3014.

30. Karishma, P.; Agarwal, D. S.; Laha, B.; Mandal, S. K.; Sakhuja, R. *Chemistry–An Asian Journal* **2019**, *14*, 4274-4288.

31. Pan, C.; Yuan, C.; Yu, J. T. *Asian Journal of Organic Chemistry* **2022**, *11*, e202200346.

32. Zheng, Y.-C.; Shu, B.; Zeng, Y.-F.; Chen, S.-Y.; Song, J.-L.; Liu, Y.-Z.; Xiao, L.; Liu, X.-G.; Zhang, X.; Zhang, S.-S. *Organic Chemistry Frontiers* **2022**, *9*, 5185-5190.

33. Huang, G.; Yu, J. T.; Pan, C. *European Journal of Organic Chemistry* **2022**, *2022*, e202200279.

34. Zhang, X.; Bai, R.; Xiong, H.; Xu, H.; Hou, W. *Bioorganic & Medicinal Chemistry Letters* **2020**, *30*, 126916.

35. Hou, W.; Xiong, H.; Bai, R.; Xiao, Z.; Su, L.; Ruan, B. H.; Xu, H. *Tetrahedron* **2019**, *75*, 4005-4009.

36. Trost, B. M.; Müller, C. *Journal of the American Chemical Society* **2008**, *130*, 2438-2439.

37. Ishii, T.; Fujioka, S.; Sekiguchi, Y.; Kotsuki, H. *Journal of the American Chemical Society* **2004**, *126*, 9558-9559.

38. Quan, X.-J.; Ren, Z.-H.; Wang, Y.-Y.; Guan, Z.-H. *Organic Letters* **2014**, *16*, 5728-5731.

39. Albrecht, Ł.; Dickmeiss, G.; Acosta, F. C.; Rodríguez-Escrich, C.; Davis, R. L.; Jørgensen, K. A. *Journal of the American Chemical Society* **2012**, *134*, 2543-2546.

40. Devi, L.; Mishra, P.; Pokhriyal, A.; Rastogi, N. *SynOpen* **2022**, *6*, 198-207.

41. Wu, J.; Yin, W.; Huang, Z.; Zhang, Y.; Jia, J.; Cheng, H.; Kang, F.; Huang, K.; Sun, T.; Tian, J. *Journal of Medicinal Chemistry* **2021**, *64*, 10919-10933.

42. Deb, I.; Shanbhag, P.; Mobin, S. M.; Namboothiri, I. N. *European Journal of Organic Chemistry* **2009**, *2009*, 4091-4101.

43. Kuczmera, T. J.; Boelke, A.; Nachtsheim, B. J. *European Journal of Organic Chemistry* **2022**, *2022*, e202200276.

44. Basavaiah, D.; Reddy, B. S.; Badsara, S. S. *Chemical Reviews* **2010**, *110*, 5447-5674.

45. Li, J.-l.; Li, W.-z.; Wang, Y.-c.; Ren, Q.; Wang, H.-s.; Pan, Y.-m. *Chemical Communications* **2016**, *52*, 10028-10031.

46. Potter, T. J.; Kamber, D. N.; Mercado, B. Q.; Ellman, J. A. *ACS Catalysis* **2017**, *7*, 150-153.

47. Bai, D.; Jia, Q.; Xu, T.; Zhang, Q.; Wu, F.; Ma, C.; Liu, B.; Chang, J.; Li, X. *The Journal of Organic Chemistry* **2017**, *82*, 9877-9884.

48. Lv, N.; Chen, Z.; Liu, Y.; Liu, Z.; Zhang, Y. *Advanced Synthesis & Catalysis* **2019**, *361*, 4140-4146.

49. Han, S. H.; Mishra, N. K.; Jeon, M.; Kim, S.; Kim, H. S.; Jung, S. Y.; Jung, Y. H.; Ku, J. M.; Kim, I. S. *Advanced Synthesis & Catalysis* **2017**, *359*, 3900-3904.

50. Potter, T. J.; Li, Y.; Ward, M. D.; Ellman, J. A. *European Journal of Organic Chemistry* **2018**, *2018*, 4381-4388.

51. Mishra, A.; Mukherjee, U.; Sarkar, W.; Meduri, S. L.; Bhowmik, A.; Deb, I. *Organic Letters* **2019**, *21*, 2056-2059.

52. Mishra, A.; Bhowmik, A.; Samanta, S.; Sarkar, W.; Das, S.; Deb, I. *Organic Letters* **2020**, *22*, 1340-1344.

53. Hu, W.-B.; Qiu, Y.-Q.; Wei, W.-Y.; Li, Q.; Xu, Y.-J. *The Journal of Organic Chemistry* **2022**, *87*, 6179-6188.

54. Shi, X. Y.; Renzetti, A.; Kundu, S.; Li, C. J. *Advanced Synthesis & Catalysis* **2014**, *356*, 723-728.

55. Jalal, S.; Sarkar, S.; Bera, K.; Maiti, S.; Jana, U. *European Journal of Organic Chemistry* **2013**, *2013*, 4823-4828.

56. Wang, C.; Wang, S. *Synthetic Communications* **2002**, *32*, 3481-3486.

57. Kumar, M. S.; Rajanna, K.; Reddy, K. R.; Venkateswarlu, M.; Venkanna, P. *Synthetic Communications* **2013**, *43*, 2672-2677.

58. *APEX2, SADABS and SAINT*; Bruker AXS inc: Madison, Wisconsin, USA, **2008**.

59. Sheldrick, G. M. SHELXT- *Acta Crystallography Section A: Foundations and Advances* **2015**, *71*, 3-8.

60. Sheldrick, G. M. Crystal Structure Refinement with SHELXL. *Acta Crystallography Section C: Foundations and Advances* **2015**, *71*, 3-8.

61. Macrae, C. F.; Bruno, I. J.; Chisholm, J. A.; Edginton, P. R.; McCabe, P.; Pidocck, E.; RodriguezMonge, L.; Taylor, T.; Van de Streek, J.; Wood, P. A. Mercury CSD 2.0- *Journal of Appllied Crystallography* **2008**, *41*, 466-470.

Chapter 2B

Iridium-Catalyzed [4+2] Annulation of *N*-Arylindazolones with *α*-Diazo Carbonyl Compounds to access Indazolo[1,2-*a*]cinnoline Carboxylates

2B.1 Introduction

α-Diazo carbonyl compounds are C-1 or C-2 synthons that have been extensively used in the domain of C-H activation to architect various functionalized and fused-(hetero)arenes in the past decade.[1-3] Importantly, electrophilic metal carbenoids formed by the interaction of negatively polarized carbon with a transition metal catalyst, followed by dinitrogen extrusion serve as a powerful intermediate for the construction of C-C bonds.[4-7] Moreover, *α*-diazo carbonyl compounds featured with ease of preparation and ease of handling have attracted the attention of chemists to for preparing complicated organic scaffolds in an atom- and step-economical manner.[8-9] In fact, the complete reactivity of diazo compounds depends on the nature of two substituents attached on it, and can be broadly categorized into three sub-groups, (i) acceptor/acceptor, (ii) acceptor/donor, and (iii) donor/donor groups containing diazo compounds.[10-16]

Pioneering work on transition metal-catalyzed directing group-assisted C-H functionalization by using *α*-diazo carbonyl compounds was showcased in 2012 by Yu's group. Following this, numerous fused *N*-heterocycles have been constructed successfully by exploring the strategy of chelation-assisted C-H activation, and subsequent coupling with diazo compounds through the formation of new C-C and C-N bonds.[17-26]

In this domain, Rovis *et al.* in 2013, documented amide-directed Rh^{III}-catalyzed annulation of *O*-pivaloyl benzhydroxamic acids (**1**) with *α*-diazo carbonyl compounds (**2**), providing a range of isoindolones (**3**) in high yields with the usage of CsOAc base in acetonitrile (Scheme 2B.1.1).[27]

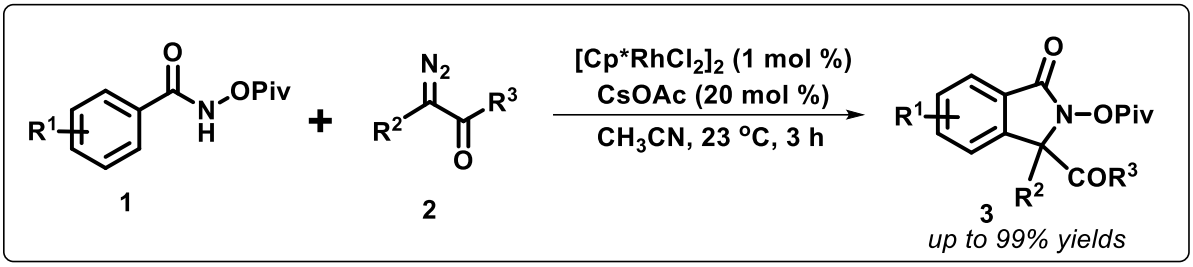

Scheme 2B.1.1 Rh-catalyzed [4+1] annulation strategy for the synthesis of isoindolones using *α*-diazo carbonyl compounds

Wang's group reported a mild and efficient protocol for the preparation of multisubstituted isoquinolones (**5**) from *N*-methoxybenzamide (**4**) and diazo compounds (**2**) *via* C-H activation by using $Rh^{III}/AgSbF_6$ -catalytic system in THF (Scheme 2B.1.2).[28]

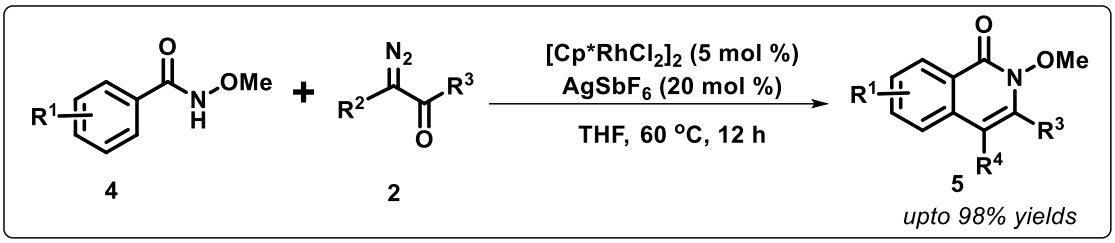

Scheme 2B.1.2 Rh-catalyzed [4+2] annulation strategy for the synthesis of isoquinolones using *α*-diazo carbonyl compounds

Glorius and coworkers disclosed a facile route for the synthesis of multi-substituted isoquinoline *N*-oxides (**7**) *via* Rh^{III}-catalyzed cyclization of oximes (**6**) with *α*-diazo carbonyl compounds (**2**) through aryl and vinylic C-H activation, cyclization and condensation steps under mild conditions. This oxidant-free methodology showed broad range of substituents scope and releases N_2 and H_2O as the by-products (Scheme 2B.1.3a).[29] Patel *et al*. stabilized another oxidant-free, indistinguishable mild approach to obtain substituted isoquinoline *N*-oxides (**7**) by Ir^{III}-catalyzed C-H activation and annulation of (hetero)aryl oxime (**6**) with *α*-diazo carbonyl compounds (**2**) (Scheme 2B.1.3b).[30]

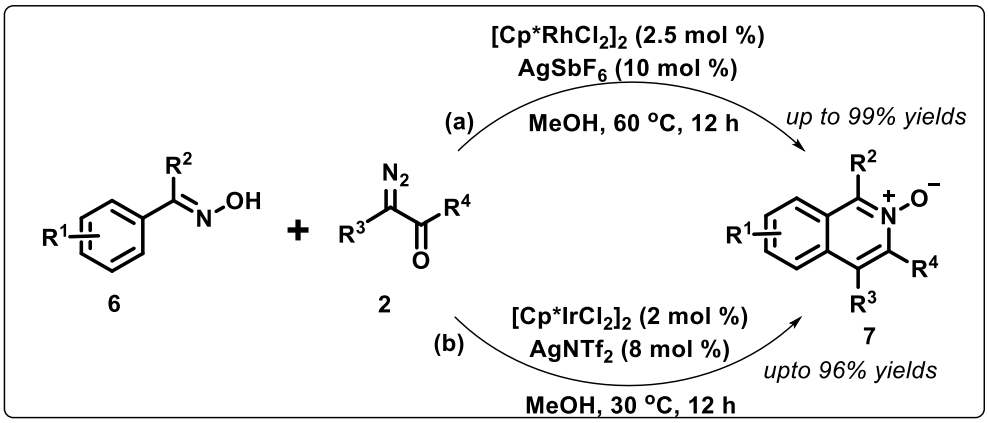

Scheme 2B.1.3 Rh/Ir-catalyzed [4+2] annulation strategies for the synthesis of isoquinoline-*N*-oxides using *α*-diazo carbonyl compounds

Afterward, the same Glorius group displayed the synthesis of isoquinolin-3-ones (**10**) through a Co^{III}-catalyzed C-H bond activation of imines **(8)** with *α*-diazo carbonyl compounds (**9**). The strategy applied a Cobalt catalyst and additionally catalytic amounts of $B(C_6F_5)_3$, which promoted the reaction efficiency by enabling unstable NH imines to serve as directing group (Scheme 2B.1.4a).[31] Ackermann *et al*. made an excellent effort by exploring the directing group ability of imine NH to synthesize isoquinolines (**12**) from aryl amidines (**11**) and *α*-diazo carbonyl

compounds (**2**) in a simple oxidant-free Co^{III}-catalyzed strategy through C-H/N-H bond functionalization (Scheme 2B.1.4b).[32]

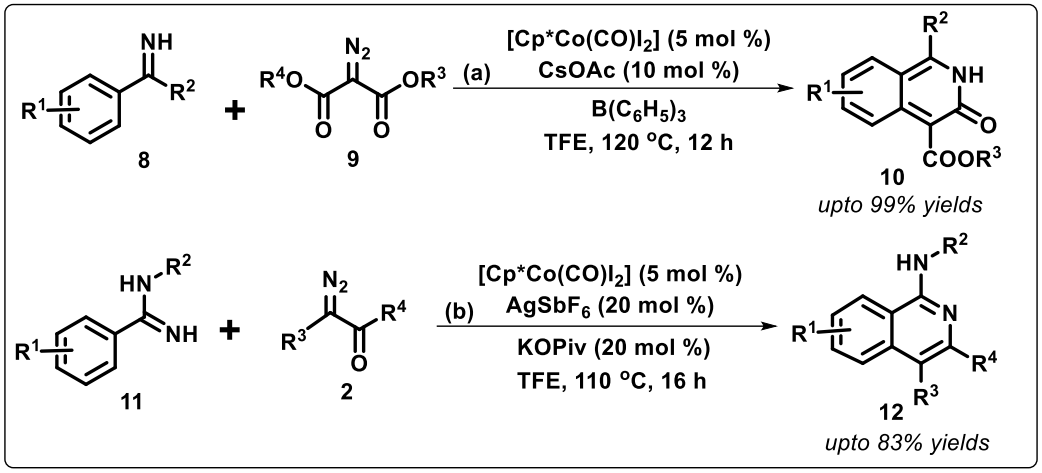

Scheme 2B.1.4 Co-catalyzed [4+2] annulation strategies for the synthesis of isoquinolines using *α*-diazo carbonyl compounds

Gratifyingly, Wu *et al*. utilized a three-carbon component substrate, vinly-*α*-diazo carbonyl compounds (**13**) in Rh^{III}-catalyzed [4+3] annulation with benzamides (**1**) substituted with *O*-pivaloyl groups to obtain acyl azepines (**14**) under mild conditions (Scheme 2B.1.5a).[33]

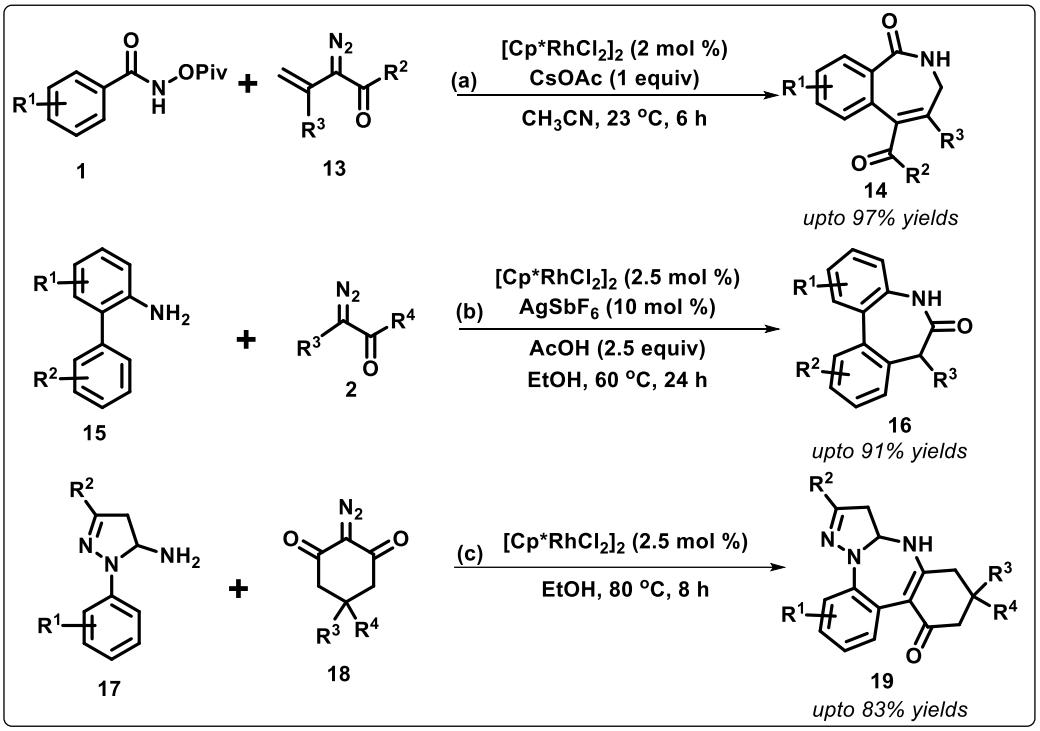

Scheme 2B.1.5 Rh-catalyzed annulation strategies for the synthesis of azepines and diazepines using *α*-diazo carbonyl compounds

Further, Huang and coworkers added another potential procedure to synthesize substituted azepinones (**16**) *via* cascade C-H functionalization/amidation reaction of aminobiaryls (**15**) with *α*-diazo malonates (**2**) under Rh^{III}-catalysis. In this [5+2] annulation strategy, amine group served as a strong directing group for the formation of 6-membered rhodacyclic key intermediate, avoiding the pre-functionalization of starting materials (Scheme 2B.1.5b).[34] Likewise, Shang and coworkers developed uncomplicated Rh^{III}-catalyzed strategy for the synthesis of tetracyclic diazepines (**19**) by [5+2] annulation of 1-aryl-1*H*-pyrazole-5-amines (**17**) with cyclic 2-diazo-1,3-diketones (**18**). Notably, mild reaction conditions with no usage of external oxidant/additive eliminates N_2 and H_2O as by-products with high functional group tolerance (Scheme 2B.1.5c).[35]

Bolm *et al*. developed a [4+2] annulation strategy for Rh^{III}-catalyzed domino C-H activation/cyclization/condensation process accessing substituted 1,2-benzothiazines (**22**) from NH-sulfoximines (**21**) and *α*-diazo compounds **(2)** (Scheme 2B.1.6a).[36] Similarly, Pawar's group attempted the synthesis of 1,2-benzothiazines (**22**) under redox-neutral conditions *via* Ir^{III}-catalyzed C-H/N-H bond functionalization of sulfoximines (**21**) with *α*-diazo carbonyl compounds (**2**) (Scheme 2B.1.6b).[37]

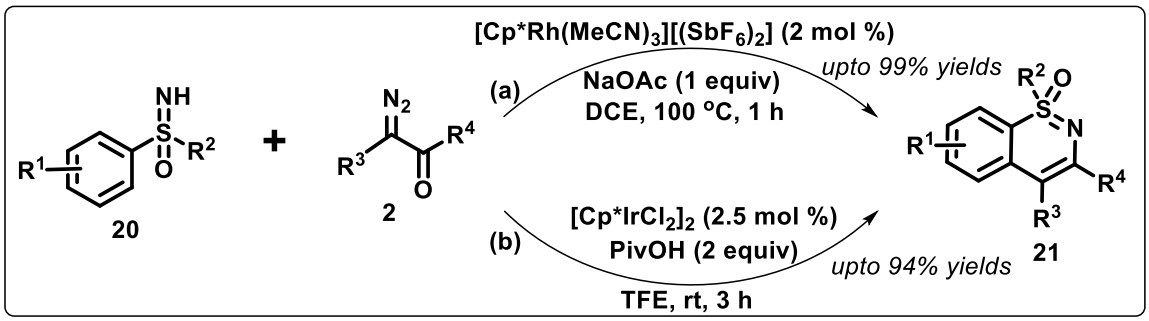

Scheme 2B.1.6 Rh/Ir- catalyzed [4+2] annulation strategies for the synthesis of 1,2-benzothiazines using *α*-diazo carbonyl compounds

Another efficient [4+2] cycloaddition reaction was exposed by Yi's group to access diverse *N*-methoxy isoquinoline-diones (**23**) *via* Rh^{III}-catalyzed regioselective C-H activation, carbenoid insertion and cyclization of *N*-methoxybenzamides (**4**) with *α*-diazotized Meldrum's acid (**22**). The methodology highlighted mild reaction conditions without use of any external ligands or additives (Scheme 2B.1.7a).[38] Patel *et al*. also utilized *α*-diazotized meldrum's acid (**22**) and achieved the synthesis of various *N*-substituted oxindoles (**25**) from acetanilide (**24**) *via* Ir^{III}-catalyzed intermolecular C-H functionalization. The protocol featured with the elimination of acetone, N_2 and CO_2 (Scheme 2B.1.7b).[39]

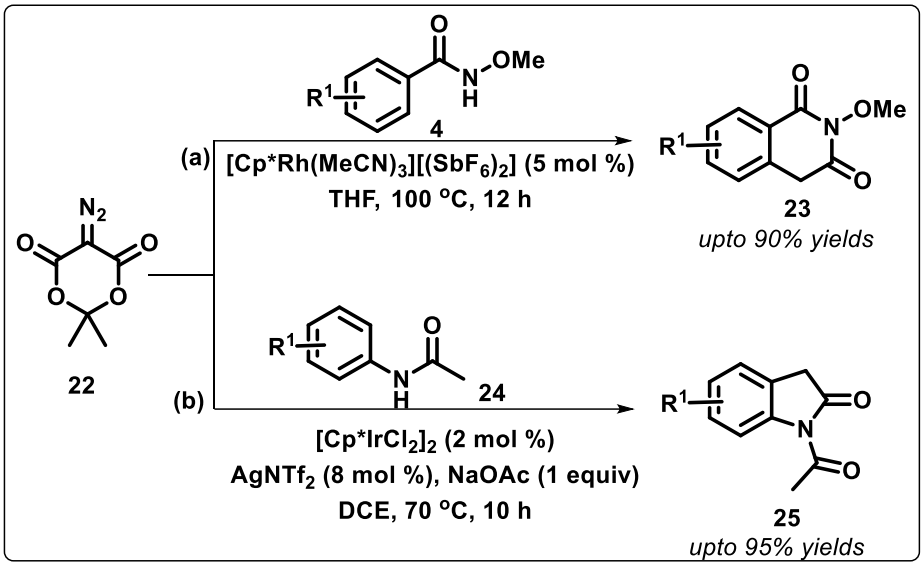

Scheme 2B.1.7 Rh/Ir-catalyzed annulation strategies for the synthesis of isoquinoline-diones and oxaindoles using *α*-diazotized meldrum's acid

Li's group described a straightforward strategy to access functionalized cinnoline triflates (**27**) *via* Rh^{III}-catalyzed annulation of azobenzenes (**26**) with *α*-diazo carbonyl compounds (**2**). The established protocol used zinc triflate that served as Lewis acid as well as source of counter ion for the product formation (Scheme 2B.1.8).[40]

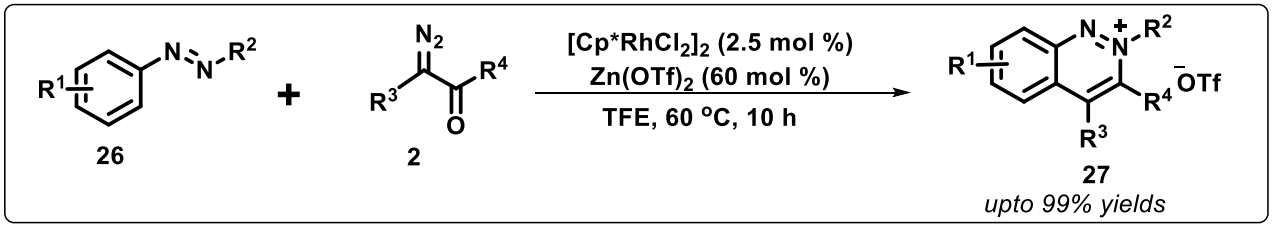

Scheme 2B.1.8 Rh-catalyzed [4+2] annulation strategy for the synthesis of cinnoline triflates using *α*-diazo carbonyl compounds

Dong's group disclosed a Ir^{III}-catalyzed cascade cyclization of 2-arylindoles (**28**) with *α*-diazo carbonyl compounds (**2**) to access pentacyclic fused-carbazoles (**29**) *via* two-fold C-H activation/alkylation, thereby forming three new C-C and one new C-N bond formations in one-pot (Scheme 2B.1.9).[41]

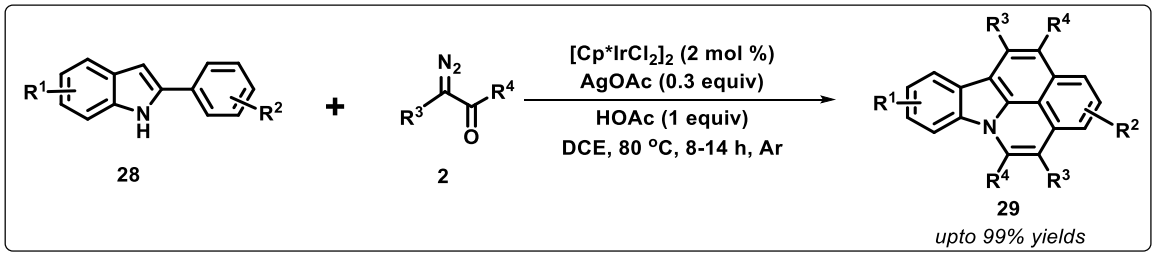

Scheme 2B.1.9 Ir-catalyzed annulation strategy for the synthesis of fused-carbazoles

In 2018, Zeng and Ke *et al.* presented a valuable synthetic methodology to furnish 3,3-disubstituted 2-oxindoles (**31**) through a Co^{III}-catalyzed strategy, involving cross-coupling/cyclization of *N*-nitrosoanilines (**30**) with *α*-diazo-*β*-ketoesters (**2**). This protocol highlighted a unique combination of C-H activation and Wolff rearrangement process (Scheme 2B.1.10).[42]

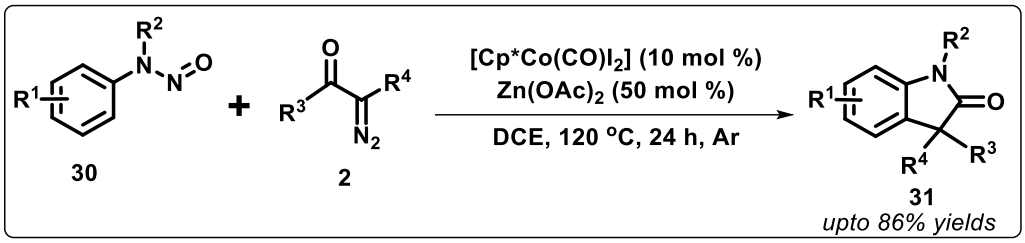

Scheme 2B.1.10 Co-catalyzed annulation strategy for the synthesis of indolin-2-ones using *α*-diazo carbonyl compounds

Interestingly, the functionalization of *N*-arylindazolones remains unexplored with *α*-diazo carbonyl compounds. Anticipating integral directing group ability of cyclic amidic group in *N*-arylindazolones, we envisioned that *N*-arylindazolones could be selectively functionalized using *α*-diazo carbonyl compounds under metal-catalyzed conditions in a one-pot manner. In this chapter, we present our systematic results on the accomplished Ir^{I}-catalyzed [4+2] annulation between 1-aryl-1,2-dihydro-3*H*-indazol-3-ones (**32**) and *α*-diazo carbonyl compounds (**2**) *via* sequential C–H activation/carbene insertion/intramolecular cyclization pathway to afford indazolo[1,2-*a*]cinnolines-5-carboxylates in high yields (Scheme 2B.1.11).

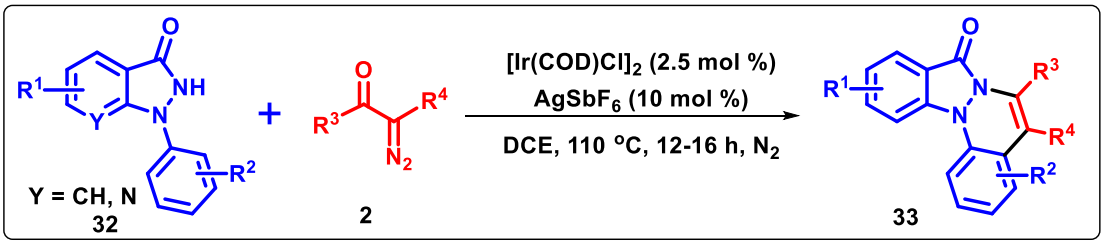

Scheme 2B.1.11 Ir-catalyzed annulation strategy for the synthesis of indazolo-fused cinnolines using *α*-diazo carbonyl compounds

2B.2 Results and Discussion

Our initial investigations started with the optimization study for the reaction of 1-phenyl-1*H*-indazol-3(2*H*)-one (**32a**) with ethyl 2-diazo-3-oxobutanoate (**2a**) as model substrates (Table 2B.2.1). The use of dimeric $[Ir(COD)Cl]_2$ (2.5 mol %) as the catalyst in 1,2-dichloroethane (DCE) at 80 °C for 16 h under a nitrogen atmosphere did not promote the reaction between **32a** and **2a** (Table 2B.2.1, entry 1). The use of additives such as NaOAc, KOAc, AgOAc, $Cu(OAc)_2 \cdot H_2O$, and KPF_6 typically required to generate Ir^I-species failed to produce any annulation product under the following reaction conditions: 80 °C, DCE, 16 h, nitrogen atmosphere (Table 2B.2.1, entries 2–6). Interestingly, the use of $AgSbF_6$ (5 mol %) and $[Ir(COD)Cl]_2$ (2.5 mol %) produced the [4+2] annulation product **33aa** in 52% yield (Table 2B.2.1, entry 7). The structure of **33aa** was unambiguously confirmed by detailed ^1H NMR, ^{13}C NMR, COSY, HSQC, HMBC, and HRMS analysis. Gratifyingly, an increase in the concentration of $AgSbF_6$ from 5 mol % to 10 mol % led to the formation of **33aa** in 64% yield (Table 2B.2.1, entry 8). However, further increase in either the catalyst loading to 5 mol % or the additive concentration to 15 mol % in two separate sets of experiments did not substantially increase the yield of **33aa** (Table 2B.2.1, entries 9 – 10). On the other hand, using 2 mol % of $[Ir(COD)Cl]_2$ afforded 56% of **33aa** in DCE at 80 °C after 16 h (Table 2B.2.1, entry 11). Delightfully, a high reaction temperature of 110 °C facilitated the reaction, affording 88% of **33aa** in 14 h under a nitrogen atmosphere (Table 2B.2.1, entry 12). Surprisingly, the corresponding reaction between **32a** and **2a** under Ir-catalyzed conditions in air led to the formation of **33aa** in <10% yield (Table 2B.2.1, entry 13). Solvent screening studies suggested no other solvent to be superior compared to the non-coordinating solvent DCE (Table 2B.2.1, entries 14–24). Alternatively, the use of comparatively more expensive and well-exemplified dimeric $[Cp^*IrCl_2]_2$ and $[Cp^*RhCl_2]_2$ catalysts afforded **33aa** in 81% and 80% yield, respectively, in DCE at 110 °C for 14 h (Table 2B.2.1, entries 25–26). The optimization studies suggested that both $[Ir(COD)Cl]_2$ and $AgSbF_6$ were essential for the desired transformation under the nitrogen atmosphere.

Table 2B.2.1 Selective optimization[a] studies for the synthesis of **33aa**

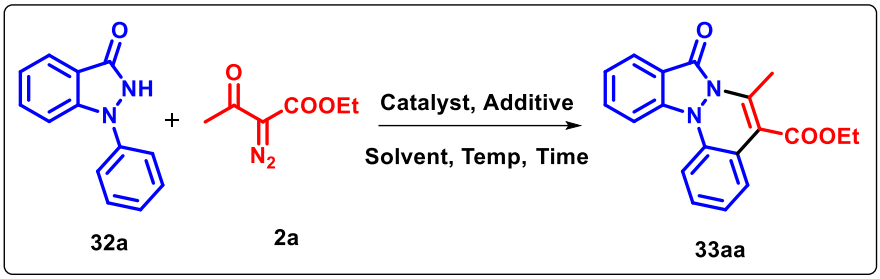

Entry	Catalyst (mol%)	Additive (mol %)	Solvent	Yield of 33aa (%)[b]
1	$[Ir(COD)Cl]_2$ (2.5)	—	DCE	-
2	$[Ir(COD)Cl]_2$ (2.5)	NaOAc (5)	DCE	-
3	$[Ir(COD)Cl]_2$ (2.5)	KOAc (5)	DCE	-
4	$[Ir(COD)Cl]_2$ (2.5)	AgOAc (5)	DCE	-
5	$[Ir(COD)Cl]_2$ (2.5)	$Cu(OAc)_2 \cdot H_2O$ (5)	DCE	-
6	$[Ir(COD)Cl]_2$ (2.5)	KPF_6 (5)	DCE	-
7	$[Ir(COD)Cl]_2$ (2.5)	$AgSbF_6$ (5)	DCE	52
8	$[Ir(COD)Cl]_2$ (2.5)	$AgSbF_6$ (10)	DCE	64
9	$[Ir(COD)Cl]_2$ (2.5)	$AgSbF_6$ (15)	DCE	65
10	$[Ir(COD)Cl]_2$ (5.0)	$AgSbF_6$ (10)	DCE	67
11	$[Ir(COD)Cl]_2$ (2.0)	$AgSbF_6$ (10)	DCE	56
12[c]	$[Ir(COD)Cl]_2$ (2.5)	$AgSbF_6$ (10)	DCE	88
13[d]	$[Ir(COD)Cl]_2$ (2.5)	$AgSbF_6$ (10)	DCE	<10
14[c]	$[Ir(COD)Cl]_2$ (2.5)	$AgSbF_6$ (10)	Toluene	68
15[c]	$[Ir(COD)Cl]_2$ (2.5)	$AgSbF_6$ (10)	Xylene	65
16[c]	$[Ir(COD)Cl]_2$ (2.5)	$AgSbF_6$ (10)	DMF	-
17[c]	$[Ir(COD)Cl]_2$ (2.5)	$AgSbF_6$ (10)	THF	30
18[c]	$[Ir(COD)Cl]_2$ (2.5)	$AgSbF_6$ (10)	MeOH	46
19[c]	$[Ir(COD)Cl]_2$ (2.5)	$AgSbF_6$ (10)	ACN	-
20[e]	$[Ir(COD)Cl]_2$ (2.5)	$AgSbF_6$ (10)	DCM	-
21[c]	$[Ir(COD)Cl]_2$ (2.5)	$AgSbF_6$ (10)	DMSO	-
22[c]	$[Ir(COD)Cl]_2$ (2.5)	$AgSbF_6$ (10)	DMA	-
23[e]	$[Ir(COD)Cl]_2$ (2.5)	$AgSbF_6$ (10)	$CHCl_3$	60
24[c]	$[Ir(COD)Cl]_2$ (2.5)	$AgSbF_6$ (10)	TFE	-
25[c]	$[Cp^*IrCl_2]_2$ (2.5)	$AgSbF_6$ (10)	DCE	81
26[c]	$[Cp^*RhCl_2]_2$ (2.5)	$AgSbF_6$ (10)	DCE	80

[a]Reaction conditions: The reactions were carried out with **32a** (0.23 mmol) and **2a** (0.35 mmol) in the presence of a catalyst/additive (as indicated in the table) in 5 mL of solvent at 80 °C for 16 h under a nitrogen atmosphere. [b]Isolated yields after column chromatography. [c]Reaction temperature = 110 °C for 14 h under a nitrogen atmosphere. [d]Reaction temperature = 110 °C for 16 h under air. [e]Reaction temperature = 60 °C for 14 h under a nitrogen atmosphere.

With the optimized reaction conditions in hand, the substrate scope of this Ir-catalyzed [4+2] annulation with several 1-aryl-1,2-dihydro-3*H*-indazol-3-ones (**32**) and *α*-diazo compounds (**2**) was investigated (Scheme 2B.2.1). 1-Aryl-1,2-dihydro-3*H*-indazol-3-ones containing electron-donating groups, such as Me and OMe [substrates: **32b**,**c** (R^2 = 4-CH_3 and 4-OCH_3)], and electron-withdrawing groups, such as Br, F, and Cl at the *para*-position of the aryl group [substrates: **32d**,**e**,**f** (R^2 = Br, F and Cl)] underwent annulation reactions smoothly with different *α*-diazoketoesters (**2a**–**c**), furnishing the corresponding indazolone-fused cinnolines (**33aa**–**33fc**) in good-to-excellent yields (Scheme 2B.2.1). Similarly, 1-aryl-1,2-dihydro-3*H*-indazol-3-ones substituted with an electron-donating group [substrate: **32h** (R^1 = 5-OCH_3)] or an electron-withdrawing group [substrate: **32i** (R^1 = 5-Br)] on the indazolone moiety were observed to be good substrates, affording high yields of the expected annulation products (**33ha**, **33hb**, **33ia**, and **33ib**). The yield of annulation product **33ga** slightly decreased when dichloro-substituted 1-aryl-1,2-dihydro-3*H*-indazol-3-one [substrate: **32g** (R^2 = 2,4-Cl_2)] was used in place of monochloro-substituted 1-aryl-1,2-dihydro-3*H*-indazol-3-one [substrate: **32f** (R^2 = 4-Cl)] with **2a**. Contentedly, *m*-nitro-substituted 1-aryl-1,2-dihydro-3*H*-indazol-3-one (**32j**) on coupling with **2a** afforded 48% of the corresponding fused cinnoline (**33ja**), while *p*-COOEt substituted 1-aryl-1,2-dihydro-3*H*-indazol-3-one [substrate: **32k** (R^2 = 4-COOEt)] (**32k**) failed to react with **2a** under the optimized conditions. Overall, notable differences in the reactivity of electron-rich and electron-deficient substrates clearly indicate a remarkable influence of the electronic properties of substituents on 1-aryl-1,2-dihydro-3*H*-indazol-3-one for this transformation. It is noteworthy that *p*-CN, *p*-OH, *p*-CHO and *p*-NO_2 substituted 1-aryl-1,2-dihydro-3*H*-indazol-3-ones could not be synthesized by the standard two-step protocol, followed for preparing other 1-aryl-1,2-dihydro-3*H*-indazol-3-ones, and thus their further coupling could not be attempted. On the other hand, an interesting structural aspect of the second coupling partner, *α*-diazo carbonyl compounds, was observed. *α*-Diazoketoesters (**2a**–**c**) reacted with different 1-aryl-1,2-dihydro-3*H*-indazol-3-ones, affording high yields of annulated products (Scheme 2B.2.1). Also, *α*-diazo carbonyl compounds (**2d**–**e**) obtained from symmetrical and unsymmetrical acyclic diketones smoothly reacted with **32a** under the Ir-catalyzed conditions to furnish their corresponding indazolo-fused cinnolines (**33ad**–**33ae**) in 72–76% yields. However,

dialkyl diazomalonates (**2f** and **2g**, R^3/R^4 = OEt or OMe) failed to react under the optimized conditions, indicating the requirement of an acyl/keto group in the *α*-diazo carbonyl compound. Unfortunately, methyl 2-diazo-4,4-dimethyl-3-oxopentanoate (**2h**) was also found to be an unreactive partner for the described [4+2] annulation reaction. The representative ^1H and ^{13}C NMR spectra of **33aa** are shown in Figure 2B.2.1 and Figure 2B.2.2, respectively.

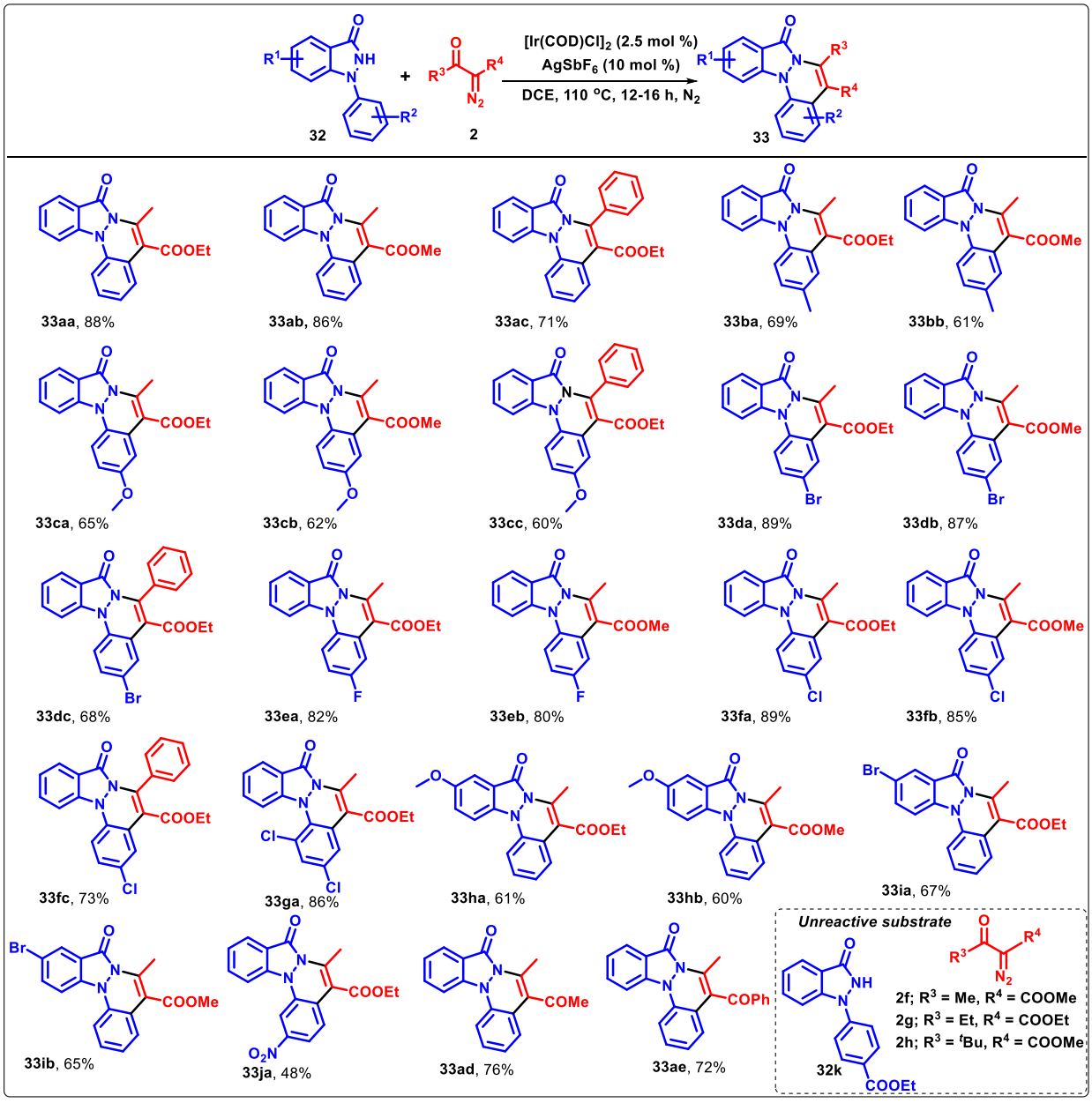

Scheme 2B.2.1 Substrate scope of 1-aryl-1,2-dihydro-3*H*-indazol-3-ones and *α*-diazo carbonyl compounds

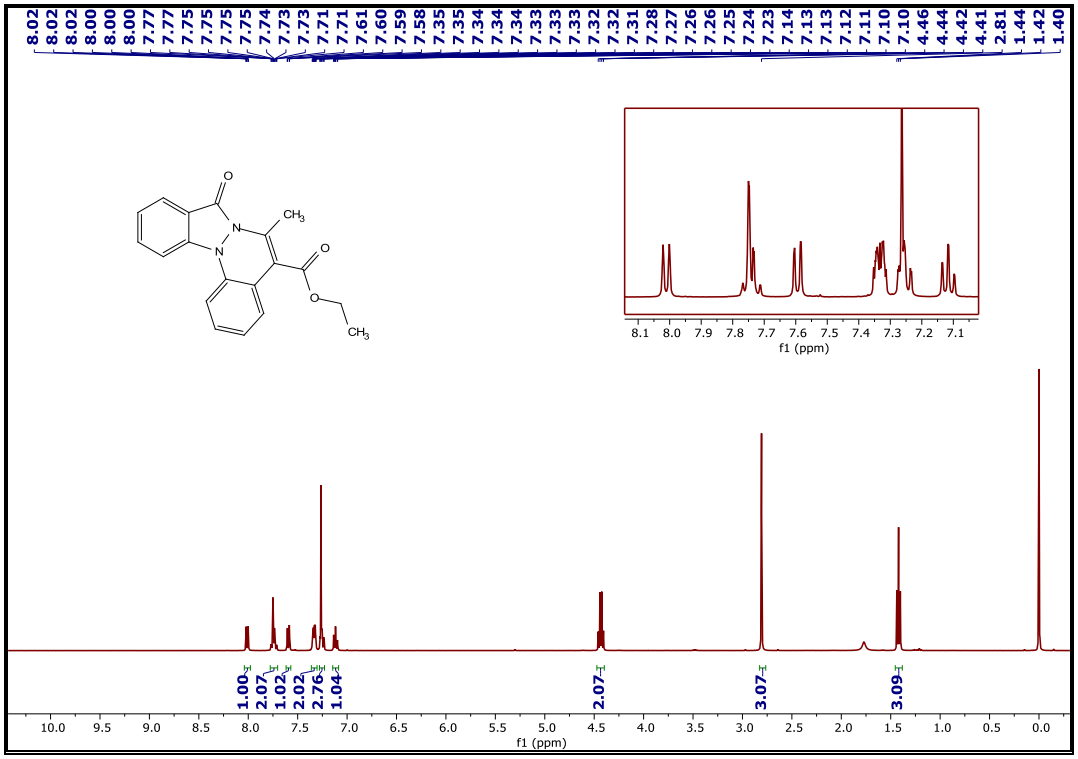

Figure 2B.2.1 ^{1}H NMR Spectrum of **33aa**

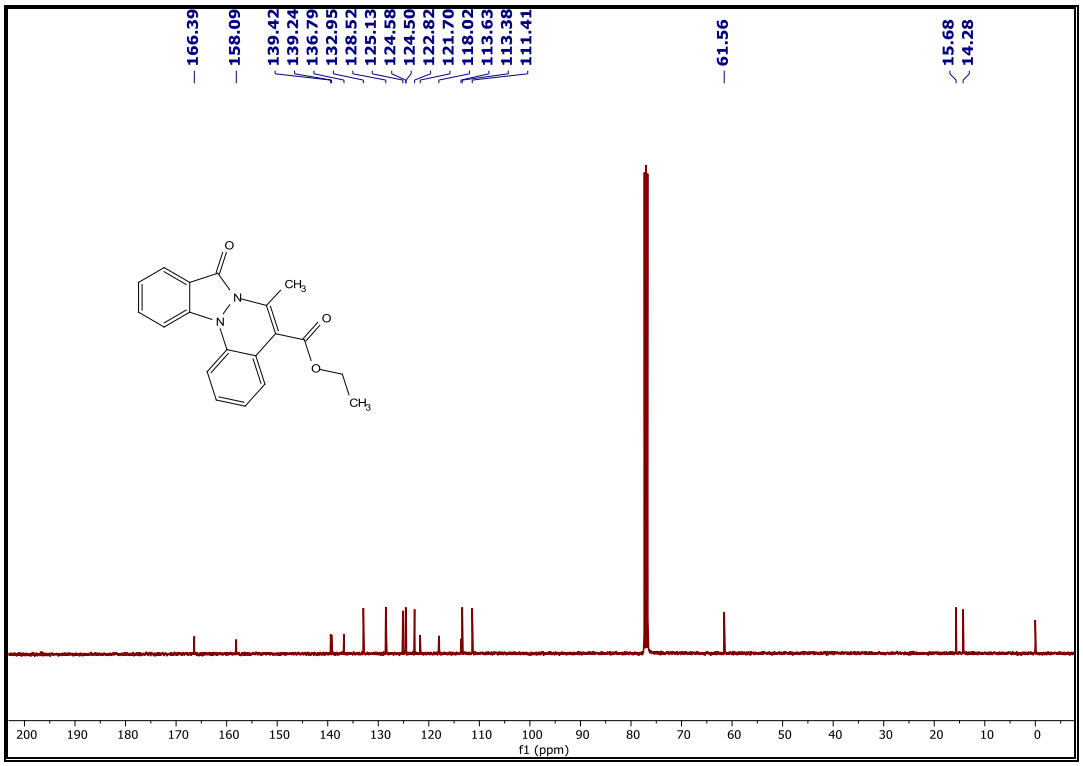

Figure 2B.2.2 ^{13}C NMR Spectrum of **33aa**

To further confirm the proposed structure of products, as a representative example, single crystals of **33fc** were grown from diethyl ether for X-ray diffraction (XRD) studies. Compound **33fc** crystallized in the triclinic P^{-1} space group. An ORTEP diagram of **33fc** (CCDC no. 1841375) is shown in Figure 2B.2.3.

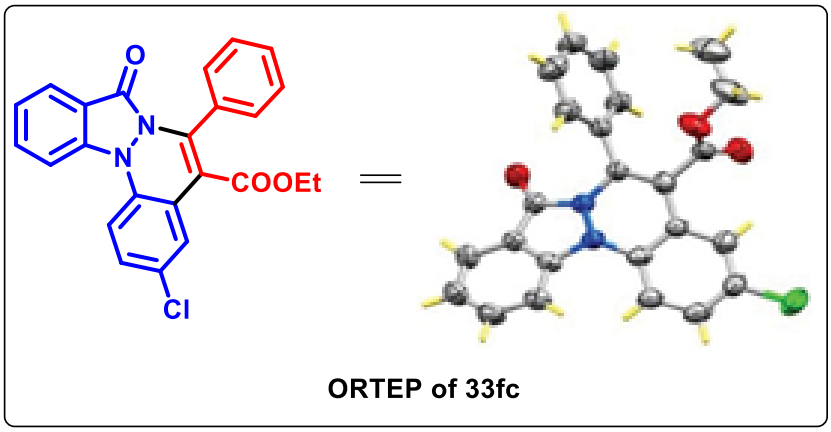

Figure 2B.2.3 ORTEP Diagram of **33fc**

Next, the substrate scope of the developed method for coupling 1-aryl-1,2-dihydro-3*H*-indazol-3-one with *α*-diazo cyclic carbonyl compounds was evaluated (Scheme 2B.2.2). The reaction of 1-phenyl-1,2-dihydro-3*H*-indazol-3-one (**32a**) with 2-diazo-5,5-dimethyl-cyclohexane-1,3-dione (**18a**) under the Ir^{I}-catalyzed optimized conditions afforded 2,2-dimethyl-2,3-dihydro-14*H*-benzo[*c*]indazolo[1,2-*a*]cinnoline-4,14(1*H*)-dione (**34aa**) in 76% yield. Similarly, a few more pentacyclic annulated products (**34ba**–**34da**) were obtained in 52–71% yields by coupling substituted 1-phenyl-1,2-dihydro-3*H*-indazol-3-one (**32b**–**d**) with **18a**. Unfortunately, diazo Meldrum's acid failed to produce any product with 1-phenyl-1,2-dihydro-3*H*-indazol-3-one (**32**). To extend the scope of our methodology, 1-phenyl-1,2-dihydro-3*H*-pyrazolo[3,4-*b*]pyridin-3-one (**32l**) was synthesized following a standard procedure, and its annulation reaction with *α*-diazo carbonyl compounds was attempted. Pleasingly, **32l** reacted comfortably with **2a** and **18a** under the Ir^{I}-catalyzed conditions to furnish ethyl 6-methyl-8-oxo-8*H*-pyrido[3′,2′:4,5]pyrazolo[1,2-*a*]cinnoline-5-carboxylate (**33la**) and 2,2-dimethyl- 2,3-dihydro-14*H*-benzo[*c*]pyrido[2′,3′:3,4]pyrazolo[1,2-*a*]cinnoline-4,14(1*H*)-dione (**34la**), respectively, in 69-76% yields (Scheme 2B.2.3).

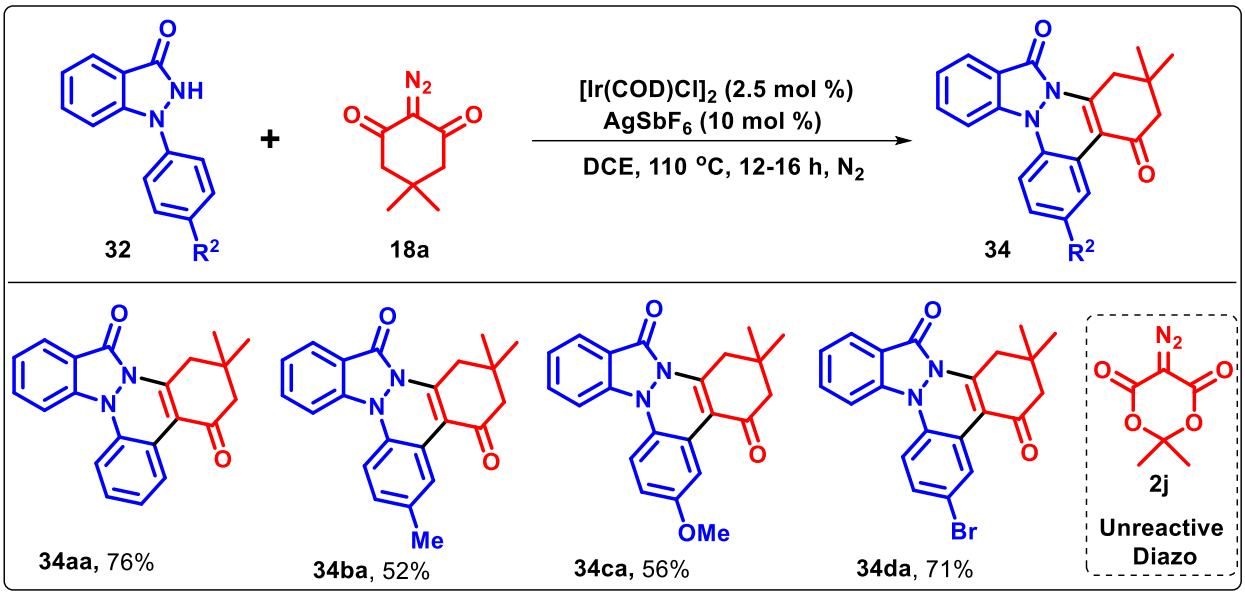

Scheme 2B.2.2 Substrate scope of 1-aryl-1,2-dihydro-3*H*-indazol-3-ones with *α*-diazo cyclic carbonyl compounds

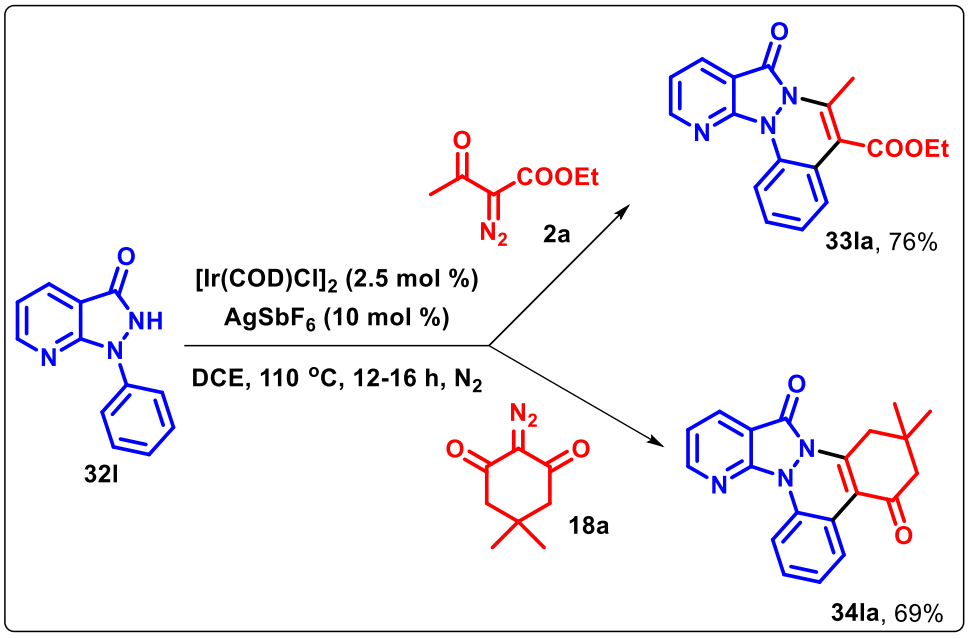

Scheme 2B.2.3 Scope of 1-phenyl-1,2-dihydro-3*H*-pyrazolo[3,4-*b*]pyridin-3-one towards [4+2] annulation with α-diazo carbonyl compounds

To demonstrate the synthetic utility of the synthesized indazolone-fused cinnolines, four different chemical transformations were performed on one of the representative examples, **33aa** (Scheme 2B.2.4). Attempted epoxidation of **33aa** using *m*-CPBA in DCM at room temperature furnished an unexpected, oxidized product **35aa** in 60% yield, whereas the alkaline hydrolysis of **33aa** using

20% aqueous NaOH in ethanol at room temperature furnished the corresponding indazolone-fused cinnoline carboxylic acid derivative (**36aa**) in 65% yield. In addition, reduction of **33aa** with LAH in THF furnished the corresponding alcohol **37aa** in 65% yield, whereas thioamidation of **33aa** using Lawesson's reagent in toluene afforded **38aa** in 71% yield (Scheme 2B.2.4).

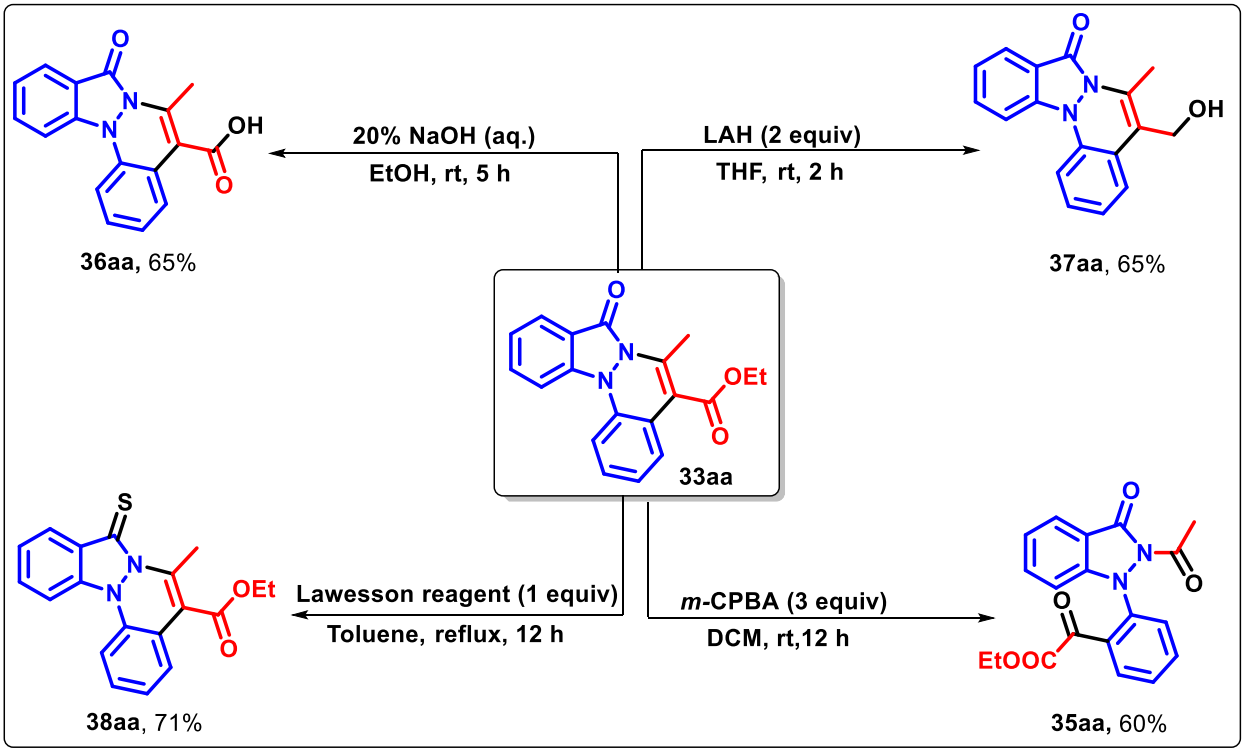

Scheme 2B.2.4 Synthetic utility of indazolone-fused cinnoline **33aa**

To elucidate the mechanism, several preliminary investigations were performed (Scheme 2B.2.5). The reaction between two model substrates (**32a** and **2a**) did not proceed without the use of an Ir catalyst either in the presence or absence of $AgSbF_6$ (Scheme 2B.2.5i). A one-pot intermolecular competitive experiment between **2a** and 1-phenyl-1,2-dihydro-3*H*-indazol-3-one containing electron-rich substrate (**32c**: R^2 = 4-OMe) and electron-deficient substrate (**32d**: R^2 = 4-Br) groups on the aryl group resulted in the formation of **33da** as the major product with a trace of **33ca** (Scheme 2B.2.5ii). However, the intermolecular competitive experiment between **2a** and 1-phenyl-1,2-dihydro-3*H*-indazol-3-one containing electron-rich substrate (**32h**: R^1 = 5-OMe) and electron-deficient substrate (**32i**: R^1 = 5-Br) groups on the indazolone moiety resulted in the formation of a mixture containing annulation products **33ha** and **33ia** in a 1:2 ratio, respectively (Scheme 2B.2.5ii). This clearly shows the higher reactivity of electron-deficient substrates over electron-rich 1-phenyl-1,2-dihydro-3*H*-indazol-3-one substrates for the desired transformation.

Repeated attempts to isolate the iridacyclic intermediate by reacting stoichiometric amounts of **32a**, $[Ir(COD)Cl]_2$ and $AgSbF_6$ in DCE at room temperature failed, probably due to the instability of the complex. Therefore, the above reaction mixture was monitored by analyzing its mass spectra at different intervals of time (Scheme 2B.2.5iii). To our delight, the ESI-HRMS spectrum of the crude mixture recorded after 2 h of stirring at room temperature indicated the presence of a five-membered iridacyclic complex **B** (Figure 2B.2.4). Then, **2a** was added to the same reaction mixture, and the mixture was stirred. The mixture was subsequently analyzed by mass spectrometry after specific intervals of time. Interestingly, the molecular masses of Ir^{III}-carbene species (**C** or **D**) and *ortho*-functionalized 1-phenyl-1,2-dihydro-3*H*-indazol-3-one (**E**) were determined after 2 h and 4 h of addition of **2a**, respectively (Figure 2B.2.5 and Figure 2B.2.6). Notably, product formation (**33aa**) was initiated (on TLC) after stirring the above reaction mixture for ~10 h at room temperature (Scheme 2B.2.5iii). Finally, a procedure used by Tsuji *et al.* was followed to isolate a stable iridacyclic complex. A stoichiometric reaction of **32a** and $[Ir(COD)Cl]_2$ was performed in the presence of $AgSbF_6$ and sodium bicarbonate in toluene under reflux for 12 h, followed by the addition of triphenylphosphine (instead of **2a**) (Scheme 2B.2.5iv). To our delight, ^1H NMR and ESI-HRMS analysis of the partially purified complex indicated the formation of an Ir-metalated complex **B1** (Figure 2B.2.7 and Figure 2B.2.8). Attempts to further purify this crude complex containing some impurities using column chromatography led to its decomposition. Thus, it is quite likely that such a five-membered iridacyclic complex (**B1**) is a key intermediate in our developed annulation method, as earlier documented by Tsuji.[43] Unfortunately, further efforts to purify this complex by column chromatography failed (Scheme 2B.2.5iv).

Based on the literature reports[39,43-44] and mechanistic investigations, a plausible mechanism is proposed (Scheme 2B.2.6). The reaction proceeds through the dissociation of an $[Ir(COD)Cl]_2$ dimer complex following anion exchange with $AgSbF_6$ to generate an Ir^I species. The Ir^I species facilitates the N–H oxidative addition of 1-phenyl-1,2-dihydro-3*H*-indazol-3-one **32a**, generating **A**, which upon C_{Ar}–H bond activation affords five-membered Ir^{III} intermediate **B**. In the next step, the iridacyclic intermediate **B** reacts with α-diazo carbonyl compound **2a** to form Ir^{III} carbene species **C**. Migratory insertion of the carbene into the Ir–C_{Ar} bond leads to the formation of intermediate **D**, which undergoes protodemetallation to afford **E** possibly as a tautomeric mixture, thus regenerating the Ir^I species for the next catalytic cycle. Finally, the desired product **33aa** is obtained from intermediate **E** by nucleophilic addition followed by dehydration.

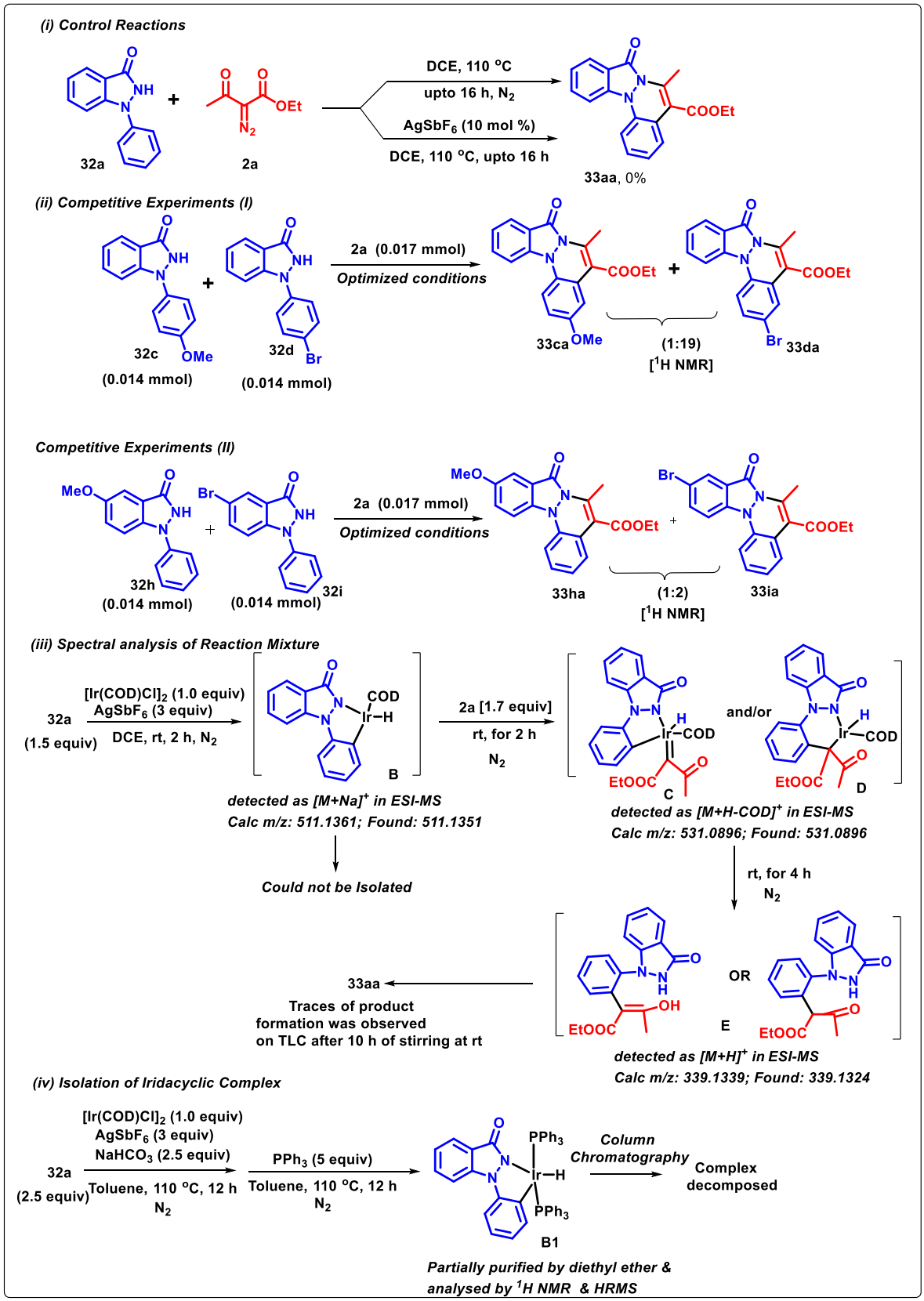

Scheme 2B.2.5 Mechanistic investigations

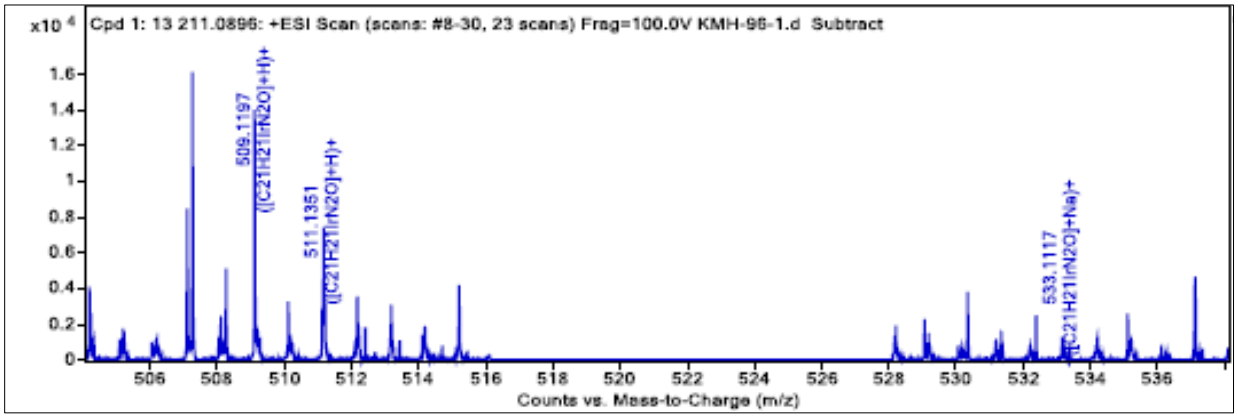

Figure 2B.2.4 HRMS Spectrum of species **B**

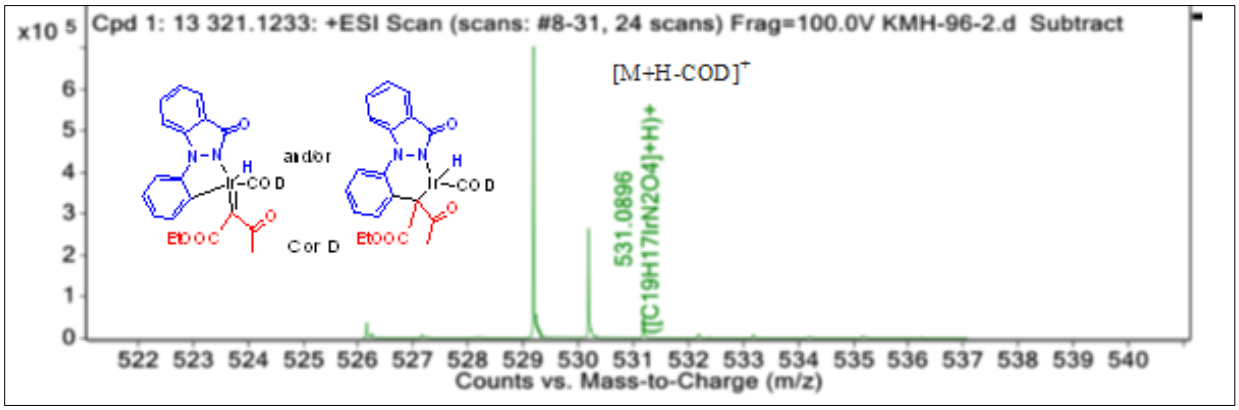

Figure 2B.2.5 HRMS Spectrum of species **C** or **D**

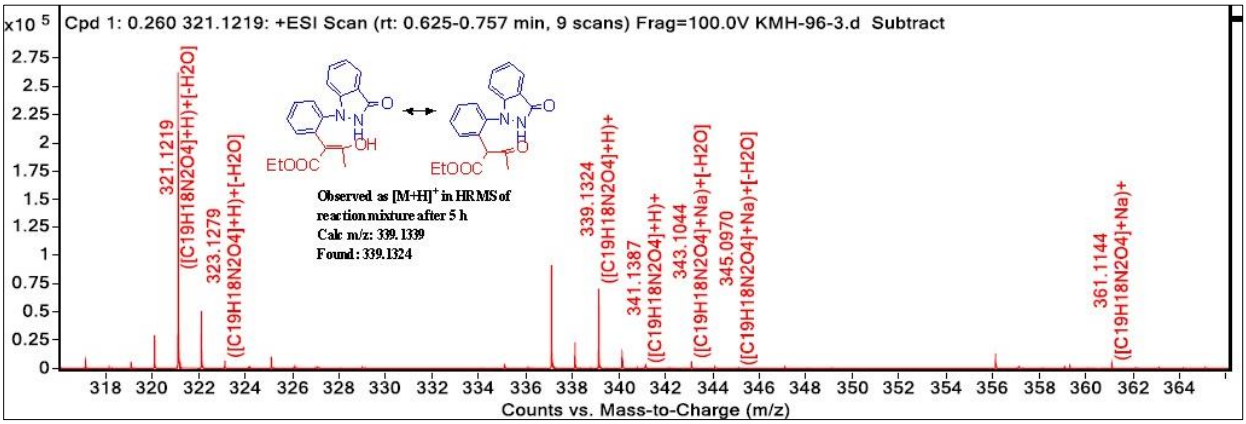

Figure 2B.2.6 HRMS Spectrum of species **E**

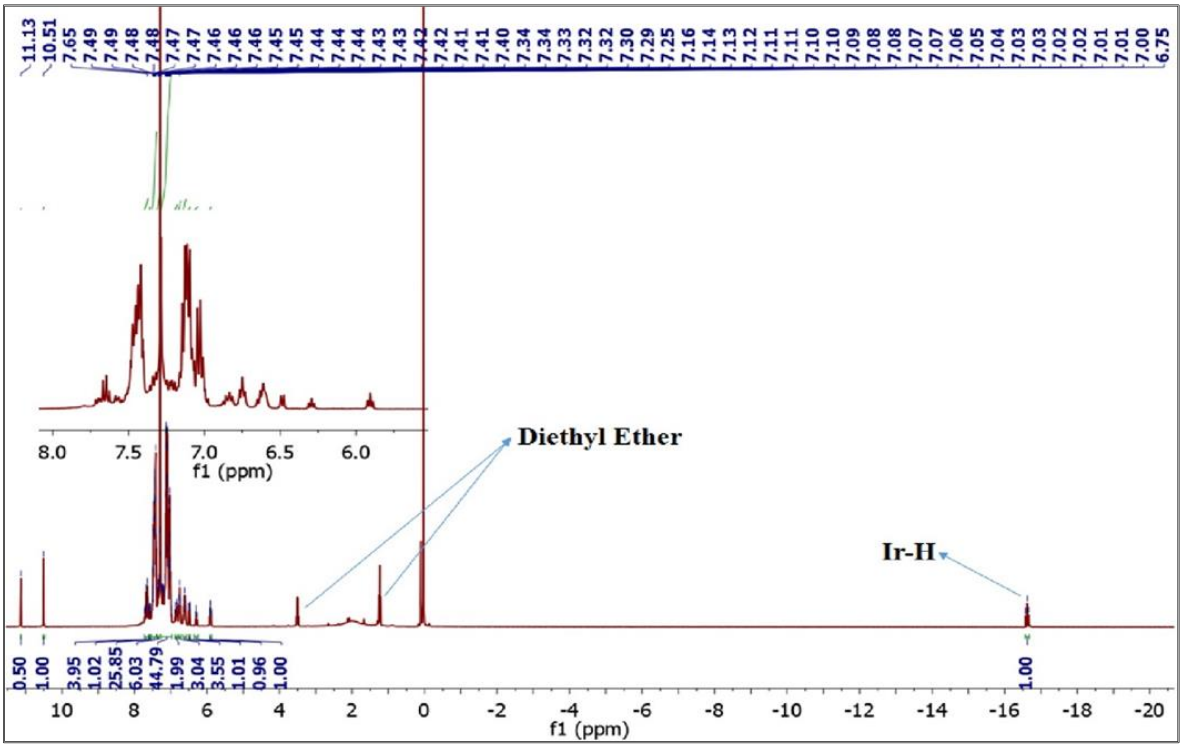

Figure 2B.2.7 ^{1}H NMR Spectrum of Crude Complex (**B1**)

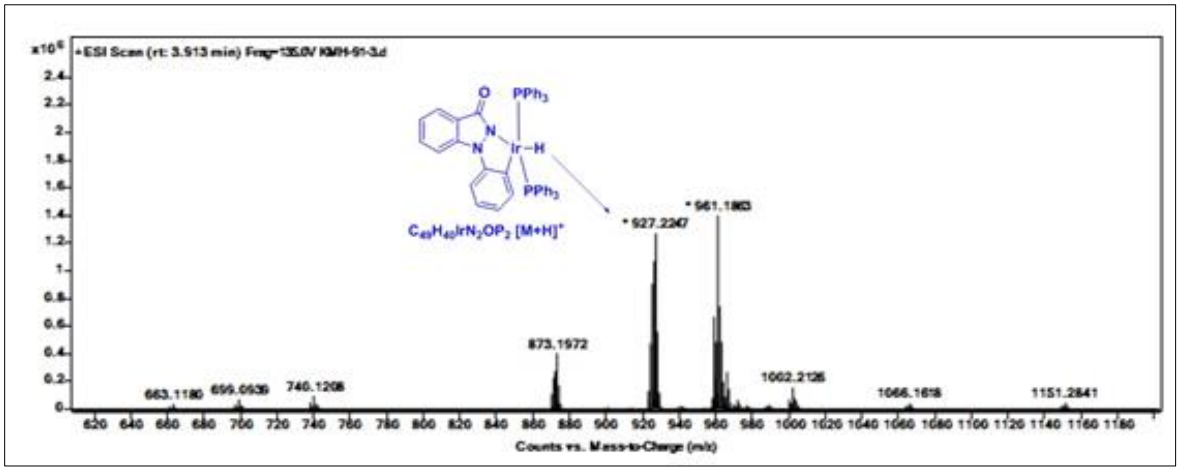

Figure 2B.2.8 HRMS Spectrum of Crude complex (**B1**)

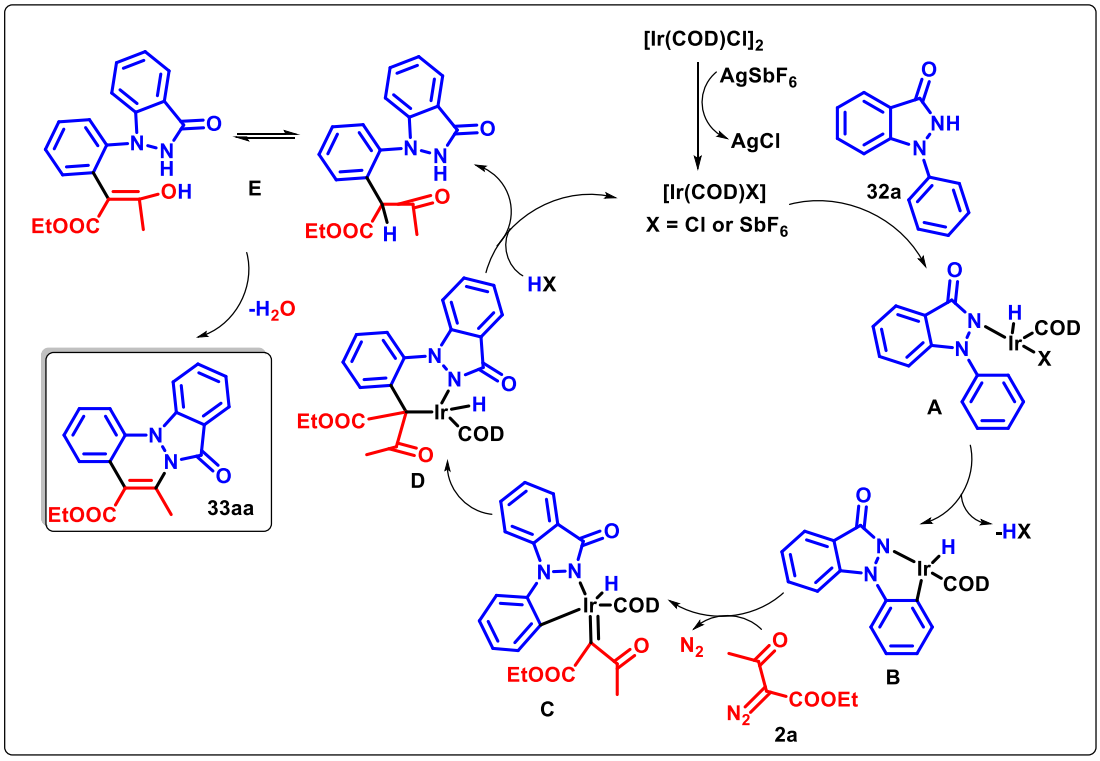

Scheme 2B.2.6 Plausible mechanistic pathway

In summary, a simple and straightforward [4+2] annulation method was developed for the synthesis of indazolone-fused cinnolines from 1-aryl-1,2-dihydro-3*H*-indazol-3-one and *α*-diazo carbonyl compounds *via* C–H bond activation using $[Ir(COD)Cl]_2$ and $AgSbF_6$ in catalytic amounts. Many tetra and pentacyclic fused heterocycles were synthesized with diverse functionalities in good-to-excellent yields. Mechanistic investigations were performed to isolate the iridacyclic intermediate, based on which a plausible mechanism is proposed. This is the first report of annulation of *α*-diazo carbonyl compounds with 1-aryl-1,2-dihydro-3*H*-indazol-3-one.

2B.3 Experimental Section

General considerations

Commercially available reagents were used without purification. *α*-Diazo carbonyl compounds were prepared as per the reported protocol.[45] Commercially available solvents were dried by standard procedures prior to use. Nuclear magnetic resonance spectra were recorded on a 400 MHz spectrometer, and chemical shifts are reported in *δ* units, parts per million (ppm), relative to residual chloroform (7.26 ppm) or DMSO (2.5 ppm) in the deuterated solvent. The following abbreviations were used to describe peak splitting patterns when appropriate: s = singlet, d = doublet, t = triplet, dd = doublet of doublets, and m = multiplet. Coupling constants *J* are reported

in Hz. The ^{13}C NMR spectra are reported in ppm relative to deuterochloroform (77.0 ppm) or [d_6] DMSO (39.5 ppm). Melting points were determined on a capillary point apparatus equipped with a digital thermometer and are uncorrected. High-resolution mass spectra were recorded on a TOF analyzer spectrometer in electrospray mode.

General procedure for the synthesis of indazolone-fused cinnolines (33)

To a stirred solution of 1-aryl-1,2-dihydro-3*H*-indazol-3-one (**32**) (50 mg, 1 equiv.) in DCE (5 mL), $[Ir(COD)Cl]_2$ (2.5 mol %) and $AgSbF_6$ (10 mol %) were added under a nitrogen atmosphere. After 15 min, the *α*-diazo carbonyl compound (**2**) (1.5 equiv.) in DCE (0.5 mL) was added. The reaction mixture was stirred at 110 °C for 12–16 h (traced by TLC). After the completion of the reaction, the reaction mixture was cooled to room temperature, diluted with water, and extracted with DCM (20 mL × 2). The organic layers were combined and concentrated under vacuum to afford a residue. The residue was purified by column chromatography (SiO_2 (100–200 mesh), eluant, (hexanes/EtOAc = 9/1) to afford the desired product (**33**).

Ethyl 6-methyl-8-oxo-8*H*-indazolo[1,2-*a*]cinnoline-5-carboxylate (33aa). Yellow solid, 67.6 mg (88%); mp 101-103 °C; ^1H NMR (400 MHz, $CDCl_3$) δ 8.04 – 7.97 (m, 1H), 7.78 – 7.70 (m, 2H), 7.59 (dd, J = 8.2, 1.1 Hz, 1H), 7.36 – 7.30 (m, 2H), 7.28 – 7.23 (m, 1H, merged with $CDCl_3$), 7.14 – 7.08 (m, 1H), 4.43 (q, J =7.1 Hz, 2H), 2.81 (s, 3H), 1.42 (t, J = 7.1 Hz, 3H); ^{13}C NMR (100 MHz, $CDCl_3$) δ 166.4, 158.1, 139.4, 139.2, 136.8, 133.0, 128.5, 125.1, 124.6, 124.5, 122.8, 121.7, 118.0, 113.6, 113.4, 111.4, 61.6, 15.7, 14.3; HRMS (ESI-TOF) (*m/z*) calculated $C_{19}H_{17}N_2O_3^+$: 321.1234, found 321.1238 $[M + H]^+$.

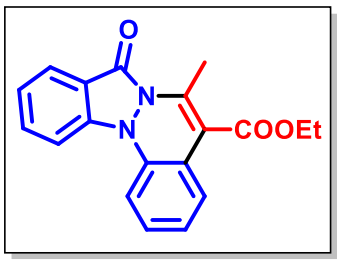

Methyl 6-methyl-8-oxo-8H-indazolo[1,2-*a*]cinnoline-5-carboxylate (33ab). Yellow solid, 63.2 mg (86%); mp 135-137 °C; ^1H NMR (400 MHz, $CDCl_3$) δ 8.04 – 7.99 (m, 1H), 7.77 – 7.72 (m, 2H), 7.59 (dd, J = 8.1, 1.2 Hz, 1H), 7.38 – 7.31 (m, 2H), 7.28 – 7.23 (m, 1H), 7.15 – 7.09 (m, 1H), 3.97 (s, 3H), 2.82 (s, 3H); ^{13}C NMR (100 MHz, $CDCl_3$) δ 166.8, 158.1, 140.0, 139.3, 136.8, 133.0, 128.5, 125.2, 124.6, 124.5, 122.8, 121.6, 118.0, 113.4, 113.3, 111.4, 52.3, 15.7; HRMS (ESI-TOF) (*m/z*) calculated $C_{18}H_{15}N_2O_3^+$: 307.1077, found 307.1082 $[M + H]^+$.

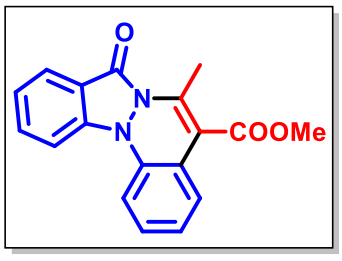

Ethyl 8-oxo-6-phenyl-8*H*-indazolo[1,2-*a*]cinnoline-5-carboxylate (33ac). Yellow solid, 65.3 mg (71%); mp 148-150 °C; ^{1}H NMR (400 MHz, $CDCl_3$) δ 7.99 – 7.94 (m, 1H), 7.85 – 7.76 (m, 3H), 7.67 (dd, J = 8.2, 1.1 Hz, 1H), 7.51 – 7.43 (m, 5H), 7.41 – 7.31 (m, 2H), 7.22 – 7.16 (m, 1H), 4.01 (q, J = 7.1 Hz, 2H), 0.88 (t, J = 7.1 Hz, 3H); ^{13}C NMR (100 MHz, $CDCl_3$) δ 165.8, 156.6, 140.4, 139.3, 137.9, 132.8, 130.9, 129.6, 129.2, 129.1, 127.9, 125.6, 124.7, 124.6, 123.4, 121.4, 118.8, 115.8, 114.3, 111.2, 61.3, 13.5; HRMS (ESI-TOF) (*m/z*) calculated $C_{24}H_{19}N_2O_3^+$: 383.1390, found 383.1405 $[M + H]^+$.

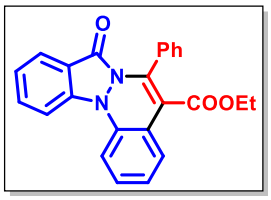

Ethyl 3,6-dimethyl-8-oxo-8*H*-indazolo[1,2-*a*]cinnoline-5-carboxylate (33ba). Yellow solid, 51.5 mg (69%); mp 138-140 °C; ^{1}H NMR (400 MHz, $CDCl_3$) δ 8.04 – 7.99 (m, 1H), 7.78 – 7.70 (m, 2H), 7.50 (d, J = 8.3 Hz, 1H), 7.36 – 7.30 (m, J = 8.0, 1H), 7.15 (d, J = 1.9 Hz, 1H), 7.09 – 7.04 (m, 1H), 4.46 (q, J = 7.1 Hz, 2H), 2.82 (s, 3H), 2.34 (s, 3H), 1.45 (t, J = 7.1 Hz, 3H);^{13}C NMR (100 MHz, $CDCl_3$) δ 166.5, 158.1, 139.3, 139.0, 134.5, 134.1, 132.8, 128.9, 125.6, 124.5, 122.5, 121.5, 117.8, 113.7, 113.2, 111.3, 61.5, 21.0, 15.7, 14.3; HRMS (ESI-TOF) (*m/z*) calculated $C_{20}H_{19}N_2O_3^+$: 335.1390, found 335.1394 $[M + H]^+$.

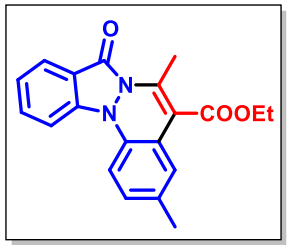

Methyl 3,6-dimethyl-8-oxo-8*H*-indazolo[1,2-a]cinnoline-5-carboxylate (33bb). Yellow solid, 43.8 mg (61%); mp133-135 °C; ^{1}H NMR (400 MHz, $CDCl_3$) δ 8.04 – 7.99 (m, 1H), 7.77 – 7.71 (m, 2H), 7.49 (d, J = 8.3 Hz, 1H), 7.36 – 7.29 (m, 1H), 7.12 (d, J = 1.9 Hz, 1H), 7.09 – 7.04 (m, 1H), 3.98 (s, 3H), 2.81 (s, 3H), 2.34 (s, 3H); ^{13}C NMR (100 MHz, $CDCl_3$) δ 167.0, 158.1, 139.5, 139.3, 134.5, 134.2, 132.9, 128.9, 125.6, 124.6, 122.6, 121.5, 117.8, 113.4, 113.3, 111.3, 52.3, 21.0, 15.7; HRMS (ESI-TOF) (*m/z*) calculated $C_{19}H_{17}N_2O_3^+$: 321.1234, found 321.1236 $[M + H]^+$.

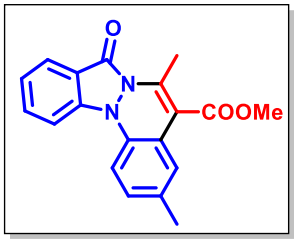

Ethyl 3-methoxy-6-methyl-8-oxo-8*H*-indazolo[1,2-*a*]cinnoline- 5-carboxylate (33ca). Yellow solid, 47.5 mg (65%); mp 85-90 °C; ^{1}H NMR (400 MHz, $CDCl_3$) δ 8.02 (dd, J = 7.9, 1.1 Hz, 1H), 7.77 – 7.68 (m, 2H), 7.52 (d, J = 8.9 Hz, 1H), 7.34 – 7.29 (m, 1H), 6.98 (d, J = 2.8 Hz, 1H), 6.80 (dd, J = 8.9, 2.8 Hz, 1H), 4.45 (q, J = 7.1 Hz, 2H), 3.83 (s, 3H), 2.84 (s, 3H), 1.45 (t, J = 7.1 Hz, 3H); ^{13}C NMR (100 MHz, $CDCl_3$) δ 166.3, 158.3, 156.5, 140.3, 139.6, 132.9, 130.6, 124.7, 123.1, 122.5, 117.7, 113.1, 112.4,

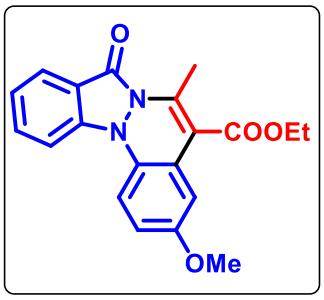

111.1, 61.5, 55.6, 15.7, 14.3; HRMS (ESI-TOF) (*m/z*) calculated $C_{20}H_{19}N_2O_4^+$: 351.1339, found 351.1343 $[M + H]^+$.

Methyl 3-methoxy-6-methyl-8-oxo-8*H*-indazolo[1,2-*a*]cinnoline-5-carboxylate (33cb).

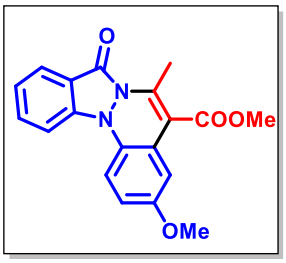

Yellow solid, 43.5 mg (62%); mp 154-157 °C; ^{1}H NMR (400 MHz, $CDCl_3$) δ 8.03 – 7.99 (m, 1H), 7.75 – 7.70 (m, 2H), 7.52 (d, *J* = 8.8 Hz, 1H), 7.34 – 7.29 (m, 1H), 6.97 (d, *J* = 2.8 Hz, 1H), 6.79 (dd, *J* = 8.9, 2.8 Hz, 1H), 3.97 (s, 3H), 3.83 (s, 3H), 2.84 (s, 3H); ^{13}C NMR (100 MHz, $CDCl_3$) δ 166.8, 158.3, 156.5, 140.8, 139.6, 133.0, 130.5, 126.5, 124.7, 123.1, 122.5, 117.7, 113.1, 112.9, 112.4, 111.3, 55.7, 52.3, 15.8; HRMS (ESI-TOF) (*m/z*) calculated $C_{19}H_{17}N_2O_4^+$: 337.1183, found 337.1179 $[M + H]^+$.

Ethyl 3-methoxy-8-oxo-6-phenyl-8*H*-indazolo[1,2-*a*]cinnoline- 5-carboxylate (**33cc**).

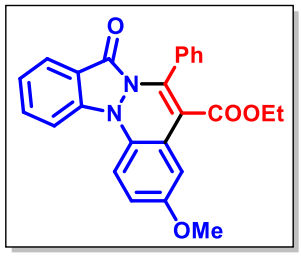

Yellow solid, 52 mg (60%); mp 138-140 °C; ^{1}H NMR (400 MHz, $CDCl_3$) δ 7.98 – 7.92 (m, 1H), 7.8 – 7.74 (m, 2H), 7.57 (d, *J* = 8.9 Hz, 1H), 7.48 – 7.41 (m, 6H), 7.38 – 7.32 (m, 1H), 6.86 (dd, *J* = 8.9, 2.9 Hz, 1H), 4.01 –3.97 (m, 2H), 3.86 (s, 3H), 0.86 (t, *J* = 7.1 Hz, 3H); ^{13}C NMR (100 MHz, $CDCl_3$) δ 166.0, 156.6, 140.8, 140.1, 132.8, 131.8, 130.9, 129.6, 129.6, 129.1, 127.9, 124.8, 123.1, 122.8, 118.6, 115.3, 114.2, 114.1, 112.2, 111.1, 61.3, 55.7, 13.5; HRMS (ESI-TOF) (*m/z*) calculated $C_{25}H_{21}N_2O_4^+$: 413.1496, found 413.1515 $[M + H]^+$.

Ethyl 3-bromo-6-methyl-8-oxo-8*H*-indazolo[1,2-*a*]cinnoline-5-carboxylate (33da). Yellow

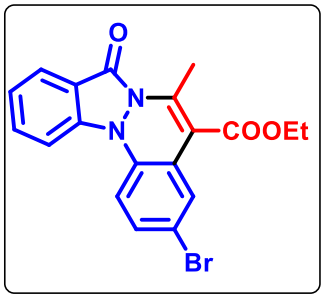

solid, 61.5 mg (89%); mp 155-158 °C; ^{1}H NMR (400 MHz, $CDCl_3$) δ 8.03 – 7.98 (m, 1H), 7.78 – 7.72 (m, 1H), 7.70 – 7.66 (m, 1H), 7.52 (d, *J* = 2.2 Hz, 1H), 7.43 (d, *J* = 8.6 Hz, 1H), 7.38 – 7.32 (m, 2H), 4.45 (q, *J* = 7.2 Hz, 2H), 2.82 (s, 3H), 1.44 (t, *J* = 7.2 Hz, 3H); ^{13}C NMR (100 MHz, $CDCl_3$) δ 165.8, 158.0, 141.4, 139.2, 135.8, 133.3, 130.9, 128.0, 124.8, 123.8, 123.2, 118.1, 117.3, 113.2, 112.8, 112.2, 61.7, 15.7, 14.2; HRMS (ESI-TOF) (*m/z*) calculated $C_{19}H_{16}BrN_2O_3^+$: 401.0321, found 401.0323 $[M + H]^+$.

Methyl 3-bromo-6-methyl-8-oxo-8*H*-indazolo[1,2-*a*]cinnoline- 5-carboxylate (33db). Yellow

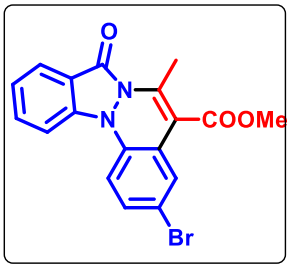

solid, 58.2 mg (87%); mp 150-153 °C; ^{1}H NMR (400 MHz, $CDCl_3$) δ 8.06 – 8.00 (m, 1H), 7.80 – 7.74 (m, 1H), 7.73 – 7.69 (m, 1H), 7.52 (d, J = 2.1 Hz, 1H), 7.45 (d, J = 8.6 Hz, 1H), 7.40 – 7.33 (m, 2H), 3.98 (s, 3H), 2.84 (s, 3H); ^{13}C NMR (100 MHz, $CDCl_3$) δ 166.3, 158.1, 141.9, 139.3, 135.9, 133.3, 131.0, 128.0, 124.8, 123.8, 123.2, 118.2, 117.4, 113.3, 112.8, 112.0, 52.5, 15.8; HRMS (ESI-TOF) (*m/z*) calculated $C_{18}H_{14}BrN_2O_3^+$: 385.0182, found 385.0189 $[M + H]^+$.

Ethyl 3-bromo-8-oxo-6-phenyl-8H-indazolo[1,2-*a*]cinnoline-5- carboxylate (33dc). Yellow

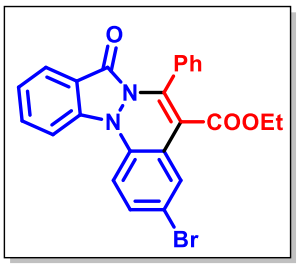

solid, 54 mg (68%); mp: 159-161 °C; ^{1}H NMR (400 MHz, $CDCl_3$) δ 7.98 (d, J = 2.2 Hz, 1H), 7.83 –7.77 (m, 2H), 7.55 – 7.39 (m, 9H), 3.99 (q, J = 7.2 Hz, 2H), 0.85 (t, J = 7.2 Hz, 3H); ^{13}C NMR (100 MHz, $CDCl_3$) δ 165.4, 156.6, 140.4, 134.3, 133.2, 131.6, 130.6, 129.9, 128.3, 128.0, 124.9, 123.8, 118.9, 117.6, 114.3, 112.7, 61.4, 13.4; HRMS (ESI-TOF) (*m/z*) calculated $C_{24}H_{18}BrN_2O_3^+$: 461.0495; found 461.0509 $[M + H]^+$.

Ethyl 3-fluoro-6-methyl-8-oxo-8*H*-indazolo[1,2-*a*]cinnoline-5- carboxylate (33ea). Yellow

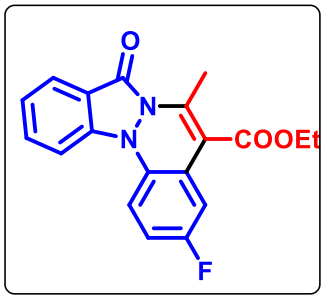

solid, 63.8 mg (82%); mp 126-129 °C; ^{1}H NMR (400 MHz, $CDCl_3$) δ 8.05 – 7.99 (m, 1H), 7.79 – 7.74 (m, 1H), 7.73 – 7.68 (m, 1H), 7.53 (dd, J = 8.9, 4.6 Hz, 1H), 7.39 – 7.32 (m, 1H), 7.19 (dd, J = 9.6, 2.8 Hz, 1H), 6.99 – 6.91 (m, 1H), 4.45 (q, J = 7.2 Hz, 2H), 2.85 (s, 3H), 1.45 (t, J = 7.1 Hz, 3H); ^{13}C NMR (100 MHz, $CDCl_3$) δ 165.9, 160.7, 158.3, 141.8, 139.6, 133.2, 133.1 (d, J_{C-F} = 2.55 Hz), 124.8, 124.0 (d, J_{C-F} = 8.73 Hz) 123.0, 118.0, 114.5 (d, J_{C-F} = 23.21 Hz), 113.2, 112.6 (d, J_{C-F} = 5.27 Hz), 112.5 (d, J_{C-F} = 12.2 Hz), 112.4 (d, J_{C-F} = 2.27 Hz), 61.7, 15.7, 14.3; ^{19}F NMR (100 MHz, $CDCl_3$) δ −117.14 to −117.20 (m, 1F); HRMS (ESI-TOF) (*m/z*) calculated $C_{19}H_{16}FN_2O_3^+$: 339.1139, found 339.1139 $[M + H]^+$.

Methyl 3-fluoro-6-methyl-8-oxo-8*H*-indazolo[1,2-*a*]cinnoline- 5-carboxylate (33eb). Yellow solid, 50.6 mg (80%); mp 135-138 °C; ^{1}H NMR (400 MHz, $CDCl_3$) δ 8.06 – 8.00 (m, 1H), 7.80 – 7.74 (m, 1H), 7.74 – 7.69 (m, 1H), 7.53 (dd, J = 8.9, 4.6 Hz, 1H), 7.40 – 7.33 (m, 1H), 7.19 (dd, J = 9.6, 2.8 Hz, 1H), 6.99 – 6.91 (m, 1H), 3.98 (s, 3H), 2.86 (s, 3H); ^{13}C NMR (100 MHz, $CDCl_3$) δ 166.3, 160.7, 158.3, 142.3, 139.7, 133.3, 133.1 (J_{C-F} = 2.58 Hz) 124.8, 124.0 (J_{C-F} = 8.7 Hz), 123.1, 118.1, 114.5 (J_{C-F} = 23.2 Hz), 113.2, 112.8, 112.6 (J_{C-F} = 7.3 Hz), 112.2 (d, J_{C-F} = 2.3 Hz), 52.4, 15.7; ^{19}F NMR (100 MHz, $CDCl_3$) δ −117.08 to −117.13 (m, 1F); HRMS (ESI-TOF) (*m/z*) calculated $C_{18}H_{14}FN_2O_3^+$: 325.0983, found 325.0995 $[M + H]^+$.

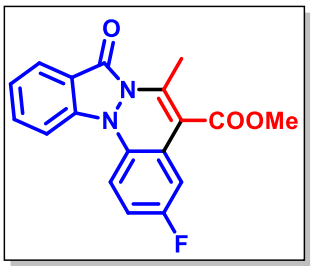

Ethyl 3-chloro-6-methyl-8-oxo-8*H*-indazolo[1,2-*a*]cinnoline-5-carboxylate (33fa). Yellow solid, 65.0 mg (89%); mp 106-108 °C; ^{1}H NMR (400 MHz, $CDCl_3$) δ 8.06 – 8.00 (m, 1H), 7.74 – 7.68 (m, 1H), 7.73 – 7.68 (m, 1H), 7.51 (d, J = 8.6 Hz, 1H), 7.41 – 7.34 (m, 2H), 7.21 (dd, J = 8.7, 2.3 Hz, 1H), 4.46 (q, J = 7.1 Hz, 2H), 2.84 (s, 3H), 1.45 (t, J = 7.1 Hz, 3H); ^{13}C NMR (100 MHz, $CDCl_3$) δ 165.8, 158.1, 141.4, 139.3, 135.4, 133.2, 129.9, 127.9, 125.1, 124.8, 123.6, 123.1, 118.1, 113.2, 112.5, 112.3, 61.7, 15.7, 14.2; HRMS (ESI-TOF) (*m/z*) calculated $C_{19}H_{16}ClN_2O_3^+$: 355.0844, found 355.0860 $[M + H]^+$.

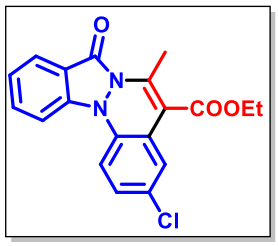

Methyl 3-chloro-6-methyl-8-oxo-8H-indazolo[1,2-*a*]cinnoline- 5-carboxylate (33fb). Yellow solid, 59.5 mg (85%); mp 140-143 °C; ^{1}H NMR (400 MHz, $CDCl_3$) δ 8.06 – 8.01 (m, 1H), 7.80 – 7.75 (m, 1H), 7.71 (d, J = 8.4 Hz, 1H), 7.51 (d, J = 8.7 Hz, 1H), 7.41 – 7.35 (m, 2H), 7.22 (dd, J = 8.7, 2.3 Hz, 1H), 3.98 (s, 3H), 2.84 (s, 3H); ^{13}C NMR (100 MHz, $CDCl_3$) δ 166.3, 158.1, 141.9, 139.4, 135.4, 133.3, 129.9, 128.0, 125.2, 124.8, 123.6, 123.2, 118.1, 113.3, 112.5, 112.1, 52.4, 15.8; HRMS (ESI-TOF) (*m/z*) calculated $C_{18}H_{14}ClN_2O_3^+$: 341.0687, found 341.0693 $[M + H]^+$.

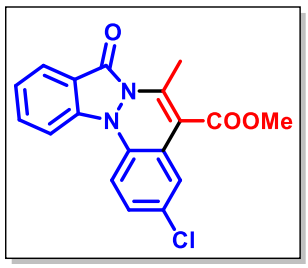

Ethyl 3-chloro-8-oxo-6-phenyl-8*H*-indazolo[1,2-*a*]cinnoline-5-carboxylate (33fc). Yellow

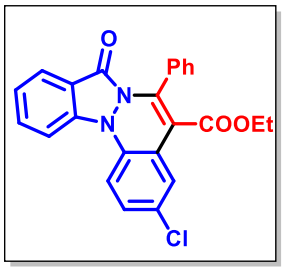

solid, 62.5 mg (73%); mp 135-138 °C; ^{1}H NMR (400 MHz, $CDCl_3$) δ 7.98 – 7.94 (m, 1H), 7.85 (d, J = 2.4 Hz, 1H), 7.82 – 7.76 (m, 2H), 7.56 (d, J = 8.7 Hz, 1H), 7.51 – 7.44 (m, 5H), 7.42 – 7.38 (m, 1H), 7.30 – 7.26 (m, 1H), 4.02 – 3.96 (m, 2H), 0.85 (t, J = 7.2 Hz, 3H); ^{13}C NMR (100 MHz, $CDCl_3$) δ 165.5, 156.6, 141.0, 140.5, 136.5, 133.2, 130.6, 130.1, 129.9, 129.0, 128.7, 128.0, 125.5, 124.9, 123.8, 123.3, 118.9, 114.3, 112.4, 61.4, 13.4; HRMS (ESI-TOF) (*m/z*) calculated $C_{24}H_{18}ClN_2O_3^+$: 417.1004, found 417.1000 $[M + H]^+$.

Ethyl 1,3-dichloro-6-methyl-8-oxo-8*H*-indazolo[1,2-*a*]cinnoline-5-carboxylate (33ga).

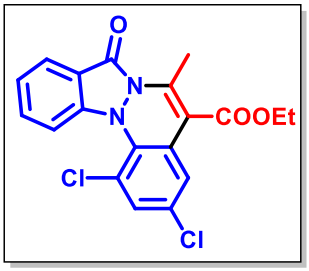

Yellow solid, 60.0 mg (86%); mp 142-145 °C; ^{1}H NMR (400 MHz, $CDCl_3$) δ 7.96 – 7.90 (m, 1H), 7.71 –7.64 (m, 1H), 7.31 – 7.23 (m, 4H), 4.44 (q, J = 7.2 Hz, 2H), 2.81 (s, 3H), 1.43 (t, J = 7.1 Hz, 3H); ^{13}C NMR (100 MHz, $CDCl_3$) δ 165.7, 159.3, 144.3, 141.2, 132.3, 131.4, 129.2, 128.9, 124.0, 122.4, 122.0, 121.5, 116.1, 114.6, 109.7, 61.8, 15.1, 14.2; HRMS (ESI-TOF) (*m/z*) calculated $C_{19}H_{15}Cl_2N_2O_3^+$: 389.0454, found 389.0465 $[M + H]^+$.

Ethyl 10-methoxy-6-methyl-8-oxo-8*H*-indazolo[1,2-*a*]cinnoline-5-carboxylate (33ha).

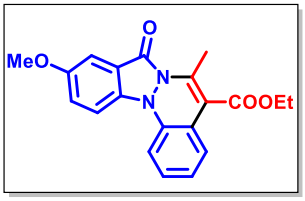

Yellow solid, 44.6 mg (61%); mp 160-164 °C; ^{1}H NMR (400 MHz, $CDCl_3$) δ 7.70 (dd, J = 8.8, 0.8 Hz, 1H), 7.53 (dd, J = 8.1, 1.0 Hz, 1H), 7.41 – 7.34 (m, 3H), 7.28 – 7.23 (m, 1H), 7.16 – 7.10 (m, 1H), 4.45 (q, J = 7.1 Hz, 2H), 3.92 (s, 3H), 2.83 (s, 3H), 1.44 (t, J = 7.1 Hz, 3H); ^{13}C NMR (100 MHz, $CDCl_3$) δ 166.4, 158.1, 156.0, 139.2, 137.3, 134.4, 128.6, 125.2, 124.2, 123.7, 121.5, 118.9, 115.0, 114.0, 111.2, 104.2, 61.5, 55.9, 15.7, 14.3; HRMS (ESI-TOF) (*m/z*) calculated $C_{20}H_{19}N_2O_4^+$: 351.1333, found 351.1339 $[M + H]^+$.

Methyl 10-methoxy-6-methyl-8-oxo-8*H*-indazolo[1,2-*a*]cinnoline-5-carboxylate (33hb).

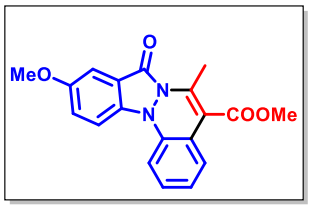

Yellow solid, 40.5 mg (60%); mp 158-160 °C; ^{1}H NMR (400 MHz, $CDCl_3$) δ 7.69 (dd, J = 8.4, 1.2 Hz, 1H), 7.52 (dd, J = 8.1, 1.1 Hz, 1H), 7.41 – 7.36 (m, 2H), 7.34 (dd, J = 7.7, 1.5 Hz, 1H), 7.25 (dd, J = 8.0, 1.5 Hz, 1H), 7.14 – 7.08 (m, 1H), 3.97 (s, 3H), 3.92 (s, 3H), 2.83 (s, 3H); ^{13}C NMR (100 MHz, $CDCl_3$) δ 166.8, 158.1, 156.0, 139.9, 137.3, 134.4, 128.6, 125.3,

124.2, 123.7, 121.5, 119.0, 115.0, 113.6, 111.1, 104.2, 55.9, 52.3, 15.7; HRMS (ESI-TOF) (*m/z*) calculated $C_{19}H_{17}N_2O_4^+$: 337.1183, found 337.1191 $[M + H]^+$.

Ethyl 10-bromo-6-methyl-8-oxo-8*H*-indazolo[1,2-*a*]cinnoline-5-carboxylate (33ia). Yellow

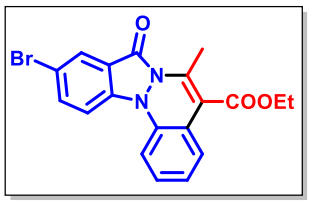

solid, 46.8 mg (67%); mp 115-119 °C; ^{1}H NMR (400 MHz, $CDCl_3$) δ 8.15 (d, J = 2.0 Hz, 1H), 7.83 (dd, J = 8.8, 2.0 Hz, 1H), 7.68 (d, J = 8.9 Hz, 1H), 7.54 (dd, J = 8.2, 1.1 Hz, 1H), 7.36 (dd, J = 7.8, 1.5 Hz, 1H), 7.32 – 7.29 (m, 1H), 7.19 – 7.13 (m, 1H), 4.46 (q, J = 7.1 Hz, 2H), 2.81 (s, 3H), 1.44 (t, J = 7.1 Hz, 3H); ^{13}C NMR (100 MHz, $CDCl_3$) δ 166.2, 156.6, 138.9, 137.6, 136.2, 135.9, 128.7, 127.2, 125.3, 124.8, 121.5, 119.6, 115.5, 114.8, 113.9, 111.5, 61.7, 15.7, 14.3; HRMS (ESI-TOF) (*m/z*) calculated $C_{19}H_{16}BrN_2O_3^+$: 399.0359, found 399.0350 $[M + H]^+$.

Methyl 10-bromo-6-methyl-8-oxo-8*H*-indazolo[1,2-*a*]cinnoline-5-carboxylate (33ib). Yellow

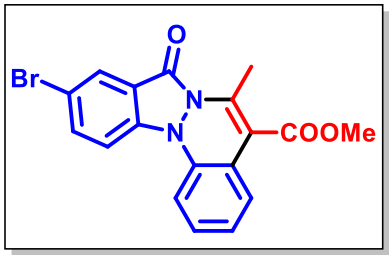

solid, 43.8 mg (65%); mp 170-172 °C; ^{1}H NMR (400 MHz, $CDCl_3$) δ 8.13 (d, J = 1.9 Hz, 1H), 7.81 (dd, J = 8.8, 2.0 Hz, 1H), 7.66 (d, J = 8.8 Hz, 1H), 7.51 (dd, J = 8.2, 1.1 Hz, 1H), 7.35 – 7.25 (m, 2H), 7.18 – 7.11 (m, 1H), 3.97 (s, 3H), 2.79 (s, 3H); ^{13}C NMR (100 MHz, $CDCl_3$) δ 166.6, 156.6, 139.5, 137.7, 136.2, 135.9, 128.7, 127.2, 125.4, 124.8, 121.5, 119.6, 115.5, 114.8, 113.6, 111.4, 52.4, 15.7; HRMS (ESI-TOF) (*m/z*) calculated $C_{18}H_{14}BrN_2O_3^+$: 385.0182, found 385.0198 $[M + H]^+$.

Ethyl 6-methyl-2-nitro-8-oxo-8*H*-indazolo[1,2-*a*]cinnoline-5-carboxylate (33ja). Yellow

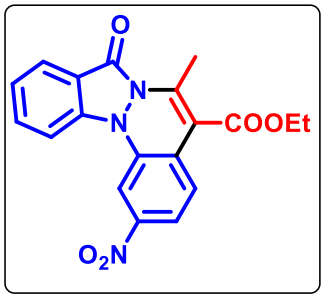

solid, 34.5 mg (48%); mp 204-205 °C; ^{1}H NMR (400 MHz, $CDCl_3$) δ 8.39 (d, J = 2.2 Hz, 1H), 8.07 (d, J = 7.9 Hz, 1H), 7.99 (dd, J = 8.7, 2.2 Hz, 1H), 7.92 –7.82 (m, 2H), 7.55 (d, J = 8.6 Hz, 1H), 7.46 (t, J = 7.4 Hz, 1H), 4.47 (q, J = 7.1 Hz, 2H), 2.88 (s, 3H), 1.45 (t, J = 7.1 Hz, 3H); ^{13}C NMR (100 MHz, $CDCl_3$) δ 164.9, 158.0, 144.2, 139.2, 137.5, 134.3, 128.6, 125.4, 125.1, 124.1, 119.9, 118.2, 113.2, 112.0, 106.5, 62.0, 16.0, 14.2; HRMS (ESI-TOF) (*m/z*) calculated $C_{19}H_{16}N_3O_5^+$: 366.1084, found 366.1104 $[M + H]^+$.

5-Acetyl-6-methyl-8*H*-indazolo[1,2-*a*]cinnolin-8-one (33ad). Yellow solid, 58.4 mg (76%); mp 159-160 °C; ^{1}H NMR (400 MHz, $CDCl_3$) δ 8.03 (dd, J = 7.8, 1.1 Hz, 1H), 7.82 – 7.73 (m, 2H), 7.64 (d, J = 8.1 Hz, 1H), 7.39 – 7.33 (m, 1H), 7.32 – 7.28 (m, 1H), 7.16 – 7.09 (m, 1H), 7.05 (dd, J = 7.8, 1.4 Hz, 1H), 2.71 (s, 3H), 2.55 (s, 3H); ^{13}C NMR (100 MHz, $CDCl_3$) δ 201.9, 158.1, 139.1, 137.0, 135.6, 132.9, 128.7, 124.6, 124.5, 124.5, 122.9, 121.6, 121.5, 118.1, 113.3, 111.7, 32.1, 15.5; HRMS (ESI-TOF) (*m/z*) calculated $C_{18}H_{15}N_2O_2^+$: 391.1128, found 391.1146, found $[M + H]^+$.

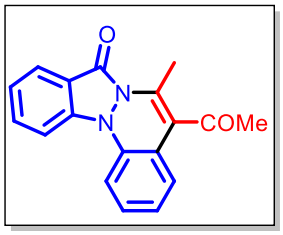

5-Benzoyl-6-methyl-8*H*-indazolo[1,2-*a*]cinnolin-8-one (33ae). Yellow solid, 60.5 mg (72%); mp 158-159 °C; ^{1}H NMR (400 MHz, $CDCl_3$) δ 8.13 – 8.03 (m, 3H), 7.88 – 7.82 (m, 1H), 7.81 – 7.75 (m, 1H), 7.71 – 7.61 (m, 2H), 7.52 (dd, J = 8.4, 7.1 Hz, 2H), 7.42 – 7.34 (m, 1H), 7.27 – 7.21 (td, J = 7.9, 1.5 Hz, 1H), 6.99 (td, J = 7.6, 1.1 Hz, 1H), 6.91 (dd, J = 7.8, 1.5 Hz, 1H), 2.59 (s, 3H); ^{13}C NMR (100 MHz, $CDCl_3$) δ 191.2, 157.8, 138.9, 137.0, 136.5, 135.6, 134.2, 132.8, 129.7, 129.0, 128.6, 125.0, 124.5, 124.4, 122.7, 122.5, 118.6, 117.9, 113.2, 111.6, 16.2; HRMS (ESI-TOF) (*m/z*) calculated $C_{23}H_{17}N_2O_2^+$: 353.1285, found 353.1308, found $[M + H]^+$.

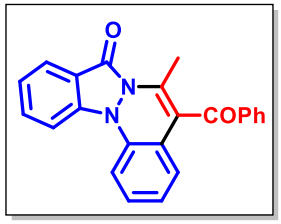

2,2-Dimethyl-2,3-dihydro-14*H*-benzo[c]indazolo[1,2-*a*]cinnoline-4,14(1*H*)-dione (34aa). Orange red solid, 60.0 mg (76%); mp 185-188 °C; ^{1}H NMR (400 MHz, $CDCl_3$) δ 8.49 (dd, J = 7.9, 1.5 Hz, 1H), 8.06 – 8.01 (m, 1H), 7.81 – 7.77 (m, 2H), 7.62 (dd, J = 8.1, 1.3 Hz, 1H), 7.38 – 7.34 (m, 1H), 7.31 (dd, J = 7.6, 1.6 Hz, 1H), 7.24 –7.19 (m, 1H), 3.53 (s, 2H), 2.52 (s, 2H), 1.23 (s, 6H); ^{13}C NMR (100 MHz, $CDCl_3$) δ 195.9, 158.7, 150.7, 140.0, 136.6, 133.6, 128.4, 127.6, 124.9, 124.8, 122.9, 120.9, 117.5, 113.6, 112.7, 111.2, 52.2, 38.2, 32.5, 28.4; HRMS (ESI-TOF) (*m/z*) calculated $C_{21}H_{19}N_2O_2^+$: 331.1441, found 331.1457 $[M + H]^+$.

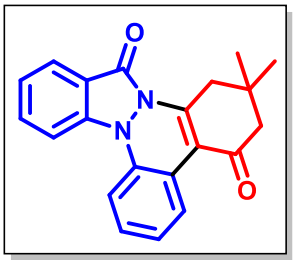

2,2,6-Trimethyl-2,3-dihydro-14*H*-benzo[c]indazolo[1,2-*a*]cinnoline-4,14(1*H*)-dione (34ba).

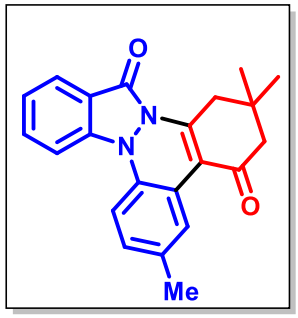

Orange red solid, 40.6 mg (52%); mp 163-166 °C; ^{1}H NMR (400 MHz, $CDCl_3$) δ 8.31 (d, J = 2.0 Hz, 1H), 8.04 – 7.99 (m, 1H), 7.79 – 7.74 (m, 2H), 7.50 (d, J = 8.2 Hz, 1H), 7.34 (dd, J = 5.3, 2.7 Hz, 1H), 7.09 (d, J = 8.1 Hz, 1H), 3.53 (s, 2H), 2.52 (s, 2H), 2.39 (s, 3H), 1.22 (s, 6H); ^{13}C NMR (100 MHz, $CDCl_3$) δ 196.1, 158.8, 150.7, 134.7, 134.3, 133.6, 128.7, 128.1, 124.8, 122.7, 120.7, 117.3, 113.5, 112.8, 111.1, 52.2, 38.2, 32.5, 28.4, 21.2; HRMS (ESI-TOF) (*m/z*) calculated $C_{22}H_{21}N_2O_3^+$: 345.1598, found 345.1575 $[M + H]^+$.

5-Methoxy-2,2-dimethyl-2,3-dihydro-14*H*-benzo[c]indazolo [1,2-*a*]cinnoline-4,14(1*H*)-dione

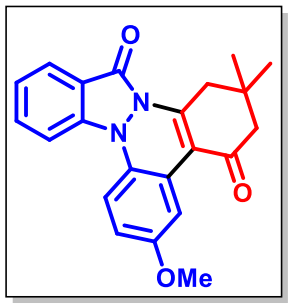

(34ca). Orange red solid, 42.4 mg (56%); mp 152-155 °C; ^{1}H NMR (400 MHz, $CDCl_3$) δ 8.17 (d, J = 2.9 Hz, 1H), 8.02 (d, J = 7.9 Hz, 1H), 7.80 – 7.72 (m, 2H), 7.52 (d, J = 8.9 Hz, 1H), 7.36 – 7.31 (m, 1H), 6.83 (dd, J = 8.9, 2.9 Hz, 1H), 3.88 (s, 3H), 3.55 (s, 2H), 2.52 (s, 2H), 1.23 (s, 6H); ^{13}C NMR (100 MHz, $CDCl_3$) δ 196.1, 158.9, 156.7, 151.2, 140.1, 133.7, 130.2, 124.8, 122.6, 117.0, 114.0, 113.2, 112.5, 112.4, 112.2, 55.7, 52.2, 38.2, 32.4, 28.4; HRMS (ESI-TOF) (*m/z*) calculated $C_{22}H_{21}N_2O_3^+$: 361.1547, found 361.1554 $[M + H]^+$.

6-Bromo-2,2-dimethyl-2,3-dihydro-14*H*-benzo[c]indazolo[1,2-*a*]cinnoline-4,14(1*H*)-dione

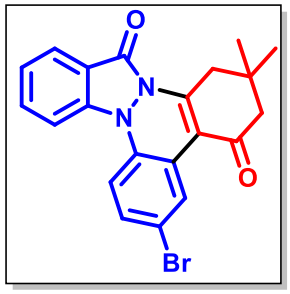

(**34da**). Orange red solid, 50.6 mg (71%); mp 220-223 °C; ^{1}H NMR (400 MHz, $CDCl_3$) δ 8.68 (d, J = 2.3 Hz, 1H), 8.02 (d, J = 7.9 Hz, 1H), 7.82 – 7.77 (m, 1H), 7.71 (d, J = 8.4 Hz, 1H), 7.44 (d, J = 8.6 Hz, 1H), 7.40 – 7.35 (m, 2H), 3.51 (s, 2H), 2.51 (s, 2H), 1.21 (s, 6H); ^{13}C NMR (100 MHz, $CDCl_3$) δ 195.5, 158.6, 151.7, 139.9, 135.6, 134.0, 130.9, 130.3, 125.0, 123.2, 122.8, 118.0, 117.5, 113.4, 112.7, 111.5, 52.0, 38.2, 32.4, 28.3; HRMS (ESI-TOF) (*m/z*) calculated $C_{21}H_{18}BrN_2O_2^+$: 410.0578, found 410.0526 $[M + H]^+$.

Ethyl 6-methyl-8-oxo-8*H*-pyrido[3′,2′:4,5]pyrazolo[1,2-*a*]cinnoline-5-carboxylate (33la).

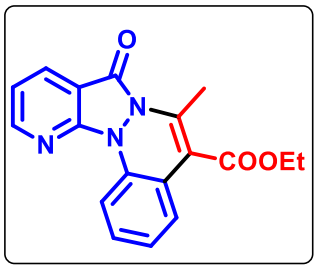

Yellow solid, 58.4 mg (76%); mp 159-160 °C; ^{1}H NMR (400 MHz, $CDCl_3$) δ 8.97 (dd, J = 8.3, 1.1 Hz, 1H), 8.80 (dd, J = 4.7, 1.8 Hz, 1H), 8.35 (dd, J = 7.8, 1.8 Hz, 1H), 7.37 – 7.28 (m, 2H), 7.23 – 7.07 (m, 2H), 4.46 (q, J = 7.2 Hz, 2H), 2.82 (s, 3H), 1.44 (t, J = 7.1 Hz, 3H); ^{13}C NMR (100 MHz, $CDCl_3$) δ 166.4, 155.7, 153.5, 149.6, 136.0, 135.1, 133.5, 129.0, 124.4, 124.2, 118.9, 117.7, 114.6, 113.9, 108.9, 61.7, 16.6, 14.2; HRMS (ESI-TOF) (*m/z*) calculated $C_{18}H_{16}N_3O_6^+$: 322.1186, found 322.1182 $[M + H]^+$.

2,2-Dimethyl-2,3-dihydro-14*H*-benzo[c]pyrido[2′,3′:3,4]pyrazolo[1,2-*a*]cinnoline 4,14(1*H*)-dione (34la).

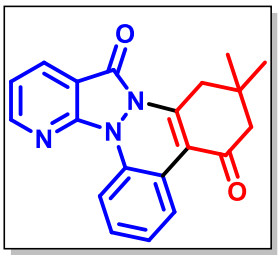

Orange solid, 54.5 mg (69%); mp 185-186 °C; ^{1}H NMR (400 MHz, $CDCl_3$) δ 8.90 (dd, J = 8.4, 1.2 Hz, 1H), 8.82 (dd, J = 4.7, 1.8 Hz, 1H), 8.57 (dd, J = 8.0, 1.5 Hz, 1H), 8.33 (dd, J = 7.9, 1.8 Hz, 1H), 7.36 – 7.31 (m, 1H), 7.31 –7.27 (m, 1H), 7.22 – 7.16 (m, 1H), 3.56 (s, 2H), 2.52 (s, 2H), 1.22 (s, 6H); ^{13}C NMR (100 MHz, $CDCl_3$) δ 196.1, 156.6, 154.3, 150.6, 149.2, 135.3, 133.7, 128.7, 127.0, 124.7, 118.4, 117.9, 114.1, 112.1, 108.7, 52.3, 39.1, 32.5, 28.3; HRMS (ESI-TOF) (*m/z*) calculated $C_{20}H_{18}N_3O_2^+$: 332.1394, found 332.1390 $[M + H]^+$.

Ethyl 2-(2-(2-acetyl-3-oxo-2,3-dihydro-1*H*-indazol-1-yl)phenyl)- 2-oxoacetate (35aa).

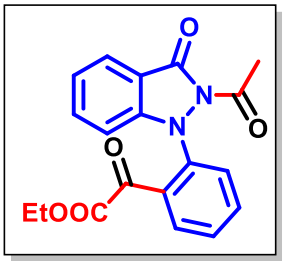

White solid, 25.4 mg (60%); ^{1}H NMR (400 MHz, $CDCl_3$) δ 8.05 – 7.93 (m, 1H), 7.94 (d, J = 7.8 Hz, 1H), 7.66 – 7.62 (m, 1H), 7.59 – 7.52 (m, 2H), 7.33 (t, J = 7.3 Hz, 1H), 7.04 (d, J = 8.3 Hz, 1H), 6.90 – 6.87 (m, 1H), 4.22 – 4.04 (m, 2H), 2.62 (s, 3H), 1.06 (t, J = 7.1 Hz, 3H); ^{13}C NMR (100 MHz, $CDCl_3$) δ 186.5, 166.2, 164.1, 163.2, 151.9, 144.3, 135.6, 135.0, 134.5, 130.1, 129.6, 125.4, 124.9, 124.6, 117.9, 115.2, 62.0, 24.7, 13.7; HRMS (ESI-TOF) (*m/z*) calculated $C_{19}H_{17}N_2O_5^+$: 353.1132, found 353.1126 $[M + H]^+$.

6-Methyl-8-oxo-8*H*-indazolo[1,2-*a*]cinnoline-5-carboxylic acid (36aa).

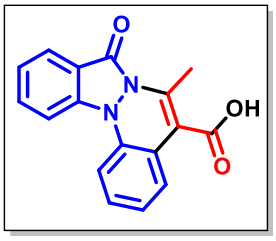

Yellow solid, 23.7 mg (65%); ^{1}H NMR (400 MHz, DMSO-d_6) δ 13.54 (brs, 1H), 8.05 (d, J = 8.5 Hz, 1H), 7.92 (d, J = 7.7 Hz, 1H), 7.89 –7.86 (m, 1H), 7.72 (d, J = 8.0 Hz, 1H), 7.42 (t, J = 7.6 Hz, 1H), 7.37 – 7.33 (m, 2H), 7.19 (t, J = 8.2 Hz, 1H), 2.69 (s, 3H); ^{13}C NMR (100 MHz, DMSO-d_6) δ 167.6, 157.6, 139.3, 136.9, 133.9, 129.5, 125.5, 125.0, 124.2, 123.7, 121.5, 117.7, 114.7,

112.2,15.7; HRMS (ESI-TOF) (*m/z*) calculated $C_{17}H_{13}N_2O_3^+$: 293.0926, found 293.0916 $[M + H]^+$.

5-(Hydroxymethyl)-6-methyl-8*H*-indazolo[1,2-*a*]cinnolin-8-one (37aa). Yellow solid, 28 mg (65%); ^{1}H NMR (400 MHz, DMSO-d_6) δ 8.03 (d, J = 8.5 Hz, 1H), 7.90 (d, J = 7.8 Hz, 1H), 7.82 (t, J = 7.9 Hz, 1H), 7.68 (d, J = 8.1 Hz, 1H), 7.58 (d, J = 7.7 Hz, 1H), 7.40 (t, J = 7.5 Hz, 1H), 7.30 (t, J = 7.7 Hz, 1H), 7.19 (t, J = 7.5 Hz, 1H), 5.06 (t, J = 5.3 Hz, 1H), 4.48 (d, J = 5.1 Hz, 2H), 2.65 (s, 3H); ^{13}C NMR (100 MHz, DMSO-d_6) δ 157.1, 139.1, 137.4, 134.5, 133.3, 128.7, 124.9, 124.7, 124.2, 123.9, 123.5, 118.1, 117.8, 114.8, 111.7, 55.8, 13.7; HRMS (ESI-TOF) (*m/z*) calculated $C_{17}H_{15}N_2O_2^+$: 279.1128, found 279.1128 $[M + H]^+$.

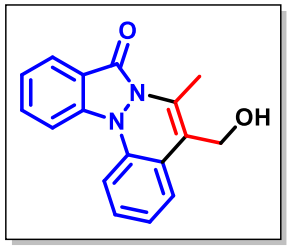

Ethyl 6-methyl-8-thioxo-8H-indazolo[1,2-*a*]cinnoline-5-carboxylate (38aa). Yellow solid, 37.5 mg (71%); ^{1}H NMR (400 MHz, $CDCl_3$) δ 8.32 –8.26 (m, 1H), 7.87 (d, J = 8.4 Hz, 1H), 7.83 – 7.78 (m, 1H), 7.74 (d, J = 8.2 Hz, 1H), 7.48 – 7.43 (m, 1H), 7.40 – 7.34 (m, 2H), 7.25 – 7.18 (m, 1H), 4.50 (q, J = 7.1 Hz, 2H), 3.14 (s, 3H), 1.46 (t, J = 7.1 Hz, 3H); ^{13}C NMR (100 MHz, $CDCl_3$) δ 171.6, 166.2, 138.4, 136.7, 136.7, 132.6, 129.9, 129.3, 125.6, 125.4, 124.9, 124.2, 120.1, 119.0, 113.2, 111.5, 62.0, 18.7, 14.2; HRMS (ESI-TOF) (*m/z*) calculated $C_{19}H_{17}N_2O_2S^+$: 337.1005, found 337.0996 $[M + H]^+$.

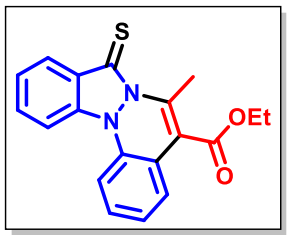

Procedure for the isolation of the iridacyclic complex

$[Ir(COD)Cl]_2$ (25 mg, 0.037 mmol) was added to a two-necked round-bottom flask containing dry toluene (5 mL) fitted with a reflux condenser, maintained under a nitrogen gas atmosphere. To this, **32a** (19.56 mg, 0.093 mmol), $AgSbF_6$ (38.07 mg, 0.111 mmol), and $NaHCO_3$ (7.7 mg, 0.092 mmol) were added. The mixture was stirred at 110 °C for 12 h under the nitrogen atmosphere. Subsequently, PPh_3 (48.6 mg, 0.185 mmol) was added to the solution and the stirring continued for further 12 h. After cooling, the reaction mixture was diluted with $CHCl_3$ (10.0 mL) and filtered to remove insoluble solids. The filtrate was evaporated, and the crude product was washed with diethyl ether (5 mL × 4) to yield a white solid (**B1**).

2B.4 Single Crystal X-Ray Diffraction Studies

Crystals of **33fc** were screened under a microscope for mounting in a nylon loop attached to a goniometer head. Initial crystal evaluation and data collection were performed on a Kappa APEX II diffractometer equipped with a CCD detector (with the crystal-to-detector distance fixed at 60

mm) and sealed-tube monochromated MoKα radiation using the program APEX2.[46] By using the program SAINT[46] for the integration of the data, reflection profiles were fitted, and values of F^2 and $\sigma(F^2)$ for each reflection were obtained. Data were also corrected for Lorentz and polarization effects. The subroutine XPREP[46] was used for the processing of data that included determination of space group, application of an absorption correction (SADABS),[46] merging of data, and generation of files necessary for solution and refinement. The crystal structure was solved and refined using SHELX 97.[47] In each case, the space group was chosen based on systematic absences and confirmed by the successful refinement of the structure. Positions of most of the non-hydrogen atoms were obtained from a direct methods solution. Several full-matrix least-squares/difference Fourier cycles were performed, locating the remainder of the non-hydrogen atoms. All non-hydrogen atoms were refined with anisotropic displacement parameters. All hydrogen atoms were placed in ideal positions and refined as riding atoms with individual isotropic displacement parameters. All figures were drawn using MERCURY V 3.0[48] and Platon.[49]

2B. 4.1 Crystal data for 33fc (CCDC No. 1841375). $C_{24}H_{17}ClN_2O_3$, *Mr* = 416.84, *T* = 273(2) K,

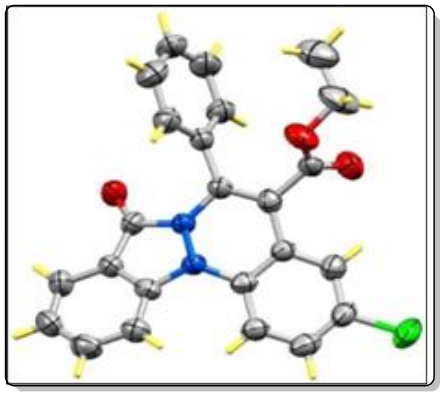

triclinic, space group *P*-1 (No. 2), *a* = 8.5002(7) Å, *b* = 9.3931(8) Å, *c* = 13.1098(11) Å, α = 83.94(2)°, β = 80.207(2)°, γ = 80.262(2)°, *V* = 1012.10(15) Å^3, *Z* = 2, *Dc* = 1.368 g cm^{-3}, μ = 0.218 mm^{-1}, R_{int} = 0.0283, final R_1 = 0.0400, wR_2 = 0.1147 for 2899 observed reflections [I > 2σ(I)] and R_1 = 0.0509, wR_2 = 0.1316 for all 3563 reflections; GOF = 1.085.

2B.5 References

1. Gaber, H. M.; Bagley, M. C.; Muhammad, Z. A.; Gomha, S. M. *RSC Advances* **2017**, *7*, 14562-14610.
2. Jha, N.; Khot, N. P.; Kapur, M. *The Chemical Record* **2021**, *21*, 4088-4122.
3. Happy, S.; Junaid, M.; Yadagiri, D. *Chemical Communications* **2023**, *59*, 29-42.
4. Vaitla, J.; Bayer, A. *Synthesis* **2019**, *51*, 612-628.
5. Xing, D.; Hu, W. *Tetrahedron Letters* **2014**, *55*, 777-783.
6. Padwa, A.; Austin, D. J. *Angewandte Chemie International Edition* **1994**, *33*, 1797-1815.
7. Doyle, M. P. *Accounts of Chemical Research.* **1986**, *19*, 348-356.

8. Rani, G.; Luxami, V.; Paul, K. *Chemical Communications* **2020**, *56*, 12479-12521.
9. Mehta, G.; Muthusamy, S. *Tetrahedron* **2002**, *58*, 9477-9504.
10. Zhu, D.; Cao, T.; Chen, K.; Zhu, S. *Chemical Science* **2022**, *13*, 1992-2000.
11. Zhu, D.; Ma, J.; Luo, K.; Fu, H.; Zhang, L.; Zhu, S. *Angewandte Chemie International Edition* **2016**, *55*, 8452-8456.
12. Liu, P.; Sun, J. *Organic Letters* **2017**, *19*, 3482-3485.
13. Guo, H.; Zhang, S.; Yu, X.; Feng, X.; Yamamoto, Y.; Bao, M. *ACS Catalysis* **2021**, *11*, 10789-10795.
14. Etesami, H.; Mansouri, M.; Habibi, A.; Jahantigh, F. *Journal of Molecular Structure* **2020**, *1203*, 127432.
15. Tan, X.; Zhu, S.; Show, P. L.; Qi, H.; Ho, S.-H. *Journal of Hazardous Materials* **2020**, *393*, 122435.
16. Xuan, Z.; Chen, Z. S. *European Journal of Organic Chemistry* **2022**, *2022*, e202200499.
17. Prabagar, B.; Yang, Y.; Shi, Z. *Chemical Society Reviews* **2021**, *50*, 11249-11269.
18. Rej, S.; Ano, Y.; Chatani, N. *Chemical Reviews* **2020**, *120*, 1788-1887.
19. Sarkar, T.; Shah, T. A.; Maharana, P. K.; Talukdar, K.; Das, B. K.; Punniyamurthy, T. *The Chemical Record* **2021**, *21*, 3758-3778.
20. Zhang, J.; Lu, X.; Shen, C.; Xu, L.; Ding, L.; Zhong, G. *Chemical Society Reviews* **2021**, *50*, 3263-3314.
21. Chen, Z.; Wang, B.; Zhang, J.; Yu, W.; Liu, Z.; Zhang, Y. *Organic Chemistry Frontiers* **2015**, *2*, 1107-1295.
22. Padwa, A.; Austin, D. J. *Angewandte Chemie International Edition* **1994**, *33*, 1797-1815.
23. Colby, D. A.; Bergman, R. G.; Ellman, J. A. *Chemical Reviews* **2010**, *110*, 624-655.
24. Ramachandran, K.; Anbarasan, P. *Chemical Science* **2021**, *12*, 13442-13449.
25. Girard, S. A.; Knauber, T.; Li, C. J. *Angewandte Chemie International Edition* **2014**, *53*, 74-100.
26. Yang, K.; Li, Z.; Hu, Q.; Elsaid, M.; Liu, C.; Chen, J.; Ge, H. *Catalysts* **2022**, *12*, 1163.
27. Hyster, T. K.; Ruhl, K. E.; Rovis, T. *Journal of the American Chemical Society* **2013**, *135*, 5364-5367.
28. Shi, L.; Yu, K.; Wang, B. *Chemical Communications* **2015**, *51*, 17277-17280.
29. Shi, Z.; Koester, D. C.; Boultadakis-Arapinis, M.; Glorius, F. *Journal of the American Chemical Society* **2013**, *135*, 12204-12207.

30. Phatake, R. S.; Patel, P.; Ramana, C. V. *Organic Letters* **2016**, *18*, 292-295.
31. Kim, J. H.; Gressies, S.; Glorius, F. *Angewandte Chemie International Edition* **2016**, *55*, 5577-5581.
32. Li, J.; Tang, M.; Zang, L.; Zhang, X.; Zhang, Z.; Ackermann, L. *Organic Letters* **2016**, *18*, 2742-2745.
33. Cui, S.; Zhang, Y.; Wang, D.; Wu, Q. *Chemical Science* **2013**, *4*, 3912-3916.
34. Bai, P.; Huang, X.-F.; Xu, G.-D.; Huang, Z.-Z. *Organic Letters* **2016**, *18*, 3058-3061.
35. Ning, Y.; He, X.; Zuo, Y.; Wang, J.; Tang, Q.; Xie, M.; Li, R.; Shang, Y. *Organic & Biomolecular Chemistry* **2020**, *18*, 2893-2901.
36. Cheng, Y.; Bolm, C. *Angewandte Chemie International Edition* **2015**, *54*, 12349-12352.
37. Aher, Y. N.; Lade, D. M.; Pawar, A. B. *Chemical Communications* **2018**, *54*, 6288-6291.
38. Shi, J.; Zhou, J.; Yan, Y.; Jia, J.; Liu, X.; Song, H.; Xu, H. E.; Yi, W. *Chemical Communications* **2015**, *51*, 668-671.
39. Patel, P.; Borah, G. *Chemical Communications* **2017**, *53*, 443-446.
40. Chen, X.; Zheng, G.; Song, G.; Li, X. *Advanced Synthesis & Catalysis* **2018**, *360*, 2836-2842.
41. Li, S. S.; Xia, Y. Q.; Hu, F. Z.; Liu, C. F.; Su, F.; Dong, L. *Chemistry–An Asian Journal* **2016**, *11*, 3165-3168.
42. Hu, X.; Chen, X.; Shao, Y.; Xie, H.; Deng, Y.; Ke, Z.; Jiang, H.; Zeng, W. *ACS Catalysis* **2018**, *8*, 1308-1312.
43. Iwai, T.; Fujihara, T.; Terao, J.; Tsuji, Y. *Journal of the American Chemical Society* **2010**, *132*, 9602-9603.
44. Li, P.; Xu, X.; Chen, J.; Yao, H.; Lin, A. *Organic Chemistry Frontiers* **2018**, *5*, 1777-1781.
45. Presset, M.; Mailhol, D.; Coquerel, Y.; Rodriguez, J. *Synthesis* **2011**, *2011*, 2549-2552.
46. *APEX2, SADABS and SAINT*; Bruker AXS inc: Madison, WI, USA, **2008**.
47. Sheldrick, G. M. *Acta Crystallography* **2008**, *A64*, 112.
48. Macrae, C. F.; Bruno, I. J.; Chisholm, J. A.; Edginton, P. R.; McCabe, P.; Pidocck, E.; RodriguezMonge, L.; Taylor, T.; Van de Streek, J.; Wood, P. A. *Journal of Applied Crystallography* **2008**, *41*, 466.
49. Spek, A. L. PLATON, Version 1.62, University of Utrecht, **1999**.

Chapter 2C

Palladium-Catalyzed [4+2] Annulation of *N*-Arylindazolones with Allenoates to access Indazolo[1,2-*a*]cinnoline Carboxylates

2C.1 Introduction

Similar to alkenes and alkynes, allenes have also emerged as a valuable coupling partners for allenylation,[1-3] alkenylation,[4-6] allylation,[7-9] dienylation,[6,10-11] alkylation,[12] and annulation[13-17] of electron-rich (hetero)/arenes under transition metal catalysis at the expense of an appropriately attached directing group (DG). However, due to the presence of orthogonal cumulative carbon-carbon double bonds, allenes showed distinct reactivity from alkenes and alkynes. Also, substituted allenes have been explored with amine containing arenes to construct nitrogen-containing heterocycles *via* simultaneous C-C and C-N bond formations using suitable transition metal-catalysts.

In 2012, Glorius *et al*. explored a mild Rh^{III}-catalyzed intermolecular oxidative coupling of *N*-pivaloyloxybenzamides (**1**) with allenes (**2**) to access 3,4-dihydroisoquinolin-1(2*H*)-ones (**3**), possessing exocyclic double bonds. The methodology featured low catalyst loading, impressive substrate scope of both the starting materials, and does not require any external oxidants (Scheme 2C.1.1).[18]

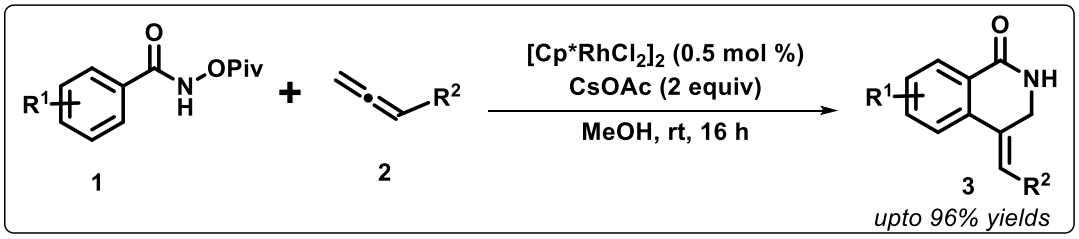

Scheme 2C.1.1 Rh-catalyzed annulation strategy for the synthesis of 3,4-dihydroisoquinolin-1(2*H*)-ones possessing exocyclic double bonds using allenes

In 2015, Ma and coworkers established another Rh^{III}-catalyzed strategy in which formal [4+2+2] cyclization of *N*-pivaloyloxybenzamides (**1**) with 1,6-allene-enes (**2**) generated eight-membered lactams (**4**) in moderate yields. The reaction progressed at room temperature under air and moisture conditions, showcasing a broad range of functional group tolerance (Scheme 2C.1.2).[19]

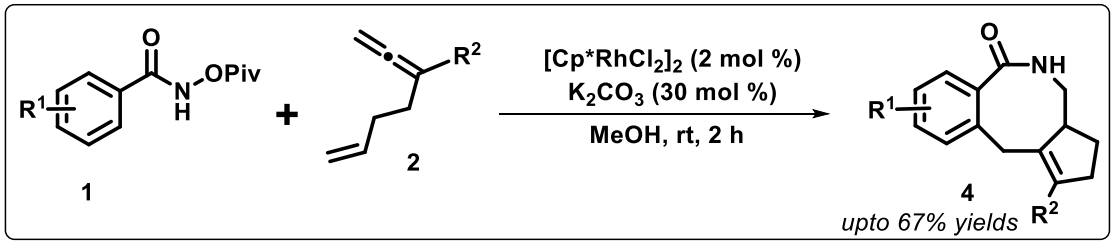

Scheme 2C.1.2 Rh-catalyzed cycloaddition/cyclization for the synthesis of eight-membered lactams using allenes

In 2014, Nicolas's group demonstrated the synthesis of tetrahydro-3-benzazepines (**6a**) and tetrahydroisoquinolines (**6b**) from allenes (**2**) and phenylethylamines (**5a**) or benzylamines (**5b**), respectively using catalytic amount of palladium acetate in acetic acid. This strategy proceeded through the activation of C-H bond of the aromatic ring with an assistance of simple primary amine as a directing group (Scheme 2C.1.3).[20]

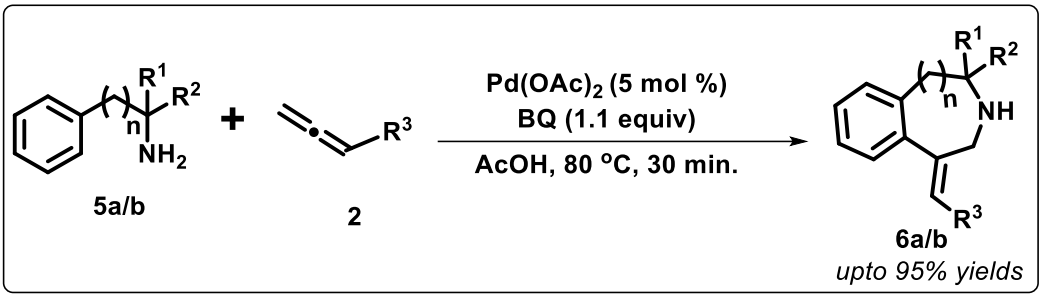

Scheme 2C.1.3 Pd-catalyzed annulation strategy for the synthesis of tetrahydro-3-benzazepines and tetrahydroisoquinolines using allenes

In 2014, Liang's group developed an efficient strategy for the Pd^{II}-catalyzed [4+2] annulation of *N*-benzoylsulfonamides (**7**) and allenes (**2**) for preparing 3,4-dihydroisoquinolin-1(2*H*)-ones (**8**) in moderate-to-good yields. The strategy highlighted the application of sulfonamide group as a well behaved directing group in the presence of electron rich as well as electron poor substituents on the tosyl moiety (Scheme 2C.1.4).[21]

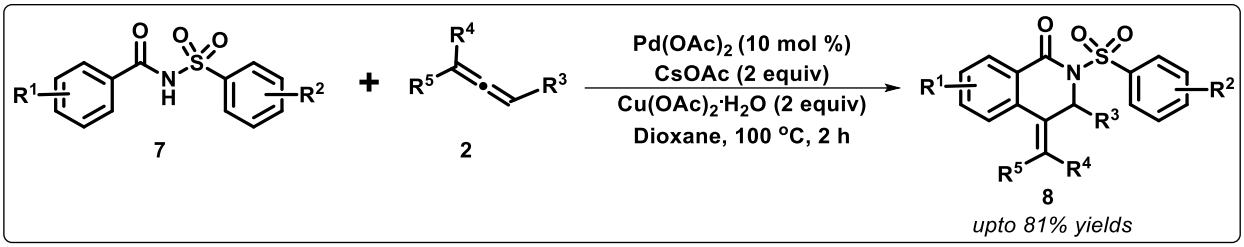

Scheme 2C.1.4 Pd-catalyzed annulation strategy for the synthesis of 3,4-dihydroisoquinolin-1(2*H*)-ones using allenes

In 2018, Ackermann *et al*. developed an efficient triazole-directed strategy for the synthesis of isoquinolones (**10**) from *N*-substituted benzamides (**9**) and allenes (**2**) under Fe^{III}-catalyzed conditions. The optimization results revealed that inexpensive and non-toxic $Fe(acac)_3$/dppe catalyst system works well to produce the target products in good yields with broad substrate scope, in addition to the advantage of easily removable triazole group (Scheme 2C.1.5).[22]

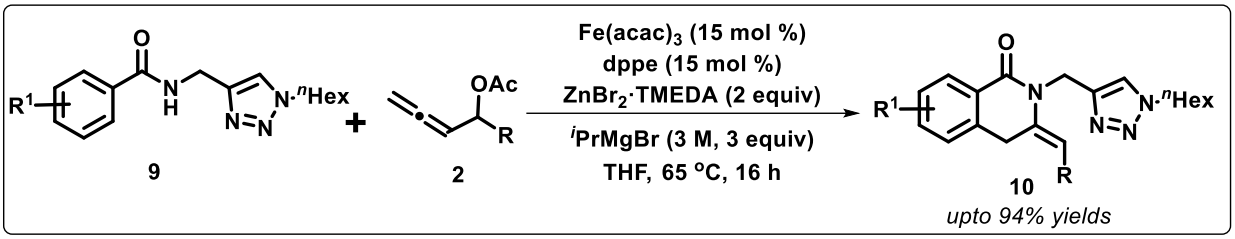

Scheme 2C.1.5 Fe-catalyzed annulation strategy for the synthesis of isoquinolones using allenes

In 2016, Cheng's group established a Co^{II}-catalyzed oxidative protocol for the coupling of a variety of functionalized benzamides (**11**) and allenes (**2**) to access isoquinolin-1(2*H*)-ones (**12**) *via* aminoquinoline-directed C-H activation, regioselective insertion followed by annulation and isomerization sequential process (Scheme 2C.1.6).[23]

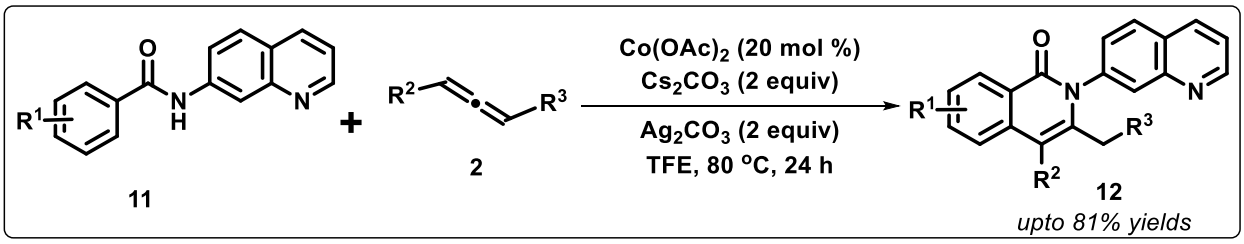

Scheme 2C.1.6 Co-catalyzed annulation strategy for the synthesis of isoquinolin-1(2*H*)-ones using allenes

Volla and coworkers studied the reactivity pattern of allenes and established that it is completely depending on electronic properties of the attached substituents to it. Based on this rationale, the authors successfully achieved the synthesis of regioisomeric isoquinolinones (**13** & **14**) possessing exocyclic and internal double bonds *via* Co^{II}-catalyzed heterocyclization reaction of various benzamides (**11**) with disubsutututed allenes (**2**) (Scheme 2C.1.7).[24]

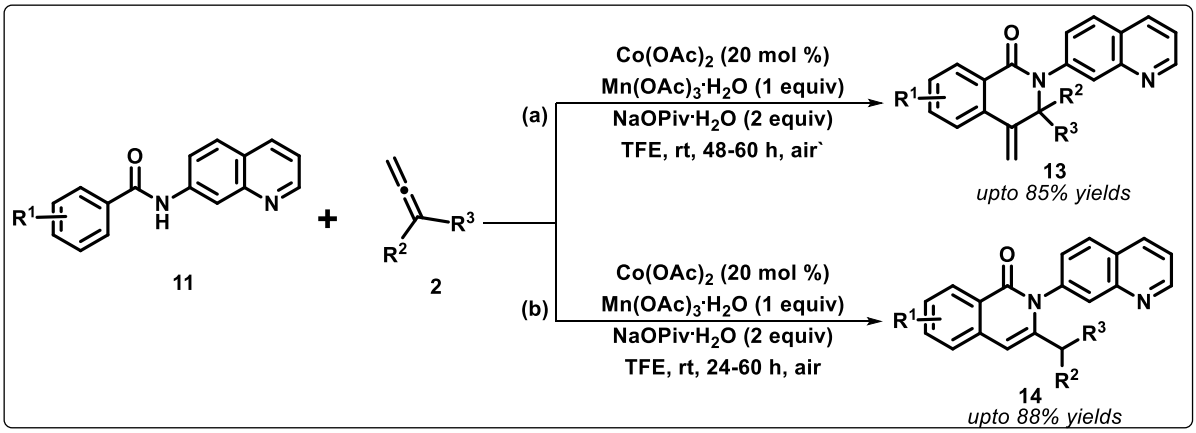

Scheme 2C.1.7 Co-catalyzed annulation strategy for the synthesis of isoquinolinones using allenes

Li, Liu and coworkers demonstrated [4+1] annulation of aromatic (**15a**) and vinylic amides (**15b**) with *α*-allenols (**2**) to synthesize a series of isoindolinones (**16a**) and 1,5-dihydro-pyrrol-2-ones (**16b**) *via* Rh^{III}-catalyzed amide-directing C-H activation approach (Scheme 2C.1.8).[25]

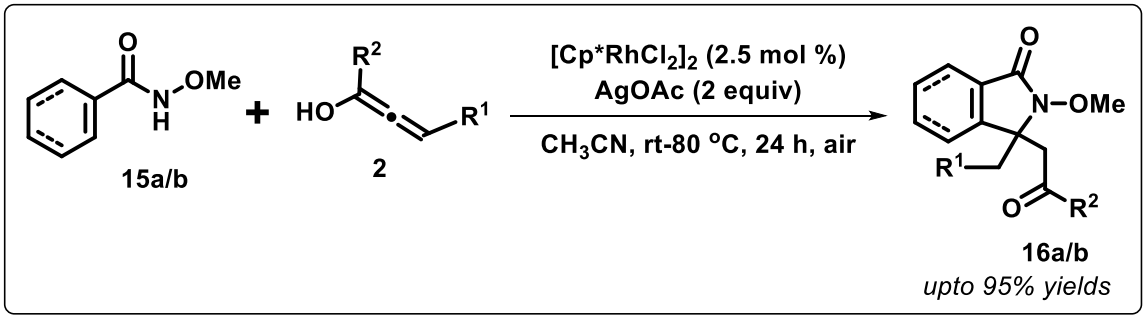

Scheme 2C.1.8 Rh-catalyzed [4+1] annulation strategy for the synthesis of isoindolinones and 1,5-dihydro-pyrrol-2-ones using allenols

In 2018, Zhai *et al*. established a novel protocol for the synthesis of versatile 3-acylquinolinones (**18**) by using electron-rich and electron-deficient benzoic hydrazides (**17**), allenes (**2**) and molecular oxygen under Co^{II}-catalysis. In this methodology, 2-(1′-methylhydrazinyl)pyridine (MHP) group acted as a directing group for the C-H bond functionalization, and no reaction was observed in absence of O_2 (Scheme 2C.1.9).[26]

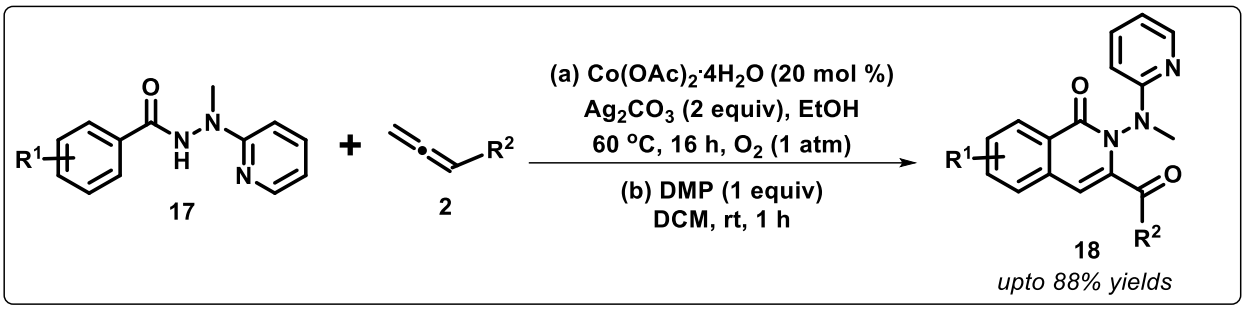

Scheme 2C.1.9 Co-catalyzed annulation strategy for the synthesis of 3-acylquinolinones using allenes

In 2018, Cheng and coworkers demonstrated a Co^{II}-catalyzed oxidative [3+3] cycloaddition strategy for the synthesis of 1,2-dihydroquinolines (**20**) from various anilides (**19**) and benzyl allenes (**2**). From the optimization study, it was proved that acetate salts enhances the productivity, and the reaction was believed to proceed through chelation-assisted C-H activation by oxygen of amidic carbonyl, followed by subsequent allene insertion, *β*-hydride elimination and a 1,4-addition of N–H to diene to furnish the target products (Scheme 2C.1.10).[27]

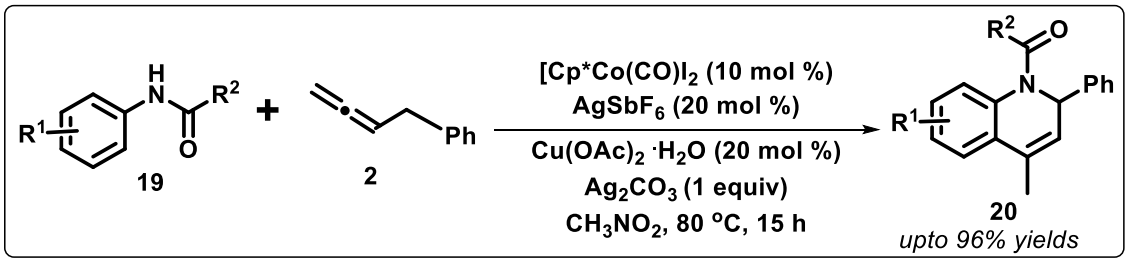

Scheme 2C.1.10 Co-catalyzed oxidative [3+3] cycloadditive strategy for the synthesis of 1,2-dihydroquinolines using benzyl allenes

The same group disclosed Co^{II}-catalyzed strategy for [4+1] annulation of *N*-alkyl amides (**21**) with allenes (**2**) to obtain isoindolones (**22**) in good-to-excellent yields. It was believed that the reaction has progressed through the path of C-H activation, diene formation, followed by intramolecular 1,2-hydroamination (Scheme 2C.1.11).[28]

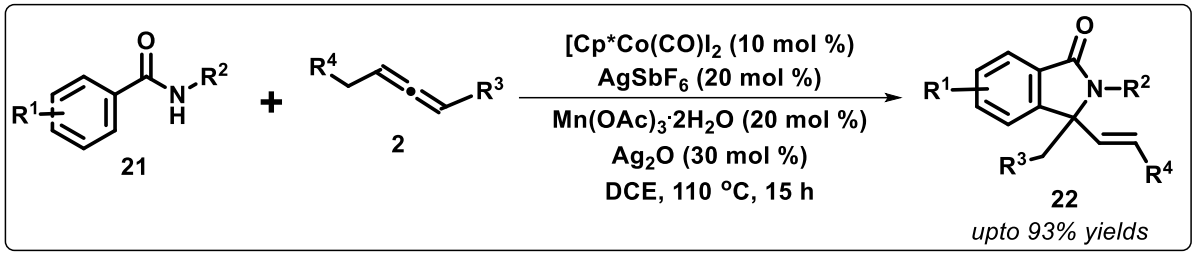

Scheme 2C.1.11 Co-catalyzed [4+1] annulation strategy for the synthesis of isoindolones using allenes

Recently, Yu's group reported Rh^{III}-catalyzed annulation of various functionalized phthalazinones or pyridazinones (**23**) with various benzyl allenes (**2**), leading to the formation of fused indazole derivatives (**24**), bearing a quaternary carbon in moderate-to-good yields with high atom economy. Mechanistic studies indicated that the products were obtained through sequential C-H activation and olefin insertion, followed by *β*-hydride elimination and intramolecular cyclization (Scheme 2C.1.12).[29]

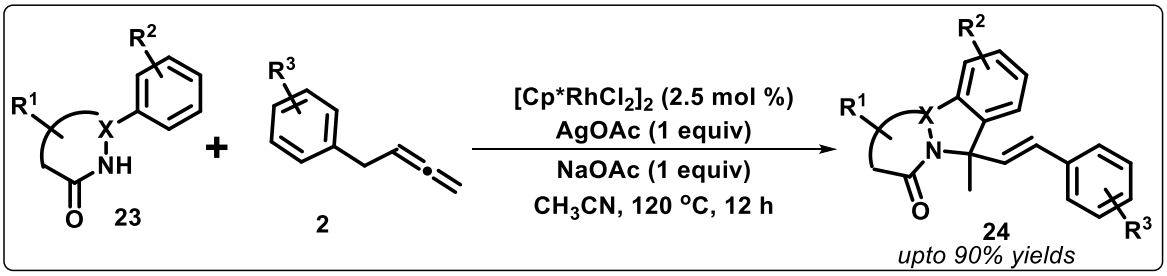

Scheme 2C.1.12 Rh-catalyzed annulation strategy for the synthesis of fused-indazole derivatives using benzyl allenes

Very recently, Baidya *et al*. presented an unprecedented Ru^{II}-catalyzed [4+2] annulation between *N*-methoxybenzamides (**15a**) and allenylphosphine oxides (**2**), furnishing phosphinyl functionalized NH-free isoquinolinone derivatives (**25**) in high yields. Notably, the C-H activation/functionalization proceeded by the aid of amidic-directing group (Scheme 2C.1.13).[30]

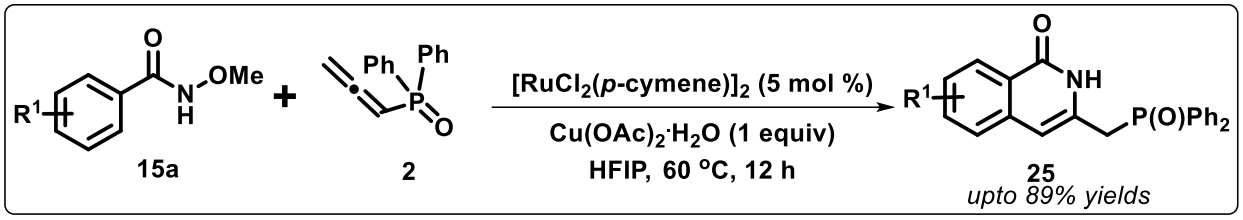

Scheme 2C.1.13 Ru-catalyzed annulation strategy for the synthesis of phosphinyl functionalized isoquinolinones using allenylphosphine oxides

Strikingly, it has been observed that the reactivity of an allene gets further enhanced by attaching electron-withdrawing substituents at the terminal positions. In this regard, allenoates have been identified as appropriate coupling partners in the cross-dehydrogenative reactions with electron-rich organic substrates. However, very limited examples have been reported on the annulation with allenoates *via* C-H activation strategy to develop *N*-heterocycles.

For the first time, Li's group employed allenoates (2,3-allenoic acid esters) (**26**) for their annulation with *N*-methoxybenzamides (**15a**) to access 3,4-substituted hydroisoquinolones, possessing exocyclic double bond (**27**) with excellent regioselectivity *via* Pd^{II}-catalyzed C-H activation/annulation approach (Scheme 2C.1.14).[31]

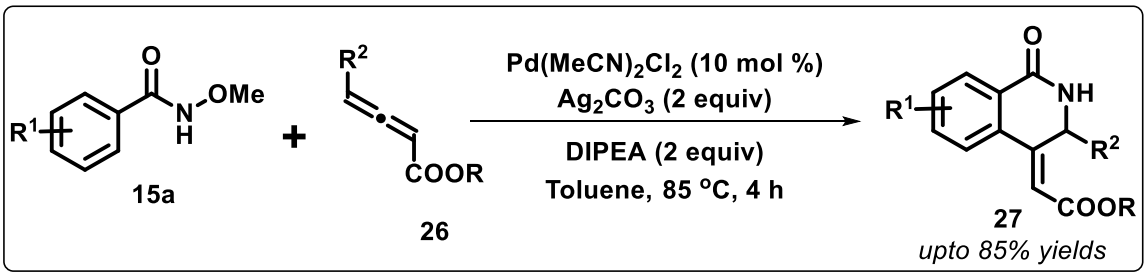

Scheme 2C.1.14 Pd-catalyzed [4+2] annulation strategy for the synthesis of 3,4-dihydroisoquinolones possessing exocyclic double bond using allenoates

In the year 2017, Rao and coworkers reported an intermolecular annulation strategy for coupling *N*-(quinolin-8-yl)benzamides (**11**) with allenoates (**26**) *via* Co^{II}-catalyzed C-H activation to synthesize regiodivergent isoquinolin-1(2*H*)-one derivatives (**28 & 29**), possessing endocyclic and exocyclic double bonds respectively in high yields (Scheme 2C.1.15).[32]

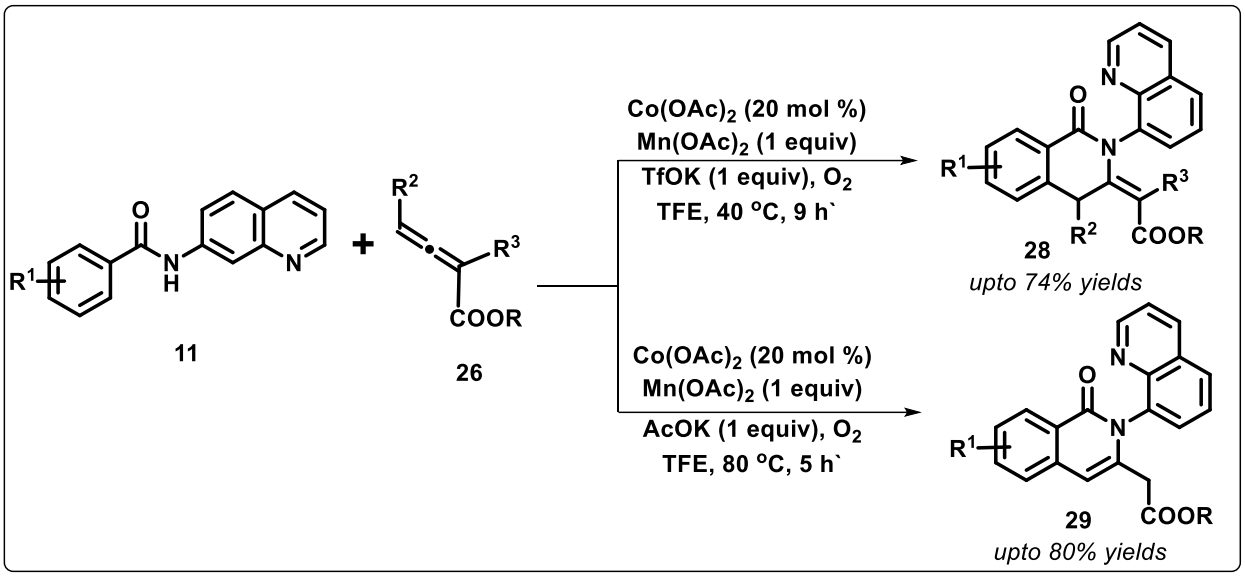

Scheme 2C.1.15 Co-catalyzed [4+2] annulation strategies for the synthesis of regiodivergent isoquinolin-1(2*H*)-ones using allenoates

Xu *et al*. described a straightforward synthesis of 2,3-dihydroisoquinolin-ylidenes (**30**) from readily available *N*-tosylacrylamides (**7**) and allenoates (**26**) *via* Pd^{II}-catalyzed direct oxidative C–H olefination with the assistance of sulfonamide as a directing group (Scheme 2C.1.16).[33]

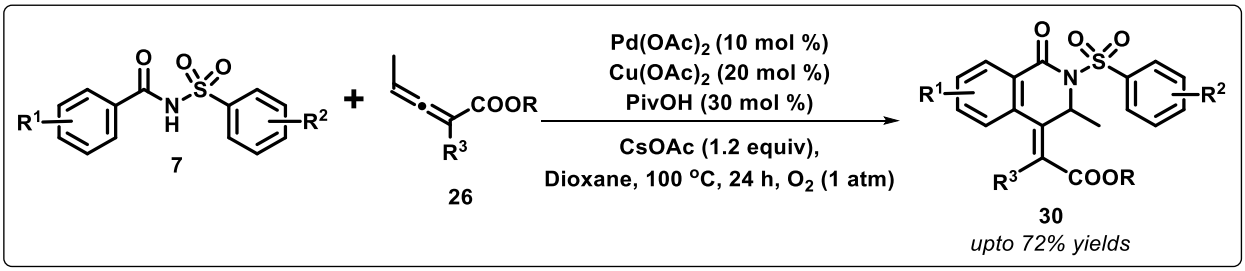

Scheme 2C.1.16 Pd-catalyzed annulation strategy for the synthesis of 2,3-dihydroisoquinolin-ylidenes using allenoates

In 2019, Yu's group established Rh^{III}-catalyzed [4+2] annulation of various acetophenone *O*-acetyl oximes (**31**) with terminal as well as internal allenoates (**26**) to access a series of functionalized isoquinolines (**32**) under redox-neutral conditions with high regioselectivity. Mechanistic studies revealed that the reaction proceeded through arene C-H activation, allene insertion followed by C-N coupling (Scheme 2C.1.17).[34]

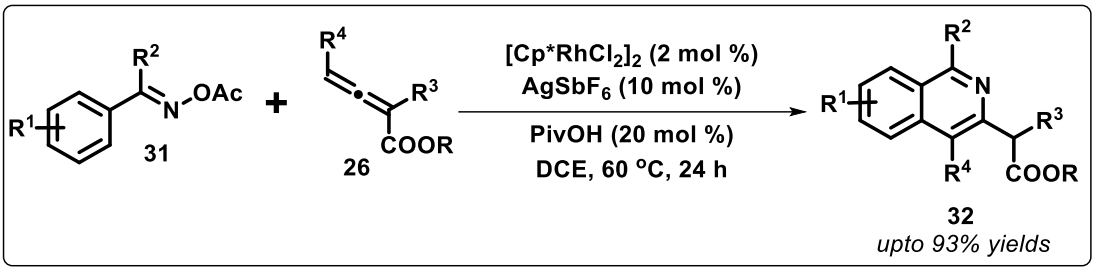

Scheme 2C.1.17 Rh-catalyzed annulation strategy for the synthesis of isoquinolines using allenoates

From the above examples it could be inferred that the presence of three reactive carbon centers in substituted allenes/allenoates unveils complex reactivity patterns based on steric and electronic properties of the attached substituents, furnishing five- and/or six-membered annulated products. Interestingly, the functionalization of *N*-arylindazolones remains unexplored with allenoates. Anticipating integral directing group ability of cyclic amidic group in *N*-arylindazolones, we envisioned that *N*-arylindazolones could be regioselectively functionalized/annulated using allenoates under metal-catalyzed conditions in a one-pot manner.

In this chapter, we disclose solvent/additive-controlled strategies for the synthesis of two regioisomeric forms of cinnoline-fused indazolones possessing internal and exocyclic double bonds through Pd^{II}-catalyzed C-H functionalization and subsequent oxidative annulation of *N*-arylindazolones with allenoates (Scheme 2C.1.18).

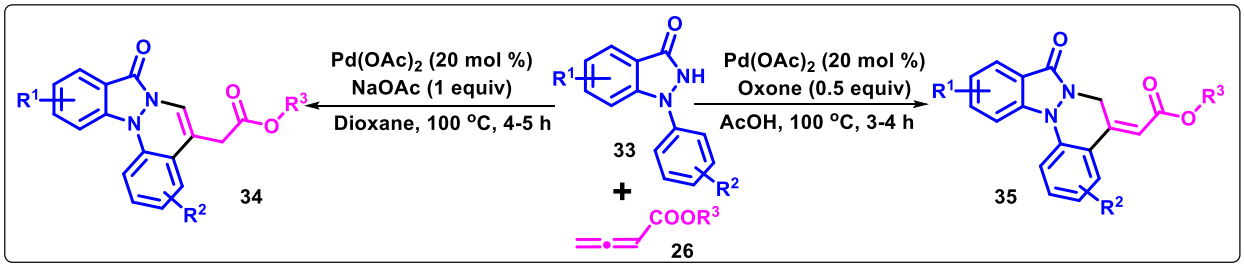

Scheme 2C.1.18 Pd-catalyzed [4+2] annulations strategy for the synthesis of regiodivergent indazolo-fused cinnolines possessing internal and exocyclic double bonds using allenoates

2C.2 Results and Discussion

Envisioning annulation between the two model substrates, 1-phenyl-1,2-dihydro-3*H*-indazol-3-one (**33a**) and phenyl butat-2,3-dienoate (**26a**), optimizing studies were initiated (Table 2C.2.1). Unfortunately, no coupling was observed between the model substrates using a catalytic amount of $Pd(OAc)_2$ in a variety of solvents including DCE, CH_3CN, toluene, and EtOH at temperatures ranging from 25 to 80 °C up to 12 h (Table 2C.2.1, entry 1). Interestingly, the reaction between

33a and **26a** using 5 mol % of $Pd(OAc)_2$ in 1,4-dioxane at 100 °C for 3 h afforded two new spots on TLC, along with the visibility of a reasonable amount of **33a** (Table 2C.2.1, entry 2). Purification of the products by column chromatography and their subsequent characterization using detailed spectroscopic analysis confirmed the formation of the two regioisomeric cinnoline-fused indazolones, **34aa** and **35aa**, in 30% and 15% yields, respectively. Almost inverse reactivity was observed by performing the model reaction in acetic acid, yielding **35aa** in 14%, with a trace amount of **34aa** (Table 2C.2.1, entry 3). The application of a stoichiometric amount of $Cu(OAc)_2$ as an additive with $Pd(OAc)_2$ gave a mixture of **34aa** and **35aa** in 20% and 35% yields, respectively (Table 2C.2.1, entry 4). Gratifyingly, a substantial increase in reactivity and selectivity was observed by replacing $Cu(OAc)_2$ with KOAc and LiOAc affording **34aa** in 61% and 63% yields, respectively, while the reaction with CsOAc was sluggish and did not produce any product (Table 2C.2.1, entries 5-7), while the application of NaOAc in dioxane afforded **34aa** in 69% yield (Table 2C.2.1, entry 8). Further, increasing the catalyst loading from 5 mol % to 15 mol % made an incremental effect on the product's yield, while no pronounced impact of catalyst overloading thereafter to 25 mol % or additive loading (NaOAc) to 1.5 equiv was observed (Table 2C.2.1, entries 9-12). Solvent screening studies indicated comparatively lower efficiency of toluene, acetonitrile (CH_3CN), and ethanol over dioxane to drive the coupling between the model substrates, while DMF and DMSO completely failed to produce any desired product resulting in messy reaction mixtures (Table 2C.2.1, entries 13-16). Notably, the model reaction using NaOAc in acetic acid produces 15% of **35aa** and a trace amount of **34aa** (Table 2C.2.1, entry 17). Thus, the use of $Pd(OAc)_2$/NaOAc in dioxane was found to be ideal reaction conditions to accomplish [4+2] annulation between **33a** and **26a** to generate phenyl 2-oxo-3-(8-oxo-8*H*-indazolo[1,2-*a*]cinnolin-5-yl)-propanoate (**34aa**) in high yield. Inspired by some of the above optimization results (Table 2C.2.1, entries 3 and 17), we continued our efforts toward standardizing optimal conditions to exclusively obtain **35aa** possessing an exocyclic double bond, which is the other regioisomeric form of **34aa**. Substituting NaOAc with oxidants such as $Cu(OAc)_2$, benzoquinone, and DDQ in acetic acid furnished higher amounts of **35aa** over **34aa** in overall moderate yields (Table 2C.2.1, entries 18-20), while oxone yielded 79% of **35aa** with a very trace amount of **34aa** (Table 2C.2.1, entry 21). Finally, decreasing the oxone concentration to 0.5 equiv with catalyst loading of 15 mol % had no detrimental effect (Table 2C.2.1, entry 22) on the reactivity and selectivity of the reaction in acetic acid, reemphasizing the importance of oxidant and solvent in

regioselectively generating phenyl (*Z*)-2-(8-oxo-8*H*-indazolo[1,2-*a*]cinnolin-5(6*H*)-ylidene)acetate (**35aa**) in a high yield.

Table 2C.2.1 Selective optimization[a] studies for the synthesis of **34aa** or **35aa**

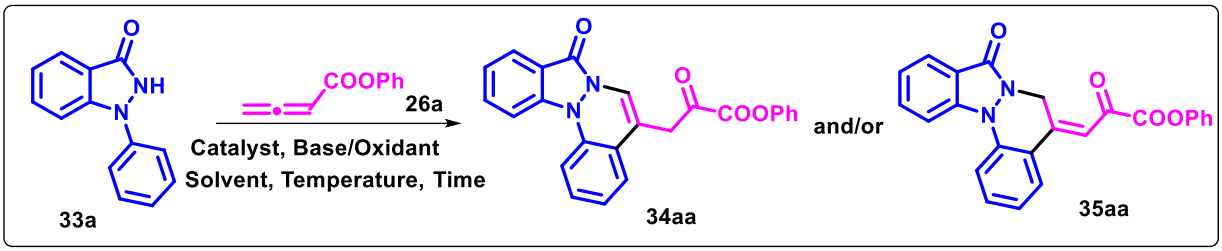

Entry	Catalyst (mol %)	Base/Oxidant (equiv)	Solvent	Yields of 34aa/35aa (%)[b]
1	$Pd(OAc)_2$ (5)	-	Solv.[c]	-
2	$Pd(OAc)_2$ (5)	-	Dioxane	30/15
3	$Pd(OAc)_2$ (5)	-	AcOH	trace/14
4	$Pd(OAc)_2$ (5)	$Cu(OAc)_2$ (1)	Dioxane	20/35
5	$Pd(OAc)_2$ (5)	KOAc (1)	Dioxane	61/0
6	$Pd(OAc)_2$ (5)	LiOAc (1)	Dioxane	63/0
7	$Pd(OAc)_2$ (5)	NaOAc (1)	Dioxane	69/0
8	$Pd(OAc)_2$ (5)	CsOAc (1)	Dioxane	-[d]
9	$Pd(OAc)_2$ (10)	NaOAc (1)	Dioxane	75/0
10	$Pd(OAc)_2$ (20)	NaOAc (1)	Dioxane	80/0
11	$Pd(OAc)_2$ (25)	NaOAc (1)	Dioxane	81/0
12	$Pd(OAc)_2$ (20)	NaOAc (1.5)	Dioxane	79/0
13	$Pd(OAc)_2$ (20)	NaOAc (1)	Toluene	35/0
14	$Pd(OAc)_2$ (20)	NaOAc (1)	CH_3CN	40/0
15	$Pd(OAc)_2$ (20)	NaOAc (1)	EtOH	38/0
16	$Pd(OAc)_2$ (20)	NaOAc (1)	DMF/ DMSO	-[d]
17	$Pd(OAc)_2$ (20)	NaOAc (1)	AcOH	trace/17
18	$Pd(OAc)_2$ (20)	$Cu(OAc)_2$ (1)	AcOH	15/45
19	$Pd(OAc)_2$ (20)	Benzoquinone (1)	AcOH	23/40
20	$Pd(OAc)_2$ (20)	DDQ (1)	AcOH	18/52
21	$Pd(OAc)_2$ (20)	Oxone (1)	AcOH	trace/79
22	$Pd(OAc)_2$ (20)	Oxone (0.5)	AcOH	trace/78

[a]Reaction conditions: The reactions were carried out with **33a** (0.237 mmol) and **26a** (0.713 mmol) in the presence of base/oxidant (as indicated in the table) using 4 mL of solvent at 100 °C for 4 h. [b]Isolated yields; [c]Solvent = DCE/CH_3CN/Toluene/EtOH at temperatures ranging from 25 °C - 80 °C up to 12 h; [d]Sluggish/messy reaction mixture.

Having optimized conditions in hand, we first investigated the generality of the developed dioxane-controlled [4+2] annulation strategy using diversely substituted 1-aryl-1,2-dihydro-3*H*-

indazol-3-one (**33a-s**) and a few allenoates (**26a-c**) (Scheme 2C.2.1). Overall, the electronic effect of substituents on the aryl and indazolone rings had a pronounced effect on the yields of the desired products. For example, electronically-rich substitutents at *para*-position of aryl moiety 1-aryl-1,2-dihydro-3*H*-indazol-3-ones [substrates: R^2 = *p*-Me (**33b**), *p*-OMe (**33c**), *p*-^{i}Pr (**33d**)] reacted efficiently with phenyl buta-2,3-dienoate (**26a**) to furnish their corresponding cinnoline-fused indazolones (**34ba-da**) in 83%, 86%, and 87% yields, respectively. The slight deterioration in the reaction efficiency was observed for halogenated arylindazolones at different positions on an aryl moiety [substrates: R^2 = *p*-Cl (**33e**), *p*-Br (**33f**), *m*-Cl (**33g**), *m*-Br (**33h**)], yielding their respective annulated products **34ea-ha** in 68−77% yields. Di-substitution on the aryl ring [substrate: R^2 = 3-Cl-4-Me (**33i**)] facilitated the reaction to produce **34ia** in 72% yield. Electron-donating and weakly electron-withdrawing substituents on an indazolone moiety [substrates: R^1 = 5-Me (**33j**), 5-OMe (**33k**), 5-Cl (**33l**), 5-Br (**33m**)] were well tolerated on 1-aryl-1,2-dihydro-3*H*-indazol-3-one to produce respective desired products **34ja**−**ma** in 74−82% yields. However, drastic decrement in the yield was observed in the case of a strong electron-withdrawing substituent on an indazolone moiety [substrate: R^1 = 5-NO_2 (**33n**)], which reacted quite inefficiently with allenoate (**26a**) to furnish the expected annulation product **34na** in only 39% yield. Intriguingly, the substrate, 1-phenyl-1,2-dihydro-3*H*-pyrazolo[3,4-*b*]pyridin-3-one (**33o**), showcased comparatively lower reactivity under standard conditions to afford **34oa** in 60% yield. Other allenoates, such as naphthalen-2-yl buta-2,3-dienoate (**26b**) and benzyl buta-2,3-dienoate (**26c**) reacted with **33a** in moderate reactivity to generate **34ab** and **34ac** in 60% and 70% yields, respectively. Unfortunately, a highly electron-deficient substrate [substrate: R^2 = 3-NO_2 (**33q**)] and *ortho*-substituted substrates [substrates: R^2 = 2-Me (**33r**), 2-Br (**33s**)] failed to react with **26a** under the described condition A. The representative ^{1}H and ^{13}C NMR spectra of **34aa** are shown in Figure 2C.2.1 and Figure 2C.2.2, respectively.

Subsequently, the substrate scope of the two coupling partners was scrutinized toward acetic acid/oxone-controlled [4+2] annulation (Scheme 2C.2.2). The electronic consequence of substituents on the aryl moiety indicated that electron-rich substrates (**33b**−**d**) possessing *p*-Me, *p*-OMe, and *p*-^{i}Pr groups showcased high reactivity, while the weakly electron-deficient substrate possessing *m*-Cl (**33g**) and *m*-Br (**33h**) functionality exhibited moderate reactivity, furnishing their respective annulated products **35ba**−**35da** and **35ga**−**35ha** possessing exocyclic double bonds, in 60−82% yields. Further, disubstituted 1-aryl-1,2-dihydro-3*H*-indazol-3-one with electron-

donating/withdrawing groups [substrates: R^2 = 3-Cl-4-Me (**33i**)] and 3,4-di-Me (**33p**)] reacted quite well with **26a** to yield **35ia** and **35pa** in 70% and 80% yields, respectively. Similarly, substrates **33j**–**l** were smoothly transformed into desired products **35ja**–**35la** in 70–75% yields. Unfortunately, [R^2 = 5-NO_2] failed to react with **26a** to produce the corresponding annulated product (**35na**) in only a trace amount that could not be isolated. The established Pd-catalyzed acetic acid-controlled condition also holds good for the coupling between **33a** and naphthalen-2-yl buta-2,3-dienoate (**26b**), leading to furnish **35ab** in a decent yield. In this condition also, a highly electron-deficient substrate [substrate: R^2 = 3-NO_2 (**33q**)] and *ortho*-substituted substrates [substrates: R^2 = 2-Me (**33r**), 2-Br (**33s**)] failed to react with **26a**. The representative ^{1}H and ^{13}C NMR spectra of **35aa** are shown in Figure 2C.2.3 and Figure 2C.2.4, respectively.

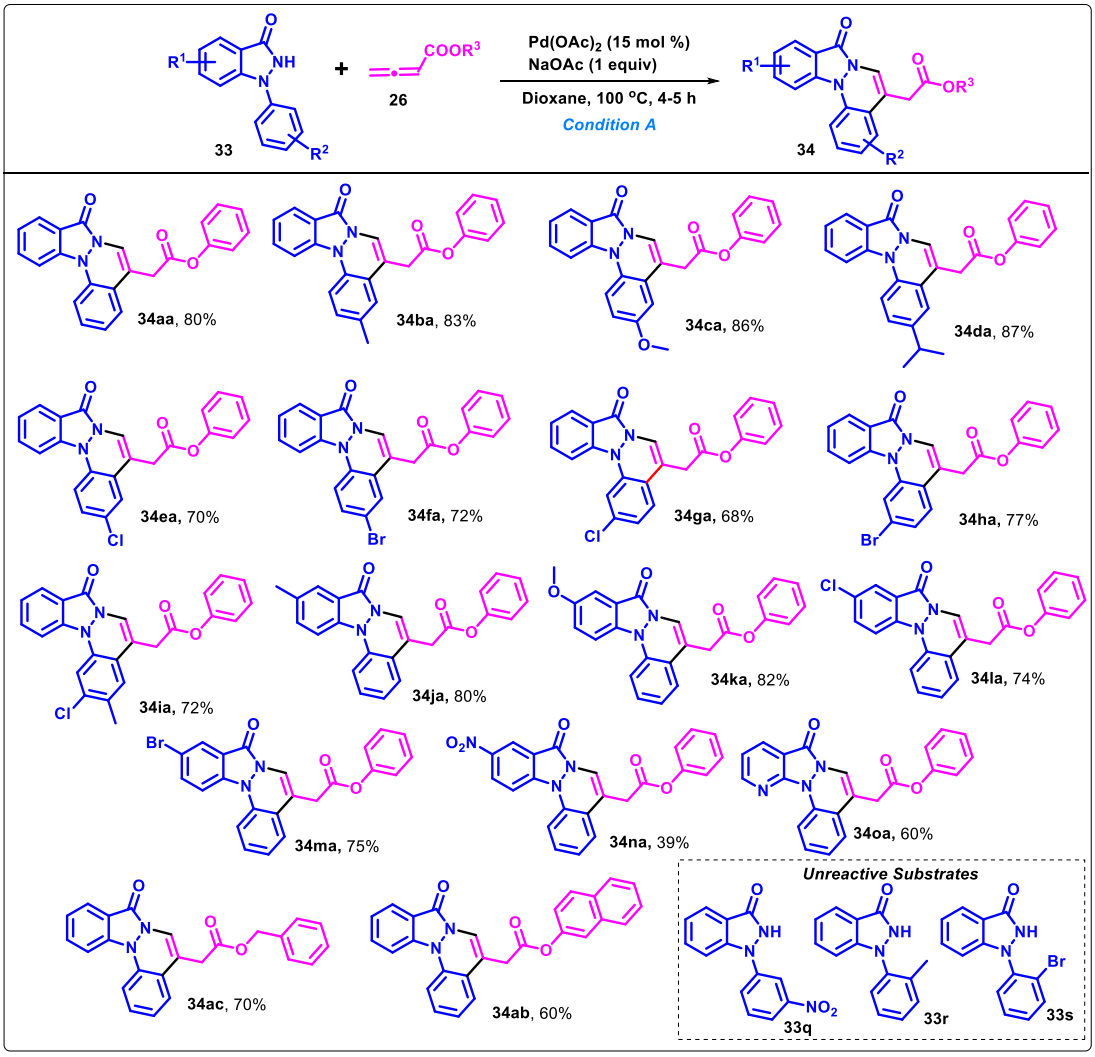

Scheme 2C.2.1. Substrate scope for the annulation of 1-aryl-1,2-dihydro-3*H*-indazol-3-ones and allenoates in dioxane

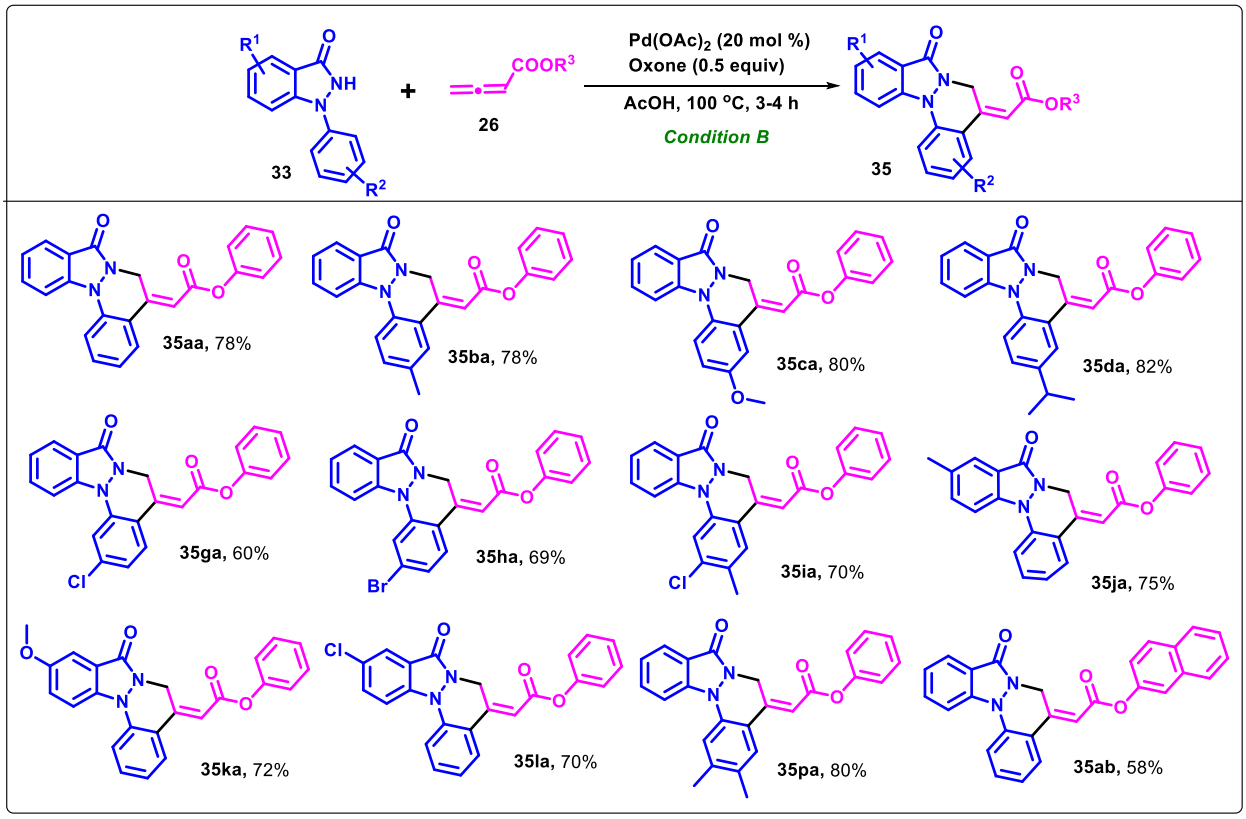

Scheme 2C.2.2. Substrate scope for the annulation of 1-aryl-1,2-dihydro-3*H*-indazol-3-ones with allenoates in acetic acid

To show the synthetic utility of the established strategy gram scale reactions were performed under both the conditions by using **33a** and **26a**. Bothe the optimized conditions revel best results in the formation of annulation products **34aa** and **35aa** (Scheme 2C.2.3).

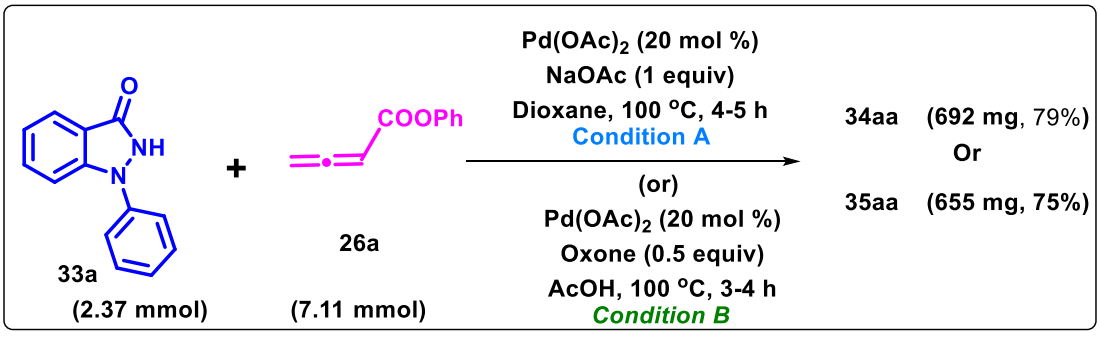

Scheme 2C.2.3. Gram Scale Synthesis of **34aa** and **35aa**

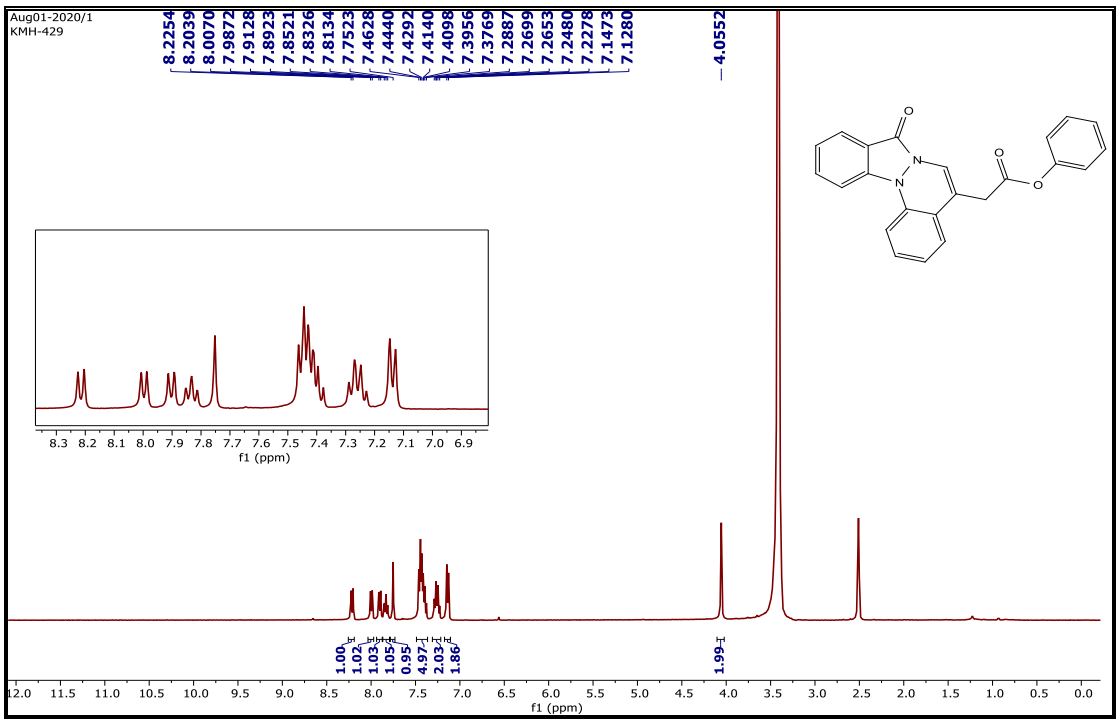

Figure 2C.2.1 ^{1}H NMR Spectrum of **34aa**

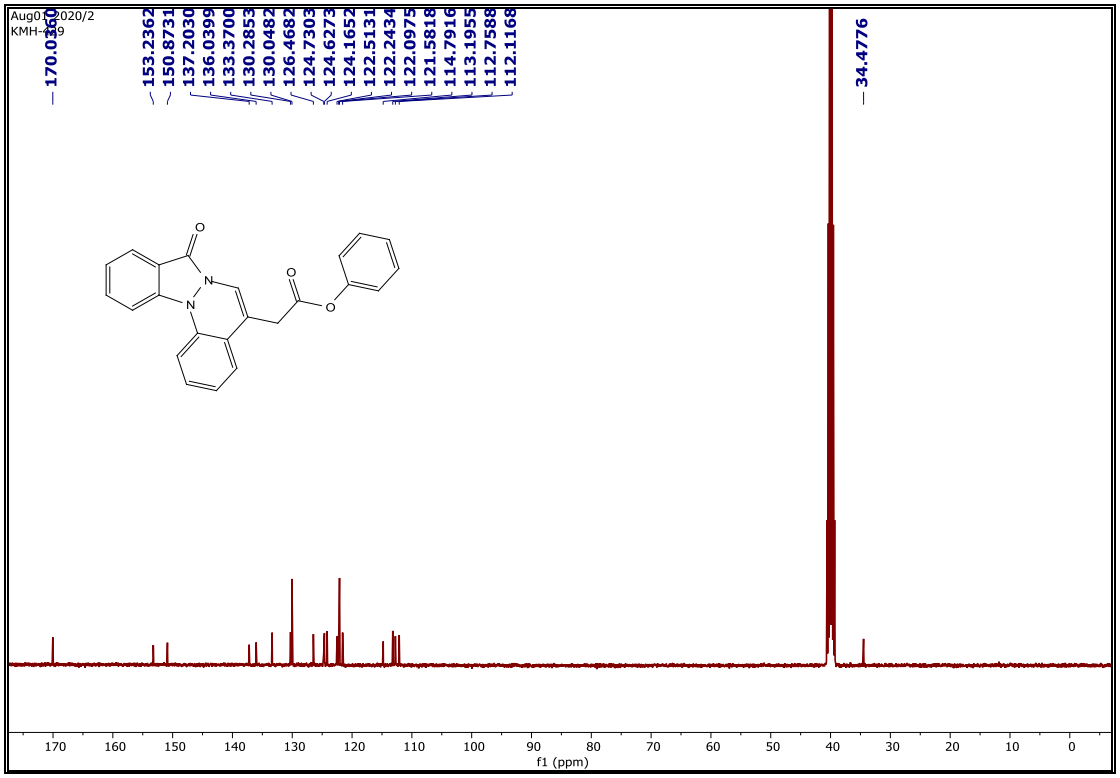

Figure 2C.2.2 ^{13}C NMR Spectrum of **34aa**

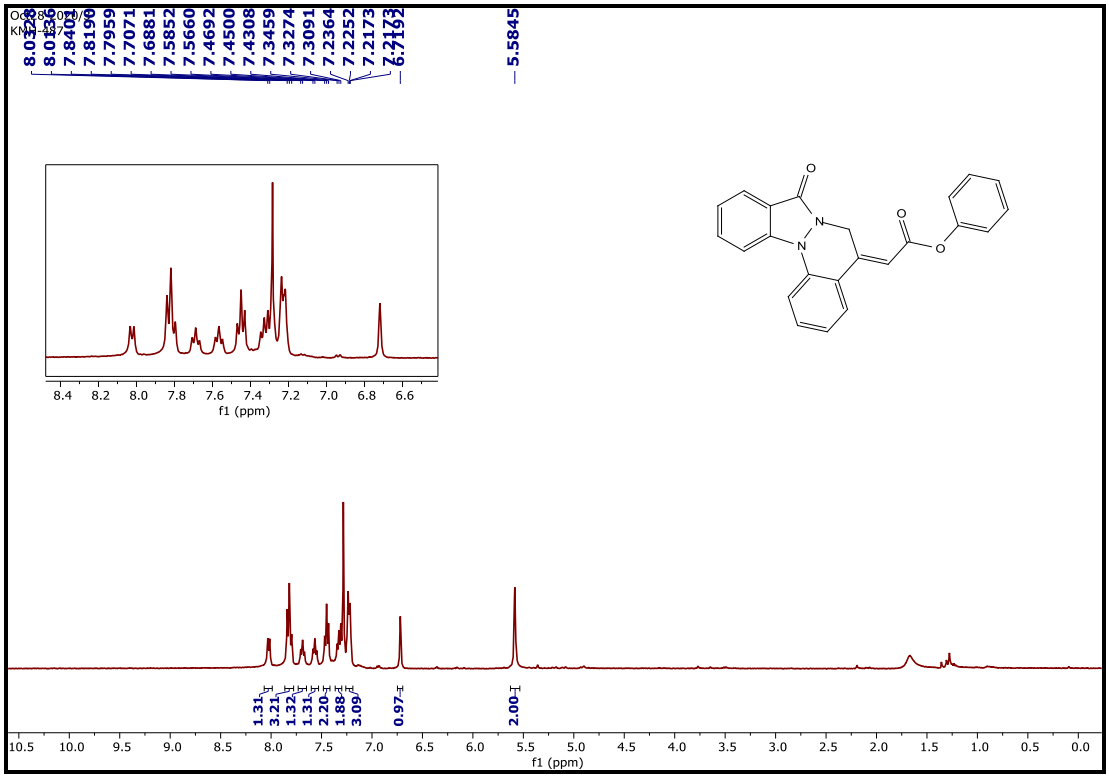

Figure 2C.2.3 ^{1}H NMR Spectrum of **35aa**

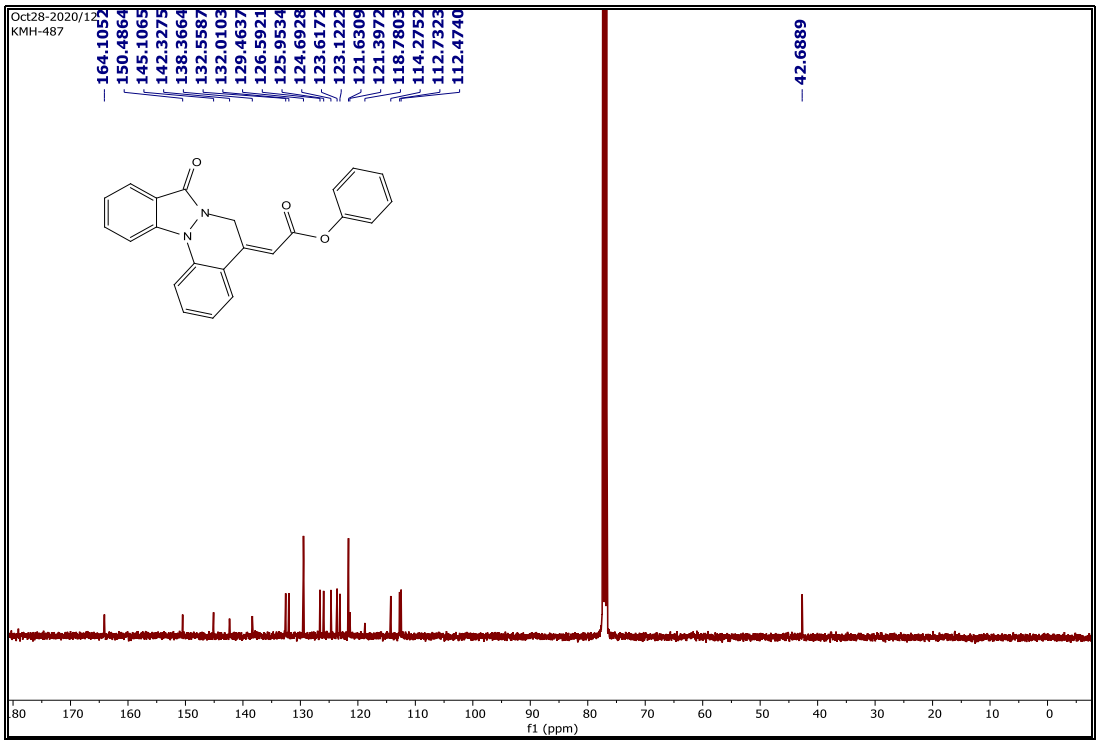

Figure 2C.2.4 ^{13}C NMR Spectrum of **35aa**

Surprisingly, the allenoates possessing substitution at the terminal double bond selectively produced the annulation products possessing an exocyclic double bond, under either of the two earlier described solvent-controlled conditions (Scheme 2C.2.4). For example, the coupling of phenyl hepta-2,3- dienoate (**26d**), phenyl 4-phenylbuta-2,3-dienoate (**26e**), and ethyl 4-phenylbuta-2,3-dienoate (**26f**) with **33a** proceeded in moderate efficiency in dioxane or acetic acid to produce **35ad**, **35ae**, and **35af** in almost similar yields. Unfortunately, trisubstituted allenoates such as phenyl 4-methylpenta-2,3-dienoate (**26g**) and ethyl 2-methylhepta-2,3-dienoate (**26h**) failed to react with **33a** in either of the described conditions. Also, aryl-substituted allene, such as 1-phenyl-3-propylallene (**26a′**), behaved in a similar fashion.

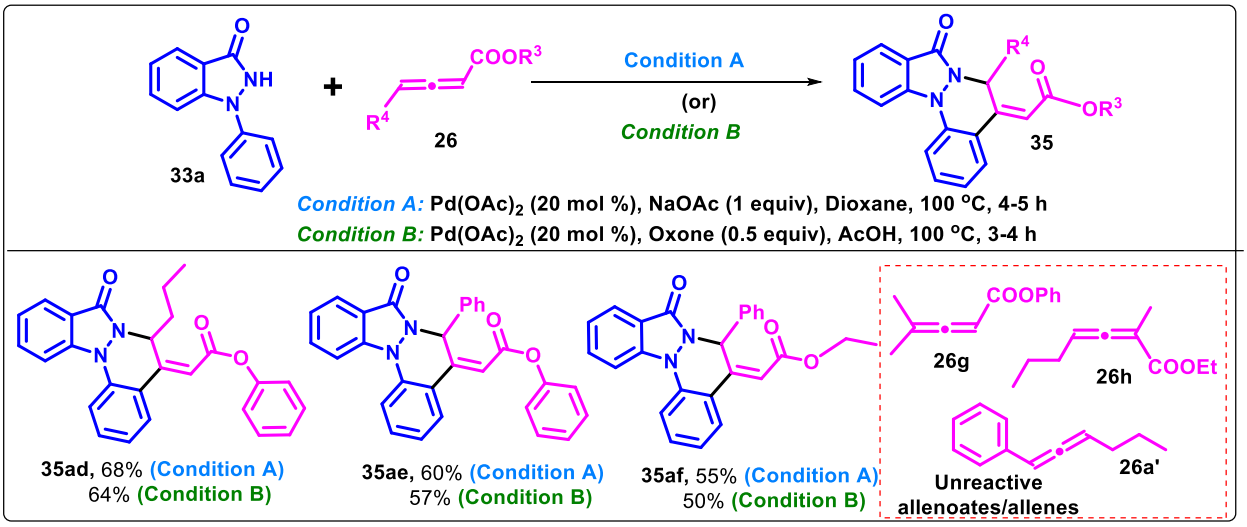

Scheme 2C.2.4 Substrate scope for the annulation of 1-phenyl-1,2-dihydro-3*H*-indazol-3-one with di- or tri-substituted allenoates

Moreover, single crystals of **35ad** and **35ae** were grown from dichloromethane *via* single solvent slow evaporation at room temperature for X-ray diffraction (XRD) studies as representative examples, which further confirmed their assigned structures (Figure 2C.2.3). ORTEP Diagrams of **35ad** (CCDC No. 2117498) and **35ae** (CCDC No. 2117499) are shown in Figure 2B.2.5.

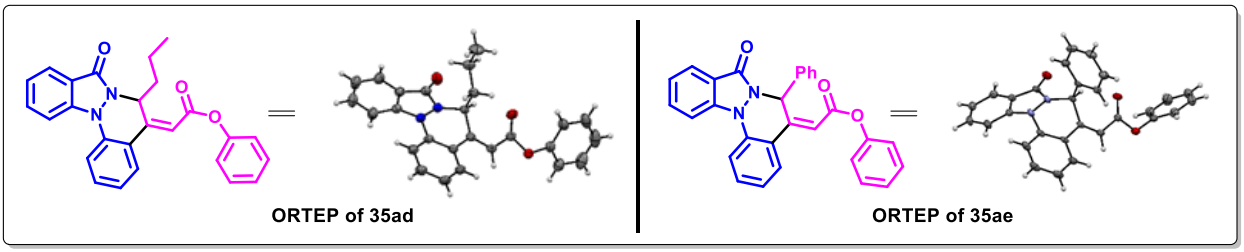

Figure 2C.2.5 ORTEP Diagrams of **35ad** and **35ae**

To gain insight into the reaction mechanism, a few control experiments, deuteration experiments, and kinetic isotope effect (KIE) studies were conducted (Scheme 2C.2.5). From the optimization results, it was evident that the two Pd-catalyzed strategies either require a base or an oxidant in respective solvents to exclusively produce two regioisomeric forms of cinnoline-fused indazolones **34aa** or **35aa**. However, the formation of *N*-alkenylated indazolone (**36aa**) by the addition of **26a** to **33a**, followed by isomerization, was obtained in 83% using NaOAc in dioxane in the absence of $Pd(OAc)_2$. This indicated a crucial role of Pd in the proposed C−H activation step. Further transformation of **36aa** into **34aa** or **35aa** was not observed by applying the two described Pd-catalyzed conditions, excluding the possibility of **36aa** to be an active intermediate (Scheme 2C.2.5i). The possibility of a radical pathway was eliminated as the reaction efficiency between **33a** and **26a** under standard conditions remains unaffected using 3 equiv of TEMPO (Scheme 2C.2.5ii). Further, a spot-to-spot conversion of **35aa** to **34aa** on TLC was monitored upon its heating in dioxane with 1 equiv of NaOAc, indicating the generation of a more stable regioisomeric form (**34**) under base-mediated conditions. However, this conversion was not observed for the compounds **35ad**−**ae** under similar reaction conditions. On the other hand, the conversion of **34aa** to **35aa** was not observed by heating it under acetic acid/oxone-mediated conditions (Scheme 2C.2.5iii). Further, negligible H/D exchange at the *ortho*-positions of **33j** was monitored by performing its reaction under standard conditions in either D_2O, CD_3OD, or CD_3COOD, indicating the cleavage of the *ortho*-C−H bond to be irreversible in nature (Scheme 2C.2.5iv). Thus, **33j-*d*$_2$** was prepared by our earlier reported procedure and used for KIE studies. The intermolecular competition experiment of **33j** and **33j-*d*$_2$** with **26a** under dioxane and acetic acid-driven Pd-catalyzed conditions gave a kinetic isotopic effect (P_H/P_D) of 2.4 and 2.1, respectively, while k_H/k_D values of 1.5 and 1.4 were computed by performing two parallel reactions of **33j** and **33j-*d*$_2$** with **26a** under the two independently described standard conditions in dioxane and acetic acid, respectively (Scheme 2C.2.5v). These results indicated that the C-H activation step might be involved in the rate-determining step.

Based on the literature studies[20-21,34-35] and our preliminary investigation, a plausible mechanism is proposed (Scheme 2C.2.6). The reaction could be believed to be proceeded by ligand exchange between 1-aryl-1,2-dihydro-3*H*-indazol-3-one (**33)** and $Pd(OAc)_2$ to furnish species **A**, which undergoes a C_{Ar}−H activation to form a five-membered palladacycle complex (**B**). Subsequently, coordination of allenoate to the palladium center followed by regioselective 1,2-migratory

insertion between the C_{Ar}–pd bond would probably afford a seven-membered palladacycle intermediate (**D**) *via* **C**. Finally, **D** would undergo reductive elimination to give **35** along with the generation of Pd^0 species. This would regenerate Pd^{II} species by oxidation with either air or oxone in dioxane and acetic acid, respectively. The reaction would cease in acetic acid-producing **35** in major amounts, while NaOAc-mediated isomerization of **35** produces **34** in dioxane.

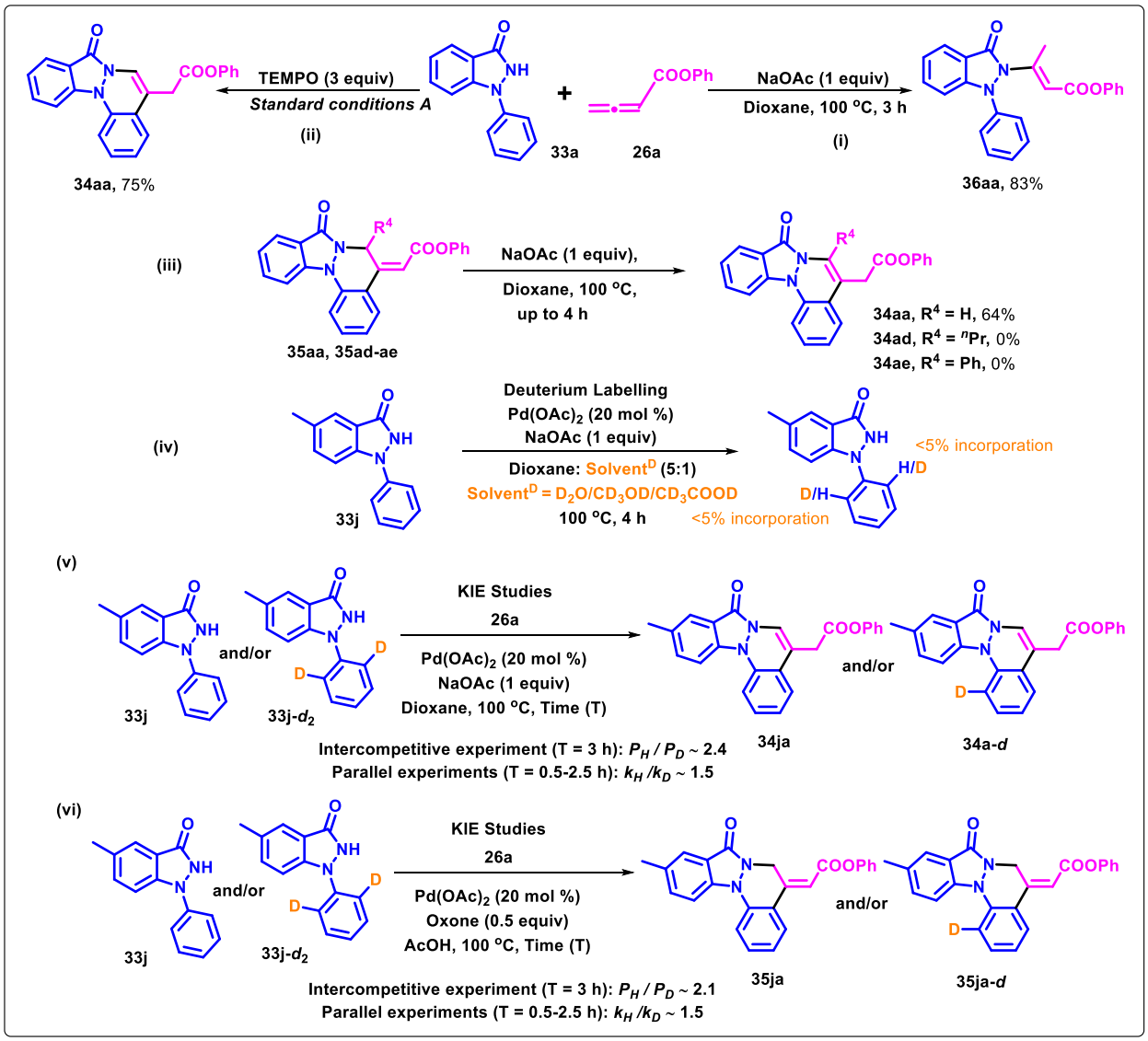

Scheme 2C.2.5. Mechanistic investigations

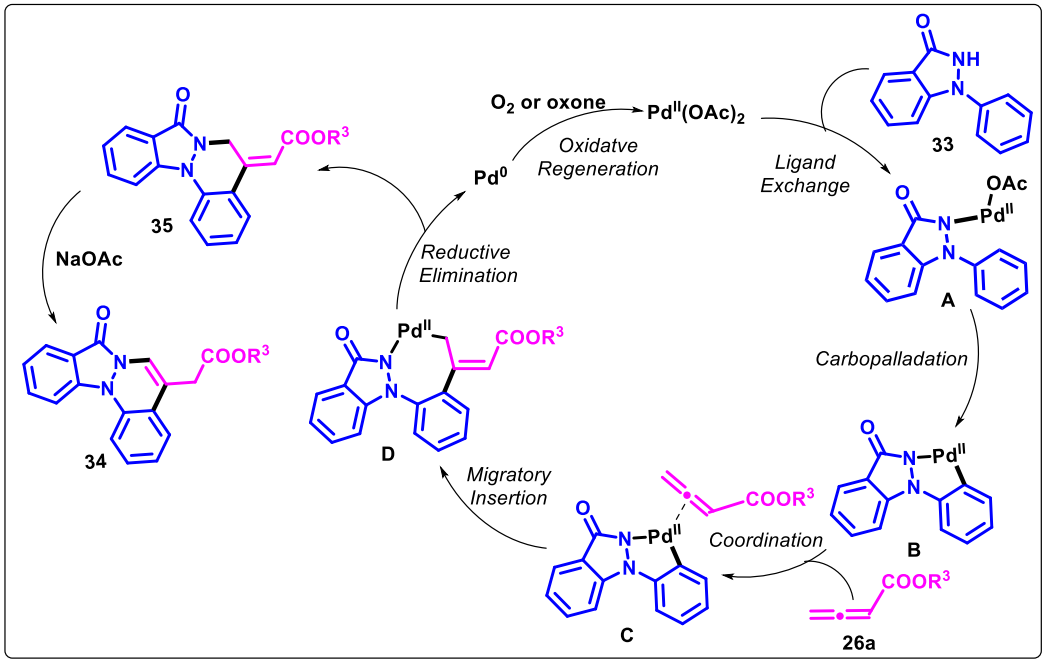

Scheme 2C.2.6. Plausible mechanistic pathway

In conclusion, the present work provides an illumination account for the reactivity comparison of the coupling between 1-aryl-1,2-dihydro-3*H*-indazol-3-one and allenoates in dioxane and acetic acid to selectively access two different regioisomeric forms of indazolo[1,2-*a*]cinnolines possessing internal and exocyclic double bonds, respectively. Terminally substituted allenoates preferred to afford only one isomeric form possessing an exocyclic double bond in either of the two solvent-controlled conditions. The described Pd^{II}-catalyzed [4+2] annulation strategies highlight the synthesis of cinnoline-fused indazolones in appreciable yields and represent a significant addition to the armory of Pd-catalyzed C–H activation protocols.

2C.3 Experimental Section

General Considerations

Commercially available reagents were used without purification. Commercially available solvents were dried by standard procedures prior to use. Allenoates were prepared according to the reported procedures.[36-37] Nuclear magnetic resonance spectra were recorded on a 400 MHz spectrometer, and the chemical shifts are reported in δ units, parts per million (ppm), relative to residual chloroform (7.26 ppm) or DMSO (2.5 ppm) in the deuterated solvent. The following abbreviations were used to describe peak splitting patterns when appropriate: s = singlet, d = doublet, t = triplet, dd = doublet of doublets, and m = multiplet. Coupling constants *J* are reported in Hz. The ^{13}C NMR spectra are reported in ppm relative to deuterochloroform (77.0 ppm) or DMSO-d_6 (39.5

ppm). Melting points were determined on a capillary point apparatus equipped with a digital thermometer and are uncorrected. High-resolution mass spectra were recorded on Agilent Technologies 6545 Q-TOF LC/MS by using electrospray mode. Column chromatography was performed on silica gel (100-200) mesh using varying ratio of ethyl acetate/hexanes as eluent.

General procedure for the synthesis of indazolo[1,2-*a*]cinnolines (34/35)

To an oven-dried 10-mL round-bottom flask containing 1-aryl-1,2-dihydro-3*H*-indazol-3-one (**33**) (50 mg, 1 equiv) in dioxane (Method A) or acetic acid (Method B) (4 mL), allenoate (**26**) (3 equiv), $Pd(OAc)_2$ (0.020 equiv), NaOAc (1 equiv) (**Method A**) or oxone (0.5 equiv) (**Method B**) were added under atmospheric air. The reaction mixture was stirred and heated on a heating mantle at 100 ºC for 3-5 h (traced by TLC). After the completion of the reaction, the reaction mixture was cooled to room temperature, concentrated, diluted with water and extracted with EtOAc (20 mL x 2). The organic layers were combined and concentrated under reduced pressure to afford a residue, which was purified by column chromatography (SiO_2 100−200 mesh) using hexanes/EtOAc (8/2) as eluent system to afford the desired product (**34/35**).

Phenyl 2-(8-oxo-8*H*-indazolo[1,2-*a*]cinnolin-5-yl)acetate (34aa). Yellow solid, 70 mg (80%);

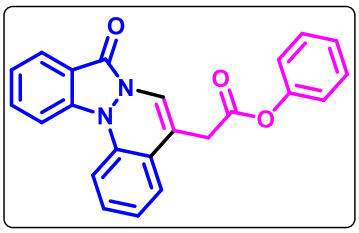

mp 150-151 ºC; ^{1}H NMR (400 MHz, DMSO-d_6) δ 8.21 (d, J = 8.6 Hz, 1H), 8.00 (d, J = 7.9 Hz, 1H), 7.90 (d, J = 8.2 Hz, 1H), 7.83 (t, J = 7.7 Hz, 1H), 7.75 (s, 1H), 7.46 – 7.38 (m, 5H), 7.29 – 7.23 (m, 2H), 7.14 (d, J = 7.7 Hz, 2H), 4.06 (s, 2H); ^{13}C NMR (100 MHz, DMSO-d_6) δ 170.0, 153.2, 150.9, 137.2, 136.0, 133.4, 130.3, 130.1, 126.5, 124.7, 124.6, 124.2, 122.5, 122.2, 122.1, 121.6, 114.8, 113.2, 112.8, 112.1, 34.5; HRMS (ESI-TOF) (*m/z*) calculated $C_{23}H_{17}N_2O_3^+$: 369.1239, found 369.1228 $[M + H]^+$.

Phenyl 2-(3-methyl-8-oxo-8*H*-indazolo[1,2-*a*]cinnolin-5-yl)acetate (34ba). Yellow solid, 71.0

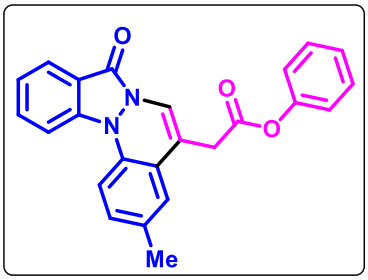

mg (83%); mp 161-162 ºC; ^{1}H NMR (400 MHz, DMSO-d_6) δ 8.17 (d, J = 8.7 Hz, 1H), 7.98 (d, J = 7.9 Hz, 1H), 7.83 – 7.78 (m, 2H), 7.75 (s, 1H), 7.44 (t, J = 7.7 Hz, 2H), 7.37 (t, J = 7.5 Hz, 1H), 7.30 – 7.22 (m, 3H), 7.14 (d, J = 7.9 Hz, 2H), 4.05 (s, 2H), 2.35 (s, 3H); ^{13}C NMR (100 MHz, DMSO-d_6) δ 170.1, 153.2, 150.9, 137.1, 133.8, 133.8, 133.2, 130.4, 130.1, 126.5, 125.2, 124.1, 122.2, 122.1, 122.1, 121.5, 114.5, 113.0, 112.7, 112.0, 34.4, 20.9; HRMS (ESI-TOF) (*m/z*) calculated $C_{24}H_{19}N_2O_3^+$: 383.1395, found 383.1392 $[M + H]^+$.

Phenyl 2-(3-methoxy-8-oxo-8*H*-indazolo[1,2-*a*]cinnolin-5-yl)acetate (34ca). Yellow solid 71 mg (86%); mp 160-161 °C; ^{1}H NMR (400 MHz, $CDCl_3$) δ 8.12 (d, J = 8.0 Hz, 1H), 7.87 (d, J = 8.6 Hz, 1H), 7.73 (t, J = 7.9 Hz, 1H), 7.70 – 7.65 (m, 2H), 7.39 (t, J = 7.8 Hz, 2H), 7.32 (t, J = 7.5 Hz, 1H), 7.25 (t, J = 7.4 Hz, 1H), 7.10 (d, J = 7.9 Hz, 2H), 7.02 (d, J = 2.8 Hz, 1H), 6.91 (dd, J = 8.8, 2.8 Hz, 1H), 3.87 (s, 3H), 3.80 (s, 2H); ^{13}C NMR (100 MHz, $CDCl_3$) δ 168.8, 156.2, 153.8, 150.5, 137.2, 132.5, 130.0, 129.5, 126.1, 124.7, 123.8, 121.8, 121.4, 121.3, 114.7, 113.4, 113.0, 111.4, 110.9, 110.5, 55.7, 36.0; HRMS (ESI-TOF) (*m/z*) calculated $C_{24}H_{19}N_2O_4^+$: 399.1344, found 399.1327 $[M + H]^+$.

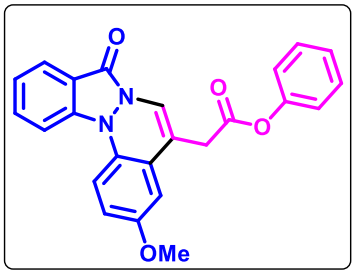

Phenyl 2-(3-isopropyl-8-oxo-8*H*-indazolo[1,2-*a*]cinnolin-5-yl)acetate (34da). Yellow solid, 71 mg (87%); mp 152-153 °C; ^{1}H NMR (400 MHz, $CDCl_3$) δ 8.14 (d, J = 7.9 Hz, 1H), 7.91 (d, J = 8.6 Hz, 1H), 7.75 (t, J = 7.8 Hz, 1H), 7.69 (d, J = 8.4 Hz, 1H), 7.66 (s, 1H), 7.38 (t, J = 7.9 Hz, 2H), 7.33 (t, J = 7.5 Hz, 1H), 7.30 (d, J = 2.0 Hz, 1H), 7.28 – 7.24 (m, 2H), 7.07 (dd, J = 8.6, 1.2 Hz, 2H), 3.83 (s, 2H), 2.96 (hept, J = 7.0 Hz, 1H), 1.30 (d, J = 6.9 Hz, 6H); ^{13}C NMR (100 MHz, $CDCl_3$) δ 169.0, 150.5, 144.9, 137.1, 134.2, 132.5, 129.5, 127.3, 126.1, 124.6, 122.2, 122.0, 121.6, 121.3, 121.1, 112.1, 111.7, 111.5, 36.0, 33.7, 23.9; HRMS (ESI-TOF) (*m/z*) calculated $C_{26}H_{23}N_2O_3^+$: 411.1708, found 411.1667 $[M + H]^+$.

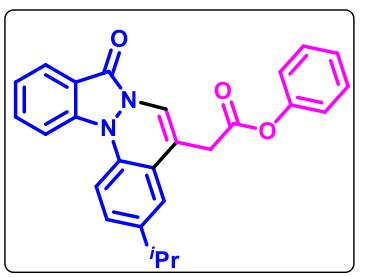

Phenyl 2-(3-chloro-8-oxo-8*H*-indazolo[1,2-*a*]cinnolin-5-yl)acetate (34ea). Yellow solid, 58 mg (70%); mp 203-204 °C; ^{1}H NMR (400 MHz, $CDCl_3$) δ 8.13 (d, J = 7.7 Hz, 1H), 7.85 (d, J = 8.6 Hz, 1H) 7.76 (td, J = 7.0, 1.3 Hz, 1H), 7.65 – 7.61 (m, 2H), 7.43 – 7.38 (m, 2H), 7.36 – 7.31 (m, 3H), 7.28 – 7.24 (m, 1H), 7.13 – 7.11 (m, 2H), 3.77 (s, 2H); ^{13}C NMR (100 MHz, $CDCl_3$) δ 168.5, 153.8, 150.5, 137.2, 134.8, 132.9, 129.5, 129.4, 129.0, 126.2, 124.8, 124.1, 124.0, 122.4, 122.2, 121.3, 115.3, 113.0, 111.7, 110.2, 35.6; HRMS (ESI-TOF) (*m/z*) calculated $C_{23}H_{16}ClN_2O_3^+$: 403.0849, found 403.0823 $[M + H]^+$.

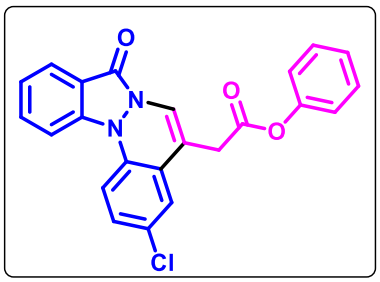

Phenyl 2-(3-bromo-8-oxo-8*H*-indazolo[1,2-*a*]cinnolin-5-yl)acetate (34fa). Yellow solid, 56 mg, (72%); mp 230-231 °C; ^{1}H NMR (400 MHz, $CDCl_3$) δ 8.13 (d, J = 7.9 Hz, 1H), 7.85 (d, J = 8.6 Hz, 1H), 7.77 (t, J = 7.8 Hz, 1H), 7.64 (s, 1H), 7.58 (d, J = 8.6 Hz, 1H), 7.50 – 7.46 (m, 2H), 7.43 – 7.35 (m, 3H), 7.27 – 7.25 (m, 1H), 7.12 (dd, J = 8.9, 1.4 Hz, 2H), 3.77 (s, 2H); ^{13}C NMR (100 MHz, $CDCl_3$) δ 168.5, 153.8, 150.5, 137.3, 135.3, 132.9, 131.9, 129.6, 126.8, 126.2, 124.8, 124.4, 122.4, 122.3, 121.3, 116.8, 115.4, 113.3, 111.7, 110.1, 35.6; HRMS (ESI-TOF) (*m/z*) calculated $C_{23}H_{16}BrN_2O_3^+$: 447.0344, found 447.0324 $[M + H]^+$.

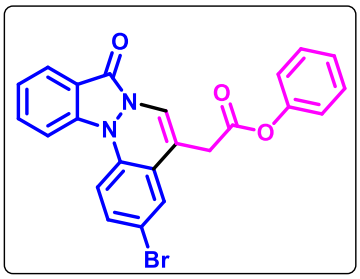

Phenyl 2-(2-chloro-8-oxo-8*H*-indazolo[1,2-*a*]cinnolin-5-yl)acetate (34ga). Yellow solid, 56 mg (68%); mp 193-194 °C; ^{1}H NMR (400 MHz, $CDCl_3$) δ 8.14 (dd, J = 7.2, 1.2 Hz, 1H), 7.90 (d, J = 8.6 Hz, 1H), 7.83 – 7.78 (m, 1H), 7.70 (d, J = 2.0 Hz, 1H), 7.62 (s, 1H), 7.44– 7.35 (m, 3H), 7.33 (d, J = 8.3 Hz, 1H), 7.27 – 7.24 (m, 1H), 7.15 (dd, J = 8.3, 1.9 Hz, 1H), 7.10 – 7.07 (m, 2H), 3.78 (s, 2H); ^{13}C NMR (100 MHz, $CDCl_3$) δ 168.6, 153.7, 150.5, 137.2, 137.2, 135.1, 132.9, 129.5, 126.2, 124.9, 124.8, 123.9, 122.5, 121.5, 121.3, 120.9, 115.6, 112.3, 111.8, 110.6, 35.8; HRMS (ESI-TOF) (*m/z*) calculated $C_{23}H_{16}ClN_2O_3^+$: 403.0849, found 403.0826 $[M + H]^+$.

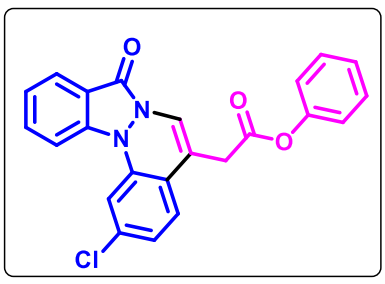

Phenyl 2-(2-bromo-8-oxo-8*H*-indazolo[1,2-*a*]cinnolin-5-yl)acetate (34ha). Yellow solid, 60 mg (77%); mp 172-173 °C; ^{1}H NMR (400 MHz, $CDCl_3$) δ 8.14 (dt, J = 7.9, 1.0 Hz, 1H), 7.88 (d, J = 8.6 Hz, 1H), 7.83 (dd, J = 5.0, 1.5 Hz, 1H), 7.82 – 7.78 (m, 1H), 7.63 (s, 1H), 7.41 – 7.37 (m, 3H), 7.31 7.29 (m, 1H), 7.27 – 7.24 (m, 2H), 7.09 – 7.07 (m, 2H), 3.77 (d, J = 1.1 Hz, 2H); ^{13}C NMR (100 MHz, $CDCl_3$) δ 168.7, 153.8, 150.5, 137.2, 137.1, 133.0, 129.5, 126.9, 126.2, 124.8, 122.9, 122.5, 121.7, 121.4, 121.3, 121.2, 115.6, 115.1, 111.9, 110.7, 35.7; HRMS (ESI-TOF) (*m/z*) calculated $C_{23}H_{16}BrN_2O_3^+$: 447.0344, found 447.0323 $[M + H]^+$.

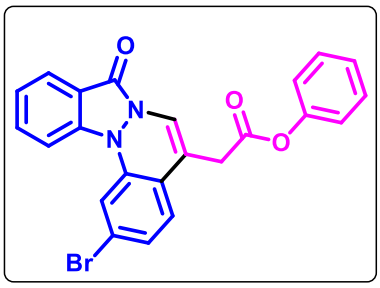

Phenyl 2-(2-chloro-3-methyl-8-oxo-8*H*-indazolo[1,2-*a*]cinnolin-5-yl)acetate (34ia). Yellow

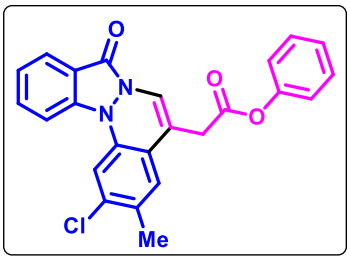

solid, 58 mg (72%); mp 144-145 °C; ^{1}H NMR (400 MHz, $CDCl_3$) δ 8.13 (dt, J = 7.9, 1.0 Hz, 1H), 7.88 (d, J = 8.6 Hz, 1H), 7.81 – 7.77 (m, 1H), 7.71 (s, 1H), 7.62 (s, 1H), 7.42 – 7.35 (m, 3H), 7.28 – 7.25 (m, 2H), 7.10 – 7.08 (m, 2H), 3.78 (d, J = 1.1 Hz, 2H), 2.41 (s, 3H); ^{13}C NMR (100 MHz, $CDCl_3$) δ 168.7, 153.8, 150.5, 137.2, 135.0, 134.7, 132.8, 131.5, 129.5, 126.2, 126.1, 124.7, 122.2, 121.4, 121.2, 120.9, 115.3, 112.7, 111.7, 110.5, 35.8, 19.6; HRMS (ESI-TOF) (*m/z*) calculated $C_{24}H_{18}ClN_2O_3^+$: 417.1005, found 417.0998 $[M + H]^+$.

Phenyl 2-(10-methyl-8-oxo-8*H*-indazolo[1,2-*a*]cinnolin-5-yl)acetate (34ja). Yellow solid, 68

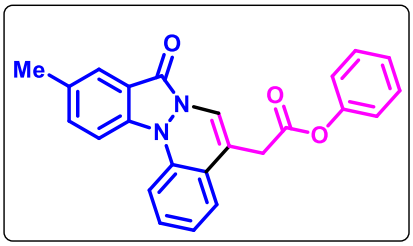

mg (80%); mp 140-141 °C; ^{1}H NMR (400 MHz, $CDCl_3$) δ 7.90 (t, J = 1.2 Hz, 1H), 7.81 (d, J = 8.7 Hz, 1H), 7.69 (dd, J = 8.2, 1.0 Hz, 1H), 7.62 (s, 1H), 7.56 (dd, J = 8.8, 1.8 Hz, 1H), 7.41 – 7.36 (m, 4H), 7.26 – 7.22 (m, 1H), 7.16 (td, J = 7.6, 1.0 Hz, 1H), 7.09 – 7.07 (m, 2H), 3.79 (s, 2H), 2.52 (s, 3H); ^{13}C NMR (100 MHz, $CDCl_3$) δ 168.9, 153.5, 150.5, 136.5, 135.6, 134.1, 131.8, 129.6, 129.5, 126.1, 124.0, 123.8, 122.0, 121.3, 121.3, 115.4, 111.8, 111.7, 111.2, 35.9, 21.1; HRMS (ESI-TOF) (*m/z*) calculated $C_{24}H_{19}N_2O_3^+$: 383.1395, found 383.1405 $[M + H]^+$.

Phenyl 2-(10-methoxy-8-oxo-8*H*-indazolo[1,2-*a*]cinnolin-5-yl)acetate (34ka). Yellow solid, 68

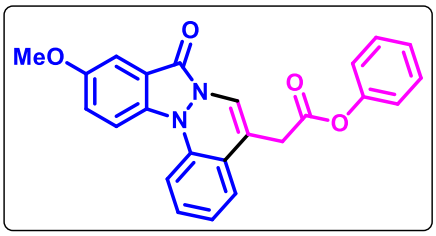

mg (82%); mp 156-157 °C; ^{1}H NMR (400 MHz, $CDCl_3$) δ 7.85 (d, J = 9.2 Hz, 1H), 7.66 (d, J = 8.2 Hz, 1H), 7.64 (s, 1H), 7.49 (d, J = 2.6 Hz, 1H), 7.43 – 7.36 (m, 5H), 7.24 (t, J = 7.4 Hz, 1H), 7.16 (t, J = 7.6 Hz, 1H), 7.09 – 7.07 (m, 2H), 3.92 (s, 3H), 3.81 (s, 2H); ^{13}C NMR (100 MHz, $CDCl_3$) δ 168.9, 155.2, 150.5, 136.4, 132.4, 129.7, 129.5, 126.1, 124.1, 123.7, 123.7, 121.7, 121.3, 121.1, 115.8, 113.4, 111.6, 111.6, 103.9, 55.9, 35.9; HRMS (ESI-TOF) (*m/z*) calculated $C_{24}H_{19}N_2O_4^+$: 399.1344, found 399.1321 $[M + H]^+$.

Phenyl 2-(10-chloro-8-oxo-8*H*-indazolo[1,2-*a*]cinnolin-5-yl)acetate (34la). Yellow solid, 61 mg (74%); mp 186-187 °C; ^{1}H NMR (400 MHz, $CDCl_3$) δ 8.07 (d, J = 2.1 Hz, 1H), 7.86 (d, J = 9.0 Hz, 1H), 7.69 – 7.65 (m, 2H), 7.62 (s, 1H), 7.44 – 7.36 (m, 4H), 7.26 – 7.19 (m, 2H), 7.09 – 7.07 (m, 2H), 3.80 (d, J = 1.0 Hz, 2H); ^{13}C NMR (100 MHz, $CDCl_3$) δ 168.8, 152.5, 150.5, 135.9, 135.3, 132.8, 129.8, 129.5, 127.4, 126.2, 124.5, 124.2, 124.0, 122.0, 121.3, 121.1, 116.3, 113.1, 112.0, 111.6, 35.8; HRMS (ESI-TOF) (*m/z*) calculated $C_{23}H_{16}ClN_2O_3^+$: 403.0849, found 403.0870 $[M + H]^+$.

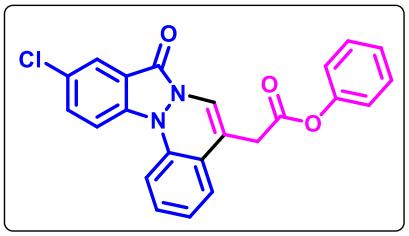

Phenyl 2-(10-bromo-8-oxo-8*H*-indazolo[1,2-*a*]cinnolin-5-yl)acetate (34ma). Yellow solid, 58 mg (75%); mp 160-161 °C; ^{1}H NMR (400 MHz, $CDCl_3$) δ 8.25 (t, J = 1.3 Hz, 1H), 7.82 (d, J = 1.8 Hz, 2H), 7.67 (d, J = 8.1 Hz, 1H), 7.63 (s, 1H), 7.45 – 7.37 (m, 4H), 7.27 – 7.20 (m, 2H), 7.08 (dd, J = 7.7, 1.6 Hz, 2H), 3.81 (s, 2H); ^{13}C NMR (100 MHz, $CDCl_3$) δ 168.7, 152.4, 150.5, 135.8, 135.5, 135.4, 129.8, 129.5, 127.2, 126.1, 124.5, 124.3, 122.0, 121.3, 121.1, 116.7, 114.5, 113.3, 112.1, 111.7, 35.8; HRMS (ESI-TOF) (*m/z*) calculated $C_{23}H_{16}BrN_2O_3^+$: 447.0344, found 447.0302 $[M + H]^+$.

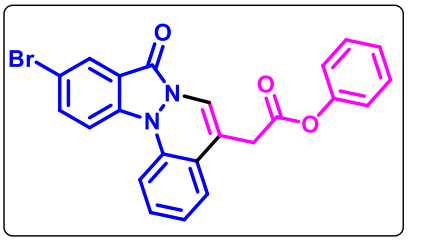

Phenyl 2-(10-nitro-8-oxo-8*H*-indazolo[1,2-*a*]cinnolin-5-yl)acetate (34na). Yellow solid, 32 mg (39%); mp 200–201 °C; ^{1}H NMR (400 MHz, DMSO-d_6) δ 8.76 (s, 1H), 8.52 (d, J = 9.4 Hz, 1H), 8.42 (d, J = 9.6 Hz, 1H), 8.02 (d, J = 8.2 Hz, 1H), 7.84 (s, 1H), 7.54 – 7.53 (m, 2H), 7.43 (t, J = 7.5 Hz, 2H), 7.36 (t, J = 7.4 Hz, 1H), 7.27 (t, J = 7.3 Hz, 1H), 7.15 (d, J = 8.0 Hz, 2H), 4.10 (s, 2H); ^{13}C NMR (100 MHz, DMSO-d_6) δ 169.9, 152.8, 150.9, 141.6, 138.1, 134.6, 130.5, 130.1, 127.4, 126.5, 126.1, 125.2, 122.4, 122.1, 121.3, 121.1, 114.2, 114.1, 113.8, 112.2, 34.4; HRMS (ESI-TOF) (*m/z*) calculated $C_{23}H_{16}N_3O_5^+$: 414.1089, found 414.1065 $[M + H]^+$.

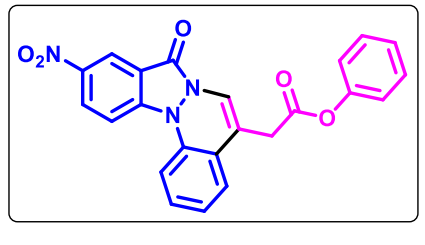

Phenyl 2-(8-oxo-8*H*-pyrido[3',2':4,5]pyrazolo[1,2-*a*]cinnolin-5-yl)acetate (34oa). Yellow solid, 53 mg (60%); mp 181-182 °C; ^{1}H NMR (400 MHz, $CDCl_3$) δ 9.15 (dd, J = 8.3, 1.1 Hz, 1H), 8.81 (d, J = 4.6 Hz, 1H), 8.46 (d, J = 7.8 Hz, 1H), 7.68 (s, 1H), 7.46 (td, J = 8.4, 8.0, 1.4 Hz, 1H), 7.41 – 7.37 (m, 3H), 7.32 – 7.30 (m, 1H), 7.27 – 7.20 (m, 2H), 7.08 (d, J = 7.7 Hz, 2H), 3.82 (s, 2H); ^{13}C NMR (100 MHz,

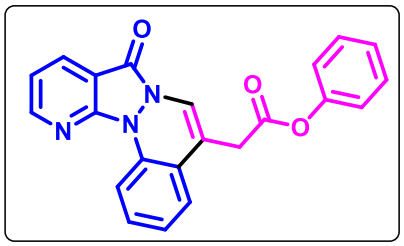

$CDCl_3$) δ 168.8, 152.9, 150.5, 148.1, 135.2, 133.5, 130.1, 129.5, 126.1, 124.4, 123.6, 121.3, 120.2, 119.7, 117.4, 115.3, 111.6, 36.1; HRMS (ESI-TOF) (*m/z*) calculated $C_{22}H_{16}N_3O_3^+$: 370.1191, found 370.1180 $[M + H]^+$.

Naphthalen-2-yl 2-(8-oxo-8*H*-indazolo[1,2-*a*]cinnolin-5-yl)acetate (34ab). Yellow solid, 60 mg

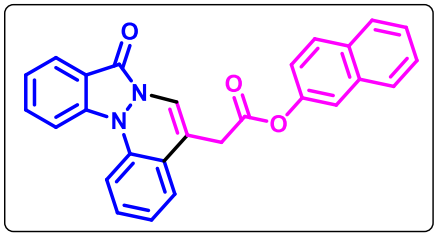

(60%); mp 140-141 °C; ^{1}H NMR (400 MHz, $CDCl_3$) δ 8.15 (d, *J* = 7.9 Hz, 1H), 7.94 (d, *J* = 8.4 Hz, 1H), 7.85 (d, *J* = 9.0 Hz, 2H), 7.87 – 7.74 (m, 3H), 7.68 (s, 1H), 7.57 (d, *J* = 2.2 Hz, 1H), 7.52 – 7.49 (m, 3H), 7.42 (t, *J* = 8.2 Hz, 1H), 7.36 (t, *J* = 7.4 Hz, 1H), 7.24 – 7.22 (m, 2H), 3.87 (s, 2H); ^{13}C NMR (100 MHz, $CDCl_3$) δ 169.0, 148.2, 137.2, 136.3, 133.7, 132.6, 131.5, 129.6, 129.5, 127.8, 127.7, 126.7, 125.8, 124.7, 124.2, 124.1, 122.2, 121.9, 121.4, 120.7, 118.4, 115.2, 112.1, 111.9, 111.3, 100.0, 36.0; HRMS (ESI-TOF) (*m/z*) calculated $C_{27}H_{19}N_2O_3^+$: 419.1395, found 419.1369 $[M + H]^+$.

Benzyl 2-(8-oxo-8*H*-indazolo[1,2-*a*]cinnolin-5-yl)acetate (34ac). Yellow solid, 64 mg (70%);

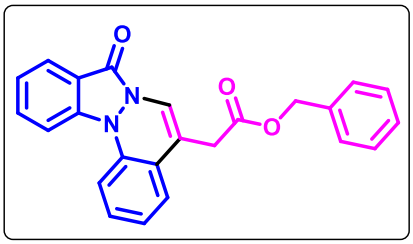

mp 126-127 °C; ^{1}H NMR (400 MHz, $CDCl_3$) δ 8.13 (d, *J* = 8.0 Hz, 1H), 7.92 (d, *J* = 8.6 Hz, 1H), 7.76 – 7.71 (m, 2H), 7.54 (s, 1H), 7.39 – 7.31 (m, 7H), 7.28 – 7.24 (m, 1H), 7.09 (t, *J* = 7.6 Hz, 1H), 5.20 (s, 2H), 3.60 (s, 2H); ^{13}C NMR (100 MHz, $CDCl_3$) δ 170.1, 153.7, 136.2, 135.5, 132.4, 129.4, 128.6, 128.4, 128.3, 124.6, 124.2, 124.0, 122.2, 121.8, 121.1, 115.3, 111.9, 111.8, 111.5, 67.1, 35.7; HRMS (ESI-TOF) (*m/z*) calculated $C_{24}H_{19}N_2O_3^+$: 383.1395, found 383.1364 $[M + H]^+$.

Phenyl (*Z*)-2-(8-oxo-8*H*-indazolo[1,2-*a*]cinnolin-5(6*H*)-ylidene)acetate (35aa). Yellow solid,

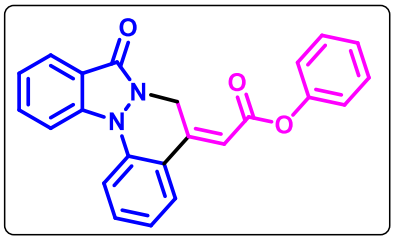

69 mg (78%); mp 139-140 °C; ^{1}H NMR (400 MHz, $CDCl_3$) δ 8.02 (d, *J* = 7.7 Hz, 1H), 7.86 – 7.77 (m, 3H), 7.69 (t, *J* = 7.8 Hz, 1H), 7.57 (t, *J* = 7.7 Hz, 1H), 7.45 (t, *J* = 7.7 Hz, 2H), 7.33 (t *J* = 7.4 Hz, 2H), 7.24 – 7.22 (m, 3H), 6.72 (s, 1H), 5.58 (s, 2H); ^{13}C NMR (100 MHz, CDCl3) δ 164.1, 150.5, 145.1, 142.3, 138.4, 132.6, 132.0, 129.5, 126.6, 126.0, 124.7, 123.6, 123.1, 121.6, 121.4, 118.8, 114.3, 112.7, 112.5, 42.7; HRMS (ESI-TOF) (*m/z*) calculated $C_{23}H_{16}N_2NaO_3^+$: 391.1058, found 391.1066 $[M + Na]^+$.

Phenyl (*Z*)-2-(3-methyl-8-oxo-8*H*-indazolo[1,2-*a*]cinnolin-5(6*H*)-ylidene)acetate (35ba).

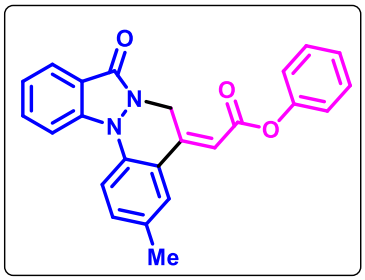

Yellow solid, 67 mg (78%); mp 150–151 °C; ^{1}H NMR (400 MHz, DMSO-d_6) δ 8.14 (d, J = 8.5 Hz, 1H), 7.95 – 7.91 (m, 2H), 7.87 (d, J = 7.7 Hz, 1H), 7.76 (t, J = 7.9 Hz, 1H), 7.54 – 7.42 (m, 3H), 7.37 – 7.30 (m, 2H), 7.25 (d, J = 7.8 Hz, 2H), 6.93 (s, 1H), 5.46 (s, 2H), 2.37 (s, 3H); ^{13}C NMR (100 MHz, DMSO-d_6) δ 164.7, 159.6, 150.7, 145.7, 142.4, 136.0, 133.8, 133.5, 133.4, 130.1, 127.4, 126.4, 124.1, 123.5, 122.3, 120.4, 117.9, 115.1, 113.9, 111.6, 41.9, 20.6; HRMS (ESI-TOF) (*m/z*) calculated $C_{24}H_{18}N_2KO_3^+$: 421.0954, found 421.0963 $[M + K]^+$.

Phenyl (*Z*)-2-(3-methoxy-8-oxo-8*H*-indazolo[1,2-*a*]cinnolin-5(6*H*)-ylidene)acetate (35ca).

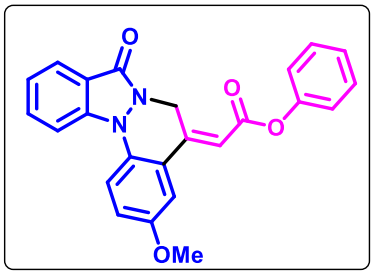

Yellow solid, 67 mg (80%); mp 159-160 °C; ^{1}H NMR (400 MHz, DMSO-d_6) δ 8.08 (d, J = 8.5 Hz, 1H), 7.95 (d, J = 9.1 Hz, 1H), 7.84 (d, J = 7.5 Hz, 1H), 7.73 (t, J = 8.1 Hz, 1H), 7.56 (d, J = 2.8 Hz, 1H), 7.50 – 7.44 (m, 2H), 7.28 – 7.35 (m, 2H), 7.25 – 7.19 (m, 3H), 7.02 (t, J = 1.7 Hz, 1H), 5.44 (s, 2H), 3.86 (s, 3H); ^{13}C NMR (100 MHz, DMSO-d_6) δ 164.8, 159.5, 155.8, 150.7, 145.4, 142.6, 133.5, 132.4, 130.1, 126.5, 124.1, 123.4, 122.3, 121.9, 120.4, 117.8, 116.7, 113.6, 112.6, 110.6, 56.3, 41.8; HRMS (ESI-TOF) (*m/z*) calculated $C_{24}H_{18}N_2NaO_4^+$: 421.1164, found 421.1152 $[M + Na]^+$.

Phenyl (*Z*)-2-(3-isopropyl-8-oxo-8*H*-indazolo[1,2-*a*]cinnolin-5(6*H*)-ylidene)acetate (35da).

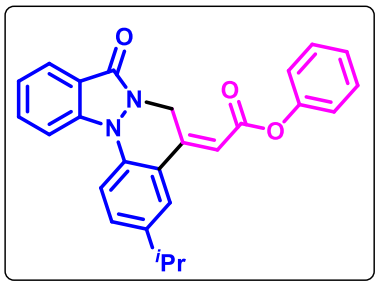

Yellow solid, 67 mg (82%); mp 144-145 °C; ^{1}H NMR (400 MHz, $CDCl_3$) δ 8.01 (d, J = 7.7 Hz, 1H), 7.80 (d, J = 8.5 Hz, 1H), 7.73 (d, J = 8.6 Hz, 1H), 7.68 (d, J = 8.0 Hz, 1H), 7.65 (d, J = 1.4 Hz, 1H), 7.48 – 7.42 (m, 3H), 7.32 – 7.26 (m, 2H, overlapped with residual peak of $CDCl_3$), 7.23 (d, J = 7.7 Hz,, 2H), 6.72 (t, J = 1.8 Hz, 1H), 5.57 (d, J = 1.8 Hz, 2H), 3.00 (hept, J = 6.9 Hz, 1H), 1.34 (d, J = 6.9 Hz, 6H); ^{13}C NMR (100 MHz, $CDCl_3$) δ 164.2, 160.0, 150.5, 145.4, 144.3, 142.4, 136.4, 132.5, 130.4, 129.5, 125.9, 124.6, 124.2, 122.9, 121.6, 121.2, 118.5, 114.4, 112.6, 112.2, 42.6, 33.7, 23.9; HRMS (ESI-TOF) (*m/z*) calculated $C_{26}H_{22}NaN_2O_3^+$: 433.1528, found 433.1498 $[M + Na]^+$.

Phenyl (*Z*)-2-(2-chloro-8-oxo-8*H*-indazolo[1,2-*a*]cinnolin-5(6*H*)-ylidene)acetate (35ga).

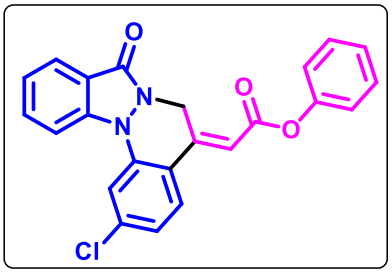

Yellow solid, 50 mg (60%); mp 179-180 °C; ^{1}H NMR (400 MHz, $CDCl_3$) δ 8.03 (d, J = 7.7 Hz, 1H), 7.82 – 7.71 (m, 4H), 7.45 (t, J = 7.8 Hz, 2H), 7.37 (t, J = 7.5 Hz, 1H), 7.32 – 7.29 (m, 1H), 7.23 – 7.17 (m, 3H), 6.69 (t, J = 1.9 Hz, 1H), 5.55 (d, J = 1.9 Hz, 2H); ^{13}C NMR (100 MHz, $CDCl_3$) δ 164.0, 160.3, 150.4, 144.2, 142.3, 139.1, 138.1, 132.9, 129.5, 127.6, 126.0, 124.9, 123.8, 123.7, 121.6, 119.7, 114.1, 112.9, 112.6, 42.8; HRMS (ESI-TOF) (*m/z*) calculated $C_{23}H_{16}ClN_2O_3^+$: 403.0849, found 403.0859 $[M + H]^+$.

Phenyl (*Z*)-2-(2-bromo-8-oxo-8*H*-indazolo[1,2-*a*]cinnolin-5(6*H*)-ylidene)acetate (35ha).

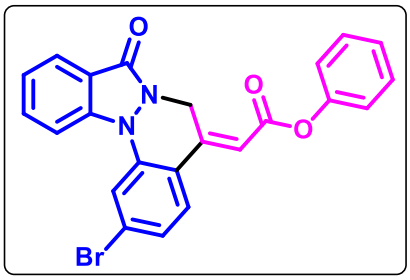

Yellow solid, 53 mg (69%); mp 162-136 °C; ^{1}H NMR (400 MHz, $CDCl_3$) δ 8.03 (d, J = 7.8 Hz, 1H), 7.94 (d, J = 1.8 Hz, 1H), 7.79 (d, J = 8.4 Hz, 1H), 7.76 – 7.72 (m, 1H), 7.69 (d, J = 8.6 Hz, 1H), 7.45 (t, J = 7.7 Hz, 2H), 7.39 – 7.35 (m, 2H), 7.33 – 7.29 (m, 1H), 7.21 (d, J = 8.0 Hz, 2H), 6.71 (d, J = 2.1 Hz, 1H), 5.55 (d, J = 1.8 Hz, 2H); ^{13}C NMR (100 MHz, DMSO-d_6) δ 164.0, 160.3, 150.4, 144.3, 142.3, 139.2, 132.9, 129.5, 127.7, 126.7, 126.2, 126.0, 124.9, 123.7, 121.6, 120.2, 119.1, 117.1, 112.9, 112.7, 42.8; HRMS (ESI-TOF) (*m/z*) calculated $C_{23}H_{16}BrN_2O_3^+$: 447.0344, found 447.0312 $[M + H]^+$.

Phenyl (*Z*)-2-(2-chloro-3-methyl-8-oxo-8*H*-indazolo[1,2-*a*]cinnolin-5(6*H*)-ylidene)acetate (35ia). Yellow solid, 57 mg (70%); mp 180-181 °C; ^{1}H NMR (400 MHz, $CDCl_3$) δ 8.02 (d, J = 7.7 Hz, 1H), 7.79 – 7.76 (m, 2H), 7.72 (t, J = 8.1 Hz, 1H), 7.68 (s, 1H), 7.45 (t, J = 7.9 Hz, 2H), 7.35 (t, J = 7.4 Hz, 1H), 7.31 – 7.26 (m, 1H, overlapped with residual $CDCl_3$), 7.22 (d, J = 8.6 Hz, 2H), 6.69 (t, J = 1.7 Hz, 1H), 5.54 (d, J = 1.8 Hz, 2H), 2.45 (s, 3H); ^{13}C NMR (100 MHz, $CDCl_3$) δ 164.0, 160.2, 150.5, 144.5, 142.4, 138.2, 137.2, 132.8, 131.4, 129.5, 128.2, 126.0, 124.8, 123.4, 121.6, 119.8, 119.0, 114.5, 112.8, 112.3, 42.9, 19.6; HRMS (ESI-TOF) (*m/z*) calculated $C_{24}H_{17}ClNaN_2O_3^+$: 439.0825, found 439.0830 $[M + Na]^+$.

Phenyl (*Z*)-2-(10-methyl-8-oxo-8*H*-indazolo[1,2-*a*]cinnolin-5(6*H*)-ylidene)acetate (35ja).

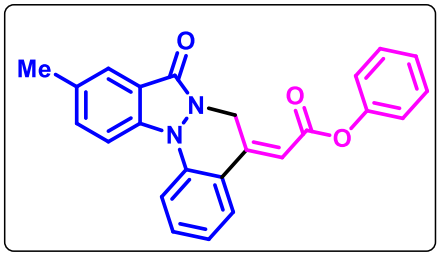

Yellow solid, 64 mg (75%); mp 149-150 °C; ^{1}H NMR (400 MHz, $CDCl_3$) δ 7.84 – 7.73 (m, 3H), 7.70 (d, J = 8.4 Hz, 1H), 7.57 – 7.41 (m, 4H), 7.32 – 7.25 (m, 1H, overlapped with residual $CDCl_3$), 7.23 – 7.16 (m, 3H), 6.70 (s, 1H), 5.55 (s, 2H), 2.48 (s, 3H); ^{13}C NMR (100 MHz, $CDCl_3$) δ 164.1, 160.1, 150.5, 145.3, 140.8, 138.7, 133.8, 133.1, 132.0, 129.4, 126.5, 125.9, 124.2, 123.3, 121.6, 121.1, 119.0, 114.1, 112.7, 112.1, 42.7, 20.9; HRMS (ESI-TOF) (*m/z*) calculated $C_{24}H_{16}KN_2O_2^+$: 403.0848, found 403.0854 $[M + K+ (-H_2O)]^+$.

Phenyl (*Z*)-2-(10-methoxy-8-oxo-8*H*-indazolo[1,2-*a*]cinnolin-5(6*H*)-ylidene)acetate (35ka).

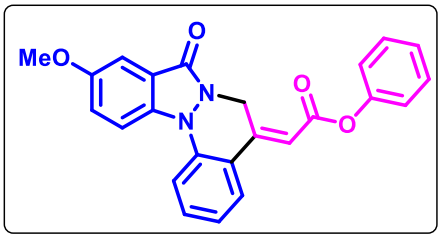

Yellow solid, 60 mg (72%); mp 149-150 °C; ^{1}H NMR (400 MHz, DMSO-d_6) δ 8.11 (d, J = 8.6 Hz, 2H), 7.95 (d, J = 8.5 Hz, 1H), 7.61 (t, J = 7.8 Hz, 1H), 7.48 (t, J = 7.7 Hz, 2H), 7.39 – 7.29 (m, 3H), 7.28 – 7.21 (m, 3H), 6.94 (s, 1H), 5.47 (s, 2H), 3.86 (s, 3H); ^{13}C NMR (100 MHz, DMSO-d_6) δ 164.7, 159.5, 156.3, 150.7, 145.8, 138.8, 137.6, 133.1, 130.0, 127.3, 126.4, 123.8, 122.6, 122.3, 120.2, 119.3, 115.7, 114.8, 111.5, 105.3, 56.3, 42.1; HRMS (ESI-TOF) (*m/z*) calculated $C_{24}H_{19}N_2O_4^+$: 399.1344, found 399.1305 $[M + H]^+$.

Phenyl (*Z*)-2-(10-chloro-8-oxo-8*H*-indazolo[1,2-*a*]cinnolin-5(6*H*)-ylidene)acetate (35la).

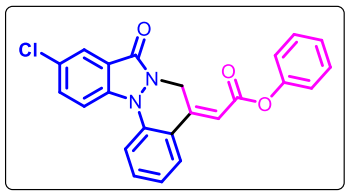

Yellow solid, 58 mg (70%); mp 177-178 °C; ^{1}H NMR (400 MHz, $CDCl_3$) δ 7.96 (d, J = 2.2 Hz, 1H), 7.82 (dd, J = 8.1, 1.5 Hz, 1H), 7.76 (d, J = 8.9 Hz, 1H), 7.71 (d, J = 8.5 Hz, 1H), 7.62 (dd, J = 8.9, 2.2 Hz, 1H), 7.57 (t, J = 7.3 Hz, 2H), 7.47 – 7.43 (m, 2H), 7.31 – 7.26 (m, 1H), 7.24 7.21 (m, 2H), 6.72 (t, J = 1.8 Hz, 1H), 5.57 (d, J = 1.8 Hz, 2H); ^{13}C NMR (100 MHz, $CDCl_3$) δ 164.0, 158.7, 150.4, 144.5, 140.4, 137.8, 132.8, 132.1, 129.5, 128.8, 126.7, 126.0, 124.2, 124.0, 121.6, 121.5, 120.0, 114.3, 113.8, 112.9, 42.6; HRMS (ESI-TOF) (*m/z*) calculated $C_{23}H_{16}ClN_2O_3^+$: 403.0849, found 403.0883 $[M + H]^+$.

Phenyl (*Z*)-2-(2,3-dimethyl-8-oxo-8*H*-indazolo[1,2-*a*]cinnolin-5(6*H*)-ylidene)acetate (35pa).

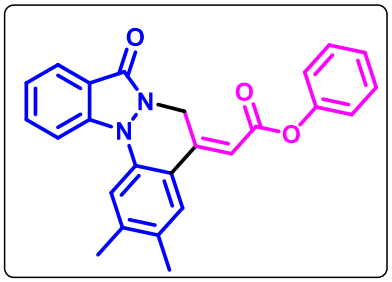

Yellow solid, 67 mg (80%); mp 185-186 °C; ^{1}H NMR (400 MHz, $CDCl_3$) δ 8.01 (d, J = 7.8 Hz, 1H), 7.82 (d, J = 8.4 Hz, 1H), 7.68 (t, J = 7.8 Hz, 1H), 7.57 (d, J = 2.1 Hz, 2H), 7.45 (t, J = 7.9 Hz, 2H), 7.32 – 7.28 (m, 2H), 7.22 (d, J = 7.6 Hz, 2H), 6.67 (t, J = 1.8 Hz, 1H), 5.55 (d, J = 1.8 Hz, 2H), 2.42 (s, 3H), 2.34 (s, 3H); ^{13}C NMR (100 MHz, $CDCl_3$) δ 164.3, 160.1, 150.6, 145.4, 142.4, 141.8, 136.6, 132.4, 132.3, 129.4, 127.1, 125.9, 124.6, 122.8, 121.7, 118.8, 118.6, 115.1, 112.8, 111.0, 42.8, 20.6, 19.3; HRMS (ESI-TOF) (*m/z*) calculated $C_{25}H_{21}N_2O_3^+$: 397.1552, found 397.1579 $[M + H]^+$.

Naphthalen-2-yl (*Z*)-2-(8-oxo-8*H*-indazolo[1,2-*a*]cinnolin-5(6*H*)-ylidene)acetate (35ab).

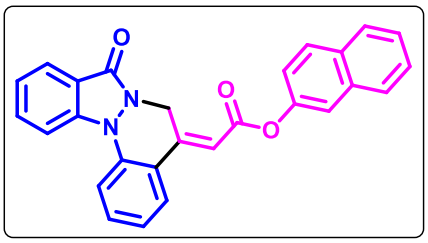

Yellow solid, 58 mg (58%); mp 120-121 °C; ^{1}H NMR (400 MHz, DMSO-d_6) δ 8.17 (t, J = 8.4 Hz, 2H), 8.09 – 7.93 (m, 4H), 7.89 (d, J = 7.2 Hz, 1H), 7.84 – 7.74 (m, 2H), 7.69 – 7.62 (m, 1H), 7.59 – 7.51 (m, 2H), 7.44 (d, J = 8.2 Hz, 1H), 7.39 – 7.34 (m, 1H), 7.31 – 7.23 (m, 1H), 7.02 (s, 1H), 5.52 (s, 2H); ^{13}C NMR (100 MHz, DMSO-d_6) δ 164.9, 159.7, 148.4, 145.8, 142.3, 138.1, 133.8, 133.6, 133.2, 131.5, 129.9, 128.2, 128.0, 127.4, 127.2, 126.4, 124.2, 124.1, 123.7, 122.1, 120.6, 119.1, 118.1, 115.2, 114.0, 111.8, 42.0; HRMS (ESI-TOF) (*m/z*) calculated $C_{27}H_{19}N_2O_3^+$: 419.1395, found 419.1366 $[M + H]^+$.

Phenyl (*Z*)-2-(8-oxo-6-propyl-8*H*-indazolo[1,2-*a*]cinnolin-5(6*H*)-ylidene)acetate (35ad).

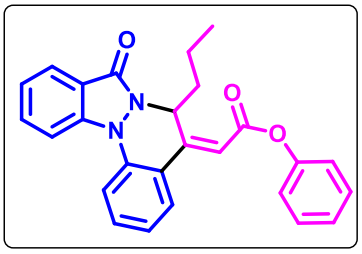

Yellow solid, 66 mg, 68% (Method A); mp 149-150 °C; ^{1}H NMR (400 MHz, $CDCl_3$) δ 8.03 (d, J = 7.7 Hz, 1H), 7.88 (d, J = 8.5 Hz, 1H), 7.84 – 7.75 (m, 2H), 7.67 (t, J = 7.7 Hz, 1H), 7.61 (t, J = 7.6 Hz, 1H), 7.45 (t, J = 7.9 Hz, 2H), 7.35 – 7.29 (m, 1H), 7.27 – 7.17 (m, 3H), 6.99 – 6.93 (m, 1H), 6.59 (s, 1H), 1.83 – 1.67 (m, 2H), 1.54 – 1.43 (m, 1H), 1.39 – 1.28 (m, 1H), 0.89 (t, J = 7.3 Hz, 3H); ^{13}C NMR (100 MHz, $CDCl_3$) 164.0, 159.3, 150.5, 149.2, 141.9, 137.2, 132.6, 131.9, 129.5, 127.3, 125.9, 124.7, 123.3, 123.0, 121.7, 120.3, 117.9, 115.0, 111.8, 111.1, 49.9, 35.8, 19.1, 13.6; HRMS (ESI-TOF) (*m/z*) calculated $C_{26}H_{22}NaN_2O_3^+$: 433.1528, found 433.1500 $[M + Na]^+$.

Phenyl (*Z*)-2-(8-oxo-6-phenyl-8*H*-indazolo[1,2-*a*]cinnolin-5(6*H*)-ylidene)acetate (35ae).

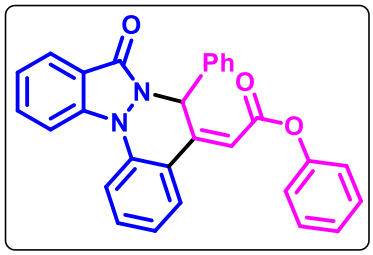

Yellow solid, 64 mg, 60% (Method A); mp 172-173 °C; ^{1}H NMR (400 MHz, $CDCl_3$) δ 8.19 (s, 1H), 8.06 (dd, *J* = 7.8, 1.2 Hz, 1H), 7.83 (t, *J* = 9.1 Hz, 2H), 7.74 (d, *J* = 8.4 Hz, 1H), 7.66 (t, *J* = 7.4 Hz, 1H), 7.56 (t, *J* = 7.8 Hz, 1H), 7.42 (t, *J* = 7.9 Hz, 2H), 7.32 (t, *J* = 7.5 Hz, 1H), 7.28 – 7.25 (m, 3H), 7.24 – 7.22 (m, 2H), 7.21 – 7.18 (m, 4H), 6.79 (s, 1H); ^{13}C NMR (100 MHz, $CDCl_3$) 163.8, 159.4, 150.4, 146.8, 141.7, 137.0, 136.7, 132.9, 132.0, 129.4, 128.7, 128.1, 127.3, 126.7, 125.9, 124.8, 123.4, 123.0, 121.7, 121.0, 117.6, 115.0, 113.4, 111.7, 52.2; HRMS (ESI-TOF) (*m/z*) calculated $C_{29}H_{21}N_2O_3^+$: 445.1552, found 445.1525 $[M + H]^+$.

Ethyl (*Z*)-2-(8-oxo-6-phenyl-8*H*-indazolo[1,2-*a*]cinnolin-5(6*H*)-ylidene)acetate (35af).

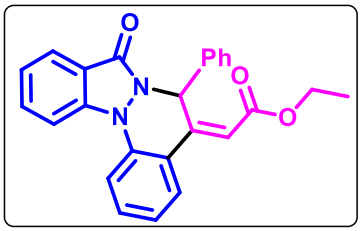

Yellow solid, 52 mg, 55% (Method A); mp 236-237 °C; ^{1}H NMR (400 MHz, $CDCl_3$) δ 8.07 (s, 1H), 7.95 (d, *J* = 7.8 Hz, 1H), 7.71 (d, *J* = 8.5 Hz, 1H), 7.62 –7.51 (m, 3H), 7.41 (t, *J* = 7.8 Hz, 1H), 7.20 (t, *J* = 7.2 Hz, 1H), 7.16 – 7.07 (m, 5H), 7.05 (t, *J* = 7.6 Hz, 1H), 6.46 (s, 1H), 4.21 (q, *J* = 7.1 Hz, 2H), 1.25 (t, *J* = 7.1 Hz, 3H); ^{13}C NMR (100 MHz, $CDCl_3$) 165.5, 159.3, 144.5, 141.6, 137.0, 136.7, 132.7, 131.5, 128.6, 127.9, 127.2, 126.6, 124.7, 123.3, 122.8, 121.3, 117.6, 115.0, 114.7, 111.5, 60.8, 52.0, 14.3; HRMS (ESI-TOF) (*m/z*) calculated $C_{25}H_{21}N_2O_3^+$: 397.1552, found 397.1513 $[M + H]^+$.

2C.4 Single Crystal X-Ray Diffraction Studies

In each case, a suitable crystal was chosen with the help of a light microscope for mounting in a nylon loop to attach to a goniometer head. A Kappa APEX II diffractometer equipped with a CCD detector (with the crystal-to-detector distance fixed at 60 mm) and sealed-tube monochromated MoKα radiation was used for centering, initial crystal evaluation and data collection by the program APEX2.[36] All data were integrated, and reflections were fitted and values of F^2 and $\sigma(F^2)$ for each reflection were obtained by using the program SAINT.[36] Finally, data were also corrected for the Lorentz and polarization effects. Using the subroutine XPREP[36] the space group was determined, and an absorption correction (SADABS)[36] and merging of data were performed to generate the necessary files for solution and refinement. A structure solution was obtained by direct methods using the SHELXS program of the SHELXTL package and was refined using SHELXL.[37] All non-hydrogen atoms were refined with anisotropic displacement parameters. All hydrogen

atoms were placed in ideal positions and refined as riding atoms with individual isotropic displacement parameters. All figures were drawn using MERCURY V 3.0.[38]

2C.4.1 Crystal data for 35ad (CCDC No. 2117498). $C_{26}H_{22}N_2O_3$, Mr = 410.45 g/mol,

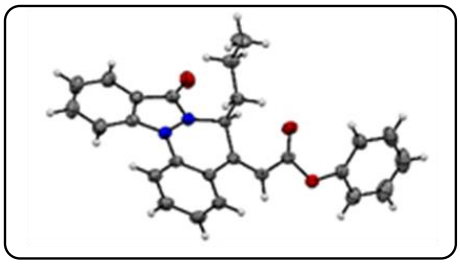

monoclinic, space group $P2_1/n$, a = 8.3687(4) Å, b = 17.1002(8) Å, c = 14.8475(8) Å, α = 90°, β = 98.068(3)°, γ = 90°, V = 2103.74(18) Å^3, Z = 4, T = 296(2) K, D_{calcd} = 1.296 g/cm^3; Full matrix least-square on F^2; R_1 = 0.044, wR_2 = 0.1177 for 2848 observed reflections [I > 2σ(I)] and R_1 = 0.0597, wR_2 = 0.1297 for all 3716 reflections; number of parameters = 281; GOF = 1.043.

2C.4.2 Crystal data for 35ae (CCDC No. 2117499). $C_{29}H_{20}N_2O_3$, Mr = 444.47 g/mol,

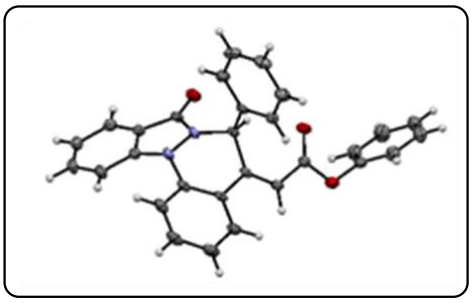

monoclinic, space group $P2_1/c$, a = 14.5420(16) Å, b = 8.2962(8) Å, c = 18.9348(17) Å, α = 90°, β = 105.545(6)°, γ = 90°, V = 2200.8(4) Å^3, Z = 4, T = 296(2) K, D_{calcd} = 1.341 g/cm^3; Full matrix least-square on F^2; R_1 = 0.0989, wR_2 = 0.2549 for 2768 observed reflections [I > 2σ(I)] and R_1 = 0.1176, wR_2 = 0.2767 for all 3862 reflections; number of parameters = 307; GOF = 1.011.

2C.5 References

1. Koschker, P.; Breit, B. *Accounts of Chemical Research* **2016**, *49*, 1524-1536.
2. Santhoshkumar, R.; Cheng, C. H. *Asian Journal of Organic Chemistry* **2018**, *7*, 1151-1163.
3. Nakanowatari, S.; Ackermann, L. *Chemistry–A European Journal* **2015**, *21*, 16246-16251.
4. Logeswaran, R.; Jeganmohan, M. *Advanced Synthesis & Catalysis* **2022**, *364*, 2113-2139.
5. Hu, Y.; Wang, C.; *Chem* **2019**, *11*, 1167-1174.
6. Shi, X.; Xu, W.; Wang, R.; Zeng, X.; Qiu, H.; Wang, M. *The Journal of Organic Chemistry* **2020**, *85*, 3911-3920.
7. Dutta, S.; Bhattacharya, T.; Werz, D. B.; Maiti, D. *Chem* **2021**, *7*, 555-605.
8. Nakanowatari, S.; Mei, R.; Feldt, M.; Ackermann, L. *Acs Catalysis* **2017**, *7*, 2511-2515.
9. Zhang, Y. J.; Skucas, E.; Krische, M. J. *Organic Letters* **2009**, *11*, 4248-4250.
10. Shukla, R. K.; Nair, A. M.; Volla, C. M. *Synlett* **2021**, *32*, 1169-1178.
11. Wang, H.; Beiring, B.; Yu, D. G.; Collins, K. D.; Glorius, F. *Angewandte Chemie International Edition* **2013**, *52*, 12430-12434.

12. Dong, Z.; Ren, Z.; Thompson, S. J.; Xu, Y.; Dong, G. *Chemical Reviews* **2017**, *117*, 9333-9403.

13. Casanova, N.; Seoane, A.; Mascareñas, J. L.; Gulías, M.; *Angewandte Chemie International Edition* **2015**, *127*, 2404-2407.

14. Tran, D. N.; Cramer, N. *Angewandte Chemie International Edition* **2010**, *122*, 8357-8360.

15. Tran, D. N.; Cramer, N. *Angewandte Chemie International Edition* **2013**, *125*, 10824-10828.

16. Han, X.-L.; Lin, P.-P.; Li, Q. *Chinese Chemical Letters* **2019**, *30*, 1495-1502.

17. Cendón, B.; Casanova, N.; Comanescu, C.; García-Fandiño, R.; Seoane, A.; Gulías, M.; Mascareñas, J. L. *Organic Letters* **2017**, *19*, 1674-1677.

18. Wang, H.; Glorius, F. *Angewandte Chemie International Edition* **2012**, *51*, 7318-7322.

19. Wu, S.; Zeng, R.; Fu, C.; Yu, Y.; Zhang, X.; Ma, S. *Chemical Science* **2015**, *6*, 2275-2285.

20. Rodriguez, A.; Albert, J.; Ariza, X.; Garcia, J.; Granell, J.; Farras, J.; La Mela, A.; Nicolas, E. *The Journal of Organic Chemistry* **2014**, *79*, 9578-9585.

21. Xia, X. F.; Wang, Y. Q.; Zhang, L. L.; Song, X. R.; Liu, X. Y.; Liang, Y. M. *Chemistry–A European Journal* **2014**, *20*, 5087-5091.

22. Mo, J.; Müller, T.; Oliveira, J. C.; Ackermann, L. *Angewandte Chemie International Edition* **2018**, *57*, 7719-7723.

23. Boobalan, R.; Kuppusamy, R.; Santhoshkumar, R.; Gandeepan, P.; Cheng, C. H. *Chem* **2017**, *9*, 273-277.

24. Thrimurtulu, N.; Dey, A.; Maiti, D.; Volla, C. M. *Angewandte Chemie International Edition* **2016**, *128*, 12549-12553.

25. Zhou, Z.; Liu, G.; Lu, X. *Organic Letters* **2016**, *18*, 5668-5671.

26. Zhai, S.; Qiu, S.; Chen, X.; Tao, C.; Li, Y.; Cheng, B.; Wang, H.; Zhai, H. *ACS Catalysis* **2018**, *8*, 6645-6649.

27. Kuppusamy, R.; Santhoshkumar, R.; Boobalan, R.; Wu, H.-R.; Cheng, C.-H. *ACS Catalysis* **2018**, *8*, 1880-1883.

28. Boobalan, R.; Santhoshkumar, R.; Cheng, C. H. *Advanced Synthesis & Catalysis* **2019**, *361*, 1140-1145.

29. Yin, C.; Zhong, T.; Zheng, X.; Li, L.; Zhou, J.; Yu, C. *Organic & Biomolecular Chemistry* **2021**, *19*, 7701-7705.

30. Chowdhury, D.; Koner, M.; Ghosh, S.; Baidya, M. *Organic Letters* **2022**, *24*, 3604-3608.

31. Qi, W.; Wu, Y.; Han, Y.; Li, Y. *Catalysts* **2017**, *7*, 320.

32. Li, T.; Zhang, C.; Tan, Y.; Pan, W.; Rao, Y. *Organic Chemistry Frontiers* **2017**, *4*, 204-209.

33. Xia, X.-F.; Zhu, S.-L.; Hu, Q.; Li, Y.; Xu, X. *Tetrahedron* **2017**, *73*, 3529-3535.

34. Wang, Q.; Lou, J.; Huang, Z.; Yu, Z. *The Journal of Organic Chemistry* **2019**, *84*, 2083-2092.

35. Vidal, X.; Mascareñas, J. L.; Gulias, M. *Journal of the American Chemical Society* **2019**, *141*, 1862-1866.

36. Song, Z.; Jia, Y.; Zhang, D.; Wang, D. *European Journal of Organic Chemistry* **2021**, *2021*, 1942-1948.

37. Hossain, M. L.; Ye, F.; Zhang, Y.; Wang, J. *The Journal of Organic Chemistry* **2013**, 78, 1236-1241.

38. *APEX2, SADABS and SAINT*; Bruker AXS inc: Madison, WI, USA, 2008.

39. Sheldrick, G. M. *Acta Crystallographic Section* C: Foundations and Advances., **2015**, 71, 3-8.

40. Macrae, C. F.; Bruno, I. J.; Chisholm, J. A.; Edginton, P. R.; McCabe, P.; Pidocck, E.; RodriguezMonge, L.; Taylor, T.; Van de Streek, J.; Wood, P. A. Jornal of Appllied Crystalography **2008**, 41, 466.

Chapter 3

Palladium-Catalyzed Tandem Transformation of *N*-Arylindazolones to Disubstituted Quinazolinones through Carbene Insertion into N-N Bond

3.1 Introduction

Quinazolinone is a privileged diazaheterocyclic scaffold found in numerous naturally-occurring alkaloids (*e.g.* Aniquinazoline D,[1] Febrifugine,[2] Arborine[3]), and a number of synthetic drug candidates (*e.g.* Quinethazone,[4] Methaqualone,[5] (*E*)-Bogorine) with varied pharmacological implications (Figure 3.1.1).

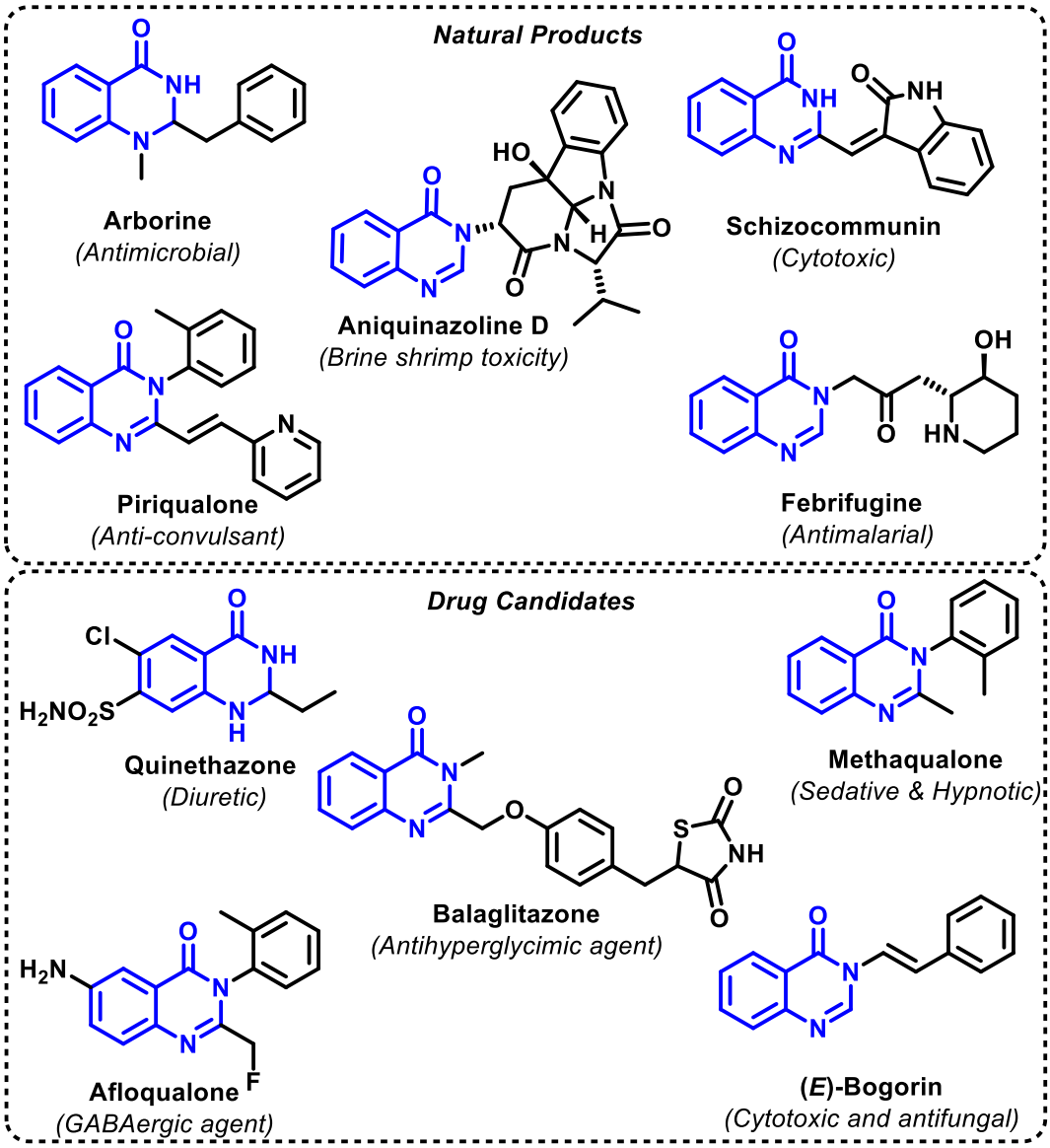

Figure 3.1.1 Selective examples of quinazolinone-based natural products and drug candidates

Consequently, focused efforts have been made towards the synthesis of natural and synthetic derivatives of quinazolinones due to wide range of biological activities possessed by them, including antimalarial, antiviral, antiparasitic, analgesic, antibacterial, anticonvulsant, anticancer, antihypertensive, anti-inflammatory, muscle relaxant, diuretic and plant growth regulators.[6-13]

In this regard, various metal-free synthetic strategies have been established from time-to-time to access quinazolinones in the past decade. Among these, a well-explored protocol utilizes 2-aminobenzamide derivatives (**1**) as starting materials to prepare substituted quinazolin-4(3*H*)-ones (**3a** or **3b)** under acid/base or oxidant-mediated conditions (Scheme 3.1.1). Some of the examples, include (i) reaction of ketoalkynes (**2**) with 2-aminobenzamides (**1**) in presence of trifluoroacetic acid (Scheme 3.1.1a),[14] (ii) phosphorous acid-catalyzed selective C–C bond cleavage and cyclocondensation of *β*-ketoesters (**4**) to 2-aminobenzamides (**1**) (Scheme 3.1.1b),[15] (iii) $Ph_2P(O)OH$-catalyzed reaction of tertiary amines (**5**) with 2-aminobenzamides (**1**) (Scheme 3.11.c),[16] (iv) reaction of *α*-ketoacids (**6**) with 2-aminobenzamides (**1**) using $K_2S_2O_8$ as an oxidant in water (Scheme 3.1.1d),[17] (v) condensation of primary alcohols (**7**) with 2-aminobenzaldehyde (**1**) in the presence of DMSO as the oxidant (Scheme 3.1.1e),[18] and (vi) cyclization of 2-aminobenzamides (**1**) with 1,3-diketones (**8**) under the catalysis of camphorsulfonic acid *via* the selective cleavage of C-C bond (Scheme 3.1.1f).[19]

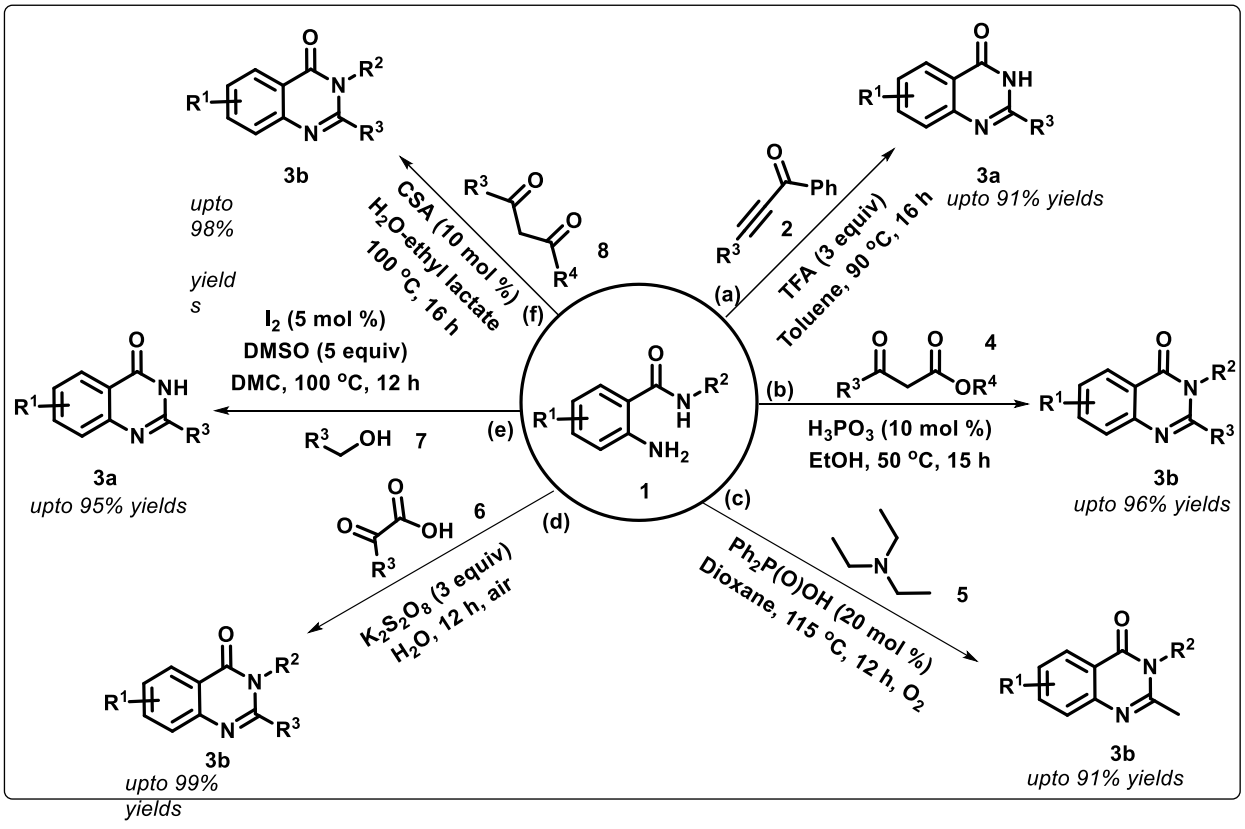

Scheme 3.1.1 Synthesis of substituted quinazolin-4(3*H*)-ones from 2-aminobenzamides

In spite of reasonable advancements, some of these strategies suffer from demerits, such as use of harsh conditions, prolonged reaction time, stoichiometric or excess amounts of toxic oxidants

resulting in toxic wastage products, and poor yields. As a result, metal-catalyzed approaches have been either developed paralleled or subsequently to overcome some of these demerits. Remarkably, Cu- and Pd-catalyzed cross-coupling reactions have contributed substantially in the success story for the construction of quinazolinone scaffolds. For example, in 2008, Zhao's group established the synthesis of 2-substituted quinazolin-4(3*H*)-ones (**3a**) *via* Cu^{I}-catalyzed cascade coupling of amidine hydrochlorides (**9**) with 2-halobenzoates (**10**) using L-proline, Cs_2CO_3 in DMF (Scheme 3.1.2a).[20] The same products were obtained by the reaction of amidine hydrochlorides (**9**) with 2-halobenzoic acids (**11**) using CuI as a catalyst in absence of any ligands (Scheme 3.1.2b).[21] Similarly, in 2018, Kumar *et al.* synthesized 2-substituted quinazolin-4(3*H*)-ones by a domino cross-coupling reaction of 2-halobenzoic acids (**11**) and amidines (**9**) using a copper−glucose catalytic system (Scheme 3.1.2c).[22]

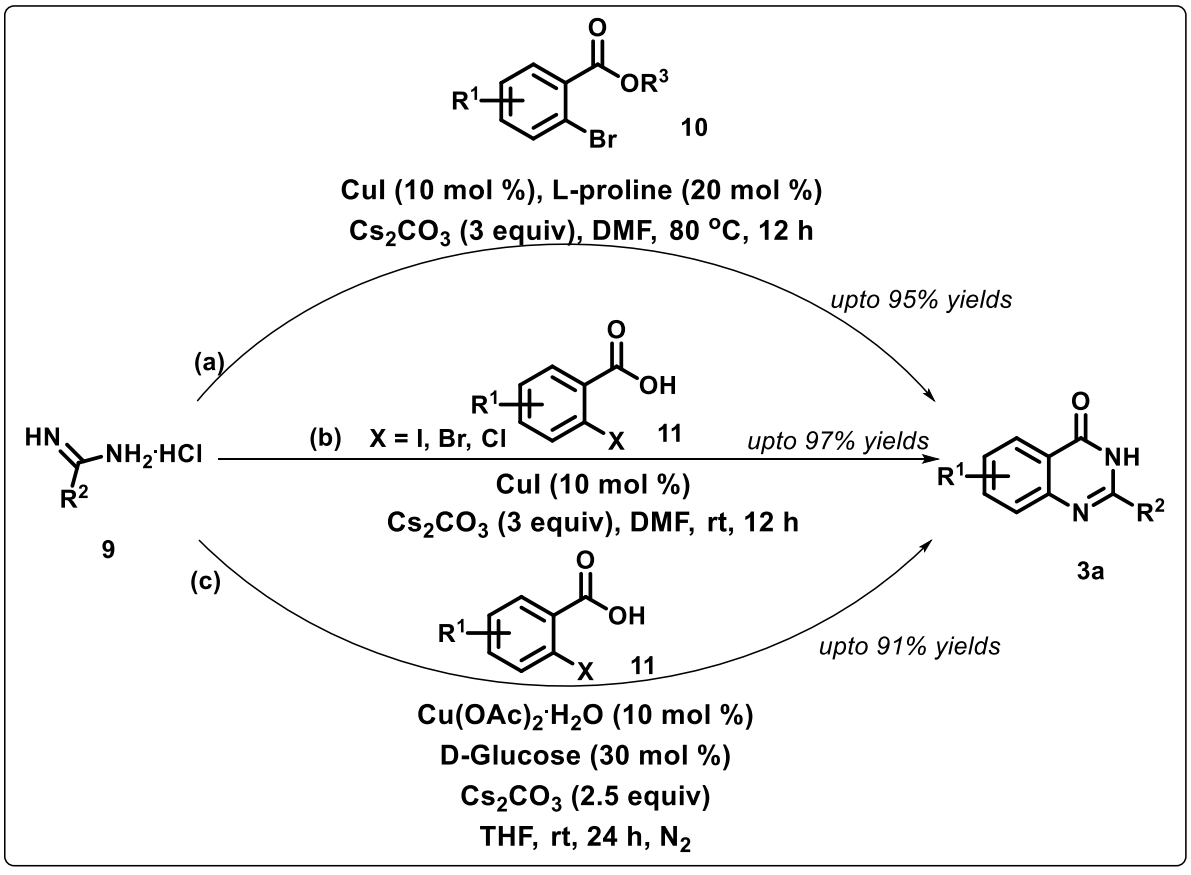

Scheme 3.1.2 Cu-catalyzed synthesis of 2-substituted quinazolin-4(3*H*)-ones from amidine hydrochlorides

Furthermore, Tripathi and coworkers developed an efficient Cu^{I}-catalyzed ligand- and base-free strategy for the synthesis of 2-substituted quinazolin-4(3*H*)-ones (**3a**), starting from 2-

bromobenzamides (**12**) and multiform substrates, such as aldehydes (**13**), alcohols (**7**), and methyl arenes (**14**) using $TMSN_3$ as a nitrogen source (Scheme 3.1.3).[23]

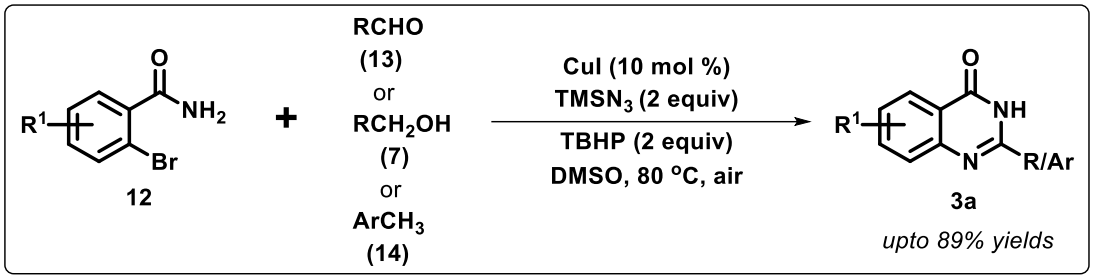

Scheme 3.1.3 Cu-catalyzed synthesis of 2-substituted quinazolin-4(3*H*)-ones from 2-bromobenzamides

In 2021, Pal and coworkers provided a one-pot two-step protocol for the synthesis of 2-substituted quinazolin-4(3*H*)-ones (**3a**) by coupling 2-nitrobenzaldehydes (**15**), urea and aldehyde (**13**) *via* Cu^{II}-catalyzed nitrile formation (**16**), hydrolysis and reduction using atmospheric oxygen as the sole oxidant (Scheme 3.1.4).[24]

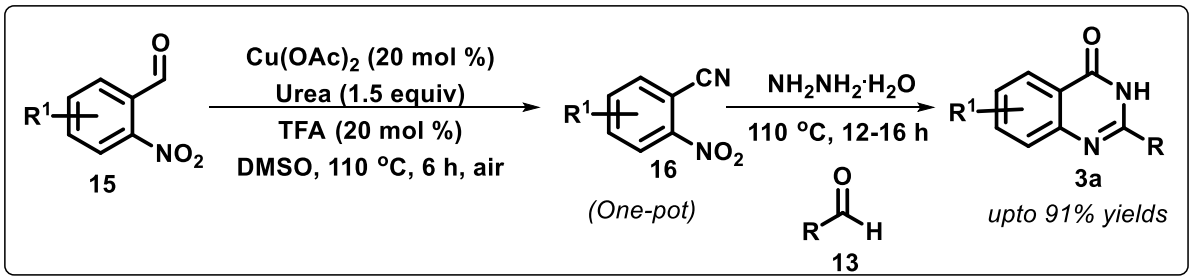

Scheme 3.1.4 Cu-catalyzed synthesis of 2-substituted quinazolin-4(3*H*)-ones from 2-nitrobenzaldehydes

In 2018, Bao *et al.* described a convenient method to synthesize 2-substituted quinazolin-4(3*H*)-ones (**3a**) from simple and readily available 2-halobenzamides (**12**) and nitriles (**17**) under the catalysis of environmentally benign copper acetate (Scheme 3.1.5).[25]

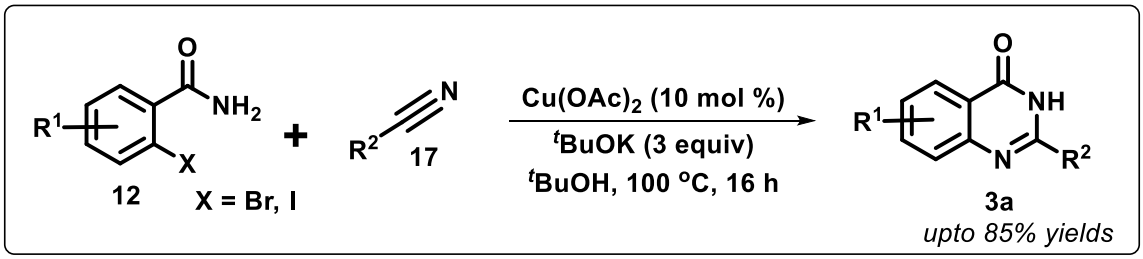

Scheme 3.1.5 Cu-catalyzed synthesis of 2-substituted quinazolin-4(3*H*)-ones from 2-halobenzamides

Orru's group reported Cu^{I}-catalyzed cyclocondensation reaction between 2-isocyanobenzoates (**18**) and amines (**19**) to prepare 3-substituted quinazolin-4(3*H*)-ones (**3c**) under microwave conditions that negated the necessity for longer reaction time and dry conditions or inert atmosphere for optimal performance (Scheme 3.1.6).[26]

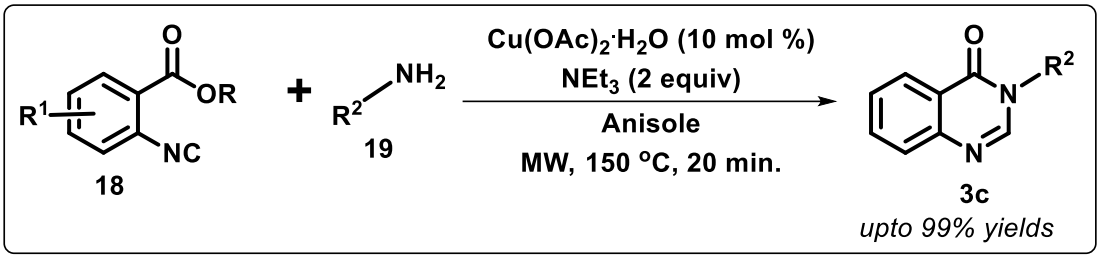

Scheme 3.1.6 Cu-catalyzed synthesis of 3-substituted quinazolin-4(3*H*)-ones from 2-isocyanobenzoates

In 2019, Zhang and coworkers established an aerobic Cu^{I}-catalyzed multicomponent annulation reaction for direct synthesis of 3-substituted quinazolin-4(*3H*)-ones (**3c**) by using readily available anilines (**19a**), primary amines (**19**) and formaldehyde (**13a**). The reaction proceeded through the formation of three C-N and one C-C bonds in conjunction with the benzylic functionalization (Scheme 3.1.7).[27]

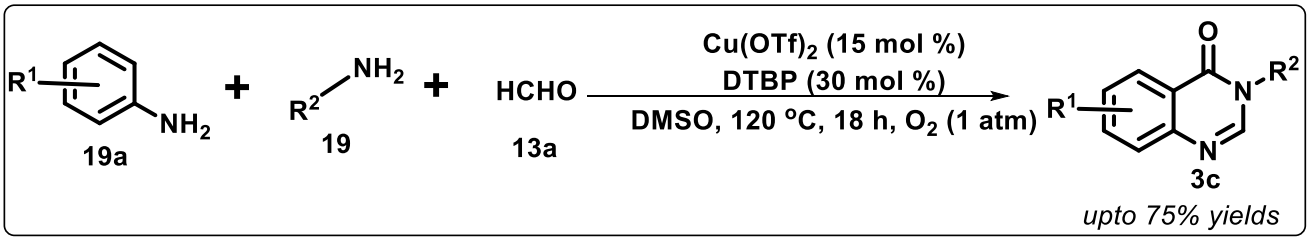

Scheme 3.1.7 Cu-catalyzed synthesis of 3-substituted quinazolin-4(*3H*)-ones from anilines

Similarly, continuous efforts have been documented towards the synthesis of substituted quinazolin-4(*3H*)-ones using palladium catalysts. For instance, in 2012, Yokoyama's group synthesized 2,3-disbstituted quinazolin-4(*3H*)-ones (**3b**) from 2-aminobenzamides (**1**) and benzyl alcohols (**7**) under Pd^{II}-catalysis. The reaction involves a series of sub-steps, including *N*-benzylation, benzylic C-H amidation, and dehydrogenation in water to form the expected products (Scheme 3.1.8).[28]

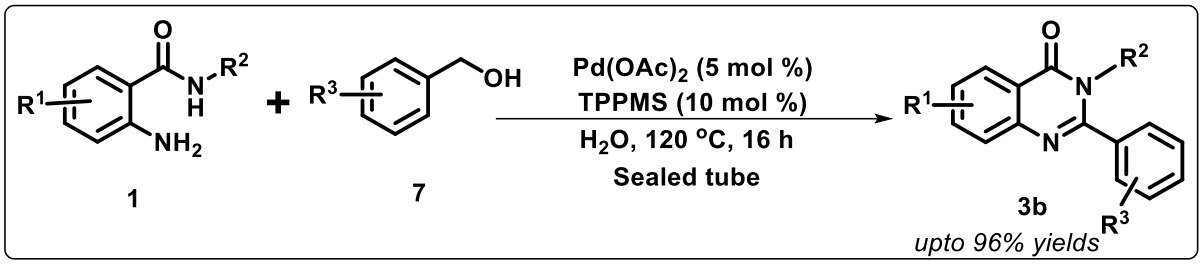

Scheme 3.1.8 Pd-catalyzed synthesis of 2,3-disubstituted quinazolin-4(3*H*)-ones from 2-aminobenzamides

Willi's group also synthesized 2,3-disubstituted quinazolin-4(3*H*)-ones (**3b**) *via* Pd^{II}-catalyzed aminocarbonylation of *N*-(*o*-halophenyl)imidates (**20**) with primary amines (**19**) in presence of carbon monoxide as carbonyl source (Scheme 3.1.9).[29]

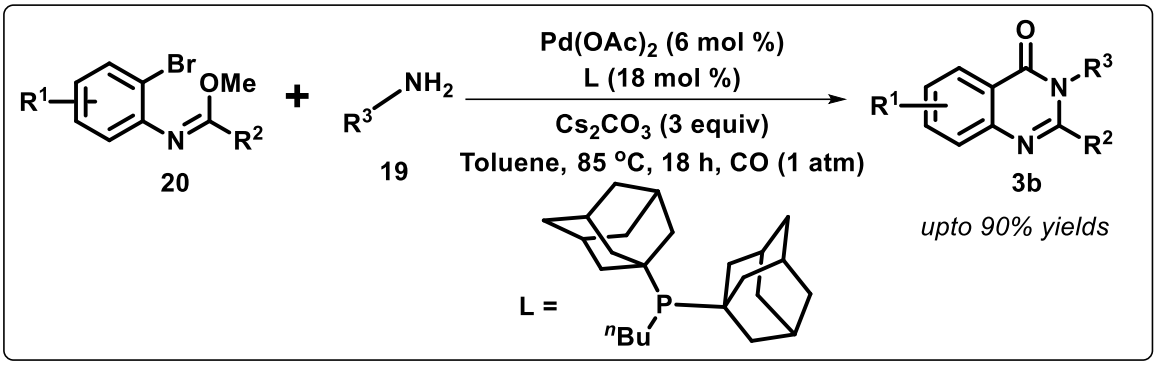

Scheme 3.1.9 Pd-catalyzed synthesis of 2,3-substituted quinazolin-4(3*H*)-ones from *N*-(*o*-halophenyl)imidates

Wu *et al.* developed a strategy to synthesize various 2-substituted quinazolin-4(3*H*)-ones (**3a**) through a Pd^{II}-catalyzed carbonylation reaction of 2-aminobenzonitriles (**21**) and aryl bromides (**22**) using carbon monoxide (Scheme 3.1.10).[30]

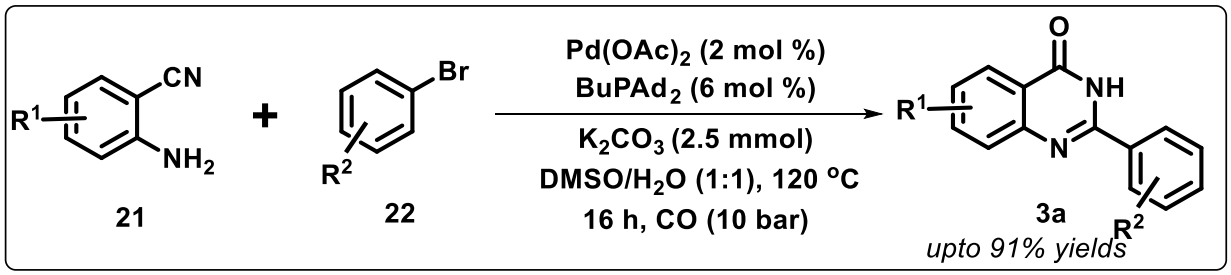

Scheme 3.1.10 Pd-catalyzed synthesis of 2-substituted quinazolin-4(3*H*)-ones from 2-aminobenzonitriles

Ji and coworkers reported a multicomponent synthesis of 2-substituted quinazolin-4(3*H*)-ones (**3a**) in moderate-to-excellent yields from readily available 2-aminobenzamides (**1**) and aryl halides (**22**) through a Pd^{II}-catalyzed isocyanide (**23a**) insertion/cyclization sequence (Scheme 3.1.11).[31]

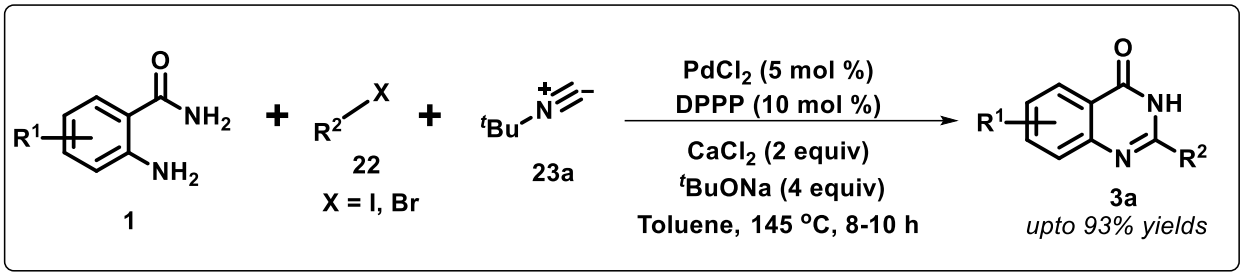

Scheme 3.1.11 Pd-catalyzed synthesis of substituted quinazolin-4(3*H*)-ones from 2-aminobenzamides

Cai's group established an efficient two-step protocol for the synthesis of 2-amino-4(3*H*) quinazolin-4(3*H*)ones (**25**) *via* ring-opening of isatoic anhydride (**24**) by primary amines (**19**) and Pd^{II}-catalyzed oxidative isocyanide (**23**) insertion in a one-pot protocol (Scheme 3.1.12).[32]

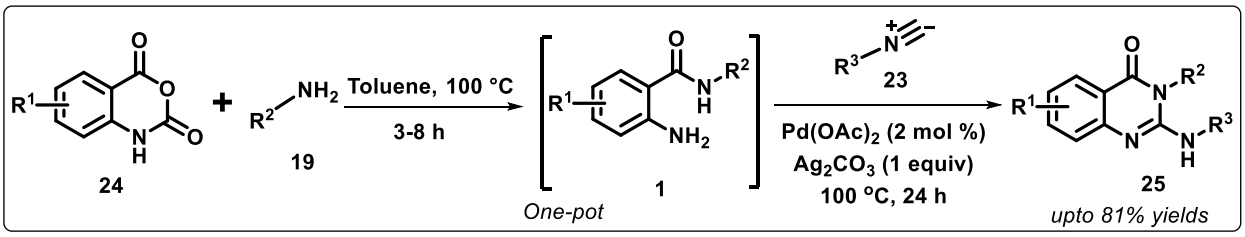

Scheme 3.1.12 Pd-catalyzed synthesis of 2-amino-4(3*H*) quinazolin-4(3*H*)ones from isatoic anhydrides

In 2018, Yang and group achieved the synthesis of 2,3-disubstituted quinazolin-4(3*H*)ones (**3b**) by the oxidative coupling of various *N*-substituted anthranilamides (**1**) with isocyanides (**23a**) and arylboronic acids (**26**) under Pd^{II} catalysis in good-to-excellent yields (Scheme 3.1.13).[33]

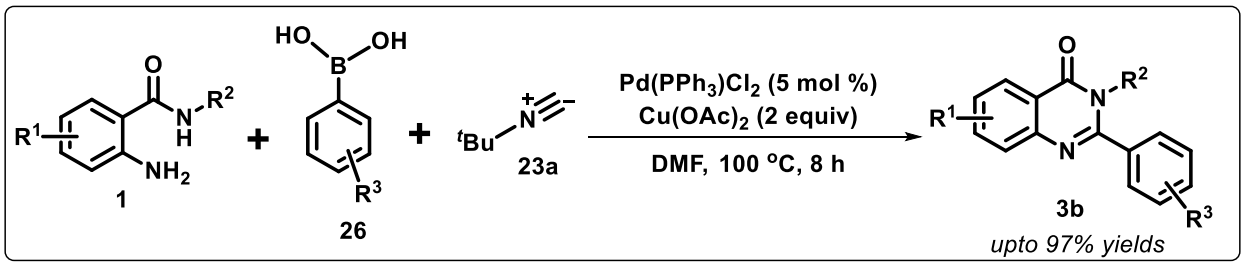

Scheme 3.1.13 Pd-catalyzed synthesis of 2,3-disubstituted quinazolin-4(3*H*)ones from *N*-substituted anthranilamides

In 2021, Feng *et al.* demonstrated the synthesis of various quinazolin-4(3*H*)-ones (**3a**) in good-to -high yields using readily available *o*-nitrobenzamides (**27**) and benzyl alcohols (**7**) under Pd^{II}-catalysis. This reaction proceeds through the hydrogen transfer from alcohol to nitrobenzamide, thereby *in-suit* generating aldehyde and amine that condenses to furnish the target products (Scheme 3.1.14).[34]

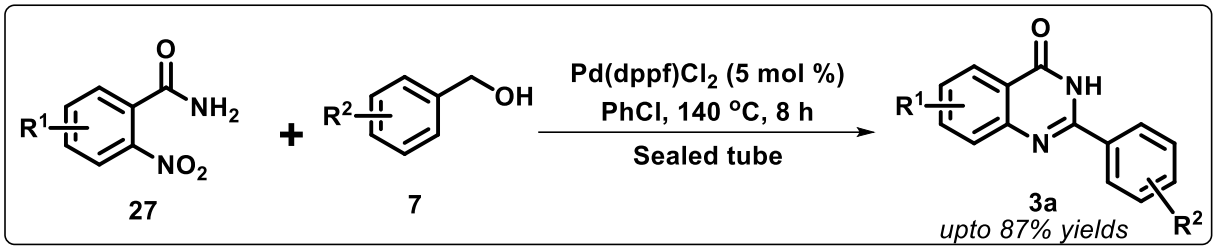

Scheme 3.1.14 Pd-catalyzed synthesis of 2-substituted quinazolin-4(3*H*)-ones from 2-nitrobenzamides

It is noteworthy that the synthetic strategies for 1,2-di(hetero)aryl 2,3-dihydroquinazolin-4(1*H*)-ones (**28**) are scarce; one such protocol involves a two-step procedure involving ammonium hydroxide-mediated conversion of *N*-aryl isatoic anhydrides (**24**) to 2-arylaminobenzamides (**1a**), followed by its condensation with aldehyde (**13**) under acidic condition (Scheme 3.1.15).[35]

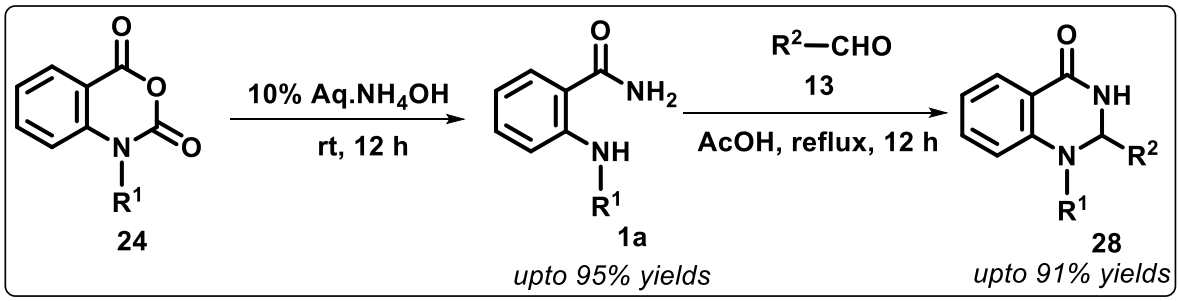

Scheme 3.1.15 Synthesis of 1,2-disubstituted 2,3-dihydroquinazolin-4(1*H*)-ones from *N*-aryl isatoic anhydrides

Moreover, the synthesis of 2,3-di(hetero)aryl 2,3-dihydroquinazolin-4(1*H*)-ones (**29**) have also received special attention. Particularly, the zest for developing newer (nano)catalytic systems (Lewis/organic acids/transition-metal catalysts,[36-37] nanoparticles,[38-45] ionic liquids and silica-supported reagents[46-47]) for the commonly employed multicomponent reaction between isatoic anhydride (**24**), amine (**19**) and aldehydes (**13**) has increased many folds (Scheme 3.1.16).[48-51]

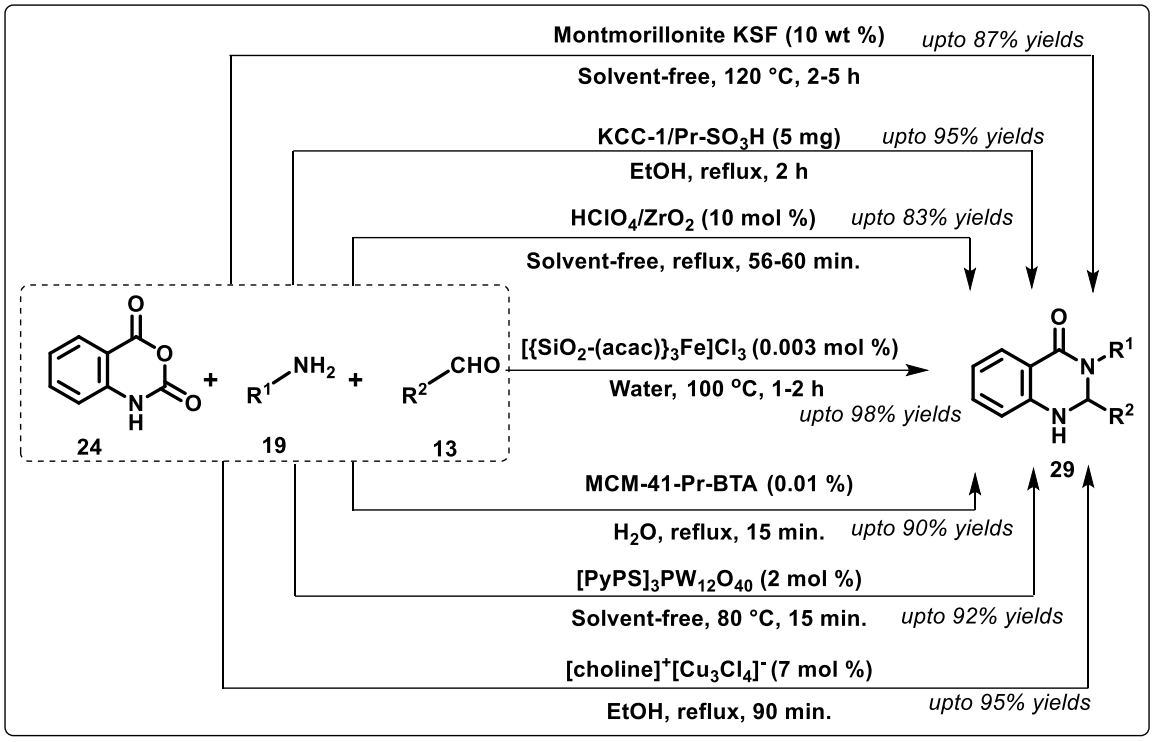

Scheme 3.1.16 Synthesis of 2,3-disubstituted 2,3-dihydroquinazolin-4(1*H*)-ones from isatoic anhydride

Alternatively, the condensation between 2-amino *N*-arylbenzamides (**1**) with aldehydes (**13**) under various metal-free conditions have also delivered rewarding outcomes in terms of yielding 2,3-disubstituted 2,3-dihydroquinazolin-4(1*H*)-ones (**29**) in good-to-excellent yields (Scheme 3.1.17).[52-54]

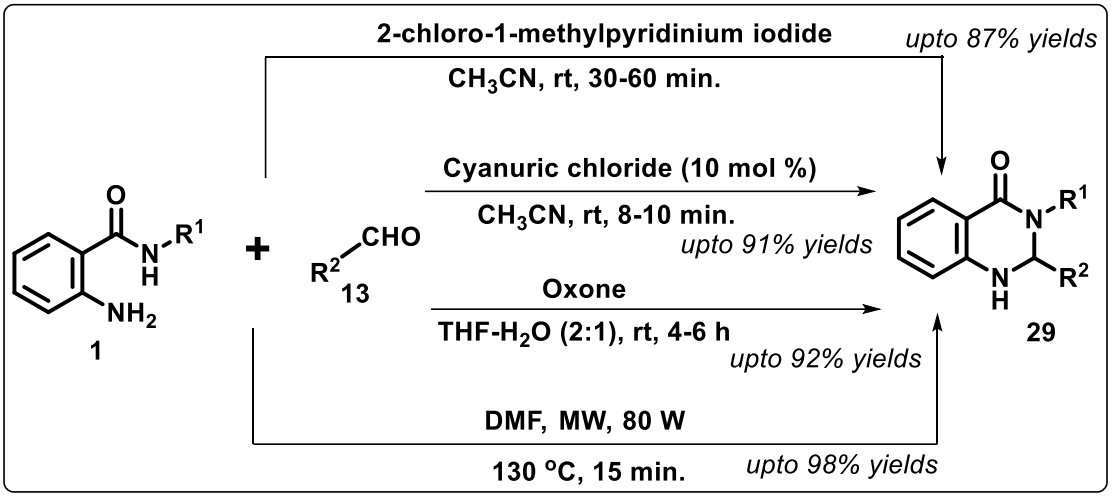

Scheme 3.1.17 Synthesis of 2,3-disubstituted 2,3-dihydroquinazolin-4(1*H*)-ones from 2-amino *N*-arylbenzamides

With regard to our continuing interest in exploring the chemistry on *N*-arylindazolones, we could not trace a direct method for its transformation to quinazolinones. However, very interestingly, Gogoi and coworkers achieved unprecedented transformation of *N*-aryl 1,2-dihydro-3*H*-indazol-3-ones (**30**) to indolo[1,2-*a*]quinazolinones (**32**) by its Ru^{II}-catalyzed annulation with diaryl alkynes (**31**) through a cascade process involving N-N bond cleavage (Scheme 3.1.18).[55]

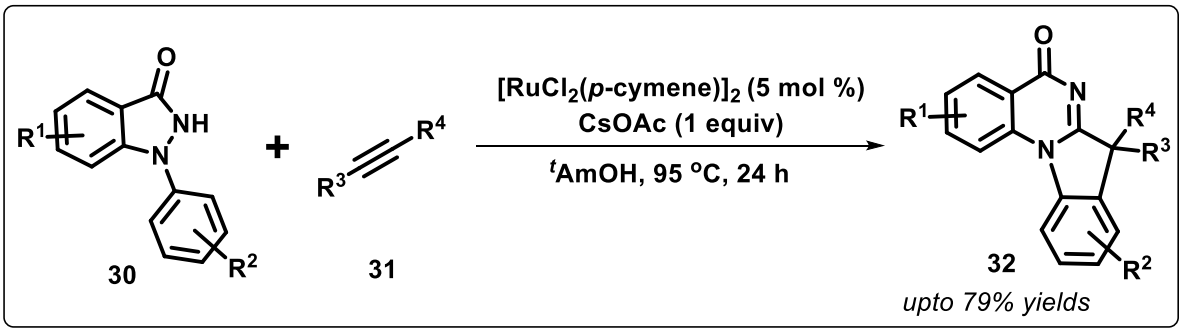

Scheme 3.1.18 Ru-catalyzed synthesis of indolo[1,2-*a*]quinazolinones from *N*-arylindazolones

Though, these reported protocols are associated with their own merits and demerits, yet the evolution of eye-catching strategies with significant advancement in chemistry for preparing 1,2-di(hetero)aryl (**28**) and 2,3-di(hetero)aryl 2,3-dihydroquinazolin-4(1*H*)-ones (**29**), are still in great demand.

In sharp contrast, the exemplification of safer yet reactive *N*-tosylhydrazones (**33**) as alkylating agents have resulted in the construction of one or more C-C/C-N bonds *via* C-H/N-H insertions. Especially, the transition-metal catalyzed *N*-tosylhydrazone-based carbene coupling reactions have enriched chemist's toolbox with elegant cyclization strategies (Scheme 3.1.19).[56-60]

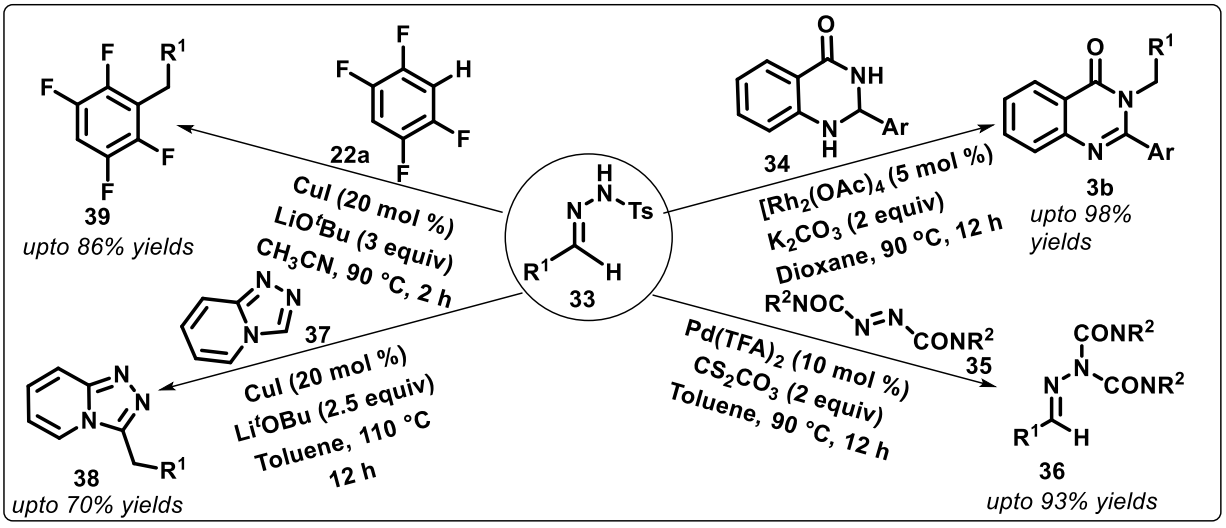

Scheme 3.1.19 Transition-metal catalyzed *N*-tosylhydrazone-based carbene coupling reactions

Interestingly, the functionalization of *N*-arylindazolones remains unexplored with *N*-tosylhydrazones. In the backdrop of the above discussion, we envisioned that *N*-arylindazolones could be selectively functionalized using aldehydic *N*-tosylhydrazones under metal-catalyzed conditions in a one-pot manner.

In this chapter, we present our unprecedented results obtained by annulating 1-aryl- or 2-aryl 1,2-dihydro-3*H*-indazol-3-ones (**30** or **40**) with aldehydic *N*-tosylhydrazones (**33**), which serendipitously led to formation of 1,2-(hetero)aryl and 2,3-(hetero)aryl 2,3-dihydroquinazolin-4(1*H*)-ones (**28** & **29**), respectively under Pd-catalyzed conditions (Scheme 3.1.20).

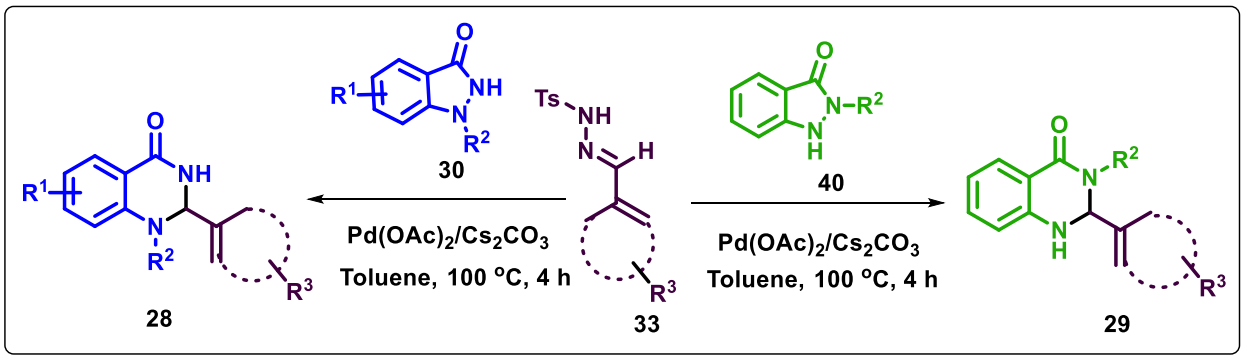

Scheme 3.1.20 Pd-catalyzed synthesis of 1,2- and 2,3-disubstituted-2,3-dihydroquinazolin-4(1*H*)-ones from *N*-arylindazolones and aldehydic *N*-tosylhydrazones

3.2 Results and Discussion

We began our investigation by scrutinizing the reaction conditions for the envisioned annulation between the model substrates, 1-phenyl-1,2-dihydro-3*H*-indazol-3-one (**30a**) and benzaldehyde *N*-tosylhydrazone (**33a**) (Table 3.2.1). In absence of a metal-catalyst and Cs_2CO_3-mediated conditions, no reaction was initiated by heating the model substrates in toluene up to 100 °C for several hours (Table 3.2.1, entry 1). Similar results were obtained by carrying the model reaction under Pd-catalyzed conditions, albeit in absence of Cs_2CO_3 (Table 3.2.1, entry 2). Gratifyingly, the use of combination of $Pd(OAc)_2$ (2.5 mol %) with Cs_2CO_3 (1 equiv) in toluene under ambient conditions commenced the coupling between **30a** and **33a** to afford a major serendipitous product, 1,2-diphenyl-2,3-dihydroquinazolin-4(1*H*)-one (**28a)** in 59% (Table 3.2.1, entry 3); the structure of this product was confirmed through attentive spectroscopic analysis such as ^1H & ^{13}C NMR, HRMS. Interestingly, the appearance of two vicinal coupled doublets at δ 6.20 & 7.55 ppm in its ^1H NMR spectra provided strong evidence for the formation of a disubstituted quinazolinone *via* insertion of a substituted methylene between N-N bond. The yield of **28a** was not affected

considerably under nitrogen atmosphere (Table 3.2.1, entry 4). Next, the optimization investigation was performed by screening a variety of bases. The replacement of Cs_2CO_3 by K_2CO_3 and Na_2CO_3 produced detrimental effects, producing **28a** in 48% and 23% yields respectively (Table 3.2.1, entries 5-6). In contrast, either trace or no product formation was observed (on TLC) by using other carbonates such as Li_2CO_3 or Ag_2CO_3, or acetates such as NaOAc, KOAc or CsOAc (Table 3.2.1, entries 7-8). In contrast, the use of stronger bases such as ^{t}BuOK and NaH furnished much poorer yields of **28a** (Table 3.2.1, entries 9-10).

Table 3.2.1 Selective optimization[a] studies for the synthesis of **28a**

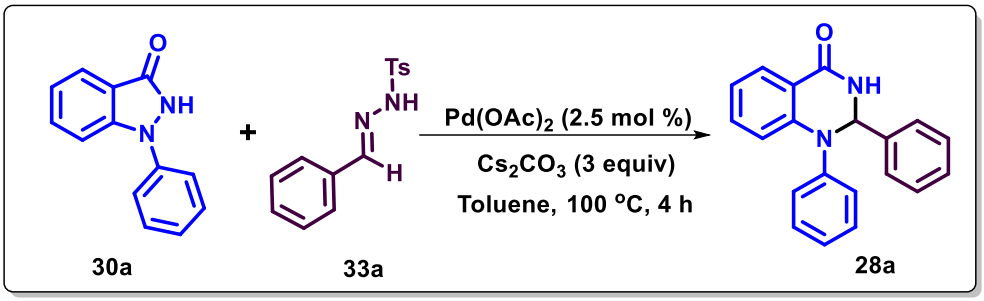

Entry	Deviation from standard conditions	Yield of 28a (%)[b]
1	no metal catalyst	-
2	no base	NR
3	1 equiv of Cs_2CO_3	59
4	under nitrogen atmosphere	56
5	K_2CO_3 (1 equiv) in place of Cs_2CO_3	48
6	Na_2CO_3 (1 equiv) in place of Cs_2CO_3	23
7	Li_2CO_3/Ag_2CO_3 (1 equiv) in place of Cs_2CO_3	Trace
8	NaOAc/KOAc/CsOAc (1 equiv) in place of Cs_2CO_3	NR
9	^{t}BuOK (1 equiv) in place of Cs_2CO_3	22
10	NaH (1 equiv) in place of Cs_2CO_3	36
11	2 equiv of Cs_2CO_3	70
12	3 equiv of Cs_2CO_3	79
13	4 equiv of Cs_2CO_3	81
14	5 mol % of $Pd(OAc)_2$	80
15	MeOH/TFE/^{t}AmOH in place of toluene	65/58/62
16	THF/CH_3CN/DMF in place of toluene	20/30/15

[a]The reaction was carried out with **30a** (0.24 mmol), **33a** (0.72 mmol), catalyst (0.006 mmol), base (0.72 mmol) under ambient conditions in solvent (3 mL) for 4 h. [b]Isolated yields. [c]Reaction temperature was varied from 25 °C to 100 °C up to 12 h. NR: No reaction.

Fruitful results in terms of amelioration of product's yield to 70% and 79% were observed by gradual increasing the base loading to 2 equivalents and 3 equivalents, respectively; While no dramatic change in the yield of **28a** was observed by using 4 equivalents of Cs_2CO_3 (Table 3.2.1, entries 11-13). Catalyst loading to 5 mol % did not make significant enhancement in the productivity of the reaction (Table 3.2.1, entry 14). We further studied the employability of several solvents in place of toluene on the product's yield. Polar protic solvents such as MeOH, TFE, ^{t}AmOH gave moderate yields (55-68%), while aprotic polar solvents such as THF, CH_3CN, DMF furnished inferior results (Table 3.2.1, entries 15-16).

This unprecedented tandem transformation of 1-aryl-1,2-dihydro-3*H*-indazol-3-one to 1,2-diaryl-2,3-dihydroquinazolinone was next examined with varied substituted 1-aryl-1,2-dihydro-3*H*-indazol-3-ones (**30b-l**) and different aldehydic *N*-tosylhydrazones (**33a-j**) (Scheme 3.2.1). Overall, the electronic effects of functionalities on aryl and indazolone rings had a distinct effect on the product outcome. For example, 1-aryl-1,2-dihydro-3*H*-indazol-3-ones substituted with electron-donating groups [substrates: **30b** (R^2 = 4-MeC_6H_4) and **30c** (R^2 = 4-^{i}PrC_6H_4)] on *N*-aryl ring reacted smoothly with *N*-tosylhydrazone (**33a**), producing their corresponding di-substituted quinazolinones **28ba** and **28ca** in 86% and 89% yields, respectively. However, slight decline in the reactivity of the 1-aryl-1,2-dihydro-3*H*-indazol-3-ones decorated with moderately electron-withdrawing groups at *N*-aryl ring [substrates: **30d** (R^2 = 4-ClC_6H_4), **30e** (R^2 = 4-BrC_6H_4) & **30f** (R^2 = 3-ClC_6H_4)] with **33a** was observed, furnishing their respective quinazolin-4-ones (**28da-fa**) in 75-80% yields. Further, di-substitutions on the aryl ring [substrates: **30g** (R^2 = 3,4-$Me_2C_6H_3$) & **30h** (R^2 = 3-Cl-4-MeC_6H_3)] displayed fruitful results affording the desired products **28ga** and **28ha** in 89% and 78% yields, respectively. Similarly, electron-donating as well as moderately electron-withdrawing substituents on indazolone ring [substrates: **30i** (R^1 =5-Me), **30j** (R^1 =5-OMe), **30k** (R^1 =5-Cl), **30l** (R^1 =5-Br)] were well tolerated towards the established methodology to release their corresponding quinazolin-4-ones (**28ia-la**) in 79-93%. Also, 1-(pyrid-2-yl)-1,2-dihydro-3*H*-indazol-3-one (**30m**) reacted reasonably well with *N*-tosylhydrazone (**33a**) to produce pyridyl-substituted quinazolinone **28ma** in 66% yield. Unfortunately, *N*-(*o*-substituted aryl) [substrates: **30n** (R^2 = 2,4-$Me_2C_6H_3$); **30o** (R^2 = 2,4-$Cl_2C_6H_3$)], and alkyl substituted or unsubstituted 1,2-dihydro-3*H*-indazol-3-ones [substrates: **30p** (R^2 = cyclohexyl; **30q** (R^2 = ^{t}butyl); **30r** (R^2 = H)] showed extremely poor reactivity with *N*-tosylhydrazone (**33a**) under the described conditions, producing only traces of the expected products, along with the recovery of maximum

starting materials. The representative ^{1}H and ^{13}C NMR spectra of **28aa** are shown in Figure 3.2.1 and Figure 3.2.2, respectively.

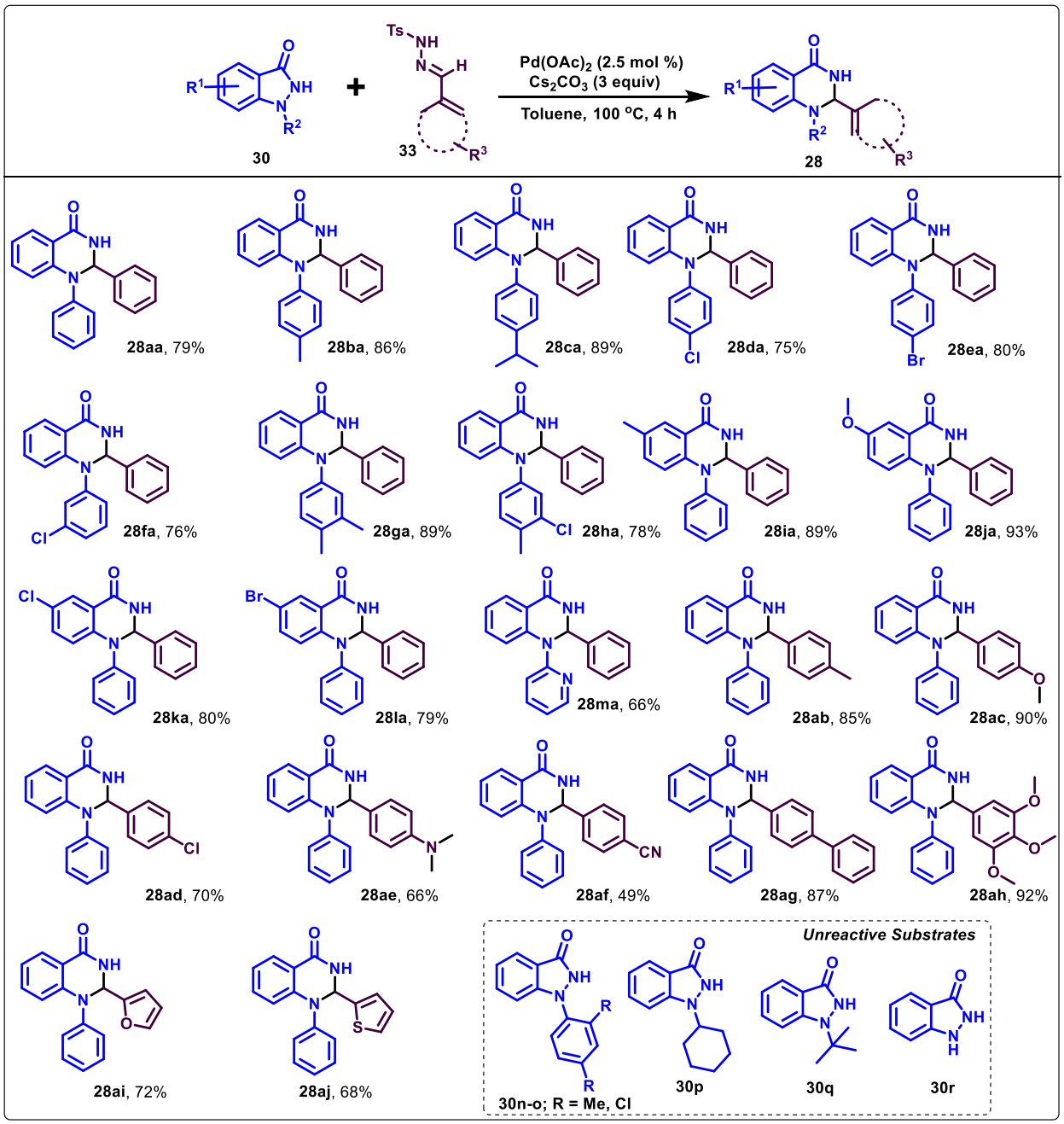

Scheme 3.2.1 Substrate scope of 1-aryl-1,2-dihydro-3*H*-indazol-3-ones and aldehydic *N*-tosylhydrazones

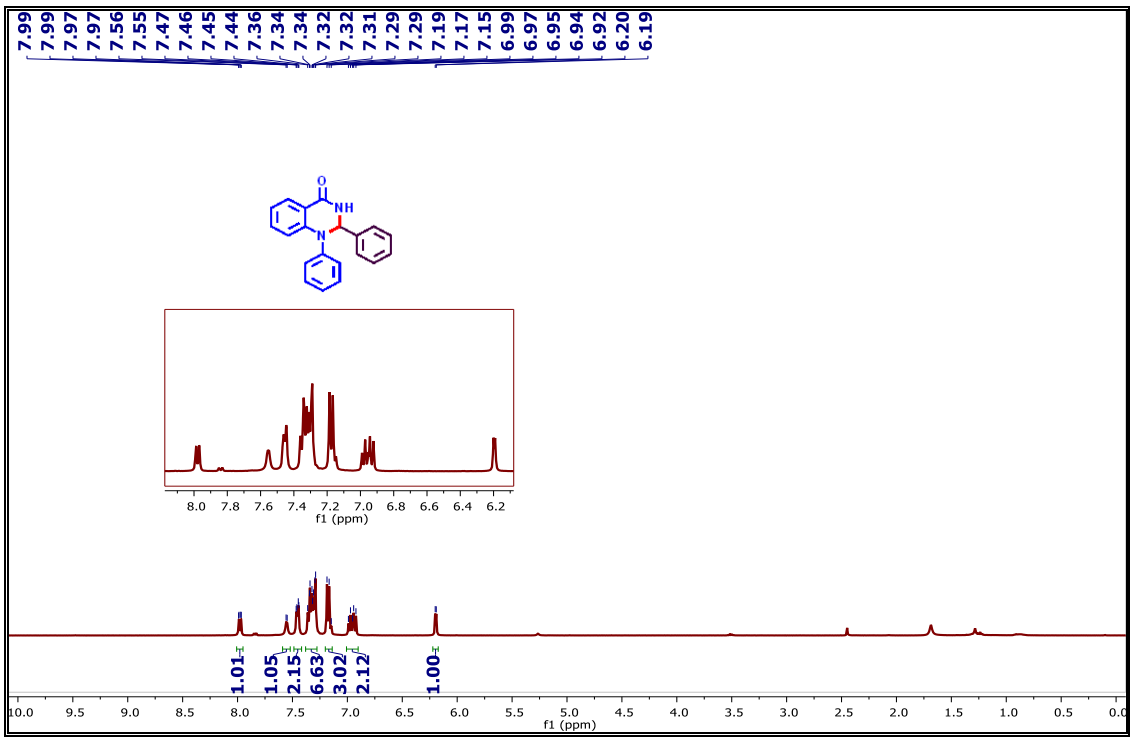

Figure 3.2.1 ^{1}H NMR Spectrum of **28aa**

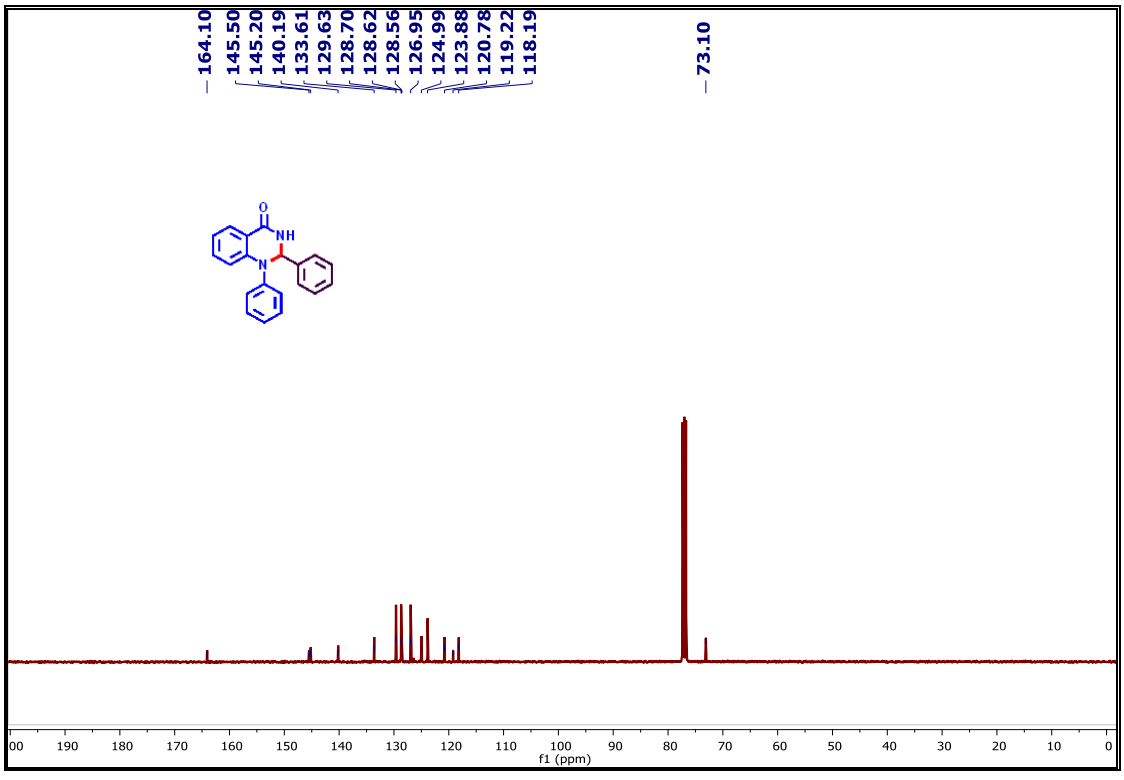

Figure 3.2.2 ^{13}C NMR Spectrum of **28aa**

While studying the substrate scope variation with respect to aldehydic *N*-tosylhydrazones, the reaction's productivity was found to be directly correlated with the electronic effect of the substituents on *N*-tosylhydrazones derived from varied benzaldehyde derivatives. For example, *N*-tosylhydrazones derived from 4-Me-benzaldehyde (**33b**), 4-OMe-benzaldehyde (**33c**) and 3,4,5-$(OMe)_3$-benzaldehyde (**33h**) reacted efficiently with **30a** under the optimized conditions to furnish the targeted quinazolin-4-ones (**28ab**, **28ac** and **28ah**) in 85-92% yields, while *N*-tosylhydrazone derived from 4-Cl-benzaldehye (**33d**) and 4-NMe_2-benzaldehyde (**33e**) reacted with moderate reactivity to give their respective products **28ad** and **28ae** in 70% and 66% yields, respectively. *N*-tosylhydrazone procured from 4-CN-benzaldehyde (**33f**) on reaction with **33a** afforded the corresponding **28af** in only 49% yield. Pleasingly, *N*-tosylhydrazones acquired from (1,1'-biphenyl)-4-carbaldehyde (**33g**), furfuraldehyde (**33i**) and thiophene-2-carbaldehyde (**33j**) reacted comfortably with **30a** to furnish their respective quinazolin-4-ones (**28ag**, **28ai and 28aj**) in 68-87% yields.

Furthermore, the optimized conditions were applicable towards the successful transformation of 2-phenyl-1,2-dihydro-3*H*-indazol-3-one (**40a**) to 2,3-diphenyl-2,3-dihydroquinazolin-4(3*H*)-one (**29aa**) in 86% yield using **33a** (Scheme 3.2.2). Notably, 2-aryl-1,2-dihydro-3*H*-indazol-3-ones produces their corresponding products with greater ease, albeit the trends with respect to the electronic effects of the substituents were similar. Under this domain, substrates with electron-donating groups **40b** (R^4 = 4-MeC_6H_4) and **40c** (R^4 = 4-$OMeC_6H_4$)] as well as moderately electron deficient substituents (R^4 = F, Cl, Br) on aryl ring of 2-aryl-1,2-dihydro-3*H*-indazol-3-ones (**40d-f**) were used as a result all the derivatives reacted very smoothly with *N*-tosylhydrazone (**33a**) granted corresponding 2,3-dihydroquinazolin-4(3*H*)-ones (**29ba-29fa**) in good-to-excellent yields (72-91%). To our delight, of 1,2-dihydro-3*H*-indazol-3-ones bearing pyridine and benzyl groups [substrates: **40g** (R^4 = 4-Pyridyl) and **40h** (R^4 = $CH_2C_6H_5$)] also provided the expected quinazolin-4-ones (**29ga** and **29ha**) in decent yields. The extremity of the reaction with respect to substituent variation on *N*-tosylhydrazones for 2-phenyl-1,2-dihydro-3*H*-indazol-3-ones was established by fruitfully coupling it with **33b** and **33f** to obtain **29ab** and **29af** in 88% and 56% respectively.

Pleasingly, single crystals of **28ab** were grown from dichloromethane *via* single solvent slow evaporation at room temperature for X-ray diffraction (XRD) studies further confirmed the assigned structures of **28**. The ORTEP of **28ab** (CCDC No. 2207706) is shown in Figure 3.2.3.

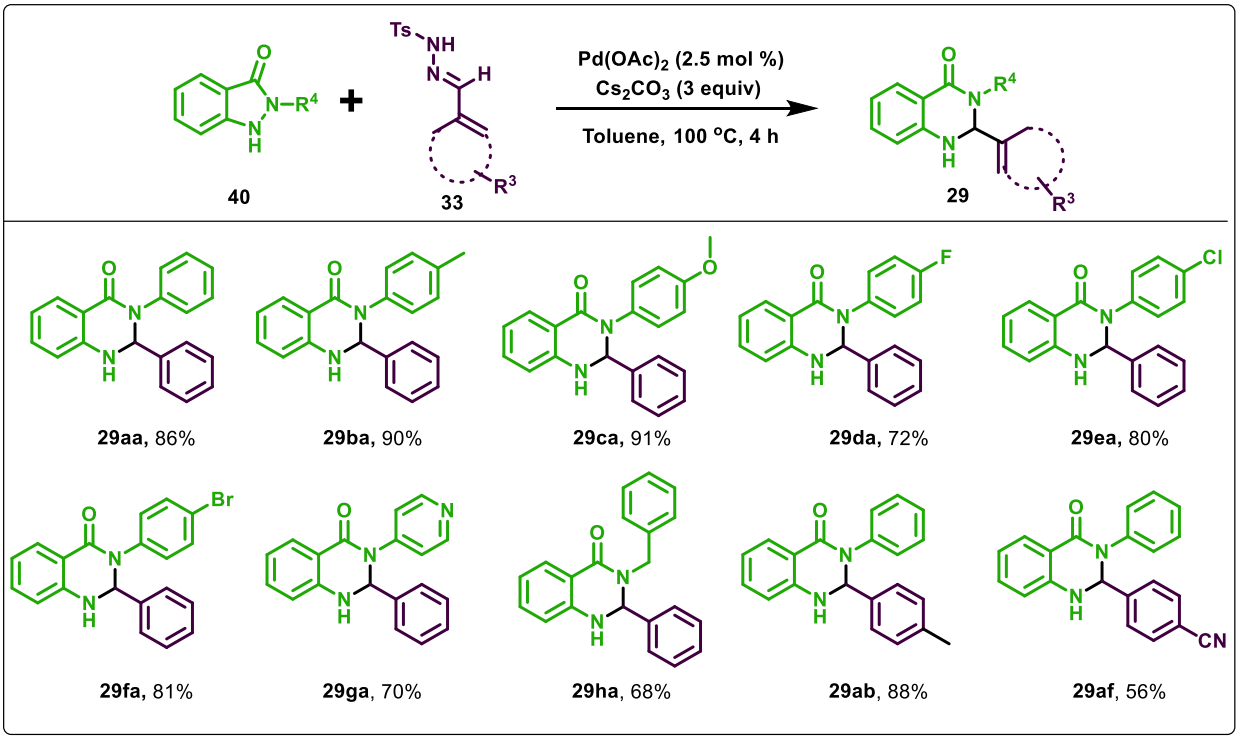

Scheme 3.2.2 Substrate scope of 2-aryl-1,2-dihydro-3*H*-indazol-3-ones and aldehydic *N*-tosylhydrazones

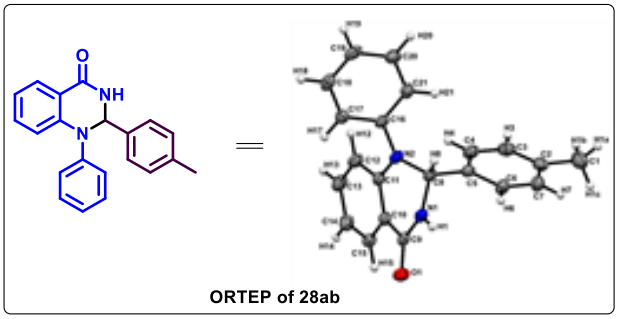

Figure 3.2.3 ORTEP Diagram of **28ab**

To demonstrate the synthetic utility of the established strategy, we undertook the task of preparing a potent calcium receptor antagonist NPS 53574, which was otherwise reported by employing several elaborated procedures. For exemplifying this, firstly the reaction of 2-phenethyl-1,2-dihydro-3*H*-indazol-3-one (**40i**) with *N*-tosylhydrazone (**33i**) derived from furfural was performed under Pd-catalyzed optimized conditions to afford 2-(furan-2-yl)-3-phenethyl-2,3-dihydroquinazolin-4(1*H*)-one (**29ii**) in 77% yield, which on dehydrogenation using DDQ in dichloromethane at room temperature furnished the targeted 2-(furan-2-yl)-3-phenethylquinazolin-4(3*H*)-one (NPS 53574, **41ii**) in 95% yield. The scalability of this

methodology was proved by performing a gram scale reaction between **40i** and **33i** under described conditions to afford **29ii** in 75%; the total of this was successfully transformed into **41ii** in 94% yield (Scheme 3.2.3).

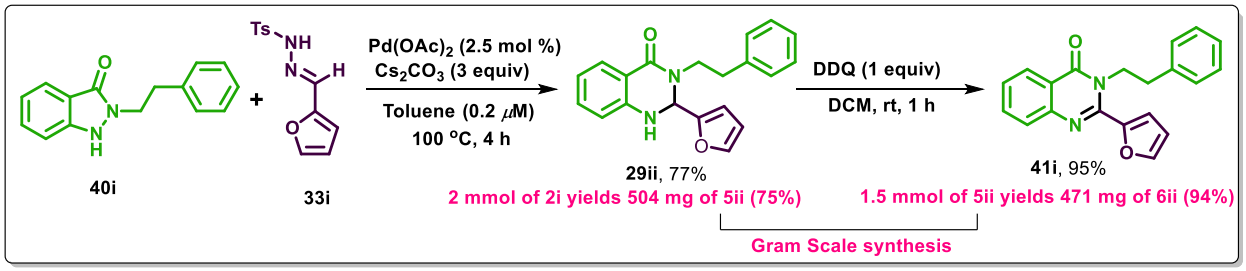

Scheme 3.2.3 Synthesis of bioactive molecule, NPS 53574

Preliminary mechanistic investigations were conducted to shed some light into the insight of reaction pathway (Scheme 3.2.4). The possibility of a radical mechanism was completely eliminated as outcome for the reaction between **30a** and **33a** under standard conditions remains un-affected in presence of TEMPO (Scheme 3.2.4i). Surprisingly, *N*-tosylhydrazones derived from *p*-hydroxybenzaldehyde (**33k**) and indole-3-carboxaldehyde (**33l**) when reacted with **30a** under the optimized conditions did not furnish the expected 1,2-disubstituted-2,3-dihydroquinazolin-4(1*H*)-one (**28ak**) and (**28al**), albeit afforded the N-H insertion products, 2-(4-hydroxybenzyl)-1-phenyl-1,2-dihydro-3*H*-indazol-3-one (**28'ak**) and 2-((1*H*-indol-3-yl)methyl)-1-phenyl-1,2-dihydro-3*H*-indazol-3-one (**28'al**) in 90% and 85% yields, respectively (Scheme 3.2.4ii) Continued heating of **28'ak** or its methyl ether derivative **28'ac** (obtained by methylation of **28'ak**) under standard conditions did not produce their respective di-substituted quinazolin-4-ones (**28ak** or **28ac**); instead decomposition of **28'aj** and **28'ac** were monitored by TLC (Scheme 3.2.4iii). Notably, the formation of **28'ac** was not at all observed (on TLC) while carefully monitoring the direct formation of **28ac** from the optimized reaction between **28a** and **33c**, even at comparatively lower temperature or lesser reaction time. Thus, the inability of transformation of N-H insertion product to the expected di-substituted quinazolin-4-one clearly indicated that N-H insertion product is not involved as an intermediate during this unprecedented transformation of five-membered indazolones to six-membered quinozolin-4-ones. Furthermore, *N*-phenyl-2,3-dihydrophthalazine-1,4-dione (**42a**) did not react at all with **33a** under standard conditions to yield any product. This provided strong evidence for the inability of amidic nitrogens and the requirement of an amine nitrogen to undergo nucleophilic attack on the palladium carbenoid species for the desired product formation (Scheme 3.2.4iv). Finally, the *in-situ* tracking of the

possible intermediates in the reaction mixture after 30 min. indicated the formation of the species **B** and **28aa**, when analyzed through mass spectrometry (Scheme 3.2.4v).

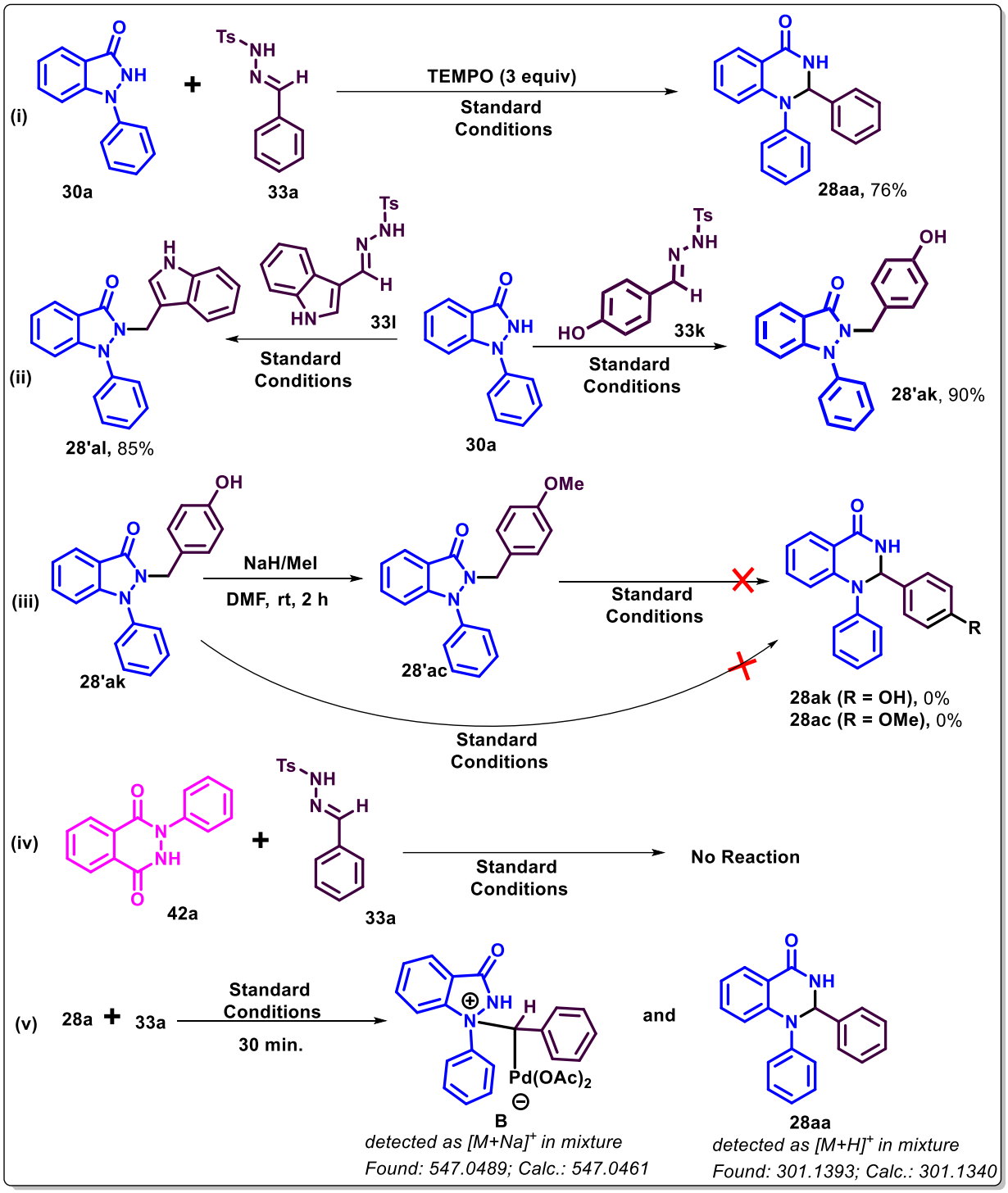

Scheme 3.2.4 Mechanistic investigations

In light of these above results and previously reported investigations,[58] a possible mechanistic pathway is proposed (Scheme 3.2.5). The reaction is believed to proceed by base-mediated decomposition of *N*-tosylhydrazone to generate diazo species, which on coordination with Pd-catalyst furnishes palladium-carbenoid complex **A**. Thereafter, the nucleophic attack of nitrogen (*tert. or sec. amine*) in 1-arylindazolone (**30**)/2-arylindazolone (**40**) on the Pd-carbenoid species **A** furnishes reactive species **B1**/**B2** *via* C-N bond formation. Subsequently, species **B1**/**B2** on intramolecular ring expansion *via* N-N bond cleavage produces disubstituted quinazolinones (**28**/**29**), along with regeneration of Pd-catalyst.

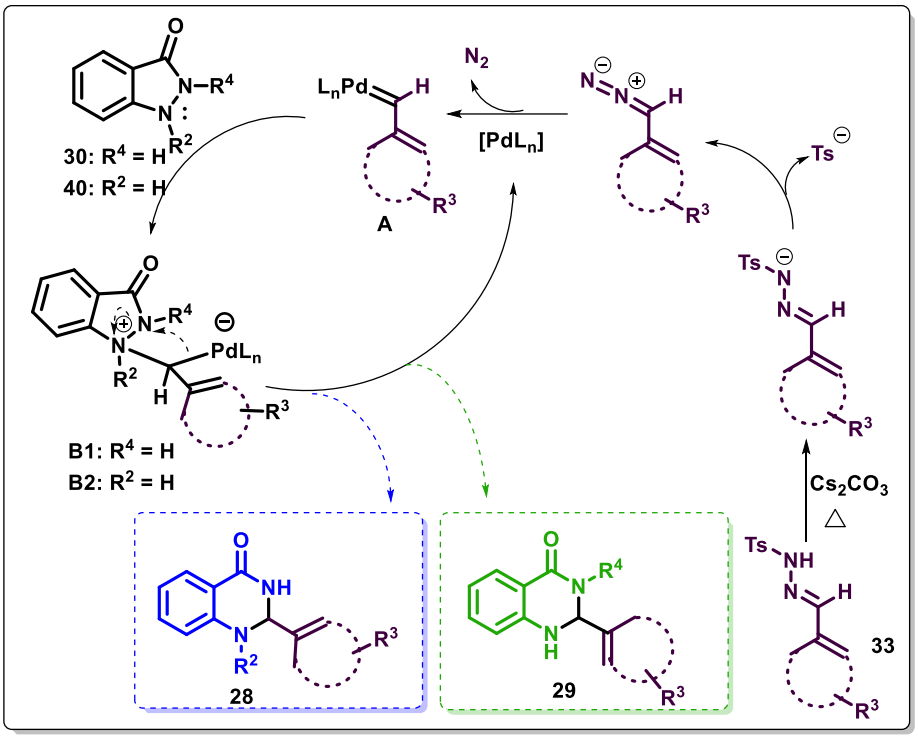

Scheme 3.2.5 Plausible mechanistic pathway

We have disclosed a simple and highly efficient methodology for the direct synthesis of 1,2-di(hetero)aryl-2,3-dihydroquinazolin-4(1*H*)-ones and 2,3-di(hetero)aryl-2,3-dihydroquinazolin-4(1*H*)-ones through palladium-catalyzed substituted carbene insertion obtained by the decomposition of aldehydic *N*-tosylhydrazones, into N-N bonds in 1-aryl- and 2-aryl 1,2-dihydro-3*H*-indazol-3-ones, respectively. The established methodology displayed good functional group tolerance on the involved coupling partners, producing disubstituted quinazolinones under ambient conditions in good-to-excellent yields. By using the established methodology, the synthesis of a potent calcium receptor antagonist, NPS 53574 was accomplished in high yield.

3.3 Experimental Section

General Considerations

Commercially available reagents were used without purification. Commercially available solvents were dried by standard procedures prior to use. Aldehydic *N*-tosylhydrazones[61] were prepared according to the reported procedure. Nuclear magnetic resonance spectra were recorded on a 400 MHz spectrometer, and the chemical shifts are reported in δ units, parts per million (ppm), relative to residual chloroform (7.26 ppm) or DMSO (2.5 ppm) in the deuterated solvent. The following abbreviations were used to describe peak splitting patterns when appropriate: s = singlet, d = doublet, t = triplet, dd = doublet of doublets, and m = multiplet. Coupling constants *J* are reported in Hz. The ^{13}C NMR spectra are reported in ppm relative to deuterochloroform (77.0 ppm) or [d_6] DMSO (39.5 ppm). Melting points were determined on a capillary point apparatus equipped with a digital thermometer and are uncorrected. High-resolution mass spectra were recorded on Agilent Technologies 6545 Q-TOF LC/MS by using electrospray mode. Column chromatography was performed on silica gel (100-200) mesh using varying ratio of ethyl acetate/hexanes as eluent.

General procedure for the transformation of substituted 1,2-dihydro-3*H*-indazol-3-ones to disubstituted 2,3-dihydroquinazolin-4(1*H*)-ones (28/29)

To an oven-dried 10-mL round-bottom flask containing 1-aryl- or 2-aryl-1,2-dihydro-3*H*-indazol-3-ones (**30/40**) (50 mg, 1 equiv) in toluene (0.2 μM), aldehydic *N*-tosylhydrazone (**33**) (3 equiv), $Pd(OAc)_2$ (0.025 equiv), Cs_2CO_3 (3 equiv) were added under atmospheric air. The reaction mixture was stirred and heated in an oil bath at 100 ^{o}C for 4 h (monitored by TLC). After the completion of the reaction, the reaction mixture was cooled to room temperature, concentrated, diluted with water and extracted with EtOAc (20 mL x 2). The organic layers were separated and concentrated under reduced pressure to afford a residue, which was purified by column chromatography (SiO_2 100−200 mesh) using hexanes/EtOAc (7/3) as eluent system to afford the desired product (**28/29**).

1,2-Diphenyl-2,3-dihydroquinazolin-4(1*H*)-one (28aa). White solid, 56 mg (79%); mp 165-166

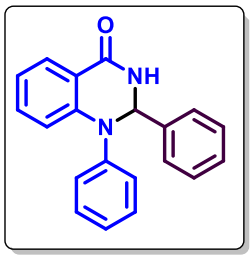

^{o}C; ^{1}H NMR (400 MHz, $CDCl_3$) δ 7.98 (dd, *J* = 7.8, 1.7 Hz, 1H), 7.56 (d, *J* = 4 Hz, 1H), 7.48 – 7.42 (m, 2H), 7.37 – 7.29 (m, 6H), 7.19 – 7.13 (m, 3H), 6.99 – 6.91 (m, 2H), 6.20 (d, *J* = 3.9 Hz, 1H); ^{13}C NMR (100 MHz, $CDCl_3$) δ 164.1, 145.5, 145.2, 140.2, 133.6, 129.6, 128.7, 128.62, 128.56, 127.0, 125.0, 123.9, 120.8, 119.2, 118.2, 73.1; HRMS (ESI-TOF) (*m/z*) calculated $C_{20}H_{17}N_2O^+$: 301.1340, found 301.1334 $[M + H]^+$.

2-Phenyl-1-(*p*-tolyl)-2,3-dihydroquinazolin-4(1*H*)-one (28ba). White solid, 60 mg (86%); mp

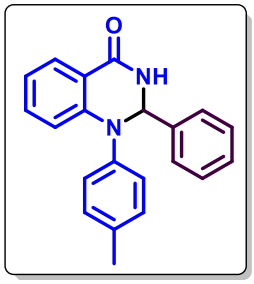

151-152 °C; ^{1}H NMR (400 MHz, $CDCl_3$) δ 7.97 (dd, J = 7.9, 1.7 Hz, 1H), 7.47 – 7.38 (m, 3H), 7.33 – 7.29 (m, 4H), 7.13 (d, J = 8.0 Hz, 2H), 7.04 (d, J = 8.3 Hz, 2H), 6.93 (t, J = 7.5 Hz, 1H), 6.81 (d, J = 8.3 Hz, 1H), 6.14 (d, J = 3.6 Hz, 1H), 2.34 (s, 3H); ^{13}C NMR (100 MHz, $CDCl_3$) δ 164.1, 146.2, 142.3, 140.2, 135.1, 133.6, 130.2, 128.7, 128.5, 127.1, 124.7, 124.6, 120.2, 118.5, 117.6, 73.4, 20.9; HRMS (ESI-TOF) (*m/z*) calculated $C_{21}H_{19}N_2O^+$: 315.1497, found 315.1482 $[M + H]^+$.

1-(4-Isopropylphenyl)-2-phenyl-2,3-dihydroquinazolin-4(1*H*)-one (28ca). White solid, 60 mg

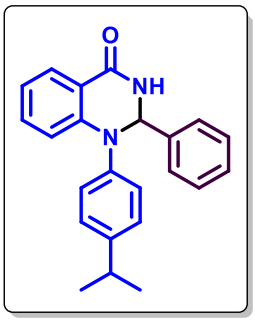

(89%); mp 164-165 °C; ^{1}H NMR (400 MHz, $CDCl_3$) δ 7.96 (d, J = 7.6 Hz, 1H), 7.77 (d, J = 3.0 Hz, 1H), 7.48 – 7.42 (m, 2H), 7.35 – 7.26 (m, 4H), 7.19 (d, J = 8.1 Hz, 2H), 7.10 (d, J = 8.1 Hz, 2H), 6.98 – 6.90 (m, 2H), 6.15 (d, J = 4.1 Hz, 1H), 2.90 (q, J = 6.9 Hz, 1H), 1.26 (d, J = 6.9 Hz, 6H); ^{13}C NMR (100 MHz, $CDCl_3$) δ 164.2, 145.8, 145.7, 143.0, 140.6, 133.5, 128.6, 128.50, 128.47, 127.5, 126.9, 123.9, 123.8, 120.4, 119.0, 118.10, 118.07, 73.1, 33.6, 24.02, 23.97; HRMS (ESI-TOF) (*m/z*) calculated $C_{23}H_{23}N_2O^+$: 343.1810, found 343.1797 $[M + H]^+$.

1-(4-Chlorophenyl)-2-phenyl-2,3-dihydroquinazolin-4(1*H*)-one (28da). White solid, 51 mg

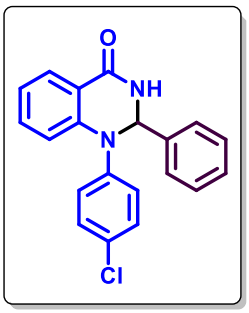

(75%); mp 179-180 °C; ^{1}H NMR (400 MHz, $CDCl_3$) δ 7.98 (dd, J = 7.9, 1.5 Hz, 1H), 7.55 (d, J = 3.9 Hz, 1H), 7.45 – 7.39 (m, 2H), 7.37 – 7.26 (m, 6H), 7.09 (d, J = 8.4 Hz, 2H), 6.99 (t, J = 7.5 Hz, 1H), 6.87 (d, J = 8.3 Hz, 1H), 6.14 (d, J = 3.8 Hz, 1H); ^{13}C NMR (100 MHz, $CDCl_3$) δ 164.0, 145.3, 143.7, 139.7, 133.8, 130.3, 129.8, 128.83, 128.82, 128.7, 126.9, 125.4, 121.2, 119.3, 118.0, 73.2; HRMS (ESI-TOF) (*m/z*) calculated $C_{20}H_{16}ClN_2O^+$: 335.0951, found 335.0944 $[M + H]^+$.

1-(4-Bromophenyl)-2-phenyl-2,3-dihydroquinazolin-4(1*H*)-one (28ea). White solid, 52 mg (80%); mp 159-160 °C; ^{1}H NMR (400 MHz, $CDCl_3$) δ 7.98 (d, J = 7.8 Hz, 1H), 7.55 (brs, 1H), 7.48 – 7.38 (m, 4H), 7.37 – 7.29 (m, 4H), 7.10 – 6.96 (m, 3H), 6.90 (d, J = 8.4 Hz, 1H), 6.14 (brs, 1H); ^{13}C NMR (100 MHz, $CDCl_3$) δ 163.9, 145.1, 144.3, 139.7, 133.7, 132.7, 128.8, 128.7, 126.9, 125.5, 121.3, 119.5, 118.2, 117.9, 73.1; HRMS (ESI-TOF) (*m/z*) calculated $C_{20}H_{16}BrN_2O^+$: 379.0445, found 379.0445 $[M + H]^+$.

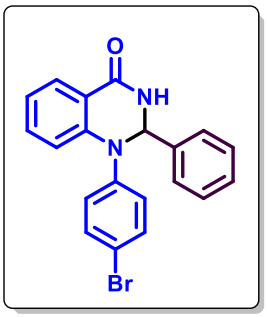

1-(3-Chlorophenyl)-2-phenyl-2,3-dihydroquinazolin-4(1*H*)-one (28fa). White solid, 52 mg (76%); mp 219-220 °C; ^{1}H NMR (400 MHz, $CDCl_3$) δ 7.98 (dd, J = 7.7, 1.7 Hz, 1H), 7.52 (d, J = 4.4 Hz, 1H), 7.46 – 7.41 (m, 2H), 7.40 – 7.35 (m, 1H), 7.33 – 7.29 (m, 3H), 7.25 (d, J = 8.0 Hz, 1H), 7.17 (t, J = 1.9 Hz, 1H), 7.13 (d, J = 8.0 Hz, 1H), 7.07 – 6.97 (m, 3H), 6.17 (d, J = 4.1 Hz, 1H); ^{13}C NMR (100 MHz, $CDCl_3$) δ 163.9, 146.8, 144.4, 139.7, 135.2, 133.8, 130.6, 128.8, 128.8, 128.7, 126.8, 124.8, 123.2, 121.8, 121.2, 120.1, 118.9, 72.9; HRMS (ESI-TOF) (*m/z*) calculated $C_{20}H_{16}ClN_2O^+$: 335.0951, found 335.0936 $[M + H]^+$.

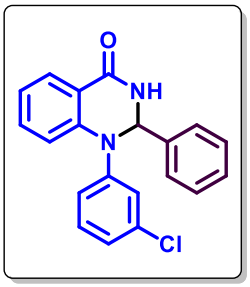

1-(3,4-Dimethylphenyl)-2-phenyl-2,3-dihydroquinazolin-4(1*H*)-one (28ga). White solid, 61 mg (89%); mp 154-155 °C; ^{1}H NMR (400 MHz, $CDCl_3$) δ 7.96 (d, J = 7.8 Hz, 1H), 7.80 (d, J = 3.9 Hz, 1H), 7.49 – 7.40 (m, 2H), 7.35 – 7.25 (m, 4H), 7.08 (d, J = 8.0 Hz, 1H), 6.98 – 6.84 (m, 4H), 6.15 (d, J = 3.8 Hz, 1H), 2.25 (s, 3H), 2.22 (s, 3H); ^{13}C NMR (100 MHz, $CDCl_3$) δ 164.3, 146.0, 142.9, 140.5, 138.0, 133.6, 133.5, 130.6, 128.6, 128.5, 128.4, 127.0, 125.4, 121.6, 120.2, 118.8, 118.1, 73.2, 19.9, 19.2; HRMS (ESI-TOF) (*m/z*) calculated $C_{22}H_{21}N_2O^+$: 329.1653, found 329.1639 $[M + H]^+$.

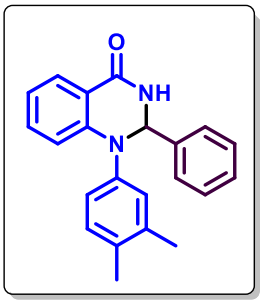

1-(3-Chloro-4-methylphenyl)-2-phenyl-2,3-dihydroquinazolin-4(1*H*)-one (28ha). White solid, 52 mg (78%); mp 194-195 °C; ^{1}H NMR (400 MHz, $CDCl_3$) δ 8.22 (d, J = 4.1 Hz, 1H), 7.96 (dd, J = 7.8, 1.7 Hz, 1H), 7.45 (dd, J = 7.3, 2.3 Hz, 2H), 7.36 (t, J = 7.8 Hz, 1H), 7.32 – 7.25 (m, 3H), 7.20 – 7.14 (m, 2H), 7.02 – 6.91 (m, 3H), 6.15 (d, J = 3.9 Hz, 1H), 2.36 (s, 3H); ^{13}C NMR (100 MHz, $CDCl_3$) δ 164.4, 145.0, 144.3, 140.0, 135.1, 133.8, 132.6, 131.6, 128.8,

128.7, 128.6, 126.9, 124.1, 121.9, 121.2, 119.5, 118.4, 72.9, 19.5; HRMS (ESI-TOF) (*m/z*) calculated $C_{21}H_{18}ClN_2O^+$: 349.1107, found 349.1103 $[M + H]^+$.

6-Methyl-1,2-diphenyl-2,3-dihydroquinazolin-4(1*H*)-one (28ia). White solid, 62 mg (89%); mp

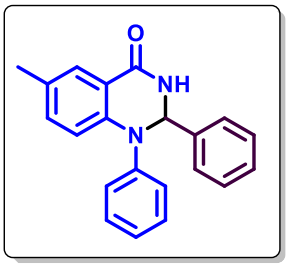

181-182 °C; ^{1}H NMR (400 MHz, $CDCl_3$) δ 8.36 (d, J = 4.4 Hz, 1H), 7.77 (d, J = 2.2 Hz, 1H), 7.49 (d, J = 6.8 Hz, 2H), 7.37 – 7.25 (m, 5H), 7.17 (d, J = 8.0 Hz, 3H), 7.13 (t, J = 7.4 Hz, 1H), 6.98 (d, J = 8.3 Hz, 1H), 6.22 (d, J = 4.3 Hz, 1H), 2.30 (s, 3H); ^{13}C NMR (100 MHz, $CDCl_3$) δ 164.6, 146.1, 142.4, 140.6, 134.5, 130.8, 129.5, 128.6, 128.4, 126.8, 124.1, 122.5, 120.0, 119.2, 72.7, 20.6; HRMS (ESI-TOF) (*m/z*) calculated $C_{21}H_{19}N_2O^+$: 315.1497, found 315.1489 $[M + H]^+$.

6-Methoxy-1,2-diphenyl-2,3-dihydroquinazolin-4(1*H*)-one (28ja). White solid, 64 mg (93%);

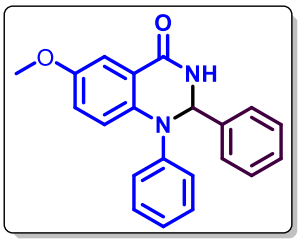

mp 176-177 °C; ^{1}H NMR (400 MHz, $CDCl_3$) δ 8.29 (d, J = 4.6 Hz, 1H), 7.52 (d, J = 7.1 Hz, 2H), 7.44 (d, J = 3.0 Hz, 1H), 7.37 – 7.25 (m, 5H), 7.16 (d, J = 7.9 Hz, 2H), 7.11 (t, J = 7.4 Hz, 1H), 7.05 (d, J = 8.9 Hz, 1H), 6.98 (dd, J = 8.9, 2.6 Hz, 1H), 6.23 (d, J = 4.7 Hz, 1H), 3.81 (s, 3H); ^{13}C NMR (100 MHz, $CDCl_3$) δ 164.3, 154.7, 147.0, 140.6, 138.0, 129.5, 128.6, 128.3, 126.7, 123.7, 122.3, 122.1, 121.8, 121.7, 109.9, 72.7, 55.7; HRMS (ESI-TOF) (*m/z*) calculated $C_{21}H_{19}N_2O_2^+$: 331.1446, found 331.1447 $[M + H]^+$.

6-Chloro-1,2-diphenyl-2,3-dihydroquinazolin-4(1*H*)-one (28ka). White solid, 54 mg (80%);

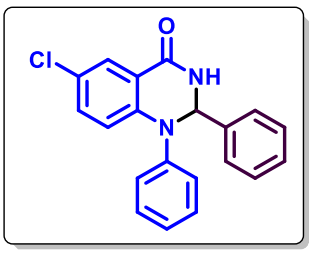

mp 136-137 °C; ^{1}H NMR (400 MHz, $CDCl_3$) δ 7.93 (d, J = 2.5 Hz, 1H), 7.79 (d, J = 4 Hz, 1H), 7.46 – 7.39 (m, 2H), 7.37 – 7.26 (m, 6H), 7.21 – 7.12 (m, 3H), 6.89 (d, J = 8.8 Hz, 1H), 6.18 (d, J = 3.9 Hz, 1H); ^{13}C NMR (100 MHz, $CDCl_3$) δ 163.1, 144.8, 143.9, 139.8, 133.6, 129.8, 128.8, 128.1, 126.9, 126.0, 125.3, 123.8, 120.3, 119.8, 73.1; HRMS (ESI-TOF) (*m/z*) calculated $C_{20}H_{16}ClN_2O^+$: 335.0951, found 335.0936 $[M + H]^+$.

6-Bromo-1,2-diphenyl-2,3-dihydroquinazolin-4(1*H*)-one (28la). White solid, 52 mg (79%); mp

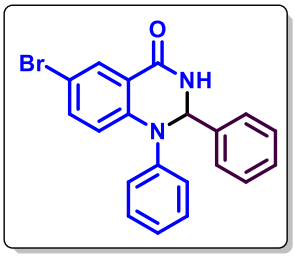

168-169 °C; ^{1}H NMR (400 MHz, $CDCl_3$) δ 8.08 (d, J = 2.5 Hz, 1H), 7.79 (d, J = 4.0 Hz, 1H), 7.44 – 7.38 (m, 3H), 7.37 – 7.27 (m, 5H), 7.20 (d, J = 7.3 Hz, 1H), 7.15 (d, J = 8.1 Hz, 2H), 6.82 (d, J = 8.8 Hz, 1H), 6.17 (d, J = 3.9 Hz, 1H); ^{13}C NMR (100 MHz, $CDCl_3$) δ 163.1, 144.7, 144.3, 139.9, 136.4, 131.1, 129.8, 128.8, 128.8, 126.8, 125.3, 123.7, 120.7,

120.0, 113.1, 73.0; HRMS (ESI-TOF) (*m/z*) calculated $C_{20}H_{16}BrN_2O^+$: 379.0445, found 379.0435 $[M + H]^+$.

2-Phenyl-1-(pyridin-2-yl)-2,3-dihydroquinazolin-4(1*H*)-one (28ma). White solid, 47 mg

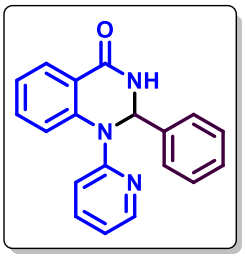

(66%); mp 202-203 °C; ^{1}H NMR (400 MHz, $CDCl_3$) δ 8.42 (d, J = 3.9 Hz, 1H), 8.02 (d, J = 7.6 Hz, 1H), 7.61 – 7.51 (m, 4H), 7.43 – 7.34 (m, 3H), 7.31 – 7.29 (m, 1H), 7.27 – 7.18 (m, 3H), 7.11 (t, J = 7.2 Hz, 1H), 6.97 – 6.94 (m, 1H); ^{13}C NMR (100 MHz, $CDCl_3$) δ 164.2, 156.1, 148.8, 140.7, 140.3, 137.8, 133.1, 128.7, 128.4, 128.0, 126.6, 123.6, 122.5, 121.4, 117.4, 110.7, 66.6; HRMS (ESI-TOF) (*m/z*) calculated $C_{19}H_{16}N_3O^+$: 302.1293, found 302.1282 $[M + H]^+$.

1-Phenyl-2-(*p*-tolyl)-2,3-dihydroquinazolin-4(1*H*)-one (28ab). White solid, 63 mg (85%); mp

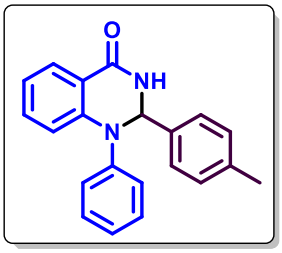

184-185 °C; ^{1}H NMR (400 MHz, $CDCl_3$) δ 7.97 (dd, J = 7.8, 1.7 Hz, 1H), 7.76 (d, J = 4.0 Hz, 1H), 7.37 – 7.30 (m, 5H), 7.20 – 7.14 (m, 3H), 7.10 (d, J = 7.8 Hz, 2H), 6.99 – 6.91 (m, 2H), 6.17 (d, J = 3.9 Hz, 1H), 2.31 (s, 3H); ^{13}C NMR (100 MHz, $CDCl_3$) δ 164.2, 145.5, 145.2, 138.3, 137.3, 133.5, 129.6, 129.4, 128.5, 126.9, 124.9, 123.8, 120.7, 119.3, 118.2, 72.9, 21.1; HRMS (ESI-TOF) (*m/z*) calculated $C_{21}H_{19}N_2O^+$: 315.1497, found 315.1484 $[M + H]^+$.

2-(4-Methoxyphenyl)-1-phenyl-2,3-dihydroquinazolin-4(1*H*)-one (28ac). White solid, 71 mg

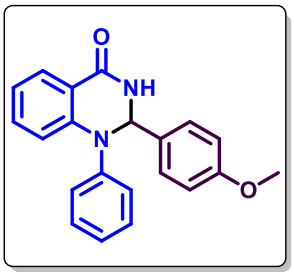

(90%); mp 170-171 °C; ^{1}H NMR (400 MHz, $CDCl_3$) δ 7.97 (dd, J = 7.8, 1.7 Hz, 1H), 7.53 (d, J = 3.4 Hz, 1H), 7.38 – 7.29 (m, 5H), 7.19 – 7.13 (m, 3H), 6.96 (t, J = 7.5 Hz, 1H), 6.86 (d, J = 8.3 Hz, 1H), 6.80 (d, J = 8.3 Hz, 2H), 6.15 (d, J = 3.7 Hz, 1H), 3.76 (s, 3H); ^{13}C NMR (100 MHz, $CDCl_3$) δ 164.2, 159.7, 145.8, 145.0, 133.6, 132.1, 129.6, 128.5, 128.3, 125.1, 124.3, 120.6, 119.0, 117.9, 114.0, 72.8, 55.2; HRMS (ESI-TOF) (*m/z*) calculated $C_{21}H_{19}N_2O_2^+$: 331.1446, found 331.1443 $[M + H]^+$.

2-(4-Chlorophenyl)-1-phenyl-2,3-dihydroquinazolin-4(1*H*)-one (28ad). White solid, 56 mg

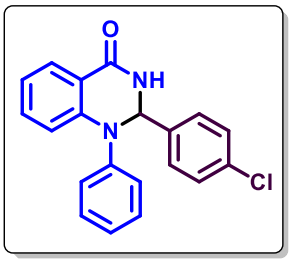

(70%); mp 150-151 °C; ^{1}H NMR (400 MHz, $CDCl_3$) δ 8.22 (d, J = 4.2 Hz, 1H), 7.95 (dd, J = 8.2, 1.7 Hz, 1H), 7.43 – 7.32 (m, 5H), 7.28 – 7.23 (m, 2H), 7.19 – 7.15 (m, 3H), 7.01 – 6.97 (m, 2H), 6.18 (d, J = 4.1 Hz, 1H); ^{13}C NMR (100 MHz, $CDCl_3$) δ 164.3, 145.2, 145.0, 139.0, 134.4, 133.7, 129.7, 128.9, 128.5, 128.3, 125.0, 123.3, 121.1, 119.4, 118.5, 72.4; HRMS (ESI-TOF) (*m/z*) calculated $C_{20}H_{16}ClN_2O^+$: 335.0951, found 335.0943 $[M + H]^+$.

2-(4-(Dimethylamino)phenyl)-1-phenyl-2,3-dihydroquinazolin-4(1*H*)-one (28ae). White solid, 54 mg (66%); mp 162-163 °C; ^{1}H NMR (400 MHz, $CDCl_3$) δ 8.00 (d, J = 7.7 Hz, 1H), 7.36 – 7.24 (m, 5H), 7.20 – 7.11 (m, 3H), 6.95 (t, J = 7.6 Hz, 1H), 6.77 (d, J = 8.3 Hz, 1H), 6.71 (brs, 1H), 6.64 (d, J = 8.2 Hz, 2H), 6.10 (brs, 1H), 2.94 (s, 6H); ^{13}C NMR (100 MHz, $CDCl_3$) δ 164.0, 150.2, 146.4, 144.8, 133.5, 129.6, 128.6, 128.1, 125.2, 125.0, 120.2, 117.6, 112.5, 73.3, 40.7; HRMS (ESI-TOF) (*m/z*) calculated $C_{22}H_{22}N_3O^+$: 344.1762, found 344.1749 $[M + H]^+$.

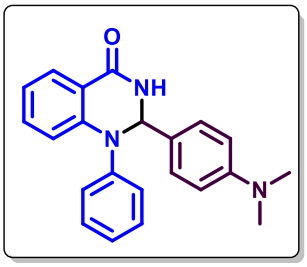

4-(4-Oxo-1-phenyl-1,2,3,4-tetrahydroquinazolin-2-yl)benzonitrile (28af). White solid, 38 mg (49%); mp 200-201 °C; ^{1}H NMR (400 MHz, $CDCl_3$) δ 8.37 (d, J = 4.4 Hz, 1H), 7.94 (d, J = 7.6 Hz, 1H), 7.66 – 7.58 (m, 4H), 7.42 – 7.34 (m, 3H), 7.20 (d, J = 7.3 Hz, 1H), 7.16 (d, J = 7.9 Hz, 2H), 7.07 – 6.99 (m, 2H), 6.23 (d, J = 4.5 Hz, 1H); ^{13}C NMR (100 MHz, $CDCl_3$) δ 163.9, 145.7, 145.3, 134.0, 132.6, 129.9, 129.1, 128.6, 127.7, 125.2, 123.1, 121.7, 119.6, 119.0, 118.3, 112.6, 72.5; HRMS (ESI-TOF) (*m/z*) calculated $C_{21}H_{16}N_3O^+$: 326.1293, found 326.1285 $[M + H]^+$.

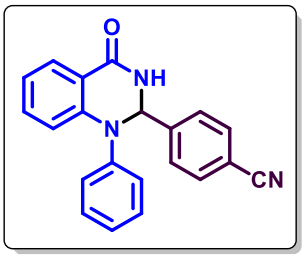

2-([1,1'-Biphenyl]-4-yl)-1-phenyl-2,3-dihydroquinazolin-4(1*H*)-one (28ag). White solid, 77 mg (87%); mp 199-200 °C; ^{1}H NMR (400 MHz, $CDCl_3$) δ 8.22 (d, J = 4.1 Hz, 1H), 7.99 (d, J = 7.8 Hz, 1H), 7.57 – 7.49 (m, 6H), 7.42 (t, J = 7.5 Hz, 2H), 7.39 – 7.31 (m, 4H), 7.22 (d, J = 7.9 Hz, 2H), 7.17 (t, J = 7.4 Hz, 1H), 7.06 – 6.96 (m, 2H), 6.26 (d, J = 4.1 Hz, 1H); ^{13}C NMR (100 MHz, $CDCl_3$) δ 164.4, 145.4, 145.2, 141.3, 140.3, 139.4, 133.6, 129.7, 128.8, 128.6, 127.5, 127.4, 127.3, 127.1, 124.8, 123.4, 120.9, 119.5, 118.4, 72.7; HRMS (ESI-TOF) (*m/z*) calculated $C_{26}H_{21}N_2O^+$: 377.1653, found 377.1645 $[M + H]^+$.

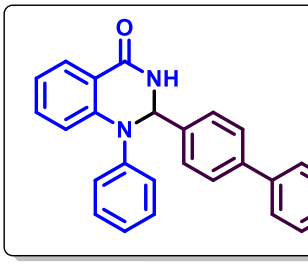

1-Phenyl-2-(3,4,5-trimethoxyphenyl)-2,3-dihydroquinazolin-4(1*H*)-one (28ah). White solid, 85 mg (92%); mp 210-211 °C; ^{1}H NMR (400 MHz, $CDCl_3$) δ 8.09 (d, J = 4.0 Hz, 1H), 7.98 (dd, J = 8.3, 1.7 Hz, 1H), 7.36 (t, J = 7.9 Hz, 3H), 7.22 – 7.15 (m, 3H), 7.02 – 6.95 (m, 2H), 6.65 (s, 2H), 6.14 (d, J = 3.8 Hz, 1H), 3.80 (s, 3H), 3.65 (s, 6H); ^{13}C NMR (100 MHz, $CDCl_3$) δ 164.3, 153.3, 145.5, 145.1, 138.0, 135.8, 133.7, 129.7, 128.5, 125.0,

123.6, 120.8, 119.2, 118.0, 104.1, 73.0, 60.8, 56.0; HRMS (ESI-TOF) (*m/z*) calculated $C_{23}H_{23}N_2O_4^+$: 391.1657, found 391.1651 $[M + H]^+$.

2-(Furan-2-yl)-1-phenyl-2,3-dihydroquinazolin-4(1*H*)-one (28ai). White solid, 50 mg (72%);

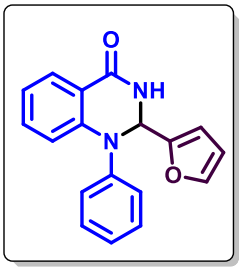

mp 175-176 °C; ^{1}H NMR (400 MHz, $CDCl_3$) δ 8.01 (d, J = 7.8 Hz, 1H), 7.45 – 7.37 (m, 4H), 7.36 – 7.30 (m, 3H), 7.20 (t, J = 7.2 Hz, 1H), 7.02 – 6.93 (m, 2H), 6.31 – 6.25 (m, 2H), 6.15 (d, J = 4.5 Hz, 1H); ^{13}C NMR (100 MHz, $CDCl_3$) δ 164.2, 152.5, 145.1, 144.2, 143.0, 133.5, 129.7, 128.5, 124.8, 123.2, 121.0, 119.1, 118.3, 110.4, 109.0, 67.7; HRMS (ESI-TOF) (*m/z*) calculated $C_{18}H_{15}N_2O_2^+$: 291.1133, found 291.1118 $[M + H]^+$.

1-Phenyl-2-(thiophen-2-yl)-2,3-dihydroquinazolin-4(1*H*)-one (28aj). White solid, 49 mg

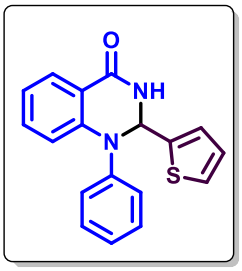

(68%); mp 165-166 °C; ^{1}H NMR (400 MHz, $CDCl_3$) δ 8.00 (d, J = 7.5 Hz, 1H), 7.68 (d, J = 4.3 Hz, 1H), 7.42 – 7.32 (m, 3H), 7.26 – 7.17 (m, 4H), 7.06 (d, J = 3.0 Hz, 1H), 7.01 (t, J = 7.5 Hz, 1H), 6.97 (d, J = 8.3 Hz, 1H), 6.89 (t, J = 4.3 Hz, 1H), 6.37 (d, J = 4.3 Hz, 1H); ^{13}C NMR (100 MHz, $CDCl_3$) δ 164.1, 145.3, 145.2, 144.5, 133.6, 129.7, 128.5, 126.8, 126.4, 126.0, 125.0, 123.4, 121.4, 119.7, 119.2, 70.2; HRMS (ESI-TOF) (*m/z*) calculated $C_{18}H_{15}N_2OS^+$: 307.0905, found 307.0902 $[M + H]^+$.

2,3-Diphenyl-2,3-dihydroquinazolin-4(1*H*)-one (29aa). White solid, 61 mg (86%); mp 205-206

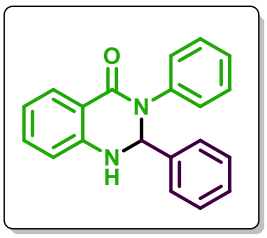

°C (Lit.[43] mp 204-206 °C); ^{1}H NMR (400 MHz, DMSO-d_6) δ 7.74 (dd, J = 7.8, 1.6 Hz, 1H), 7.66 (d, J = 2.8 Hz, 1H), 7.39 (d, J = 6.9 Hz, 2H), 7.36 – 7.30 (m, 4H), 7.29 – 7.23 (m, 4H), 7.19 (t, J = 7.1 Hz, 1H), 6.80 – 6.69 (m, 2H), 6.30 (d, J = 2.7 Hz, 1H); ^{13}C NMR (100 MHz, DMSO-d_6) δ 162.8, 147.0, 141.3, 141.2, 134.3, 129.1, 128.9, 128.8, 128.5, 127.0, 126.7, 126.5, 118.0, 115.8, 115.3, 73.1; HRMS (ESI-TOF) (*m/z*) calculated $C_{20}H_{17}N_2O^+$: 301.1340, found 301.1328 $[M + H]^+$.

2-Phenyl-3-(*p*-tolyl)-2,3-dihydroquinazolin-4(1*H*)-one (29ba). White solid, 63 mg, (90%); mp

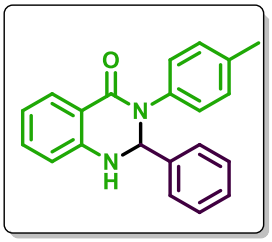

199-200 °C (Lit.[43] mp 198-199 °C); ^{1}H NMR (400 MHz, $CDCl_3$) δ 8.02 (dd, J = 7.8, 1.6 Hz, 1H), 7.39 – 7.34 (m, 2H), 7.32 – 7.26 (m, 4H), 7.09 (brs, 4H), 6.88 (t, J = 7.5 Hz, 1H), 6.61 (d, J = 8.1 Hz, 1H), 6.06 (d, J = 2.4 Hz, 1H), 4.99 (d, J = 2.2 Hz, 1H), 2.30 (s, 3H); ^{13}C NMR (100 MHz, $CDCl_3$) δ 163.2, 145.4, 140.1, 138.0, 136.6, 133.8, 129.6, 129.0, 128.9,

128.7, 126.8, 119.4, 116.8, 114.8, 74.7, 21.1; HRMS (ESI-TOF) (*m/z*) calculated $C_{21}H_{19}N_2O^+$: 315.1497, found 315.1485 $[M + H]^+$.

3-(4-Methoxyphenyl)-2-phenyl-2,3-dihydroquinazolin-4(1*H*)-one (29ca). White solid, 62 mg (91%); mp 215-216 °C (Lit.[43] mp 213-216 °C); ^{1}H NMR (400 MHz, $CDCl_3$) δ 8.01 (dd, J = 7.8, 1.6 Hz, 1H), 7.38 – 7.32 (m, 2H), 7.31 – 7.24 (m, 4H), 7.08 (d, J = 8.9 Hz, 2H), 6.88 (td, J = 7.6, 1.1 Hz, 1H), 6.80 (d, J = 8.8 Hz, 2H), 6.61 (dd, J = 8.1, 1.0 Hz, 1H), 6.04 (d, J = 2.1 Hz, 1H), 4.93 (d, J = 2.1 Hz, 1H), 3.76 (s, 3H); ^{13}C NMR (100 MHz, $CDCl_3$) δ 163.3, 158.2, 145.5, 140.0, 133.8, 133.3, 129.0, 129.0, 128.7, 128.5, 126.9, 119.4, 116.6, 114.7, 114.2, 75.0, 55.4; HRMS (ESI-TOF) (*m/z*) calculated $C_{21}H_{19}N_2O_2^+$: 331.1446, found 331.1444 $[M + H]^+$.

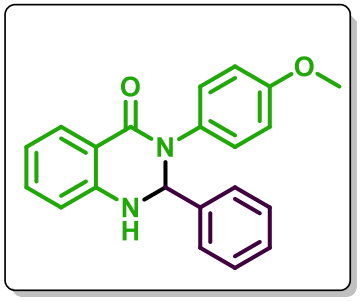

3-(4-Fluorophenyl)-2-phenyl-2,3-dihydroquinazolin-4(1*H*)-one (29da). White solid, 49 mg (72%); mp 225-226 °C; ^{1}H NMR (400 MHz, $CDCl_3$) δ 8.02 (dd, J = 7.8, 1.5 Hz, 1H), 7.37 – 7.32 (m, 3H), 7.31 – 7.26 (m, 3H), 7.16 – 7.10 (m, 2H), 6.99 – 6.93 (m, 2H), 6.91 (td, J = 7.6, 1.0 Hz, 1H), 6.64 (dd, J = 8.1, 1.0 Hz, 1H), 6.07 (d, J = 2.0 Hz, 1H), 4.88 (d, J = 2.0 Hz, 1H); ^{13}C NMR (100 MHz, $CDCl_3$) δ 163.4, 162.1 ($^1J_{C\text{-}F}$ = 245 Hz), 145.5, 139.4, 136.3, 136.3, 134.0, 129.2 ($^3J_{C\text{-}F}$ = 8.0 Hz), 129.1 ($^3J_{C\text{-}F}$ = 6.8 Hz), 128.8, 127.0, 119.6, 116.5, 115.8 ($^2J_{C\text{-}F}$ = 22 Hz), 114.7, 75.0; HRMS (ESI-TOF) (*m/z*) calculated $C_{20}H_{16}FN_2O^+$: 319.1246, found 319.1234 $[M + H]^+$.

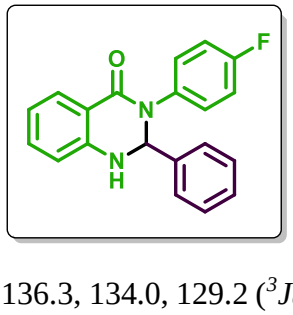

3-(4-Chlorophenyl)-2-phenyl-2,3-dihydroquinazolin-4(1*H*)-one (29ea). White solid, 54 mg (80%); mp 220-221 °C (Lit.[43] mp 217-220 °C); ^{1}H NMR (400 MHz, $CDCl_3$) δ 8.01 (dd, J = 7.8, 1.6 Hz, 1H), 7.38 – 7.28 (m, 6H), 7.25 (d, J = 8.8 Hz, 2H), 7.12 (d, J = 8.4 Hz, 2H), 6.90 (t, J = 7.5 Hz, 1H), 6.64 (d, J = 8.0 Hz, 1H), 6.08 (d, J = 2.1 Hz, 1H), 4.95 (brs, 1H); ^{13}C NMR (100 MHz, $CDCl_3$) δ 163.2, 145.4, 139.4, 139.0, 134.1, 132.4, 129.3, 129.1, 128.9, 128.4, 126.9, 119.7, 116.6, 114.9, 74.7; HRMS (ESI-TOF) (*m/z*) calculated $C_{20}H_{16}ClN_2O^+$: 335.0951, found 335.0943 $[M + H]^+$.

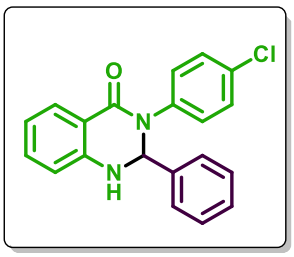

3-(4-Bromophenyl)-2-phenyl-2,3-dihydroquinazolin-4(1*H*)-one (29fa). White solid, 53 mg (81%); mp 223-224 °C (Lit.[43] mp 222-224 °C); ^{1}H NMR (400 MHz, $CDCl_3$) δ 8.02 (dd, J = 7.8, 1.6 Hz, 1H), 7.41 (d, J = 8.8 Hz, 2H), 7.38 – 7.33 (m, 3H), 7.32 – 7.27 (m, 3H), 7.08 (d, J = 8.8 Hz, 2H), 6.91 (t, J = 7.5 Hz, 1H), 6.65 (d, J = 8.0 Hz, 1H), 6.09 (d, J = 2.2 Hz, 1H), 4.84 (brs, 1H); ^{13}C NMR (100 MHz, $CDCl_3$) δ 163.1, 145.3, 139.5, 139.4, 134.1, 132.1, 129.3, 129.1, 128.9, 128.7, 126.9, 120.4, 119.8, 116.6, 114.9, 74.6; HRMS (ESI-TOF) (*m/z*) calculated $C_{20}H_{16}BrN_2O^+$: 379.0445, found 379.0436 $[M + H]^+$.

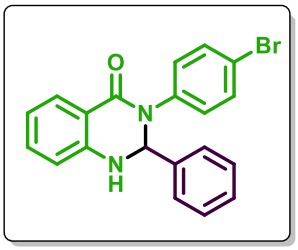

2-Phenyl-3-(pyridin-4-yl)-2,3-dihydroquinazolin-4(1*H*)-one (29ga). White solid, 51 mg (70%); mp 210-211 °C; ^{1}H NMR (400 MHz, $CDCl_3$) δ 8.53 (d, J = 5.6 Hz, 2H), 8.04 (d, J = 7.9 Hz, 1H), 7.42 – 7.29 (m, 6H), 7.27 – 7.23 (m, 2H), 6.92 (t, J = 7.5 Hz, 1H), 6.70 (d, J = 8.1 Hz, 1H), 6.21 (d, J = 3.1 Hz, 1H), 5.10 (d, J = 3.2 Hz, 1H); ^{13}C NMR (100 MHz, $CDCl_3$) δ 163.0, 150.5, 148.0, 144.7, 139.0, 134.6, 129.3, 129.2, 129.1, 126.4, 120.2, 119.0, 117.1, 115.7, 72.8; HRMS (ESI-TOF) (*m/z*) calculated $C_{19}H_{16}N_3O^+$: 302.1293, found 302.1287 $[M + H]^+$.

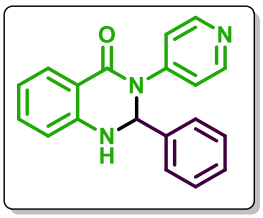

3-Benzyl-2-phenyl-2,3-dihydroquinazolin-4(1*H*)-one (29ha). White solid, 47 mg (68%); mp 163-164 °C (Lit.[41] mp 165-166 °C); ^{1}H NMR (400 MHz, $CDCl_3$) δ 8.05 (d, J = 8.0 Hz, 1H), 7.39 – 7.27 (m, 9H), 7.26 – 7.23 (m, 2H), 6.89 (t, J = 7.5 Hz, 1H), 6.53 (d, J = 8.0 Hz, 1H), 5.66 – 5.60 (m, 2H), 4.53 (brs, 1H), 3.69 (d, J = 15.3 Hz, 1H); ^{13}C NMR (100 MHz, $CDCl_3$) δ 163.2, 145.1, 139.4, 136.8, 133.7, 129.3, 129.0, 128.8, 128.6, 128.0, 127.5, 126.6, 119.2, 115.7, 114.3, 71.1, 46.9; HRMS (ESI-TOF) (*m/z*) calculated $C_{21}H_{19}N_2O^+$: 315.1497, found 315.1485 $[M + H]^+$.

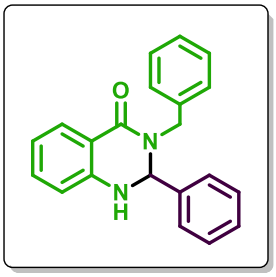

3-Phenyl-2-(*p*-tolyl)-2,3-dihydroquinazolin-4(1*H*)-one (29ab). White solid, 66 mg (88%); mp 214-215 °C (Lit.[43] mp 212-215 °C); ^{1}H NMR (400 MHz, $CDCl_3$) δ 8.02 (dd, J = 7.8, 1.6 Hz, 1H), 7.32 – 7.26 (m, 4H), 7.25 – 7.16 (m, 4H), 7.08 (d, J = 7.9 Hz, 2H), 6.88 (td, J = 7.6, 1.1 Hz, 1H), 6.61 (dd, J = 8.1, 1.0 Hz, 1H), 6.05 (d, J = 2.4 Hz, 1H), 5.01 (d, J = 2.4 Hz, 1H), 2.30 (s, 3H); ^{13}C NMR (100 MHz, $CDCl_3$) δ 163.2, 145.5, 140.7, 138.8, 137.0, 133.8, 129.4, 129.0, 128.9, 126.9, 126.7, 126.7, 119.4, 116.9, 114.9, 74.4, 21.1; HRMS (ESI-TOF) (*m/z*) calculated $C_{21}H_{19}N_2O^+$: 315.1497, found 315.1490 $[M + H]^+$.

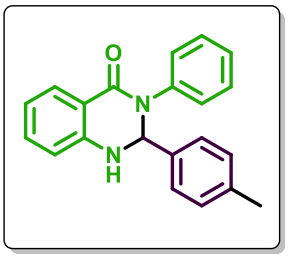

4-(4-Oxo-3-phenyl-1,2,3,4-tetrahydroquinazolin-2-yl)benzonitrile (29af). White solid, 43 mg (56%); mp 201-202 °C (Lit.[46] mp 202.4-204.6 °C); ^{1}H NMR (400 MHz, $CDCl_3$) δ 8.01 (d, J = 7.9 Hz, 1H), 7.56 (d, J = 8.0 Hz, 2H), 7.49 (d, J = 8.0 Hz, 2H), 7.38 – 7.27 (m, 3H), 7.26 – 7.18 (m, 3H), 6.93 (t, J = 7.6 Hz, 1H), 6.67 (d, J = 8.1 Hz, 1H), 6.14 (d, J = 3.0 Hz, 1H), 5.15 (d, J = 3.1 Hz, 1H); ^{13}C NMR (100 MHz, $CDCl_3$) δ 162.8, 145.1, 144.7, 140.3, 134.3, 132.6, 129.24, 129.22, 129.1, 127.6, 127.1, 126.5, 120.2, 118.2, 117.0, 115.4, 112.8, 73.7; HRMS (ESI-TOF) (*m/z*) calculated $C_{21}H_{16}N_3O^+$: 326.1293, found 326.1287 $[M + H]^+$.

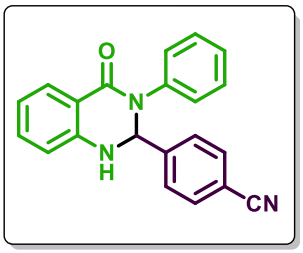

2-(Furan-2-yl)-3-phenethyl-2,3-dihydroquinazolin-4(1*H*)-one (29ii). White solid, 51 mg (77%); mp 146-147 °C (Lit.[51] mp 147-148 °C); ^{1}H NMR (400 MHz, $CDCl_3$) δ 7.97 (d, J = 7.8 Hz, 1H), 7.37 – 7.31 (m, 3H), 7.30 – 7.21 (m, 4H), 6.90 (t, J = 7.5 Hz, 1H), 6.63 (d, J = 8.0 Hz, 1H), 6.26 (brs, 1H), 6.20 (d, J = 2.6 Hz, 1H), 5.48 (d, J = 2.7 Hz, 1H), 4.61 (d, J = 2.5 Hz, 1H), 4.39 – 4.30 (m, 1H), 3.20 – 3.11 (m, 1H), 3.07 – 2.90 (m, 2H); ^{13}C NMR (100 MHz, $CDCl_3$) δ 162.9, 152.2, 145.0, 142.9, 139.1, 133.3, 129.0, 128.6, 128.4, 126.5, 119.8, 116.8, 114.8, 110.4, 108.3, 66.3, 47.6, 34.8; HRMS (ESI-TOF) (*m/z*) calculated $C_{20}H_{19}N_2O_2^+$: 319.1446, found 319.1437 $[M + H]^+$.

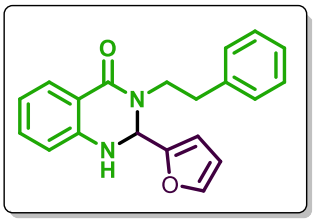

Procedure for the synthesis of 41ii

Column purified 2-(2-furyl)-3-(2-phenylethyl)-2,3-dihydroquinazolin-4(1*H*)-one (**29ii**) (30 mg, 0.09 mmol) was treated with DDQ (21 mg, 0.09 mmol) in DCM solvent (1 mL) for an hour at room temperature under atmospheric air. After the completion, the reaction mixture was quenched by addition of water. The oxidized product **41ii** was extracted using DCM and washed multiple times with water to remove by-products. The organic layer was dried over sodium sulfate and concentrated under vacuum to afford pure **41ii** as a solid product.

2-(Furan-2-yl)-3-phenethylquinazolin-4(3*H*)-one (41ii). Brown solid, 28 mg (95%); mp 110-111 °C (Lit.[62] mp 101-102 °C); ^{1}H NMR (400 MHz, $CDCl_3$) δ 8.36 (d, J = 8.0 Hz, 1H), 7.83 – 7.73 (m, 2H), 7.69 (brs, 1H), 7.53 (t, J = 7.4 Hz, 1H), 7.37 – 7.29 (m, 2H), 7.28 – 7.22 (m, 3H), 7.13 (d, J = 3.5 Hz, 1H), 6.65 (t, J = 2.5 Hz, 1H), 4.47 (t, J = 8.2 Hz, 2H), 3.15 (t, J = 8.2 Hz, 2H); ^{13}C NMR (100 MHz, $CDCl_3$) δ 162.3, 147.9, 147.4, 146.2, 144.2,

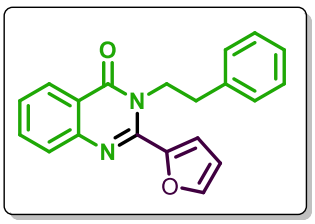

138.2, 134.4, 128.8, 128.7, 127.6, 127.2, 126.8, 126.7, 120.8, 115.4, 112.1, 47.1, 35.2; HRMS (ESI-TOF) (*m/z*) calculated $C_{20}H_{17}N_2O_2^+$: 317.1290, found 317.1286 $[M + H]^+$.

2-(4-Hydroxybenzyl)-1-phenyl-1,2-dihydro-3*H*-indazol-3-one (28'ak). White solid, 68 mg

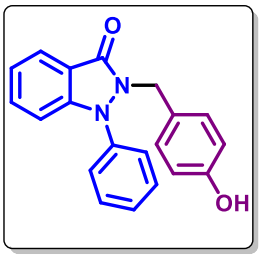

(90%); mp 120-121 °C; ^{1}H NMR (400 MHz, DMSO-d_6) δ 9.39 (s, 1H), 7.80 (d, J = 7.8 Hz, 1H), 7.60 – 7.48 (m, 3H), 7.45 (t, J = 7.3 Hz, 1H), 7.30 (d, J = 7.7 Hz, 2H), 7.25 (t, J = 7.6 Hz, 1H), 7.08 (d, J = 8.3 Hz, 1H), 6.85 (d, J = 8.0 Hz, 2H), 6.62 (d, J = 8.0 Hz, 2H), 4.76 (s, 2H); ^{13}C NMR (100 MHz, DMSO-d_6) δ 163.4, 157.3, 149.6, 140.5, 133.4, 130.5, 129.6, 128.5, 127.1, 125.5, 123.9, 123.2, 117.8, 115.6, 112.4, 45.7; HRMS (ESI-TOF) (*m/z*) calculated $C_{20}H_{17}N_2O_2^+$: 317.1290, found 317.1277 $[M + H]^+$.

2-((1*H*-indol-3-yl)methyl)-1-phenyl-1,2-dihydro-3*H*-indazol-3-one (28'al). White solid, 69 mg

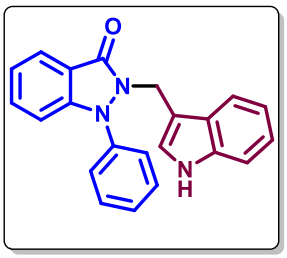

(85%); mp 125-126 °C; ^{1}H NMR (400 MHz, $CDCl_3$) δ 8.13 (s, 1H), 7.91 (d, J = 7.8 Hz, 1H), 7.59 (d, J = 7.9 Hz, 1H), 7.51 (t, J = 7.6 Hz, 2H), 7.44 – 7.36 (m, 2H), 7.32 (d, J = 8.1 Hz, 1H), 7.28 – 7.25 (m, 2H), 7.19 – 7.14 (m, 2H), 7.08 (t, J = 7.5 Hz, 1H), 6.97 – 6.94 (m, 2H), 5.18 (s, 2H); ^{13}C NMR (100 MHz, $CDCl_3$) δ 164.1, 149.7, 140.8, 135.8, 132.2, 129.8, 127.9, 126.6, 125.4, 124.3, 124.0, 122.4, 122.2, 119.9, 119.4, 118.0, 111.6, 111.5, 111.0, 37.8; HRMS (ESI-TOF) (*m/z*) calculated $C_{22}H_{18}N_3O^+$: 340.1450, found 340.1441 $[M + H]^+$.

Procedure for the methylation of 28'ak

To an oven-dried 10-mL round-bottom flask containing 2-(4-hydroxybenzyl)-1-phenyl-1,2-dihydro-3*H*-indazol-3-one (**28'ak**) (50 mg, 1 equiv) in DMF (3 mL), sodium hydride (2 equiv), methyl iodide (1.5 equiv) was added under nitrogen air. The reaction mixture was stirred at room temperature for 2 h (monitored by TLC). After the completion of the reaction, the reaction mixture was quenched by addition of ice-cold water/. The reaction mixture was extracted with EtOAc (20 mL x 2). The organic layers were separated and concentrated under reduced pressure to afford a residue, which was purified by column chromatography (SiO_2 100−200 mesh) using hexanes/EtOAc (7/3) as eluent system to afford **28'ac** in pure form.

2-(4-Methoxybenzyl)-1-phenyl-1,2-dihydro-3*H*-indazol-3-one (28'ac). Colorless liquid, 40 mg (77%); ^{1}H NMR (400 MHz, $CDCl_3$) δ 7.94 (d, J = 7.9 Hz, 1H), 7.50 (t, J = 6.9 Hz, 2H), 7.43 – 7.41 (m, 2H), 7.23 – 7.19 (m, 3H), 7.06 (d, J = 8.2 Hz, 2H), 6.96 (d, J = 8.3 Hz, 1H), 6.76 (d, J = 8.3 Hz, 2H), 4.91 (s, 2H), 3.76 (s, 3H).; ^{13}C NMR (100 MHz, $CDCl_3$) δ 163.9, 159.1, 149.8, 140.5, 132.4, 129.8, 129.7, 128.5, 128.3, 125.8, 124.1, 122.6, 118.0, 113.8, 111.8, 55.2, 45.7; HRMS (ESI-TOF) (*m/z*) calculated $C_{21}H_{19}N_2O_2^+$: 331.1446, found 331.1465 $[M + H]^+$.

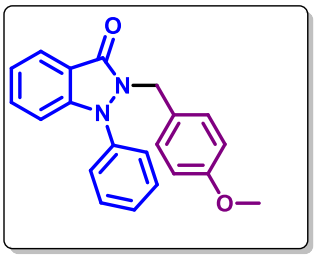

3.4 Single Crystal X-Ray Diffraction Studies

A suitable crystal was chosen with the help of a light microscope and was mounted in a nylon loop to attach to a goniometer head. A Kappa APEX II diffractometer equipped with a CCD detector and sealed-tube monochromated MoKα radiation was used for the entire measurement (centering, initial crystal evaluation, and data collection) by the program APEX. All data were integrated, and reflections were fitted and values of F^2 and $\sigma(F^2)$ for each reflection were obtained by using the program SAINT.[63] Finally, data were also corrected for the Lorentz and polarization effects. Using the subroutine XPREP[63] the space group was determined, and an absorption correction (SADABS) and merging of data were performed to generate the necessary files for solution and refinement. A structure solution was obtained by direct methods using the SHELXS program of the SHELXTL package and was refined using SHELXL.[64,65] All non-hydrogen atoms were refined with anisotropic displacement parameters. All hydrogen atoms were placed in ideal positions and refined as riding atoms with individual isotropic displacement parameters. All figures were drawn using MERCURY V 3.0.[66]

3.4.1 Crystal data for 28ab (CCDC No. 2207706). $C_{21}H_{18}N_2O$, Mr = 314.37 g/mol, triclinic, space group *P-1 (No. 2)*, a = 7.742(3) Å, b = 10.438(4) Å, c = 10.878(4) Å, α = 100.711(12)°, β = 107.441(11)°, γ = 91.506(12)°, V = 820.9(5) Å^3, Z = 2, T = 108(2) K, D_{calcd} = 1.272 g/cm^3; Full matrix least-square on F^2; R_1 = 0.039, wR_2 = 0.1003 for 2654 observed reflections [$I > 2\sigma(I)$] and R_1 = 0.0425, wR_2 = 0.1034 for all 2892 reflections; number of parameters = 222; GOF = 1.029.

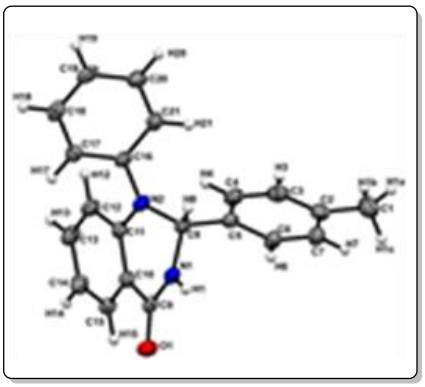

3.5 References

1. An, C.-Y.; Li, X.-M.; Li, C.-S.; Wang, M.-H.; Xu, G.-M.; Wang, B.-G. *Marine Drugs* **2013**, *11*, 2682-2694.
2. Jiang, S.; Zeng, Q.; Gettayacamin, M.; Tungtaeng, A.; Wannaying, S.; Lim, A.; Hansukjariya, P.; Okunji, C. O.; Zhu, S.; Fang, D. *Antimicrobial Agents and Chemotherapy* **2005**, *49*, 1169-1176.
3. Kametani, T.; Van Loc, C.; Higa, T.; Koizumi, M.; Ihara, M.; Fukumoto, K. *Journal of the American Chemical Society* **1977**, *99*, 2306-2309.
4. Olesen, K. H.; Dupont, B.; Flensted-Jensen, E. *Journal of Internal Medicine* **1970**, *187*, 33-40.
5. Van Zyl, E. F. *Forensic Science International* **2001**, *122*, 142-149.
6. Rajput, R.; Mishra, A. P. *International Journal of Pharmacy and Pharmaceutical Sciences* **2012**, *4*, 66-70.
7. Radwan, A. A.; Alanazi, F. K. *Quinazolinone and Quinazoline Derivatives* **2020**, *11*.
8. Kshirsagar, U. *Organic & Biomolecular Chemistry* **2015**, *13*, 9336-9352.
9. Yan, B.-R.; Lv, X.-Y.; Du, H.; Gao, M.-N.; Huang, J.; Bao, X.-P. *Chemical Papers* **2016**, *70*, 983-993.
10. Asif, M. *International Journal of Medicinal Chemistry* **2014**, *2014*, 1-28.
11. Shao, L.-H.; Fan, S.-L.; Meng, Y.-F.; Gan, Y.-Y.; Shao, W.-B.; Wang, Z.-C.; Chen, D.-P.; Ouyang, G.-P. *New Journal of Chemistry* **2021**, *45*, 4626-4631.
12. Rakesh, K.; Darshini, N.; Shubhavathi, T.; Mallesha, N. *Organic & Medicinal Chemistry International Journal* **2017**, *2*, 41-45.
13. Al-Amiery, A. A.; Kadhum, A. A. H.; Shamel, M.; Satar, M.; Khalid, Y.; Mohamad, A. B. *Medicinal Chemistry Research* **2014**, *23*, 236-242.
14. Yang, X.; Cheng, G.; Shen, J.; Kuai, C.; Cui, X. *Organic Chemistry Frontiers* **2015**, *2*, 366-368.
15. Li, Z.; Dong, J.; Chen, X.; Li, Q.; Zhou, Y.; Yin, S.-F. *The Journal of Organic Chemistry* **2015**, *80*, 9392-9400.
16. Chen, X.; Chen, T.; Zhou, Y.; Han, D.; Han, L.-B.; Yin, S.-F. *Organic & Biomolecular Chemistry* **2014**, *12*, 3802-3807.
17. Huang, J.; Chen, W.; Liang, J.; Yang, Q.; Fan, Y.; Chen, M.-W.; Peng, Y. *The Journal of Organic Chemistry* **2021**, *86*, 14866-14882.
18. Ge, W.; Zhu, X.; Wei, Y. *RSC Advances* **2013**, *3*, 10817-10822.

19. Shen, G.; Zhou, H.; Du, P.; Liu, S.; Zou, K.; Uozumi, Y. *RSC Advances* **2015**, *5*, 85646-85651.
20. Huang, C.; Fu, Y.; Fu, H.; Jiang, Y.; Zhao, Y. *Chemical Communications* **2008**, 6333-6335.
21. Liu, X.; Fu, H.; Jiang, Y.; Zhao, Y. *Angewandte Chemie International Edition* **2009**, *121*, 354-357.
22. Dubey, A. V.; Kumar, A. V. *ACS Sustainable Chemistry & Engineering* **2018**, *6*, 14283-14291.
23. Upadhyaya, K.; Thakur, R. K.; Shukla, S. K.; Tripathi, R. P. *The Journal of Organic Chemistry* **2016**, *81*, 5046-5055.
24. Sahoo, S.; Pal, S. *The Journal of Organic Chemistry* **2021**, *86*, 18067-18080.
25. Yu, X.; Gao, L.; Jia, L.; Yamamoto, Y.; Bao, M. *The Journal of Organic Chemistry* **2018**, *83*, 10352-10358.
26. Collet, J. W.; Van Der Nol, E. A.; Roose, T. R.; Maes, B. U.; Ruijter, E.; Orru, R. V. *The Journal of Organic Chemistry* **2020**, *85*, 7378-7385.
27. Liang, Y.; Tan, Z.; Jiang, H.; Zhu, Z.; Zhang, M. *Organic Letters* **2019**, *21*, 4725-4728.
28. Hikawa, H.; Ino, Y.; Suzuki, H.; Yokoyama, Y. *The Journal of Organic Chemistry* **2012**, *77*, 7046-7051.
29. Sadig, J. E.; Foster, R.; Wakenhut, F.; Willis, M. C. *The Journal of Organic Chemistry* **2012**, *77*, 9473-9486.
30. Li, H.; He, L.; Neumann, H.; Beller, M.; Wu, X.-F. *Green Chemistry* **2014**, *16*, 1336-1343.
31. Jiang, X.; Tang, T.; Wang, J.-M.; Chen, Z.; Zhu, Y.-M.; Ji, S.-J. *The Journal of Organic Chemistry* **2014**, *79*, 5082-5087.
32. Ji, F.; Lv, M.-F.; Yi, W.-B.; Cai, C. *Organic & Biomolecular Chemistry* **2014**, *12*, 5766-5772.
33. Qian, C.; Liu, K.; Tao, S.-W.; Zhang, F.-L.; Zhu, Y.-M.; Yang, S.-L. *The Journal of Organic Chemistry* **2018**, *83*, 9201-9209.
34. Wang, K.; Chen, H.; Dai, X.; Huang, X.; Feng, Z. *RSC Advances* **2021**, *11*, 13119-13123.
35. Elfeky, S. M.; Sobahi, T. R.; Gineinah, M. M.; Ahmed, N. S. *Archiv der Pharmazie* **2020**, *353*, 1900211.
36. Samim, S. A.; Roy, B. C.; Nayak, S.; Kundu, S. *The Journal of Organic Chemistry* **2020**, *85*, 11359-11367.
37. Villalba, F.; Albéniz, A. C. *Advanced Synthesis & Catalysis* **2021**, *363*, 4795-4804.
38. Nikooei, N.; Dekamin, M. G.; Valiey, E. *Research on Chemical Intermediates* **2020**, *46*, 3891-3909.

39. Ahmadian, F.; Barmak, A.; Ghaderi, E.; Bavadi, M.; Raanaei, H.; Niknam, K. *Journal of the Iranian Chemical Society* **2019**, *16*, 2647-2658.

40. Dutta, A.; Trivedi, P.; Kulshrestha, A.; Kumar, A.; Chaturvedi, V.; Sarma, D. *Applied Organometallic Chemistry* **2021**, *35*, e6116.

41. Shaabani, A.; Afshari, R.; Hooshmand, S. E. *New Journal of Chemistry* **2017**, *41*, 8469-8481.

42. Mohammadsaleh, F.; Barmak, A.; Hajipou, A.; Jajarmi, S.; Niknam, K. *Journal of Organometallic Chemistry* **2022**, *962*, 122271.

43. Azizi, S.; Soleymani, J.; Hasanzadeh, M. *Nanocomposites* **2020**, *6*, 31-40.

44. Naik, M.; Rodrigues, L.; Torney, P.; Salker, A. *Journal of Chemical Sciences* **2022**, *134*, 1-8.

45. Hamidi, Z.; Abdollahi-Alibeik, M.; Mosavian, S. Y. *Silicon* **2018**, *10*, 2491-2497.

46. Yang, Y.; Fu, R.; Liu, Y.; Cai, J.; Zeng, X. *Tetrahedron* **2020**, *76*, 131312.

47. Mohammadi, M. K.; Saghanezhad, S. J.; Razzaghi-asl, N. *Bulletin of the Chemical Society of Ethiopia* **2017**, *31*, 535-544.

48. Rajput, R. *International Journal of Pharmaceutical Sciences Review and Research* **2020**, *11*, 3912-3922.

49. Ghorbani-Choghamarani, A.; Taghipour, T. *Letters in Organic Chemistry* **2011**, *8*, 470-476.

50. Hao, X.; Deng, J.; Zhang, H.; Liang, Z.; Lei, F.; Wang, Y.; Yang, X.; Wang, Z. *Bioorganic & Medicinal Chemistry* **2022**, *55*, 116595.

51. Zaytsev, V. P.; Revutskaya, E. L.; Nikanorova, T. V.; Nikitina, E. V.; Dorovatovskii, P. V.; Khrustalev, V. N.; Yagafarov, N. Z.; Zubkov, F. I.; Varlamov, A. V. *Synthesis* **2017**, *49*, 3749-3767.

52. Sharma, M.; Pandey, S.; Chauhan, K.; Sharma, D.; Kumar, B.; Chauhan, P. M. *The Journal of Organic Chemistry* **2012**, *77*, 929-937.

53. Kumar, P.; Matta, A.; Singh, S.; Van der Eycken, J.; Len, C.; Parmar, V. S.; Van der Eycken, E. V.; Singh, B. K. *Synthetic Communications* **2017**, *47*, 756-763.

54. Sriramoju, V.; Kurva, S.; Madabhushi, S. *New Journal of Chemistry* **2018**, *42*, 3188-3191.

55. Gogoi, K.; Bora, B. R.; Borah, G.; Sarma, B.; Gogoi, S. *Chemical Communications* **2021**, *57*, 1388-1391.

56. Zhang, K.; El Bouakher, A.; Levaique, H.; Bignon, J.; Retailleau, P.; Alami, M.; Hamze, A. *The Journal of Organic Chemistry* **2019**, *84*, 13807-13823.

57. Zhu, C.; Chen, P.; Zhu, R.; Lin, Z.; Wu, W.; Jiang, H. *Chemical Communications* **2017**, *53*, 2697-2700.

58. Lingayya, R.; Vellakkaran, M.; Nagaiah, K.; Nanubolu, J. B. *Advanced Synthesis & Catalysis* **2016**, *358*, 81-89.

59. Lonka, M. R.; Zhang, J.; Gogula, T.; Zou, H. *Organic & Biomolecular Chemistry* **2019**, *17*, 7455-7460.

60. Xu, S.; Wu, G.; Ye, F.; Wang, X.; Li, H.; Zhao, X.; Zhang, Y.; Wang, J. *Angewandte Chemie International Edition* **2015**, *127*, 4752-4755.

61. Choudhary, D.; Khatri, V.; Basak, A. K. *Organic Letters* **2018**, *20*, 1703-1706.

62. Kumar, R. A.; Maheswari, C. U.; Ghantasala, S.; Jyothi, C.; Reddy, K. R. *Advanced Synthesis & Catalysis* **2011**, *353*, 401-410.

63. *APEX2, SADABS and SAINT*; Bruker AXS inc: Madison, WI, USA, **2015**.

64. Sheldrick, G. M. *Acta Crystallography Section. A Foundation Advances* **2015**, *71*, 3-8.

65. Sheldrick, G. M. *Acta Crystallography Section C: Foundation Advances* **2015**, *71*, 3-8.

66. Macrae, C. F.; Bruno, I. J.; Chisholm, J. A.; Edginton, P. R.; McCabe, P.; Pidocck, E.; Rodriguez-Monge, L.; Taylor, T.; Van de Streek, J.; Wood, P. A. *Journal of Applied Crystallography* **2008**, *41*, 466.

Chapter 4

Conclusions of the Thesis

4.1 General Conclusions

Synthesis of fused *N*-heterocycles has always been an interesting area of chemical research considering their high applications in medicinal and material chemistry as pharmaceuticals, agrochemicals, sensors, gelators *etc.* However, the development of greener methodologies by employing easily available starting materials, with minimization of synthetic steps and high atom-economy has been a long thirst for synthetic chemists. In this concern, transition metal-catalyzed directing group-assisted cross-dehydrogenative coupling strategy has emerged as a powerful tool in organic synthesis to construct C-C/C-hetero bonds.

Strikingly, indazol-3-one nucleus has been recognized as a privileged scaffold that constitute an integral part of functionalized and indazolo-fused heterocycles with interesting biological activities. Particularly, the functionalization of *N*-aryl-1,2-dihydro-3*H*-indazol-3-ones was only explored to a limited extent at the time of commencement of this research work. Thus, the demand of developing efficient methodologies for synthesizing functionalized/fused *N*-arylindazolones *via* transition metal-catalyzed C-H activation/functionalization continues unabated. The current thesis entitled "**Transition Metal-Catalyzed Transformations of *N*-Arylindazolones to Fused-Diazaheterocycles *via* C-C/C-N Bond Formations**" was successfully executed in due diligence of sustainable chemistry, and the thesis has been divided into four chapters (Figure 4.1.1).

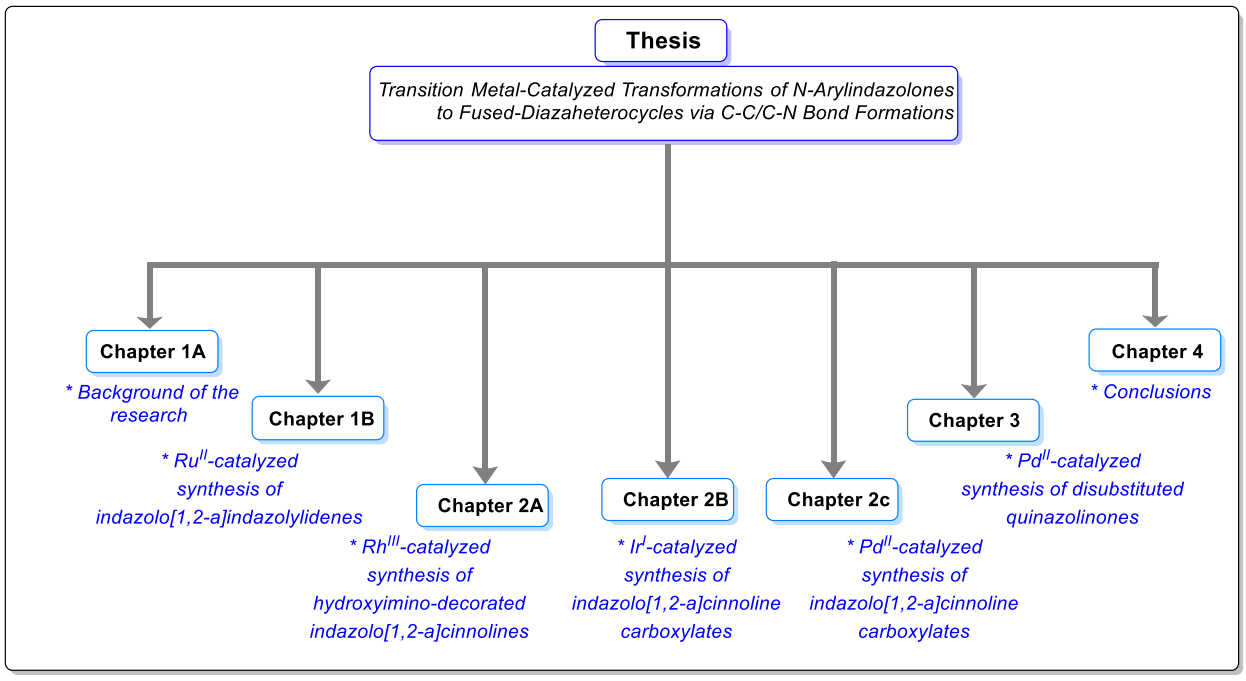

Figure 4.1.1 A diagram describing the systematic division of the thesis

4.2 Specific Conclusions

Chapter 1A: Background of the research

This chapter of the thesis commences with a brief background on transition metal-catalyzed cross-dehydrogenative coupling (CDC) strategies in C-C/C-N bond formations achieved by eminent research groups *via* C-H activation/functionalization, and general mechanistic pathways involved in these processes. This has been followed by an overview of directing group-assisted C-H activation with the focus on explaining the role of amide functionality in chelation-assisted C-H functionalization. Moreover, this chapter briefly describes the crucial role played by different transition metals (Pd, Rh, Ru, Ir) in C-H activation strategies. Finally, the chapter briefly summarizes the importance of benzodiazines, particularly 1,2-dihydro-3*H*-indazol-3-one scaffold, and the rationale for pursuing this research work by exploring the directing group ability of inbuilt cyclic amide group in *N*-aryl-1,2-dihydro-3*H*-indazol-3-ones and aiming to functionalize it with varied coupling partners primarily *via* chelation-assisted transition metal-catalyzed C-H activation notion (Figure 4.2.1).

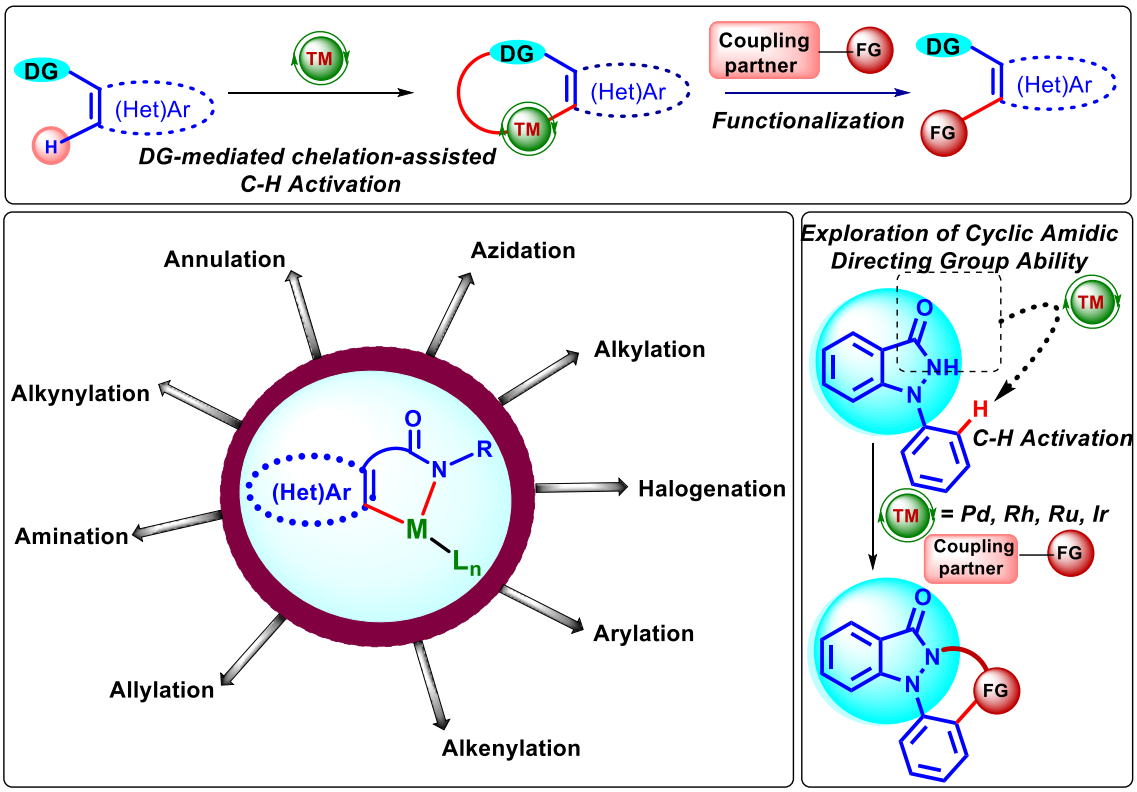

Figure 4.2.1 A graphical representation on the usage of amide-assisted C-H functionalization/annulation CDC strategies, and the rationale for the current thesis work

Chapter 1B: Ruthenium-Catalyzed [4+1] Annulation of *N*-Arylindazolones with Acrylates to access Indazolo[1,2-*a*]indazolylidenes

This chapter initially describes a brief introduction on the biological importance of functionalized/fused-indazoles, followed by an overview on the existing literature reports on synthesis of indazolo-fused heterocycles. Thereafter, the chapter summarizes significant work established by various research groups on transition metal-catalyzed protocols developed towards the synthesis of new heterocyclic frameworks for alkenylation and [*m*+*n*] annulation strategies, employing acrylates as coupling partners. Inspired from the existing literature studies, the synthesis of diversely substituted indazolo[1,2-*a*]indazolylidenes was executed by the coupling of various *N*-aryl-1,2-dihydro-3*H*-indazol-3-ones and acrylates *via* Ru^{II}-catalyzed cross-dehydrogenative strategy using KPF_6 as an additive and CsOAc as a base in toluene (Scheme 4.2.1). This methodology furnished good yields of expected tetracyclic products with electron-withdrawing (halogens or nitro) substituents on aryl ring of indazolone substrate, whereas with electron-releasing (Me or OMe) groups, moderate yields of target products were obtained. A detailed mechanistic investigation was conducted to elucidate the mechanism of the protocol, including isolation of an intermediate at lower temperature, isotopic labelling and kinetic isotopic effect studies. Parallel KIE experiment suggested a k_H/k_D value of 2.9, while a P_H/P_D value of 3.1 was determined by an intercompetitive experiment. These results suggested that the reaction proceeds through the formation of a ruthenacyclic intermediate *via* amidic N-H assisted C-H bond activation, which on vinylic coordination, migratory insertion, *β*-hydride-elimination, intramolecular aza-Michael addition and dehydrogenation produces the desired product.

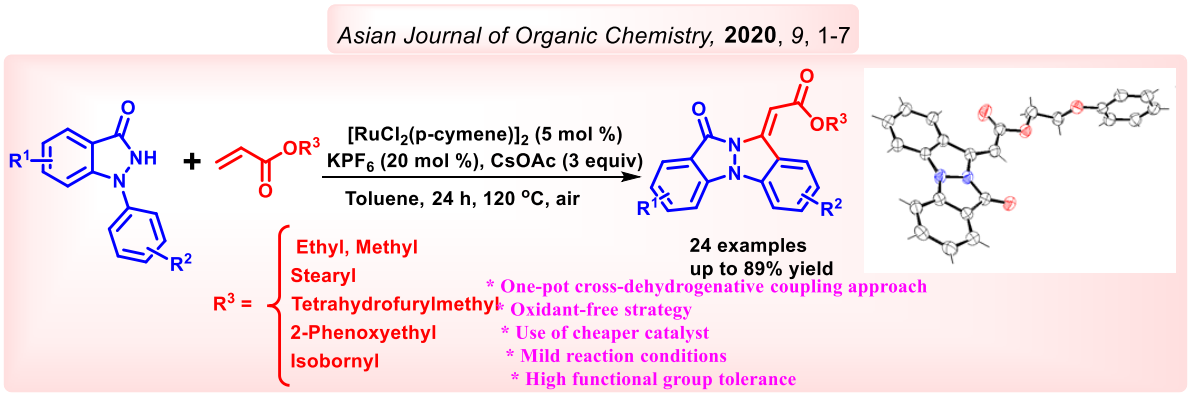

Scheme 4.2.1 Ru-catalyzed [4+1] annulation strategy for the synthesis of indazolo[1,2-*a*]indazolylidenes using acrylates

Chapter 2A: Rhodium-catalyzed [4+2] Annulation of *N*-Arylindazolones with Nitroolefins to access Hydroxyimino-decorated Indazolo[1,2-*a*]cinnolines

This chapter commences with summarizing the importance of functionalized and fused-cinnolines. Particularly, it documents the literature studies on cinnoline-fused heterocyclic frameworks constructed by oxidative annulation of various *N*-aryl heterocycles with different coupling partners *via* directing group-assisted transition metal-catalyzed C-H activation protocols. Thereafter, a brief discussion on the development of C-C/C-N bond formations by the utilization of nitroolefins under transition metal-catalysis has been included. Inspired from limited annulation/functionalization studies on nitroolefins, a reductive strategy for the [4+2] annulation of *N*-aryl-1,2-dihydro-3*H*-indazol-3-one with easily accessible nitroolefins was achieved to afford hydroxyimino-decorated indazolo[1,2-*a*]cinnolines under Rh^{III}-catalyzed conditions in ethanol (Scheme 4.2.2). Detailed spectroscopic analysis of the products, including the X-ray crystal structure of one of the products provided a clear evidence for the assigned structure. Mechanistic investigations, including deuterium labeling experiment and *in situ* ESI-MS reaction monitoring provided a support to the plausible mechanism of this external reducing agent-free strategy. These investigations suggested that the reaction initially followed a S_EAr pathway to form a five-membered rhodacyclic intermediate, which upon olefin insertion, migratory insertion, demetallation and finally reduction of nitro group by concomitant protonation of the two oxygen atoms, and subsequent dehydration generates the expected product.

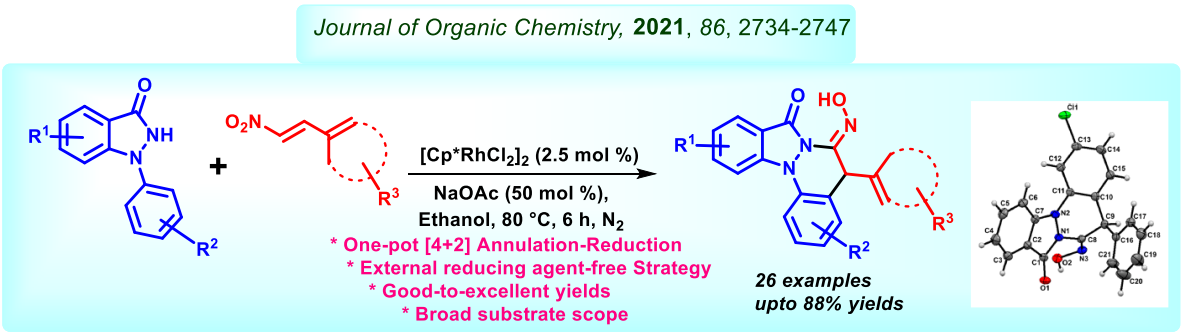

Scheme 4.2.2 Rh-catalyzed [4+2] annulation strategy for the synthesis of hydroxyimino-decorated indazolo[1,2-*a*]cinnolines using nitroolefins

Chapter 2B: Iridium-Catalyzed [4+2] Annulation of *N*-Arylindazolones with *α*-Diazo Carbonyl Compounds to access Indazolo[1,2-*a*]cinnoline Carboxylates

This chapter initially highlights the reactivity of *α*-diazo carbonyl compounds as C-1 or C-2 synthons, particularly in the annulation protocols to construct various heterocyclic scaffolds *via* directing group-assisted C-H activation using appropriate transition metal complexes. Inspired from the exiting reports, an efficient methodology for the [4+2] annulation of *N*-aryl-1,2-dihydro-3*H*-indazol-3-ones with *α*-diazo carbonyl compounds was achieved to access indazolo[1,2-*a*]cinnoline carboxylates under Ir^{I}-catalyzed conditions using $AgSbF_6$ as an additive in DCE (Scheme 4.2.3). By using the optimized conditions, various tetracyclic indazolo[1,2-*a*]cinnoline carboxylates were prepared with moderate-to-good yields; whereby moderately electron-withdrawing substituents on aryl ring of indazolone furnished good yields as compared to electron-donating substituents on aryl ring of indazolone moiety. Detailed spectroscopic analysis, including ^{1}H & ^{13}C NMR analysis and the X-ray crystal structure of one of the synthesized products provided a clear evidence for their proposed structure. The protocol was extended towards the synthesis of a few pentacyclic indazolo[1,2-*a*]cinnolines from cyclic *α*-diazo carbonyl compounds. Further, several synthetic utilities of the synthesized indazolone-fused cinnolines by performing chemical modifications on the appended ester, amidic functional groups in one of the product. Preliminary mechanistic investigations, including control and competitive experiments, *in situ* reaction monitoring by ESI-MS and isolation of an iridacyclic intermediate suggested the reaction proceeds through the N–H oxidative addition of *N*-arylindazole and subsequent C–H bond activation to afford an iridacyclic intermediate, which upon carbene coordination, migratory insertion, protodemetallation and dehydration affords the desired product.

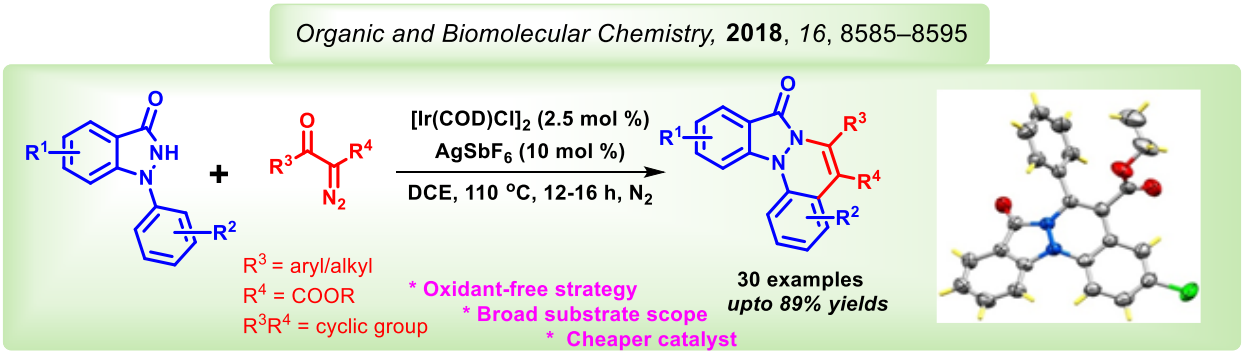

Scheme 4.2.3 Ir-catalyzed [4+2] annulation strategy for the synthesis of indazolo[1,2-*a*]cinnoline carboxylates using *α*-diazo carbonyl compounds

Chapter 2C: Palladium-Catalyzed [4+2] Annulation of *N*-Arylindazolones with Allenoates to access Indazolo[1,2-*a*]cinnoline Carboxylates

This chapter initially describes the literature study on transition metal-catalyzed C-H functionalization/annulation strategies, employing various substituted allenes and allenoates as coupling partners at the expense of an appropriately attached amidic/amine directing groups. Anticipating the versatile reactivity exhibited by allenoates in C-H functionalization processes, solvent/additive-controlled strategies for the synthesis of two regioisomeric forms of indazolo[1,2-*a*]cinnolines possessing internal and exocyclic double bonds were disclosed through Pd^{II}-catalyzed oxidative annulation of *N*-aryl-1,2-dihydro-3*H*-indazol-3-ones with allenoates (Scheme 4.2.4). A broad range of substrate scope was exhibited under dioxane- and acetic acid-controlled conditions, producing tetracyclic indazolo-fused cinnolines in moderate-to-good yields. Surprisingly, the allenoates possessing substitution at the terminal double bond selectively produced the annulation products possessing an exocyclic double bond, under either of the two described solvent-controlled conditions. All the spectroscopic data and the X-ray crystal structures of two products provided a clear evidence for their assigned structures. Further, a gram scale reactions were performed under both the described conditions to show the synthetic utility of the strategies on an industrial level. Detailed mechanistic investigations, including isotopic labelling and kinetic isotopic effect studies through parallel and intercompetitive experiments suggested that the reactions proceeds through the formation of a five-membered palladacycle complex, which upon allenoate coordination, regioselective 1,2-migratory insertion followed by reductive elimination generates the products in presence of appropriate additive/base.

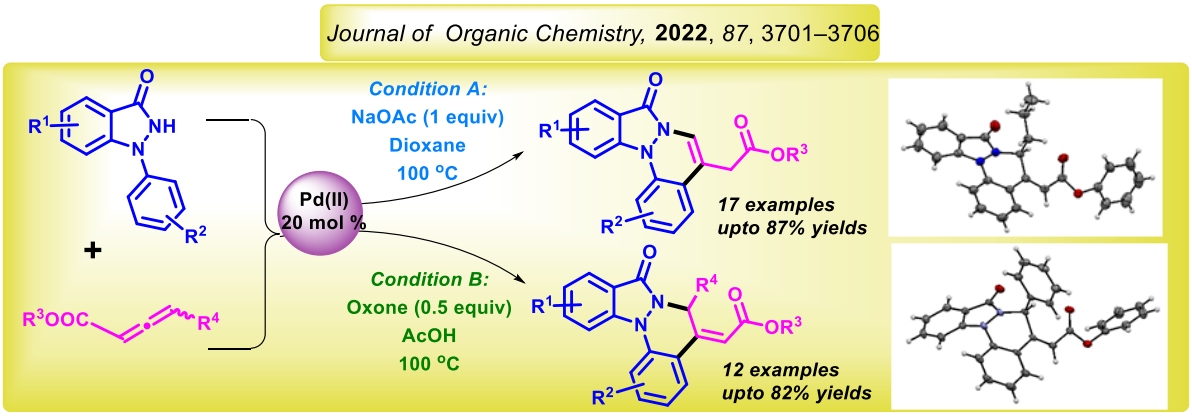

Scheme 4.2.4 Pd-catalyzed annulation strategy for the synthesis of indazolo[1,2-*a*]cinnoline carboxylates using allenoates

Chapter 3: Palladium-Catalyzed Tandem Transformation of *N*-Arylindazolones to Disubstituted Quinazolinones through Carbene Insertion into N-N Bond

This chapter first describes the biological importance of quinazolinones, and thereafter, presents an overview on various synthetic protocols applied for the construction of substituted quinazolinones *via* metal-free as well as metal-catalyzed (Cu/Pd) conditions. Further, a discussion on the existing synthetic strategies for preparing 1,2-di(hetero)aryl 2,3-dihydroquinazolin-4(1*H*)-ones and 2,3-di(hetero)aryl 2,3-dihydroquinazolin-4(1*H*)-ones has been included. Next, the exemplification of safer yet reactive *N*-tosylhydrazones as alkylating agents, leading to the construction of C-C/C-N bonds *via* C-H/N-H insertions, has been included. Anticipating limited reports on the application of aldehydic *N*-tosylhydrazones in C-H functionalization, a one-pot Pd^{II}-catalyzed protocol was developed for the unprecedented transformations of 1-aryl- and 2-arylindazolones to 1,2-(hetero)aryl and 2,3-(hetero)aryl 2,3-dihydroquinazolin-4(1*H*)-ones respectively, by reacting them with *N*-tosylhydrazones through carbene insertion into N-N Bond (Scheme 4.2.5). This protocol furnished moderate-to-excellent yields of diversely substituted quinazolinones, in which electron-rich indazolones and *N*-tosylhydrazones showcased high reactivity. Detailed spectroscopic analysis of the products and the X-ray crystal structure of one of them provided a clear evidence for the assigned structures. By using this methodology, an important bioactive molecule, NPS-53574 was synthesized in gram scale level. Detailed mechanistic investigations provided the evidence for a tentative reaction pathway.

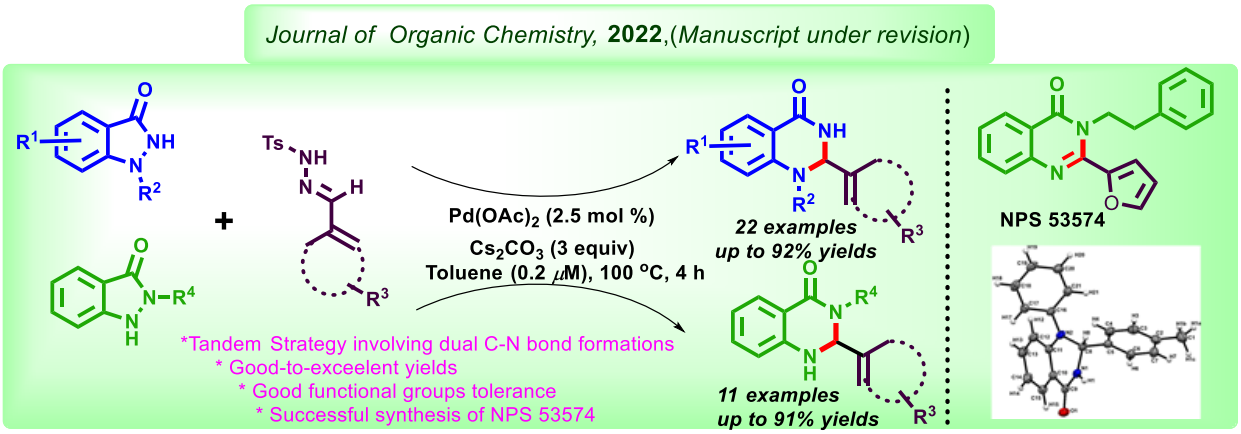

Scheme 4.2.5 Pd-catalyzed synthesis of 1,2- and 2,3-disubstituted-2,3-dihydroquinazolin-4(1*H*)-ones using aldehydic *N*-tosylhydrazones

4.3 Future Scope

In recent years, various research groups utilized *N*-arylindazolones to develop biologically relevant fused and functionalized diazaheterocycles *via* transition metal catalyzed strategies in a convenient manner. Hence, this thesis was mainly focused on developing new strategies for the synthesis of indazolo[1,2-*a*]indazol-ylidenes, indazolo[1,2-*a*]cinnolines and 2,3-dihydroquinazolin-4(1*H*)-ones under transition metal-catalyzed conditions. Expanding the scope, much more work in this field is desirable and could be efficiently executed. In this regard, the scope of the present work could be expanded by synthesizing novel fused-indazolones (**i-vi**) given in Figure 4.3.1. Further, their biological activities and the sensing ability of fluorescent molecules could be studied.

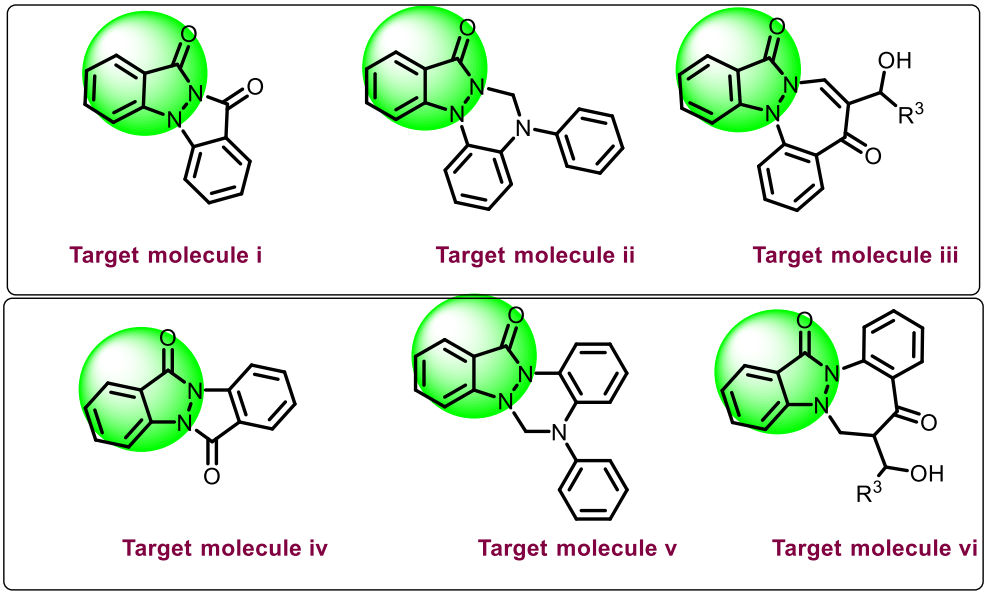

Figure 4.3.1 Structures of novel fused-indazolones for future studies

Appendices

List of Publications *[A-1]*

1. **Chikkagundagal K. Mahesha**, Somnath A. Borade, Disha Tank, Kiran Bajaj, Himanshi Bhambri, Sanjay K. Mandal, Rajeev Sakhuja, "Tandem Transformation of Indazolones to Quinazolinones through Pd-Catalyzed Carbene Insertion into N-N Bond", *J. Org. Chem.* **2023**, *88*, 1457.
2. **Chikkagundagal K. Mahesha**, Sushma Naharwal, Narendra D. Kharat, Sanjay K. Mandal, Rajeev Sakhuja, "Regiodivergent Synthesis of Cinnoline-Fused Indazolones through Pd-Catalyzed Annulation of 1-Arylindazolones with Allenoates", *J. Org. Chem.* **2022**, *87*, 3701–3706.
3. Sushma Naharwal, Pidiyara Karishma, **Chikkagundagal K. Mahesha**, Kiran Bajaj, Sanjay K. Mandal, Rajeev Sakhuja, "Ruthenium-Catalyzed (Spiro)Annulation of *N*-aryl-2,3-dihydrophthalazine-1,4-diones with Quinones to Access Pentacyclic Spiro-Indazolones and Fused-Cinnolines", *Org. Biomol. Chem.,* **2022**, *20*, 4753-4764.
4. Narendra D. Kharat, **Chikkagundagal K. Mahesha**, Kiran Bajaj, Rajeev Sakhuja, "Rhodium-Catalyzed Annulation of Vinylated Tyrosines with Internal Alkynes to Access Oxepine-Mounted Unnatural Tyrosines and its Peptide Late Stage Functionalization", *Org. Lett.* **2022**, *24*, 6857-6862.
5. Pidiyara Karishma, **Chikkagundagal K. Mahesha** *(sharing equal contribution with the first author)*, Sanjay K. Mandal, Rajeev Sakhuja, "Reducing-Agent-Free Convergent Synthesis of Hydroxyimino-Decorated Tetracyclic Fused Cinnolines *via* Rh^{III}-Catalyzed Annulation Using Nitroolefins", *J. Org. Chem.* **2021**, *86*, 2734–2747.
6. **Chikkagundagal K. Mahesha**, Sanjay K. Mandal, Rajeev Sakhuja, "Indazolone-Assisted Sequential *ortho*-Alkenylation-Oxidative Aza-Michael Addition of 1-Arylindazolone using Acrylates under Ru(II) Catalysis", *Asian J. Org. Chem.* **2020,** *9*, 1199-1204.
7. **Chikkagundagal K. Mahesha**, Devesh S. Agarwal, Pidiyara Karishma, Datta Markad, Sanjay K Mandal, Rajeev Sakhuja, "Iridium-Catalyzed [4+2] Annulation of 1-Arylindazolones with α-Diazo Carbonyl Compounds: to Access Indazolone-fused Cinnolines", *Org. Biomol. Chem.,* **2018**, *16*, 8585-8595.
8. Pidiyara Karishma, **Chikkagundagal K. Mahesha**, Devesh Agarwal, Sanjay K. Mandal, Rajeev Sakhuja, "Additive-Driven Rhodium-Catalyzed [4+1]/[4+2]

Annulations of *N*-Arylphthalazine-1,4-dione with α-Diazo Carbonyl Compounds", *J. Org. Chem.* **2018**, *83*, 11661–11673.

9. Vellekkat Jamsheena, **Chikkagundagal K. Mahesha**, M. Nibin Joy, Ravi S. Lankalapalli, "Metal-Free Diaryl Etherification of Tertiary Amines by *ortho*-C(sp^2)–H Functionalization for Synthesis of Dibenzoxazepines and –ones", *Org. Lett.* **2017**, *19*, 6614–6617.

10. Sushma Naharwal, Narendra Dinkar Kharat, **Chikkagundagal K. Mahesha**, Kiran Bajaj, Rajeev Sakhuja, "Palladium-Catalyzed Regioselective C-Arylation and C, N-Diarylation of N-Aryl 2,3-dihydrophthalazine-1,4-diones using Diaryliodonium Salts" Synthesis, **2023**, 55, A-K.

List of Presentations in Conferences *[A-2]*

Poster:

1. **Chikkagundagal K. Mahesha,** Devesh S. Agarwal, Pidiyara Karishma, Datta Markad, Sanjay K. Mandal, Rajeev Sakhuja "Iridium-Catalyzed [4+2] Annulation of 1-Arylindazolones with α-Diazo Carbonyl Compounds: Access to Indazolone-fused Cinnolines" at ISCB International Conference (ISCBC-2019), Lucknow, during January 12-14, 2019.
2. **Chikkagundagal K. Mahesha,** Pidiyara Karishma, Rajeev Sakhuja "Ruthenium Catalyzed Oxidative Annulation of 1-Arylindazolone with Acrylates: An easy access to Indazolo[1,2-*a*]indazolones possessing Exocyclic Double Bond Functionality" ISCBC-NIPiCON-2020 International Conference, Ahmedabad, during January 22-24, 2020. *(Best poster presentation award)*

Brief Bibliography of the Candidate *[A-3]*

Mahesha C. K. obtained his Master's degree from Tumkur University in the year 2013. In June 2016, he cleared the CSIR-NET-LS in Chemical Sciences conducted by CSIR-UGC (June-2016). He joined the Department of Chemistry, BITS Pilani, Pilani Campus as a junior research fellow in a DST-SERB sponsored project in January, 2018 under the project in-charge, Dr. Rajeev Sakhuja and simultaneously he enrolled into the Ph.D. program in Auguest, 2018. During the tenure of his Ph.D., he was actively involved in the synthesis and functionalization of the *N*-arylindazolone skeleton. He has published eight research articles in peer-reviewed international journals and presented papers in two international conferences.

His main research interest lies in the development of new methods for the construction of nascent chemical bonds using novel C−H activation/functionalization strategies under transition metal-catalyzed conditions.

Brief Bibliography of the Supervisor *[A-4]*

Dr. Rajeev Sakhuja obtained his M.Phil. and Ph.D. degrees from the Department of Chemistry, University of Delhi, New Delhi in the area of heterocyclic chemistry. Following this, he pursued his postdoctoral research with Prof. Alan R. Katritzky at the Center of Heterocyclic Compounds, University of Florida, Gainesville, and thereafter with Professor Raymond Booth at Department of Medicinal Chemistry, University of Florida from 2009-2012. He joined the Department of Chemistry, BITS Pilani, Pilani Campus as an Assistant Professor in March 2012. Following Ph.D., he has fourteen years of post-Ph.D. research experience in the broad field of organic synthesis. Dr. Sakhuja is presently Professor in Department of Chemistry, leading an independent research group at Birla Institute of Technology & Science, Pilani where his current area of research interests lies in the development of metal-catalyzed and metal-free strategies for the functionalization of heterocycles, synthesis of biologically important heterocyclic scaffolds, along with the development of organic materials with sensing and gelation abilities. His effective contribution in these areas has fetched him seventy research articles, 4 reviews in peer-reviewed journals of international repute and two book chapters. He has successfully completely four sponsored projects funded by government agencies (DST, SERB, UGC), and private organization (BITS seed grant & additional research grant) in the past ten years.